Magnetism in ultrathin film structures

Rep. Prog. Phys. **71** (2008) 056501 (78pp) doi:10.1088/0034-4885/71/5/056501

Magnetism in ultrathin film structures

C A F Vaz[1], J A C Bland[2] and G Lauhoff[3]

Cavendish Laboratory, Madingley Road, Cambridge, CB3 0HE, UK

E-mail: carlos.vaz@cantab.net

Received 15 October 2007, in final form 10 March 2008
Published 23 April 2008
Online at stacks.iop.org/RoPP/71/056501

Abstract

In this paper, we review some of the key concepts in ultrathin film magnetism which underpin nanomagnetism. We survey the results of recent experimental and theoretical studies of well characterized epitaxial structures based on Fe, Co and Ni to illustrate how intrinsic fundamental properties such as the magnetic exchange interactions, magnetic moment and magnetic anisotropies change markedly in ultrathin films as compared with their bulk counterparts, and to emphasize the role of atomic scale structure, strain and crystallinity in determining the magnetic properties. After introducing the key length scales in magnetism, we describe the 2D magnetic phase transition and survey studies of the thickness dependent Curie temperature and the critical exponents which characterize the paramagnetic–ferromagnetic phase transition. We next discuss recent experimental and theoretical results on the determination of the exchange constant, followed by an overview of measurements of the magnetic moment in the elemental 3d transition metal thin films in the various crystal phases that have been successfully stabilized, thereby illustrating the sensitivity of the magnetic moment to the local symmetry and to the atomic environment. Finally, we discuss briefly the magnetic anisotropies of Fe, Co and Ni in the fcc crystalline phase, to emphasize the role of structure and the details of the interface in influencing the magnetic properties. The dramatic effect that adsorbates can have on the magnetic anisotropies of thin magnetic films is also discussed. Our survey demonstrates that the fundamental properties, namely, the magnetic moment and magnetic anisotropies of ultrathin films have dramatically different behaviour compared with those of the bulk while the comparable size of the structural and magnetic contributions to the total energy of ultrathin structures results in an exquisitely sensitive dependence of the magnetic properties on the film structure.

(Some figures in this article are in colour only in the electronic version)

This article was invited by Professor J Spence.

Contents

[1] Author to whom any correspondence should be addressed. Present address: Applied Physics, Yale University, New Haven, CT 06520, USA.
[2] Deceased.
[3] Present address: Samsung Information Systems America, 75 W Plumeria Drive, San Jose, CA 95134, USA.

1. An introduction to the physics of magnetism in ultrathin films

The study of the magnetic properties of thin films started in earnest in the 1970s following the development of deposition techniques by molecular beam epitaxy—which allowed an unprecedented control over the crystal growth environment [1]—and the advent of an array of *in situ* crystallographic and spectroscopic characterization techniques. Thin film magnetism has long since matured into an active area of research, with important technological ramifications. Indeed, thin film magnetism has brought important contributions to our fundamental understanding of the physics of magnetism [2–5] in tandem with critical applications in information technology, particularly evident since the discovery of the GMR effect [6, 7] (for which Fert and Grünberg shared the 2007 Nobel Prize in Physics) and following its impact on computer read-head technology. Early research work focused strongly on the fundamental physical aspects of low-dimensional and interfacial magnetism, although a clear recognition of the potential for applications was also present (for example, leading to the development of bubble memories in garnet films [8]). With the better understanding of the physics at the nanoscale followed a more device-oriented research effort where much attention has been given to physical phenomena with potential for device applications. Examples include the intensive research on spin-valve and multilayer structures aimed at developing GMR/TMR sensors and devices (an example of which is the observation of very large magnetoresistance (MR) effects in Fe/MgO/Fe magnetic tunnel junctions [9–11]); the study of fast switching dynamics [12–15] and the developments in new storage media for reading and storing of information in magnetic RAMs [16]; the investigation of phenomena associated with transport of spin-polarized electrons across ferromagnetic/semiconductor interfaces (spin-injection and -detection) with a view to integrating the spin degree of freedom into semiconductor signal processing devices (spintronics) [17–23]; the work on the current-induced magnetic switching, first reported by Berger [24–29], has become a very topical field [30–32], with potential to allow the magnetic switching of individual bit elements by electric currents alone, via domain wall displacement [28, 33–39] or via switching of the soft layer in spin-valve elements [40–61]; and the developments in nanolithography and materials engineering for applications in high density storage media, to cite some of the current topics of research in magnetism with a very considerable emphasis on practical devices. Micromagnetic calculations [62–64] have also been used extensively for the study of the equilibrium magnetic configurations in small (patterned) elements and *ab initio* calculations [65–77] have been employed to predict new effects with real potential for applications; such approaches are fast becoming an essential counterpart of experimental physics in advancing the understanding of the material properties and in predicting new phenomena. It is likely that this recent focus on the practical aspects of physical phenomena at the nanoscale will lead to the resurgence of a research programme aimed at addressing more fundamental aspects of magnetism, since many of the physical mechanisms underlying the processes currently being investigated are still, for the most part, poorly understood. It is therefore important to take stock of some of the fundamental aspects of the physics of ultrathin magnetic films achieved thus far, so that one may tackle the current stream of new phenomena on surer ground. In fact, notwithstanding the huge impact ultrathin magnetic films have made in magnetic data storage technology, we are probably only at the beginning of a revolutionary and technological era which will harness ultrathin magnetic films, e.g. for magnetic biosensors, etc. Moreover, as the drive to realize ever smaller memory bits on magnetic media and to create ever smaller magnetic devices, the influence of the reduced size and surface/edge effects will become even more important in designing such structures, i.e. bulk properties cannot be assumed.

Some of the recent achievements in the area of thin film magnetism are worth recalling. In the early 1980s, the magnetization of sufficiently thin (few monolayer) epitaxial Fe/Ag(0 0 1) films was theoretically predicted [68] and experimentally confirmed [78] to lie perpendicular to the plane of the film. This occurs because a surface magnetic anisotropy term favouring a perpendicular spin orientation overwhelms the volume dependent dipolar energy. Perpendicular anisotropy, first reported on NiFe(1 1 1)/Cu(1 1 1) thin films by Gradmann and Müller [79, 80], has now been identified in a wide range of ultrathin ferromagnetic film structures [81–88] and has already been exploited in perpendicular recording media [89]. In such media, the stray field perpendicular to the film plane generated by the magnetic domains which store the information is sensed and external perpendicular fields are applied during the magnetic recording process. The giant magnetoresistance (GMR) effect, first identified in Fe/Cr trilayers [7] and multilayers in 1988 [6], describes the large reduction in electrical resistance which occurs when the relative alignment of the Fe layers is changed from an antiparallel to a parallel configuration by the application of an external field. Originally, this effect was identified in structures with fixed Cr thickness, for which an antiparallel alignment of the Fe layers is favoured due to the interlayer exchange coupling across the Cr spacer layer. The coupling strength was since found [90, 91] to oscillate with thickness in a wide range of spacer materials (so-called oscillatory coupling) and this behaviour has since been theoretically described in terms of RKKY interactions in the 2D geometry and magnetic quantum well effects within the spacer layer [92–104]. New applications based on these discoveries have fuelled much excitement in this field as well as creating new important technologies. For example, IBM demonstrated in 1994 that a magnetoresistive read-head based on the giant magnetoresistance behaviour of a spin-valve multilayer structure could be used to read a 1 Gb in^{-2} disk [105] and soon after spin-valve read heads became standard in disk drives whose storage densities keep increasing dramatically. This progress is remarkable, given that less than 10 years passed from the discovery of the effect to the realization of the first commercial devices.

The first commercially available hard disk drive (HDD) was introduced by IBM, called RAMAC. This HDD introduced

in September 1956 had a recording density of about 2 kb in^{-2}. Commercial HDDs reached recording densities of 200 Gb in^{-2} in 2007 (and areal density demonstration of 520 Gb in^{-2}), which corresponds to a 10^8 increase in magnetic recording density in the last 51 years, or an annual increase in recording density of about 40%. Unlike the areal density of dynamic random access memories (DRAM), which increased almost constantly at 40% per year, the progress in magnetic recording changed with time. At around 1990 the annual rate of increase of the recording density was only 25%; it increased to 60% per year after the introduction of thin film magnetoresistive heads in 1990 and with the introduction of GMR heads in 1997 the rate of increase has changed to about 100% annually. To overcome the thermal stability problem, the so-called antiferromagnetic coupled media were introduced [106, 107]. However, this strong annual growth could not be maintained beyond 2001 and perpendicular magnetic recording media (first proposed in 1970 [108]) were recently introduced. The main advantage of perpendicular compared with longitudinal magnetic recording media is that a soft magnetic underlayer is incorporated into the disk. This underlayer conducts the magnetic flux readily and the perpendicular magnetic recording layer that stores the data resides in the gap between the recording head pole-tip and the soft magnetic underlayer [89, 109, 110]. Higher fields allow higher coercivity media to be used so that further reductions in the grain size of the magnetic recording media (hence higher storage densities) become possible. Ultimately, however, the superparamagnetic limit will impose a cut-off on the storage densities which are achievable and, in addition, demanding problems associated with magnetic writing and media must be solved. Presently, the problem of the superparamagnetic limit is being 'postponed' by the introduction of perpendicular magnetic recording. Other approaches to overcome some of these problems include the use of patterned media, such as discrete track media [111, 112] or bit patterned media [113–118]. In the case of bit patterned media each grain stores one bit, enabling a large increase in the areal storage density. Both approaches are seriously considered on HDD industry road maps. Other suggestions include modulation of the magnetic anisotropy across the magnetic film to effectively create continuous media that is subdivided into small regions each capable of storing a bit of information [119–121]. Therefore, interest is inevitably shifting towards a better understanding of the physics of nanoscale structures. Another approach which is being currently developed is the so-called heat-assisted magnetic recording (HAMR), similar to magnetooptic recording: the magnetic recording media is locally heated during the writing process, followed by rapid cooling after completion of the writing. Local heating lowers the magnetic anisotropy locally, thereby assisting the magnetic writing process by reducing the required head field strength [122, 123]. The demonstration of large room temperature spin dependent tunnelling resistance for transport across thin oxide layers has generated great excitement, both for the basic physical processes involved but also because of applications [9–11, 16, 124–126]. Current magnetic recording heads have employed the tunnel magnetoresistance (TMR) effect since 2005. Future magnetic recording technologies such as magnetic random access memory cells and other devices will be expected to employ TMR elements [16, 124, 127].

Nanoscale magnetic effects were already recognized several decades ago. For example, Bloch in the 1930s [128] recognized that a 2D magnetic film would be unstable to magnetic fluctuations at finite temperatures—a result which was later treated rigorously by Mermin and Wagner [129]. Efforts in the 1960s and 1970s to prepare thin films were very often hampered by poor vacuum which led to surface contamination. For example, Liebermann *et al* [130, 131] observed a reduced moment at Ni interfaces which was interpreted as a magnetically 'dead' layer but later studies demonstrated, in fact, that surface oxidation led to the reduced moment [132, 133]. While the prospect of new applications are a driving force today, the subject of thin film magnetism owes much to the stimulus generated by the theoretical predictions during the mid-1980s of strongly enhanced magnetic moments for monolayers of the 3d ferromagnetic transition metals supported by noble metal single crystal substrates. However, it is only recently that methods of sample growth, structural and magnetic characterization have been refined to the point that accurate tests of these predictions have become possible and the issue of surface structure and surface contamination still remains of central importance today. As an illustration, recent growth studies have led to an improved understanding of the role of surfactants in controlling interface structure at the atomic scale. Such effects can be used to dramatically influence magnetic properties in ultrathin films by controlling the interface roughness—for example, the surfactant effect of minute amounts of oxygen in the 10^{-9} mbar range can significantly affect the magnitude of the giant magnetoresistance in spin-valve structures [134], while 1–3 at% carbon in Co/Cu spin-valves can eliminate the GMR effect altogether [135, 136]. Submonolayer coverages of non-magnetic materials can change the magnetic anisotropy of ultrathin films, in some cases causing a complete reorientation of the magnetic easy axis [137–140]. The interface also plays a crucial role for tunnelling magnetoresistance, where smooth, homogeneous and clean interfaces are required for optimum spin polarization and magnetic decoupling of the magnetic layers [141]. In general, the chemical and physical sharpness of the interface (absence of interdiffusion, chemical reaction at the interface or reaction with contaminants; and roughness and uniformity of the deposited layers, respectively) may influence the magnetic behaviour of the system under study, such as spin injection efficiency across ferromagnetic/semiconductor interfaces, magnetic anisotropies and magnetic moments. A substantial worldwide research effort is currently devoted to exploring the link between magnetic properties and atomic scale structure and surface chemical effects. New impetus to this field has recently been given, on the one hand, by the development of new characterization techniques with ever increasing sensitivities and spatial- and time-resolutions, such as scanning tunnelling microscopy (STM), atomic and magnetic force microscopy (AFM, STM), spin-sensitive STM and near field optical MOKE techniques, x-ray magnetic circular dichroism (XMCD), polarized neutron reflection

(PNR), scanning electron microscopy with polarization analysis (SEMPA) and photoemission electron microscopy (PEEM), to name a few; and also by the application of advanced lithography and pattern transfer techniques to the fabrication of nanoscale magnetic elements based on ultrathin magnetic films. On the other hand, the spectacular development of *ab initio* calculation methods has enabled a much deeper understanding of materials properties at the electronic level. Tight binding and density functional theory combined with other calculation methods have provided numerical values for a range of key material parameters which have proven to be, on the whole, accurate and consistent with experiments [65–77]; in fact, since first principles calculations are not constrained by the materials available in the laboratory, theoreticians are able to 'experiment' with metastable or non-equilibrium phases of materials, and to determine the respective properties *in silico*. Such studies have contributed much to a better understanding of the properties of materials and stimulated much experimental work.

The last few years have seen the emergence of an exciting and promising new field of research, magnetoelectronics or spintronics, which aims to combine the electron charge degree of freedom with that of the electron spin, thereby opening new avenues for non-volatile information storage and processing at higher speed, higher densities and lower power consumption [17–20, 142, 143]. For these applications, performance is expected to depend sensitively on the interface quality [144–147], and high-spin polarization materials are key. In addition, while interface effects are well recognized in magnetic systems, they are also actively playing a key role in other areas of condensed matter physics, including complex oxides, superconductors, ferroelectrics and multiferroic materials [148, 149]; interfacing of 3d ferromagnets with such disparate materials is already showing potential for new physics and for applications [150–161].

In this paper, particular emphasis is placed on studies conducted in well characterized epitaxial systems, since these are expected ideally to reveal more of the intrinsic magnetic properties while keeping extrinsic factors under control, although in practice such expectation is often frustrated by the complexity of the interplay between structure and magnetism. We focus on the elemental 3d transition metal systems, Fe, Co and Ni, with the occasional reference to some alloys. Further, we restrict ourselves to four fundamental aspects of magnetism which, in our opinion, merit reviewing in the light of recent developments. The magnetic moment is the most fundamental quantity in magnetism, yet it is a very difficult quantity to measure in ultrathin films; the exchange constant is yet another fundamental constant in magnetism, which is exceedingly difficult to measure accurately in bulk systems, and more so in thin films; magnetic phase transitions give important insights into the physics of critical phenomena and the role of dimensionality on the magnetic behaviour of ultrathin films; finally, the magnetic anisotropy has been perhaps the most widely studied facet of thin film magnetism, and we illustrate how intrinsic and extrinsic effects combine to affect markedly the magnetic anisotropy of ultrathin magnetic films. Several tutorial introductions to these and other aspects of ultrathin film magnetism are available in the literature: Gradmann [83], Bland and Heinrich (ed) [2–5] and Mills and Bland (ed) [162] (ultrathin film magnetism); Himpsel *et al* [96, 163], Bader [164], Kläui and Vaz [165] and Martín *et al* [166] (magnetic nanostructures); Gijs and Bauer [167], Levy [168], Hirota *et al* [169], Maekawa and Shinjo (ed) [170], and Marrows [30] (magnetoresistance); Heinrich and Cochran [171], Johnson *et al* [84] and Sander [172] (magnetic anisotropies in thin films and multilayers); Heinrich and Cochran [171], Stiles [97], Lindner and Baberschke [173] and Edwards and Umerski [104] (interlayer coupling); Sander *et al* [174, 175] (magnetoelastic effects in thin films); Eastman *et al* [176], Baberschke *et al* [177] and Stöhr and Siegmann [178] (electronic structure of magnetic 3d metals); Hillebrands, Ounadjela and Thiaville (ed) [12–14] (spin dynamics in confined magnetic structures); Awschalom *et al* [179], Žutić *et al* [20], Xu and Thompson (ed) [21], Maekawa [22] and Hirohata and Otani (ed) [180] (spintronics). The recently published volumes edited by Kronmüller and Parkin [181] also contain a wide range of reviews on topical aspects of magnetism at the nanoscale.

1.1. Length scales in magnetism

Magnetism is a quantum mechanical phenomenon that results from a combination of the Pauli exclusion principle and the electron–electron repulsive Coulomb term of the electronic potential. In simple terms, the requirement of antisymmetry couples the electron orbitals to the electron spin state (exchange energy); electrons avoid the same region in space thus lowering the electrostatic energy but at a cost of kinetic energy. While the exchange interaction arising from the exchange energy does not result from a direct atomic spin–spin coupling, it can be written phenomenologically as such; one useful description is that of the Heisenberg Hamiltonian $H = -\sum J_{ij}\boldsymbol{S}_i \cdot \boldsymbol{S}_j$, where J_{ij} is the exchange integral and $\boldsymbol{S}_i$ the spin of atom i, which is particularly suitable for localized magnetic systems (where $\boldsymbol{S}$ is the localized atomic total momentum) [182]. A description based on the rigid band model of metals is also often used (Stoner model) [183, 184], where the exchange energy is treated in a mean field fashion by considering the exchange splitting between bands as proportional to the magnetization, a correspondence which is indeed observed experimentally in Fe, Co and Ni [178, 185].

The exchange energy is at the origin of magnetic order, favouring parallel alignment of the spins in the case of ferromagnetism. Other magnetic energy terms include the magnetic anisotropy term, which originates from the spin–orbit coupling (and is therefore a quantum relativistic effect) and the classical magnetostatic energy term, including the dipole–dipole interaction and the Zeeman term (interaction with an external magnetic field). Although the strength of the exchange energy (of the order of 0.1 eV/atom) is much larger than the magnetostatic (∼0.1 meV/atom) and magnetic anisotropy (∼10 μeV/atom) energy terms [186], the latter two tend to be important in macroscopic samples with dimensions exceeding characteristic length scales which we introduce next [163]. Such length scales follow naturally from the classical expressions for the different energy terms; in the

continuum limit, the excess exchange energy density due to a non-parallel alignment of the spins is, for cubic or isotropic materials [187–189]:

$$e_{\mathrm{ex}} = A(\boldsymbol{\nabla m})^2, \tag{1}$$

where A is the exchange constant and $\boldsymbol{m} = \boldsymbol{M}/M_{\mathrm{s}}$ is the magnetization unit vector with M_{s} the saturation magnetization. The magnetic anisotropy energy term couples the direction of the magnetization with the crystal symmetry axes, and as such has at least the symmetry of the crystal lattice. Microscopically, the magnetocrystalline anisotropy originates from the spin–orbit coupling linking the spin direction to the direction of the orbital moment, and from the magnetic dipolar interaction (excluding shape anisotropy), although the latter contributes only in second order of approximation to cubic systems [190–193]. For uniaxial and cubic materials, the anisotropy energy density is usually expressed as

$$e_{\mathrm{uni}} = K_{\mathrm{u}}(1-\alpha_3^2) + K'_{\mathrm{u}}(1-\alpha_3^2)^2 + \cdots, \tag{2}$$

$$e_{\mathrm{cub}} = K_1 \sum_{i>j} \alpha_i^2\alpha_j^2 + K_2\alpha_1^2\alpha_2^2\alpha_3^2 + \cdots, \tag{3}$$

where the α_i are the direction cosines of the magnetization. It is worth noting that several terms contribute to the magnetic anisotropy other than the intrinsic magnetocrystalline anisotropy we have considered thus far; for example, strain has the effect of introducing an extra anisotropy term via the magnetoelastic interaction [188, 194, 195], and this is a term which is particularly important in epitaxial magnetic films, which tend to be grown on substrates which are not perfectly lattice matched [83, 174, 196, 197]; uniaxial or biaxial strains affect mostly the uniaxial anisotropy term of the magnetic energy, but higher anisotropy terms are also affected by strain [174, 198]. Another anisotropy contribution which is particularly important in ultrathin films is the *surface magnetic anisotropy*, first identified by Néel [199,200], and which arises from the break of symmetry at the interface. Both uniaxial and in-plane cubic anisotropy surface contributions have been identified [83] and a typical signature of this anisotropy term is a linear variation of the effective (measured) anisotropy constant with the inverse of the film thickness; this was first demonstrated experimentally by Gradmann and Müller [79,80] in $Ni_{48}Fe_{52}(1\,1\,1)$ thin films; typically the surface magnetic anisotropy in thin films are of the order of 0.1–1 erg cm^{-2} [81, 84, 132, 133, 201]. Another source of anisotropy which arises in surfaces is that associated with atomic steps, either due to islands that are created during the film growth or due to surface miscut [202–211].

Finally, the magnetostatic energy density term, which can be written as[4]

$$e_{\mathrm{ms}} = 2\pi \boldsymbol{H}_{\mathrm{d}} \cdot \boldsymbol{M} \tag{4}$$

where $\boldsymbol{H}_{\mathrm{d}}$ is the magnetic dipolar field created by the magnetization distribution itself, which in turn can be calculated from the magnetostatic potential generated by surface and volume magnetic charges, $\rho_{\mathrm{s}} = \boldsymbol{n} \cdot \boldsymbol{M}$ and $\rho_v = -\nabla \cdot \boldsymbol{M}$, respectively (where $\boldsymbol{n}$ is the unit vector normal to the surface enclosing the magnetic volume) [213,214]. From these expressions two characteristic lengths arise immediately, the *exchange length*

$$l_{\mathrm{ex}} = (A/2\pi M_{\mathrm{s}}^2)^{1/2} \tag{5}$$

and the *domain wall width*

$$l_{\mathrm{dw}} = (A/K)^{1/2}. \tag{6}$$

As the expressions show, they give an indication of the length over which the exchange energy dominates over the magnetostatic and the magnetic anisotropy terms, respectively; another quantity which is of interest is the *quality factor* corresponding to the ratio between anisotropy and magnetostatic energies,

$$Q = K/(2\pi M_{\mathrm{s}}^2). \tag{7}$$

In this context, *ultrathin magnetic films* are films whose thickness is of the order of, or below, the exchange length. An equivalent expression to l_{dw} is obtained for the length scale $l_{\mathrm{s}} = (Aw/K_{\mathrm{s}})^{1/2}$ over which spins are disturbed by the presence of an atomic step of terrace width w with step anisotropy strength K_{s}.

A simple example may be provided to illustrate the meaning of the term 'ultrathin' in terms of these characteristic length scales [171,215–217]. Consider a sheet of atomic spins which are pinned at one interface by a strong perpendicular anisotropy and let us neglect other magnetic anisotropies. Since the magnetic dipolar interactions favour an in-plane orientation of the interior spins, we expect that above a certain thickness a twist of the spins will arise in sufficiently thick films giving rise to exchange energy. The dipolar field leads to an energy density term of the form $2\pi M_{\mathrm{s}}^2 \cos^2\theta$ in a first approximation [84, 218], where θ is the angle between the magnetization and the film normal and we assume the magnetization direction varies only along the out-of-plane z-direction. The spin configuration is then obtained by minimizing the sum of the exchange and magnetostatic energy terms:

$$E = A(\mathrm{d}\theta/\mathrm{d}z)^2 + 2\pi M_{\mathrm{s}}^2 \cos^2\theta, \tag{8}$$

subject to the appropriate boundary conditions determined by the surface anisotropy which require that the surface torque vanishes [219]. Differentiating with respect to θ and searching for a minimum we obtain

$$A\mathrm{d}^2\theta/\mathrm{d}z^2 - \pi M_{\mathrm{s}}^2 \sin 2\theta = 0. \tag{9}$$

An approximate solution to this equation is given by

$$\theta = \theta_0 \mathrm{e}^{-z/l_{\mathrm{ex}}}, \tag{10}$$

which is valid for small values of θ. This indicates that, for a dominant perpendicular anisotropy, the spins will be aligned almost uniformly along the surface normal for small thicknesses and that for significant spin twist as a function

[4] The cgs system of units is used throughout as it is particularly suited to the study of magnetism; some quantities will be given in other commonly used units, such as Bohr magnetons, $\mu_{\mathrm{B}} = 9.274\,009\,15(23) \times 10^{-21}$ erg G^{-1}, eV and Å. Film thickness will be given in either Å, nm or monolayers (ML). For conversion between cgs and SI units, see [212].

of depth the film thickness must be larger than the exchange length. A rigorous treatment of this problem which takes into account the strength of the surface anisotropy has been given by several authors [215–217] who demonstrate that beneath a critical thickness, in a film with either perpendicular or in-plane anisotropy, all spins are parallel[5]: such film therefore behaves like a single giant spin or magnetic moment. Hence, ferromagnetic (FM) ultrathin films interspaced by non-magnetic (NM) spacer layers of the form [FM/NM] can be thought of as the characteristic 'building' bricks of multilayer structures.

Likewise, the domain wall width arises naturally in problems dealing with the transition region separating uniform magnetic domains and constitutes a textbook example of the competition between exchange and anisotropy terms [194, 226]. It is worth noting that this characteristic length need not coincide with the domain wall width in real materials, where a competition between all energy terms determines both the type of wall (Bloch, Néel, cross-tie) and the wall width [227]. A striking example is provided by the character of the domain wall in circular fcc Co disc elements [228, 229], where the (Néel) domain wall width is found to vary with the radial coordinate as a result of the fine balance between the different energy terms, magnetic anisotropy, exchange and dipolar interactions: close to the centre of the disk, the magnetic configuration resembles a Landau–Lifshitz domain with sharp domain walls, while close to the edge the magnetization follows the disk periphery in order to minimize surface pole charges at the disk edge, giving rise to a much widened domain wall width, see figure 1. The domain wall is said to be *geometrically constrained* [165, 228–233].

A general definition for the domain wall width is given by the expression:

$$\delta_{\mathrm{DW}} = \Delta\theta(\partial\theta/\partial x)_0^{-1}, \tag{11}$$

where $\Delta\theta$ is the angle variation between the two magnetic domains in radians and $(\partial\theta/\partial x)_0$ is the slope of the angle variation across the direction perpendicular to the wall plane (other definitions are possible, see [227]).

The two length scales introduced above are intimately related to the dimension below which a magnetic particle attains a single domain state of uniform magnetization. This is technologically important since it gives an upper limit to the storage density in particulate recording media (the breaking into domains being associated with loss of information) and has been an intensive topic of research since the first estimate of the critical dimension for a single domain particle, by Frenkel and Dorfman in 1930 [234]. Approximate expressions for the critical radius for a single domain state is [194, 235, 236]:

$$r_c/l_{\mathrm{ex}} \approx 2.121 \quad \text{(weak anisotropy)}; \tag{12}$$

$$r_c/l_{\mathrm{ex}} \approx 9Q \quad \text{(strong anisotropy)}; \tag{13}$$

[5] This does not take into account the breakup into magnetic domains, which may constitute a lower energy state of the system; this reflects the fact that the dipolar energy expression is more complex than the simple approximation used; such a breakup in domains is often observed experimentally in thin films that exhibit perpendicular magnetic anisotropy such as Co/Au(1 1 1) [220, 221], Fe/Ag(0 0 1) [222] or Ni/Cu(0 0 1) [223–225], although in the latter case the origin of the magnetic anisotropy is not due to a surface term and the film thickness is larger than in the previous examples, see section 6.5.

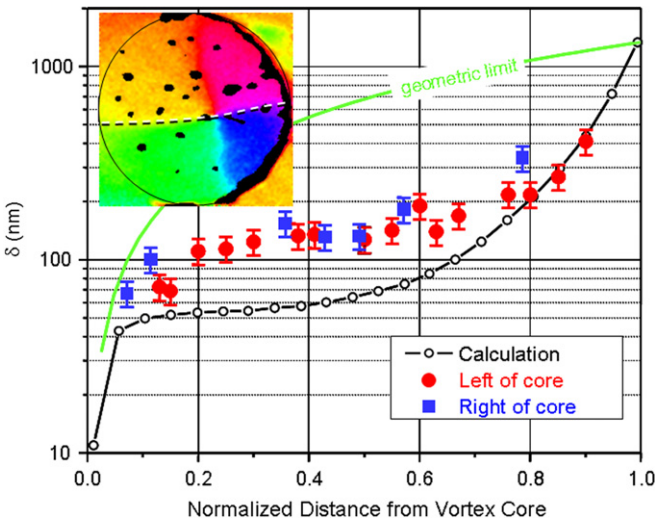

Figure 1. Domain wall width as a function of the normalized distance from the vortex core for a 1.7 μm diameter fcc Co disk, 34 nm thick. Inset shows the scanning electron microscopy with polarization analysis (SEMPA) image from which the data points were extracted [228, 229].

where $Q = K/(2\pi M_s^2)$ is the quality factor. In table 1 we list typical values for the critical radius for spherical particles of selected materials, where we have assumed that bulk parameters are still valid at such small length scales. It should be noted, however, that particles with significant shape anisotropy can remain in a single domain state for much larger dimensions as compared with spherical particles, which have no shape anisotropy [237].

When thermal excitations are introduced, one needs to consider the entropy contribution, S, in addition to the internal energy of the system U, which includes the exchange, anisotropy and magnetostatic energy terms, through the appropriate thermodynamic potential, namely, the Gibbs free energy $G = U - TS - \boldsymbol{M}\cdot\boldsymbol{B}_0$, where T is the temperature, and the last term is the Zeeman energy where $\boldsymbol{B}_0$ is the external applied magnetic field [245]. Thermal excitations affect the properties of magnetic systems very significantly; the excitation of magnons or spinwaves (elementary magnetic excitations) affects the value of the saturation magnetization and at higher temperatures spin waves and Stoner excitations (thermal reversal of the electron spin) are responsible for the destruction of magnetic order; the lattice expansion with temperature affects magnetic anisotropies and also affects the magnetic switching process by introducing excitations that assist the magnetization in overcoming local energy barriers (pinning sites). However, for temperatures much below the Curie temperature, the effect of thermal excitations may be treated as introducing small perturbations to the ground state of the system, as in the theory of spin waves.

The spin wave spectrum depends sensitively on the intrinsic parameters of the system, and therefore carries information about several important quantities, such as g-factor, magnetic anisotropy, saturation magnetization and exchange constant. Besides thermal excitation, spin waves can be excited by photons in the visible or in the radio-frequency range, which are the basis of the Brillouin light scattering

Table 1. Critical radius for single domain spherical particles for selected materials. Values of A and M_s at room temperature taken from table 11, values for the magnetic anisotropy constant K taken from [238] except [239][a] and [240, 241][b]; the reference in the last column refers to the experimental critical radius r_c. $Q = K/(2\pi M_s^2)$ is the quality factor.

Material	Anisotropy	10^6 K (erg cm^{-3})	l_{ex} (nm)	l_{dw} (nm)	Q	r_c (nm)	r_c^{exp} (nm)	Reference
bcc Fe	Weak	0.481	3.3	20.3	0.026	6.9	10	[242]
fcc Co	Weak	−1.2[a]	4.8	15.8	0.091	10.1		
hcp Co	Strong	4.12	4.7	8.3	0.324	13.7	4	[243]
fcc Ni	Weak	−0.056	7.6	39.2	0.038	16.2	10	[244]
fcc $Ni_{80}Fe_{20}$	Weak	0.0027[b]	5.1	199	0.00065	10.8		

(BLS) and ferromagnetic resonance (FMR) techniques. In this frequency range it is convenient to introduce a dynamic length scale which characterizes typical spatial variations in the rf magnetization, arising as a consequence of the surface torques exerted by the surface anisotropy [171, 246]:

$$l_{dyn} = (At/K_s)^{1/2}, \tag{14}$$

where t is the film thickness and K_s is the surface anisotropy strength. Spatial variations of the rf components of the magnetization are therefore negligible for films thinner than this length scale [171, 246]. Since the surface anisotropy field $H_s = 2K_s/(4\pi M_s t)$ is usually much smaller than the dipolar field $4\pi M_s$, the dynamic length scale usually exceeds the static exchange length l_{ex}. For instance, for a thickness t^* such that $t^* = l_{dyn}$, one obtains $t^* = A/K_s$ and rf mode spatial variations can be neglected for films of thickness $t \ll t^*$; for Fe, $t^* \sim 200$ Å at room temperature, using $A = 1.98\,\mu$erg cm^{-1} (table 11) and $K_s \sim 1$ erg cm^{-2} [171, 246].

Another aspect concerns the spin wavelength in a thin magnetic film. The spin wave dispersion in the large wave vector limit (but much smaller than the Brillouin zone boundary) is given by

$$\hbar\omega = Dk^2, \tag{15}$$

where k is the spin wave vector and D is the exchange stiffness which is related to J by (see section 4)

$$D = 2JSa^2, \tag{16}$$

where a is the lattice constant. For small wave vectors the dispersion relation is more complicated than this simple expression since the dipole fields associated with the spin variation across the film need to be taken into account [343]. The surface boundary conditions associated with the surface anisotropy field impose a constraint on the allowed values of k_z, the wave vector normal to the plane of the film. Only spin waves with discrete values of k_z are supported where $k_z \sim n\pi/d$ and d is the film thickness. For each allowed value of k_z there exists a manifold of spin wave modes with wave vector components k_x, k_y in the plane of the film. The lowest frequency mode is the so-called uniform mode corresponding to $n = 0$ and $k_z = 0$. This has no spatial variation of the spins with depth across the film and corresponds to a uniform precession of the magnetization about an effective field direction. However, for $n > 0$, standing waves of magnetization across the film thickness exist. The lowest such

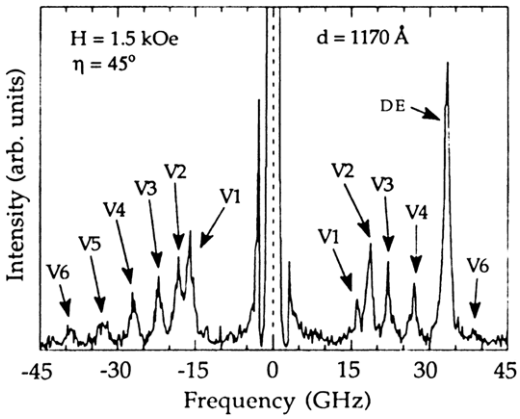

Figure 2. BLS spectrum for a 117 nm Fe/GaAs(0 0 1) film. A field of 1.5 kOe was applied along one of the in-plane ⟨0 1 1⟩ directions. The first six volume spin wave modes and the (Damon–Eshbach) surface spin wave mode are labelled by V1–V6 and DE, respectively [249]. Reprinted from R J Hicken, D E P Eley, M Gester, S J Gray, C Daboo, A J R Ives and J A C Bland 1995 Brillouin light scattering studies of magnetic anisotropy in epitaxial Fe/GaAs films *J. Magn. Magn. Mater.* **145** 278 Copyright (1995), with permission from Elsevier.

wave has a minimum frequency approximately given by Dk_1^2 where $k_1 = \pi/t$. For thermal excitation we require

$$D(\pi/t)^2 = k_B T. \tag{17}$$

Setting $T = 300$ K and using a value for the exchange stiffness for Fe of 280 meV Å^2 (see table 11) we obtain $t \sim 10$ Å. Thus films of this thickness and less will have an almost two-dimensional (2D) spin wave spectrum at room temperature [247, 248]. Figure 2 shows the spin wave spectrum for a 117 nm Fe/GaAs(0 0 1) film obtained by Brillouin light scattering [249]. The first exchange mode corresponding to $n = 1$ can be seen at a frequency of approximately 15 GHz and several higher order modes can also be observed. In a thin film (around 50 Å) the first mode lies outside the frequency scan range of figure 2. By fitting the data to a theoretical model describing the spin-wave modes in thin magnetic films [249–252], estimates of the stiffness constant can be obtained, $D = 260$ meV Å^2 for this 117 nm Fe film, a value which is comparable to that of bulk Fe, see section 4. Note that the estimated value for the crossover thickness of 10 Å is much smaller than that corresponding to l_{dyn} due to the fact that the details of the surface anisotropy field have not been included in our discussion, which takes into account a bulk-like exchange energy only. A proper discussion would include

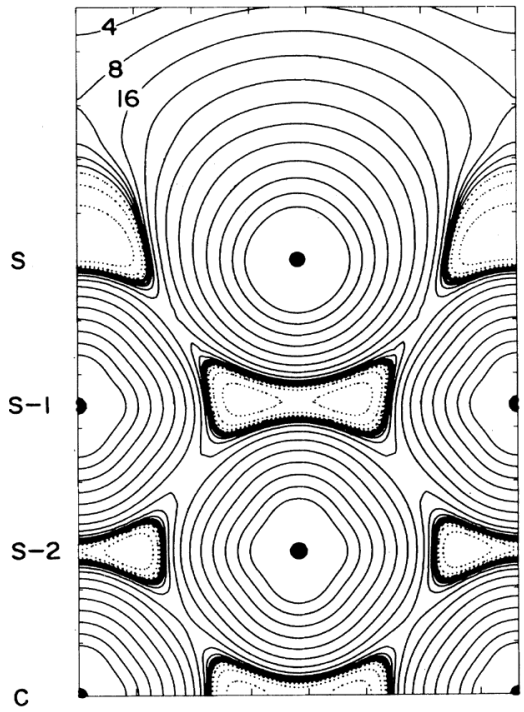

Figure 3. Spin-density map of the top three atomic layers of a seven layer Fe(0 0 1) slab in units of 10^{-5} on the (1 1 0) plane; each contour line differs by a factor of 2, dashed lines indicate negative spin density. Calculations were performed using a full-potential linearly augmented plane wave method [260]. Reprinted with permission from S Ohnishi, A J Freeman and M Weinert 1983 Surface magnetism of Fe(0 0 1) *Phys. Rev.* B **28** 6741. Copyright (1983) by the American Physical Society.

the effect of the surface anisotropy field on the spin wave energy [253, 254].

It must be emphasized that an ultrathin film is not necessarily a 2D film. The realization of a true 2D film occurs for much smaller thicknesses than the exchange length in general, and is characterized by a temperature and thickness dependent paramagnetic–ferromagnetic phase transition (see below and section 3). It is also important to recognize that, in addition to the exchange length, other physical length scales are important in describing a magnetic film system. For example, the electronic bandstructure is strongly modified at a surface or at an interface due to the broken symmetry and reduced atomic coordination which results in modified interactions. However, the bulk band structure develops surprisingly quickly as a function of depth from the interface. Typically for transition metal films, the effect of the surface or interface is only significant over a length scale of around 5–6 ML. As an illustration, we reproduce in figure 3 the calculated spin-density contours for a 7 ML Fe(0 0 1) slab, showing that only the atoms at the top three layers have spin-density contours that differ significantly from the bulk (central) atoms. Experimental examples that confirm this result include the thickness dependence of the critical exponent (from a value characteristic of a Ising system to that of a 3D system at around 7 ML [255–257], see section 3.2); the variation in the number of 3d holes as a function of film thickness probed by x-ray absorption spectrum experiments, which reaches the bulk value at around 5–7 ML, also indicates that below this thickness the electronic structure of the film is significantly different from that of the bulk [258, 259].

The thickness at which the Curie temperature begins to differ from the bulk value is a measure of the length scale of the spin–spin correlation length ξ describing the critical spin fluctuations in the vicinity of T_c. This effect has been long recognized since it can be seen in relatively thick films, several hundred angstroms thick [261]. The behaviour can be described by a so-called shift exponent λ which governs the thickness dependent Curie temperature $T_c(N)$ where N is the thickness in monolayers (see section 3.2):

$$[T_c - T_c(N)]/T_c \sim N^{-\lambda}. \tag{18}$$

Scaling arguments [262] predict $\lambda = 1/\nu$ where ν is the critical exponent for the correlation length. In the case where the film thickness is much less than the in-plane spin–spin correlation length $\xi_\parallel$ the film thickness provides a cut-off for spin correlations perpendicular to the film plane and thus the film can be regarded as 2D.

The problem of 2D ferromagnetism remains controversial. Bloch [128] pointed out that a 2D Heisenberg spin system cannot be ferromagnetically ordered at finite temperatures. This conjecture was based on the following argument. In thermal equilibrium the average value of the number of spin waves excited in the mode k is given by the Planck distribution:

$$\langle n(k)\rangle = (\exp\{\beta Dk^2\} - 1)^{-1}, \tag{19}$$

where $\beta = 1/k_B T$. The number of modes between k and $k+\mathrm{d}k$ is given by

$$g(k)\,\mathrm{d}k = 2\pi k\,\mathrm{d}k. \tag{20}$$

Now we can find an expression for the total number of modes excited by carrying out a summation over all modes:

$$n_k = \int_0^\infty g(k)\langle n(k)\rangle\,\mathrm{d}k. \tag{21}$$

At long wavelengths we can approximate

$$\exp\{\beta Dk^2\} \approx 1 + \beta Dk^2. \tag{22}$$

Hence the total number of spin wave modes diverges in 2D but is finite in 3D. This result was proved rigorously by Mermin and Wagner [129] for 2D spin systems with no anisotropy and only short-range interactions.

In practice, small symmetry breaking terms in the spin wave dispersion can prevent the divergence. Symmetry breaking introduced by magnetic anisotropies provide an example of one mechanism which can cause this behaviour. The anisotropy changes the spin wave dispersion according to

$$\hbar\omega = \Delta + Dk^2, \tag{23}$$

where the gap Δ is due to the anisotropy term. This leads to a magnetization variation as a function of temperature of the form [247, 263]

$$1 - M/M_s \propto T\ln(k_B T/\Delta). \tag{24}$$

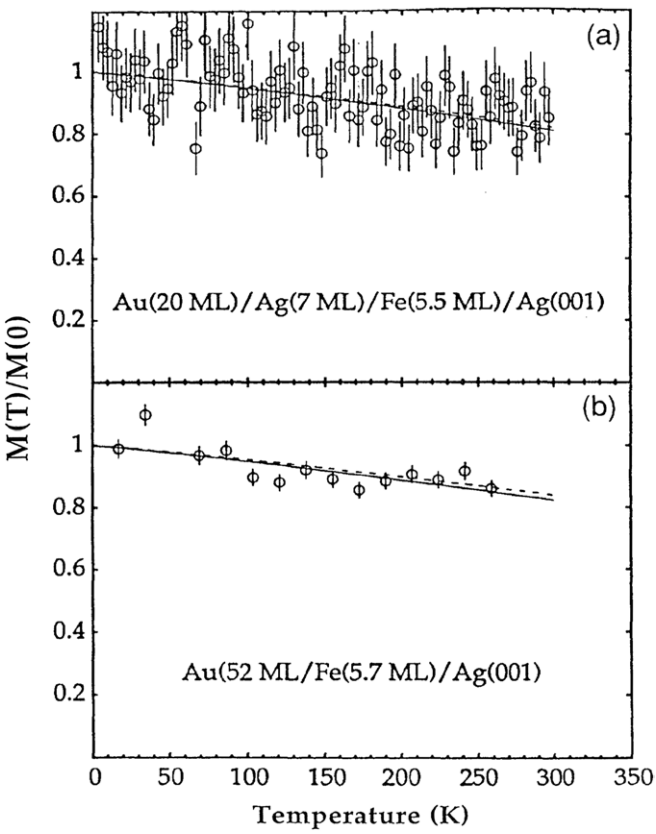

Figure 4. Normalized temperature dependence of the saturation magnetization determined from polarized neutron reflection (PNR) for (*a*) Ag/5.5 ML Fe, (*b*) Au/5.7 ML Fe films grown on Ag(0 0 1) substrates. Solid lines correspond to a best fit to (24) with Δ as the fitting parameter, and dashed lines correspond to a fit to the same expression using Δ calculated from the anisotropy constants obtained from FMR measurements; the values obtained for Δ are in the range from 0.1 to 0.3 K for these films [268]. Reprinted with permission from J A C Bland, C Daboo, B Heinrich, Z Celinski and R D Bateson 1995 Enhanced magnetic moments in bcc Fe films *Phys. Rev.* B **51** 258. Copyright (1995) by the American Physical Society.

Surprisingly, very small anisotropy fields are sufficient to stabilize the magnetization due to the logarithmic dependence. A value for $\Delta/k_B = 1$ K (corresponding to Oe range fields) is sufficient to give rise to an appreciable magnetization at 300 K. A longstanding goal of experimental physics has been to realize a supposedly 'perfect' 2D ferromagnetic monolayer through epitaxy to test whether indeed long range order develops. In practice magnetic anisotropies are almost always present which have been assumed to cause the stabilization of magnetic order in films as thin as 1 ML with Curie temperatures in excess of 100 K [264]. In addition, the dipolar interaction can stabilize the magnetization since the dipolar fields decay as $1/r^3$ and therefore break the requirement of the Mermin Wagner theorem [129] for short-range interactions only [265]. Experimental results for 1–2 ML thick fcc Co films suggest that the magnetization is stabilized by the magnetic anisotropies rather than by dipolar interactions [266, 267]; the temperature variation of the magnetization observed in 5 ML thick bcc Fe films grown on Ag(0 0 1) [268], shown in figure 4, has been interpreted also in terms of the previous expression, and similar results were observed for monolayers of Co and NiFe on Cu(1 1 1) [132] and fcc Fe/Cu(0 0 1) [269]. The observation of a change in the temperature dependence of the magnetization in 3 Å Fe/Ag multilayers by Mössbauer spectroscopy from a $T^{3/2}$ variation for small Ag thicknesses (corresponding to strong Fe interlayer coupling) to a linear variation at large Ag thicknesses (yielding isolated 3 Å Fe films) was also interpreted as a signature of a 3D to 2D crossover [270–272]. However, on a discordant note, the Mössbauer results of Przybylski *et al* [273, 274] on a 1 ML Fe(1 1 0)/W(1 1 0) indicate a magnetization variation following a $T^{3/2}$ dependence, and a similar result was found by Lugert *et al* for 4 ML Fe(1 1 0)/Ag(1 1 1) [275] and for 1, 4 ML Fe(1 1 0)/Au(1 1 1) [276]. One explanation may be the much stronger uniaxial anisotropies characteristic of the latter film systems.

One major obstacle to the observation of 2D magnetism is the existence of *superparamagnetism*. In this situation, islands with a volume V have developed an anisotropy constant K and are capable of supporting a thermally fluctuating magnetic moment. The time scale for the fluctuations at a temperature T is given by [277–280]

$$\tau = f_0^{-1} \exp(KV/k_B T), \tag{25}$$

where the frequency factor f_0 is of the order of 10^{-9} s. The quantity KV represents the energy barrier for magnetization reversal. Depending on the characteristic data collection time of the experimental measurement, a so-called *blocking temperature* exists below which the magnetization of the island is stable. Above the blocking temperature the thermal fluctuation of the spins results in zero average magnetization. For a given measurement time τ_m and temperature T_m it is straightforward to estimate the radius r of the islands at which the blocking temperature becomes equal to the measurement temperature:

$$r_B = [(-k_B T_m/\pi t K) \ln(f_0 \tau_m)]^{1/2}, \tag{26}$$

where t is the film thickness. In order to observe 2D magnetism it is necessary that the actual island size is much larger than the superparamagnetic particle size or conversely that the blocking temperature for the island size is much larger than the temperature at which the measurements are made [281–283]. Since in the superparamagnetic state the system is in thermodynamic equilibrium, it follows that the *M–H* curves have no hysteresis and, for sufficiently high temperatures, the magnetization curves scale with *H/T* (excluding effects related to interactions between particles or with the variation of the saturation magnetization with temperature and applied field [244, 284]). These are the two experimental criteria for superparamagnetism [237, 244, 284].

Other length scales appear when magnetism is considered in conjunction with other physical phenomena (see [163] for a recent overview). For example, the electron mean free path is different for majority and minority electrons, and this difference in scattering rate between up and down electrons explains the GMR effect observed in in-plane spin-valve structures [167, 285–289]. Also important is the wavelength of

electrons in metals. In metal multilayers quantization effects are to be expected at layer thicknesses much smaller than those typical in semiconductor superlattices due to the small size of the Fermi wavelength (around 1 nm in metals compared with up to 10 nm in semiconductors). Thus, interlayer coupling which is driven by the oscillatory polarization of confined electrons in the non-magnetic spacer layers occurs only for spacer layer thickness which are a few Fermi wavelengths in thickness.

The rest of this paper is organized as follows. In the next section, a brief discussion of some of the techniques employed in the characterization of thin films is given. In section 3 we give an overview of the main results available on the magnetic phase transition in thin magnetic films, with emphasis to the discussion of the 2D–3D phase transition and the problem of island percolation and the onset of ferromagnetic order. In section 4 we review the available data on the exchange constant of the elemental 3d ferromagnets; based on our survey we propose a set of values for the exchange constant for bulk Fe, fcc Co, hcp Co, Ni and $Ni_{80}Fe_{20}$. In section 5 we overview the published work on the magnetic moment of Fe, Co and Ni in their various crystalline forms, while in section 6 we discuss the magnetic anisotropies of Fe, Co and Ni in the fcc crystalline phase, to emphasize the sensitivity of the magnetic anisotropy to both intrinsic and extrinsic factors. We finish with a brief conclusion where we place in a broader perspective the relevance of the content of this review paper for the present and future work on small magnetic elements and nanomagnetism more generally.

2. Magnetic measurement techniques

Measurements of the magnetic properties of ultrathin structures are highly demanding in view of the small amount of magnetic material involved. A monolayer of Fe in a sample of area 1 cm^{-2} has a total magnetic moment of $\sim 10^{-5}$ emu, for example, which corresponds to a signal close to the detection limit of a conventional vibrating sample magnetometer. While commercial SQUID magnetometers do provide the sensitivity required, the difficulty of accurately subtracting the comparatively large response of a typically thick diamagnetic substrate remains a challenge. However, designer-built SQUID systems can achieve sensitivities and accuracies that rival any other magnetometric technique, as exemplified by the work of Baberschke and co-workers [290–294] who have used a high-T_c SQUID design operating in ultrahigh vacuum for the measurement of the magnetic moment of ultrathin films, and by the work of Wernsdorfer and co-workers [295–299] who have employed micro-SQUID junctions [300] to detect the switching fields of individual magnetic nanoparticles. The advent of commercial alternating gradient magnetometry [301] provides an alternative technique, offering the sensitivity of SQUID magnetometry with much more rapid data acquisition. However, the requirement that an alternating field is applied at the sample position in addition to the dc applied field makes it unsuitable for accurate determinations of small switching fields, while high sensitivity temperature dependent measurements are difficult. Another technique particularly suited to the accurate determination of the magnetic moment of ultrathin magnetic films is polarized neutron reflection (PNR), which relies on the magnetic moment of the neutron and its spin-dependence scattering from a magnetic media at angles near total reflection for the determination of the magnetic moment in a self-calibrated manner, in addition to structural parameters, such as layer thickness and interface roughness (in a similar fashion as x-ray reflectometry). Reviews of this technique have been given by Felcher *et al* [302–304], Zabel *et al* [305–307], Majkrzak [308], Fermon *et al* [309] and Bland and Vaz [310, 311].

Of extreme importance to our current understanding of magnetism of ultrathin films has been the contribution given by x-ray magnetic circular dichroism (XMCD) [186, 193, 312–315], which relies on the fact that light absorption in magnetic media depends on the light polarization, right or left, in this particular case. The strength of this technique is that sum rules for the dichroic and absorption signals (based on an atomic model [316, 317]) allow the determination of both orbital and spin components of the magnetization in addition to magnetic anisotropies [318], while doing so with submonolayer sensitivity and element-selectively, by tuning the x-ray energy to the absorption edge of the element under study [319]. While absolute moments are difficult to estimate with an accuracy better than ∼20%, relative variations are fairly accurate [320].

Another key technique employed in the study of magnetic thin films relies on the magnetooptic Kerr effect (MOKE), based on the fact that the state of polarization of light is modified upon reflection from a magnetized medium. Small changes in the polarization of linearly polarized light can routinely be measured very accurately by cross-polarization techniques; in addition, the surface sensitivity of the magneto-optic Kerr effect, limited to within one absorption length of the material, typically ∼20 nm for most metals, makes this technique particularly relevant in thin film magnetism. While absolute moments cannot in general be obtained with this technique, it is a sensitive probe for the magnetization and employed in studies of magnetic dynamics, magnetic phase transitions and in the determination of magnetic anisotropies. A particular advantage of the Kerr effect technique is the compatibility with *in situ* measurements [321]. Reviews of Kerr effect techniques have been given by Bader *et al* [207, 322–324], while other descriptions of this technique include that of Florczac and Dahlberg [325, 326], and Bland [327]; the theoretical formalisms applicable to multilayered magnetic media based on the electromagnetic theory of anisotropic media have been provided by, among others, Sprokel [328], Zak *et al* [329–331] and Višňovský [332–336], while the microscopic mechanisms underlying magneto-optic effects (including XMCD) have been covered by Sokolov [337], Ebert [338] and Collins *et al* [339].

In addition to magnetometry techniques, radio-frequency techniques using ferromagnetic resonance (FMR) [173, 191, 340–342] and Brillouin light scattering (BLS) [343–351] that probe directly the spin-wave spectrum of magnetic materials have played an important role in the accurate determination of magnetic anisotropies, the exchange constant and the g-factor

in thin magnetic films. While FMR probes low energy spin waves, BLS can probe a larger wave vector range, depending on the scattering geometry [173]. Mössbauer spectroscopy, and the related conversion electron Mössbauer spectroscopy (CEMS) (where photoemitted electrons are detected, instead of photons), measure the hyperfine field at the probe nuclei (^{57}Fe) and are a sensitive and powerful technique for probing the magnetic state of the system. CEMS is inherently more surface sensitive, but the ability of implanting the radioactive isotopes in specific locations, such as the interface, also makes Mössbauer spectroscopy particularly local specific [272].

Besides these techniques, an array of other techniques have been employed in the study of thin magnetic films, in particular, magnetic and surface imaging techniques [352–354], including atomic force microscopy (AFM) [355–357], magnetic force microscopy (MFM) [358–360], scanning tunnelling microscopy (STM) [361–366], spin-polarized STM [366–371], scanning Kerr microscopy [372], scanning electron microscopy with polarization analysis (SEMPA) [373–376], photoemission electron microscopy (PEEM) [123, 377–383], Lorentz microscopy [384–386], electron holography [387, 388], scanning Hall probe microscopy [389–392]. The imaging of the surface structure has contributed enormously to our understanding of the correlation between surface morphology and magnetism, in particular for monolayer and submonolayer-thick films [393, 394]. Imaging of magnetic configurations in thin films and small patterned structures have provided invaluable information about the accessible magnetic states either at remanence or during the switching of the magnetization process. This has led to a more detailed understanding of both static and dynamic magnetic processes that take place in magnetic films, but we shall not consider this aspect of thin film magnetism here (probably the most exhaustive review of magnetic domain imaging to date is that by Hubert and Schäfer [227], which also gives brief introductions to many of the techniques mentioned above). Magnetotransport measurements, usually based on the anisotropic magnetoresistance effect [395–397], have the advantage over conventional techniques in that its sensitivity does not decrease with the size of the sample, and is therefore often employed in the study of small systems, for instance to infer the magnetization structure in nanometre sized constrictions [232, 398], and in studies of the magnetoresistance of atomic contacts [399–401]. Reviews on magnetoresistance effects can be found in [167, 395–397]. Spin-resolved photoemission [178, 402–407] has been used to probe the valence/conduction band spin density of states; together with inverse photoemission spectroscopy and tunnelling resonance spectroscopy, these techniques offer a wealth of information that relates directly to the band structure, and as such probes deep into the electronic structure of the material. A fairly comprehensive and excellent review of this subject matter, and of many other aspects of contemporary magnetism, has been recently provided by Stöhr and Siegmann [178]. Volume 3 of Kronmüller and Parkin (ed) [181] is wholly dedicated to state-of-the-art techniques for characterization and sample preparation, and provides a comprehensive compilation of recent developments in this important field.

3. The two-dimensional magnetic phase transition

Critical phenomena refer to points of instability in the phase diagram of a given system. These critical points are classified as first or second order according to whether the transition is discontinuous or continuous, respectively [408]. An example of a first order transition in Co is the hcp to fcc crystalline phase transition with temperature, which occurs approximately at 710 K [409]. First order phase transitions exhibit hysteresis and are associated with a finite change in the internal energy of the system. An example of a second order phase transition in the same system, is the ferromagnetic to paramagnetic phase transition, which occurs at $T_c = 1388 \pm 2$ K [238]. In second order phase transitions, the two phases transform into each other with no energy cost and are therefore characterized by fluctuations between the two phases at the critical point [410].

The continuous character of second order phase transitions allows a close scrutiny of its behaviour close to the critical point, and it turns out that the critical behaviour follows power (*scaling*) laws[6], with exponents whose values fall within a small range of *universal* values that depend only on a small number of parameters, such as dimensionality and number of degrees of freedom of the system [412–415] (although the symmetry of the disordered phase and the interaction range may change the critical behaviour [412, 416–419]). In fact, it appears that the critical behaviour of most systems can be described by two specific microscopic interaction Hamiltonians: (i) the Q-state Potts model, where each spin i can be in one of Q possible discrete orientations ζ_i ($\zeta_i = 1, 2, ..., Q$). If two neighbouring spins have the same orientation, then they contribute an amount $-J$ to the total energy of a configuration, otherwise they contribute nothing:

$$H(d, s) = -J \sum_{\langle ij \rangle} \delta(\zeta_i, \zeta_j), \tag{27}$$

where δ is the Kronecker symbol and $\langle ij \rangle$ indicate that summation is over nearest neighbours. (ii) The n-vector model, characterized by spins capable of taking on a continuum of states:

$$H(d, n) = -J \sum_{\langle ij \rangle} \boldsymbol{S}_i \cdot \boldsymbol{S}_j, \tag{28}$$

where the spin $\boldsymbol{S}_i$ is an n-dimensional unit vector and $\boldsymbol{S}_i$ interacts isotropically with the spin $\boldsymbol{S}_j$ localized on site j [420, 421]. The cases considered here are covered by the n-vector model for $n = 1, 2, 3$: the Ising, XY and Heisenberg models, respectively (the Potts model is equivalent to the n-vector model for $n = 2, 3$) [422][7]. In table 2 we list the theoretical critical exponents for the n-model for $d = 2, 3$ and $n = 1, 2, 3$. For the linear chain of spins there is no

[6] Power laws are usually associated with multiscale phenomena [411].

[7] Near the critical point, the atomic length scale of the system and the type of short-range interactions become inconsequential, and the critical behaviour becomes universal; in particular, the critical behaviour of itinerant systems, such as 3d magnetic systems, are also described by the above localized models.

Table 2. Values of the critical exponents β, γ and ν for selected systems (d is the dimensionality and n the number of degrees of freedom). The three critical exponents are linked through the scaling relation $\gamma = d\nu - 2\beta$. RG—renormalization-group calculations.

System	d	n	β	γ	ν	Method	References
2D Ising	2	1	0.125	1.75	1	Exact	[424]
2D XY system	2	2	0.231[a]	—	—	RG	[431,432]
2D Heisenberg	2	3	—	—	—	Theory[b]	[129]
3D Ising	3	1	0.325	1.241	0.630	RG	[433,434]
3D XY system	3	2	0.345	1.316	0.669	RG	[433,434]
3D Heisenberg	3	3	0.365	1.386	0.705	RG	[433,434]

[a] For finite systems.

[b] Does not exhibit magnetic ordering at temperatures above 0 K.

finite ordering temperature in the thermodynamic limit. In two dimensions, the Ising model ($n = 1$) predicts magnetic ordering at finite temperatures, with a critical exponent of the magnetization of 1/8 [423, 424]. On the other hand, the isotropic XY and Heisenberg 2D systems do not order at finite temperatures in the thermodynamic limit [128, 129, 425, 426]. However, it turns out that the 2D XY system has a peculiar critical behaviour, corresponding to neither order nor disorder, but instead to what is described as quasi-order [427]. The critical behaviour of the 2D XY Hamiltonian was studied in detail by Kosterlitz and Thouless [418, 428, 429], who found that this system does have a critical point with long range correlations but no spontaneous magnetization[8]. This phase transition originates from the unbinding of vortices (corresponding to topological charges, such as current vortices in type II superconductors or magnetic domain walls) above the critical temperature T_{KT}, which are bound in pairs below T_{KT} [430]. In addition, Bramwell and Holdsworth [431, 432] have found, also using the renormalization approach, that finite systems order magnetically, and that the variation of the magnetization near the critical point has a critical exponent of $\approx$0.23. The value of this critical exponent becomes undefined as the size of the specimen extends to infinity, as predicted by the Kosterlitz and Thouless results. Finally, for the 3D case, all Hamiltonian systems order at finite temperatures, with critical exponents for the magnetization of 0.325 (Ising), 0.345 (XY) and 0.365 (Heisenberg) [433–436]. We see therefore that as the number of degrees of freedom or the dimensionality of the system increases, the critical exponent for the magnetization also increases in value (i.e. the onset of the magnetic order just below the critical point becomes steeper). These models correspond, however, to idealizations of real systems, which often exhibit features that break the symmetry of the Hamiltonian, such as magnetic anisotropy and long range magnetic dipolar (and/or exchange) interactions. In general, the effect of magnetic anisotropy is to drive the system away from the critical point in the phase diagram of the corresponding isotropic Hamiltonian to a new critical point with its own universality class of critical exponents. For small anisotropies, such change in the values of the critical exponents can be expected to be small, but may deviate considerably for strongly anisotropic systems [412, 417, 418, 437, 438]. In fact, Bander and Mills [438] have shown using renormalization-group analysis (by extrapolation from a large N spin-component expansion) that, in 2D, the presence of vanishingly small anisotropies with easy axis perpendicular to the film plane results in magnetic order of Ising character at a non-zero temperature (related to the critical temperature of the bulk material). This result is in agreement with Monte Carlo simulations [439] and *ab initio* calculations [264] and seems to reconcile the Mermin and Wagner result with the fact that magnetism is observed in most monolayer-thin magnetic films. For the 2D XY system with in-plane anisotropies, José *et al* [417] have shown that for quartic symmetry (in-plane cubic) anisotropies non-universal critical behaviour may result, while for hexagonal symmetries the critical behaviour is predicted to be identical to the isotropic XY system. Another complication refers to the presence of long range dipolar interactions, which can have a strong influence close to the critical point on spin states whose correlation length extends over the whole of the sample [412, 440, 441]. Part of the discrepancies observed in the critical exponent of the magnetization for real magnetic materials and the value predicted for the 3D Heisenberg model have been attributed to the effect of dipolar interactions [442], and a closer agreement has been obtained when the temperature window used for the fit is not too close to the critical temperature (the value of β tends to be larger the closer the experimental window is to T_c) [440]. For very thin films the dipolar interactions may be expected to be less significant (since the magnetostatic energy scales with the square of the film thickness for in-plane magnetized films), but their influence can still be important [443]. In fact, Yafet *et al* [265] have shown that, within the non-interacting spin-wave approximation, in a 2D lattice of spins coupled by isotropic short-range exchange interactions, the dipolar interactions can induce ferromagnetic order in the system (see also [264]). They also find that for systems with low-spin moment and large exchange coupling J, the effect of the dipolar interactions can be approximated by a small magnetic field (while such approximation is incorrect for systems with a large spin moment).

The universality class can be ascertained by the knowledge of two critical exponents, since relations between critical exponents (*scaling laws*) allow the determination of the other critical exponents [412, 415]. The 2D Ising model describes a 2D lattice of spins interacting only via the exchange interaction with nearest neighbours, where the spins are constrained to lie either up or down along a particular direction and so this corresponds to the case of a ferromagnet with uniaxial

[8] While the 2D Heisenberg system is believed not to have a phase transition, even of the Kosterlitz–Thouless type [418, 428].

anisotropy. The spin–spin correlation length is the maximum distance over which the spin directions are correlated. For instance, if a single spin is in the up direction, the probability of its nearest neighbours also having an up spin is increased which in turn biases the probability of their nearest neighbours having an up spin orientation. In this way a spin fluctuation can propagate over a large area of the lattice in a system with short-range interactions only, and which diverges at $T = T_c$. This means that any two spins however far apart are correlated and the system becomes exquisitely sensitive to small perturbations, e.g. the application of an external magnetic field. Close to the critical temperature, the magnetization M, susceptibility χ and correlation length ξ vary with temperature according to a power law

$$M \sim (T_c - T)^{\beta}, \tag{29}$$

$$\chi \sim (T_c - T)^{-\gamma}, \tag{30}$$

$$\xi \sim (T_c - T)^{-\nu}. \tag{31}$$

The accurate experimental determination of the critical exponents in ultrathin films is difficult: different techniques may give different critical temperatures, depending on the spatial and time resolution (e.g. techniques that probe a large film area may not be able to distinguish the formation of magnetic domains from a non-magnetic state, therefore giving lower estimates of the Curie temperature [444, 445]; superparamagnetism adds another difficulty, since the magnetization of the system may fluctuate faster than the measurement acquisition time while in fact magnetic order exists [281]); the film morphology [96, 446] may complicate the analysis of the experimental data. For instance, when growth proceeds by island growth, each island may have a larger Curie temperature than the equivalent deposited material would have if it were a continuous film [447, 448]; this is thought, in some cases, to be responsible for the observed increase in T_c with thickness in thin films. This point has been made by Gradmann [83], who notes that with increasing film coverage T_c should not change up to the completion of the monolayer if the film growth is in a layer-by-layer mode. This in fact was observed in Fe/W(1 1 0) films grown at elevated temperatures, in contrast to growth at low temperatures (figure 5) [447, 449]. On the other hand, Farle *et al* [448] have argued that such a variation is expected for thicker films, suggesting that one criterion for layer-by-layer growth should be the observation of a variation in T_c as predicted by the theory of size effects (see section 3.2). However, it is found that despite this variation in the Curie temperature, the critical exponent β remains constant within the first few monolayers, indicating perhaps that even these small islands exhibit the same type of critical behaviour as the 1 or 2 ML films [450]. The fact that three parameters need to be determined from one set of data (the critical temperature, amplitude and exponent, which are strongly correlated with each other) adds to the difficulty of determining the critical parameters unambiguously [443, 451, 452] and some schemes have been suggested to minimize this problem [453–456]. Other kinds of difficulties relate to the systems themselves: the choice of the appropriate temperature window for the measurement of the

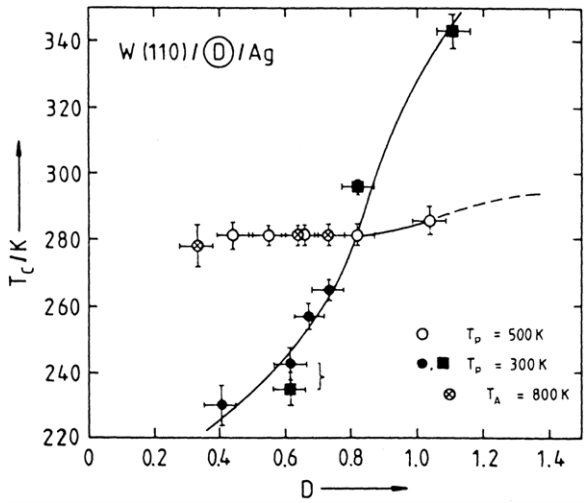

Figure 5. Variation of the Curie temperature T_c versus Fe thickness in monolayers for Ag/Fe(1 1 0)/W(1 1 0) for samples prepared at 500 K (open symbols) and at 300 K (full symbols) [449]. Reprinted with permission from M Przybylski and U Gradmann 1988 *J. Physique Colloques* **49** C8-1705. Copyright (1988) by EDP Sciences.

critical behaviour; the presence of magnetic domains which break up the long range correlations; the sensitivity of the 2D phase transition to the applied magnetic field [264]; the temperature variation of the lattice constant, which may change the value of the critical temperature [440] (the magnetization is usually measured at constant pressure while theory assumes constant volume, see section 5.3); and the presence of finite size effects, which smears the critical transition of the order parameter [451, 452]. As an example, the effect of the finite width in Fe stripes on the critical behaviour of Fe/W(1 1 0) films has been studied in detail by Elmers *et al* [457], where they show experimentally the onset of rounding effects due to the finite size of the sample (and in particular on the change on T_c with terrace size; see also [458]). These become characteristic of the critical point: for the magnetization curve, this is reflected in the presence of a tail that extends beyond the critical temperature [440, 459]. Also, few magnetic systems are sufficiently chemically stable to withstand the necessary thermal cycles, and exposure to residual gases even in *in situ* experiments may lead to changes in the magnetic properties over time due to chemical bonding or surfactant effects [281], as mentioned earlier. This has limited the study of critical phenomena to a small number of systems; Ni and Gd have been preferred due to their low Curie temperature, although other magnetic elements have been studied in the (limited) thickness range where the critical temperature is below the temperature at which the system starts to deteriorate (this can be monitored by checking for hysteresis during the temperature cycles) [460]. On the positive side, the critical transition in low-dimensional systems tend to be less abrupt and extend over a larger temperature range than their 3D counterparts [323].

For magnetic thin films, the most studied critical process is the temperature dependence of the order parameter (magnetization) near the critical point. Unlike β, the value of

T_c is a characteristic of the system (it depends on the strength of the interactions, etc). The value of β has been determined experimentally for several thin film magnetic systems, and a comprehensive list of values drawn from available literature is given in table 3 together with the magnetic anisotropy exhibited by the system (if such information is available), the critical temperature, the temperature interval and the technique employed. Elmers [461] has given a detailed description of the magnetic phase transition in 0–2 ML thick films, with emphasis on Fe/W(1 1 0), Fe/W(1 0 0) and Co/Cu(1 1 1) systems.

It has to be noted that the comparison between the values of the theoretical critical exponents and the experimental values is not without difficulties [445, 450–453]. One of the main concerns refers to the role of size effects on the magnetization curve, which tends to smear the critical transition and to complicate the estimate of the Curie temperature and of β; in addition, the proper choice of the temperature interval is sometimes criticized on the grounds that it often exceeds the temperature range over which one would expect the power law to describe correctly the temperature variation of the magnetization, while for the 2D Ising model the analytical expression of the magnetization is known [424], figure 6 (see, however, [324]). Schilbe *et al* [451, 452] have discussed this problem in some detail to conclude that the agreement between the effective critical exponents measured experimentally and the theoretical values is not fortuitous, but that they are explained by considering the equivalent effective critical exponents calculated as, e.g., $\beta_{\text{eff}} = \partial \log m(t)/\partial \log t$ ($t = 1 - T/T_c$ being the reduced temperature). Their Monte Carlo simulations show that for the temperatures normally accessible experimentally, the critical exponent thus calculated yields values close to the experimental ones and identical to the theoretical values when no size effects are present. Analytical expressions obtained from renormalization-group calculations for the thickness dependent critical exponents also support this view [484].

The 2D Ising model is expected to describe the critical behaviour of thin films with uniaxial magnetic anisotropy [438], with $\beta \approx 1/4$, while thin magnetic films with planar anisotropy are expected to show a 2D XY behaviour with $\beta = 0.23$. This is largely supported by experiment, with some exceptions. The list of critical exponents for the systems quoted in table 3 show that they cluster around three values, one close to 0.125 corresponding to Ising behaviour, another close to the XY-behaviour of 0.23, and still another close to the Heisenberg value of 0.37 for the thicker films. However, based on the expected values for the magnetic anisotropy (and since this is not measured close to the critical value, its extrapolation from room temperature measurements may not reflect the actual anisotropy near T_c—the magnetic anisotropy itself is expect to vanish at T_c, see section 6.2), it is seen that some discrepancies arise. For example, Fe(1 1 0)/Ag(1 1 1) has a small in-plane anisotropy but the β exponent is close to the Ising value; and the same for the V/Ag(1 0 0), although for this system several other experiments have failed to confirm the presence of magnetic order [480–482]. The case of the 1.7 ML Fe/W(1 1 0) studied by Back *et al* [456] also seems to be in disagreement with the expected 2D XY behaviour, but Elmers *et al* [458] have suggested that for this thickness the Fe film consists of double layer islands emerging from the monolayer film which are responsible for a large increase in the magnetic anisotropy, thus resulting in a Ising behaviour instead of what the anisotropy estimate for the monolayer film would at first suggest. The opposite case where a system with perpendicular anisotropy yields a critical exponent close to the XY value is found in one instance for two Co/Cu(1 1 1) samples, but in the same study other samples with identical film thicknesses give a critical exponent close to the Ising value [257]. Bensch *et al* [472] also find a critical exponent β for Fe/GaAs(0 0 1) close to the predicted 2D XY value, even though this system exhibits in-plane uniaxial magnetic anisotropy [326, 486–490] and should therefore be expected to follow an Ising behaviour. A few sets of studies have considered the thickness dependence of the critical exponent and were therefore able to determine the crossover between the two-dimensional Ising critical behaviour to the three-dimensional Heisenberg regime [255–257]. The transition thickness was found to occur at around 7 ML for the Ni/Cu(0 0 1) [256, 257], Ni/Cu(1 1 1) [257], Co_1Ni_9/Cu(0 0 1) [256] and Ni/W(1 1 0) [255] systems (see figure 7). We also note that the critical exponent does not seem to be affected by the large changes in the Curie temperature both with film thickness and growth conditions.

One feature that the data in table 3 allow us to consider is the dependence of the critical temperature on the crystallographic plane, which relates to different lattice coordination numbers. As a general rule, one expects the critical temperature to increase with increasing surface coordination number and the data seem roughly to bear this trend. In fact, keeping in mind the sensitivity of T_c to growth conditions and thickness, we see that layers with identical thickness grown in different crystallographic planes exhibit larger T_c as the plane of the film changes from (1 0 0) to (1 1 0) to (1 1 1). This can be observed for the (bcc) 1.6 ML Fe(1 0 0)/W(1 0 0) and 1.7 ML Fe(1 1 0)/W(1 1 0); for the (fcc) 2 ML Co(1 0 0)/Cu(1 0 0) and the 1.7 ML Co/Cu(1 1 1); for the (fcc) Ni(1 0 0)/Cu(1 0 0) and the Ni(1 1 1)/Cu(1 1 1) [257]. The differences in the Curie temperature for these examples are of the order of 100 K, but variations due to extrinsic effects are difficult to ascertain.

Another aspect refers to the effect on the critical temperature of interactions between the magnetic layer and its substrate or overlayer. The effect of the capping layer on the critical temperature provides a better illustration of this interaction; in table 3 the T_c values reported for 1 ML Fe/W(1 1 0) are systematically lower than the value of T_c when a film of identical thickness is capped with Ag. This may be due to an enhancement of the magnetic moment of Fe when in contact with Ag (see sections 5.2 and 5.5), which may lead to an enhancement of the Curie temperature [491]. More direct evidence is provided by Przybylski and Gradmann [273] who observed that for the Fe/W(1 1 0) monolayer, T_c increases from 210 to 296 K when capped with Ag. Another example is provided by Ni and Co thin films grown on Cu(0 0 1), where the effect of a Cu overlayer is to decrease the Curie temperature of the Ni and Co films [492–495]. This clearly

Table 3. Experimental values of the critical exponent β for thin magnetic transition metal films. $\Delta t = t_2 - t_1$ is the temperature interval used to determine β, with $t_1 = 1 - T_1/T_c$, $t_2 = 1 - T_2/T_c$ and T_1, T_2 are the lower and higher temperature limits, respectively. MA is the magnetic anisotropy; PMA stands for perpendicular magnetic anisotropy; when in-plane uniaxial anisotropy is present, the direction of the easy axis is given. For bulk materials, the absolute (cubic) easy axis direction is given. Acronyms for the experimental techniques: MOKE—magnetooptic Kerr effect; ECS—electron capture spectroscopy; SPLEED—spin-polarized low energy electron diffraction; SPSEE—spin-polarized secondary electron emission spectroscopy; CEMS—conversion electron Mössbauer spectroscopy; BM—bulk magnetometry; TOM—torsion oscillation magnetometry; FMR—ferromagnetic resonance spectroscopy.

System	MA	T_c (K)	β	Δt	Technique	References
5 ML V(1 0 0)/Ag(1 0 0)[a]		475.1	0.128 ± 0.01	0.002–0.4	ECM	[462, 463]
5–11 ML Fe/Cu(1 0 0)[b]	PMA	∼285	0.17 ± 0.03	0.01–0.1	MOKE	[464]
1.2 ML Fe(1 0 0)/Pd(1 0 0)	In-plane[c]	∼400	0.127 ± 0.004	0.002–0.08	MOKE	[465, 466]
2 ML Fe(1 0 0)/Pd(1 0 0)	PMA[c]	613.4	0.125 ± 0.01	0.0–0.03	ECS	[467]
2.5, 2.7 ML Fe/Ag(1 0 0)[j]	PMA	∼500	0.124 ± 0.02	0.001–0.1	MOKE	[450]
1.8 ML Fe(1 1 0)/Ag(1 1 1)	In-plane[d]	338.1	0.139 ± 0.006	0.001–0.16	MOKE	[468]
1.9 ML Fe(1 1 0)/Ag(1 1 1)	In-plane[d]	450.5	0.139 ± 0.004	0.001–0.16	MOKE	[468]
2.0 ML Fe(1 1 0)/Ag(1 1 1)	In-plane[d]	466.4	0.130 ± 0.003	0.001–0.16	MOKE	[468]
2 ML Fe/Au(1 0 0)	In-plane[c]	290.03	0.25 ± 0.01	0.0001–0.2	ECS	[463]
1–2.5 ML Fe/Au(1 0 0)	In-plane[c]	300–500	0.22 ± 0.05	0.001–0.1	SPLEED, SPSEE	[469]
1.6 ML Fe/W(1 0 0)-as grown (300 K)	Cubic, in-plane	188.6	0.210 ± 0.012	0.003–0.1	SPLEED	[470]
1.6 ML Fe/W(1 0 0)-annealed (550 K)	Cubic, in-plane	207.8	0.217 ± 0.005	0.003–0.1	SPLEED	[470]
2.0 ML Fe/W(1 0 0)-as grown (300 K)	Cubic, in-plane	223 ± 1	0.21 ± 0.02	0.02–0.1	SPLEED	[470]
2.0 ML Fe/W(1 0 0)-annealed (550 K)	Cubic, in-plane	217 ± 1	0.23 ± 0.02	0.02–0.1	SPLEED	[470]
1.6 ML Fe/W(1 0 0)		208	0.22 ± 0.03	0.001–0.1	SPLEED	[471]
Ag/2.2 ML Fe/W(1 0 0)		306	0.22 ± 0.01	0.001–0.1	CEMS	[471]
Ag/0.83 ML Fe(1 1 0)/W(1 1 0)	[1 $\bar{1}$ 0]	278 ± 1	0.19 ± 0.02	0.007–0.6	CEMS	[447]
Ag/1.0 ML Fe(1 1 0)/W(1 1 0)	[1 $\bar{1}$ 0]	282 ± 3	0.18 ± 0.01	0.01–0.7	CEMS	[447]
Ag/1.22 ML Fe(1 1 0)/W(1 1 0)	[1 $\bar{1}$ 0]	285 ± 2	0.193 ± 0.005	0.01–0.7	CEMS	[447]
1 ML Fe(1 1 0)/W(1 1 0)	PMA	230	0.123	0.004–0.05	SPLEED	[457]
1.7 ML Fe/W(1 1 0)	<1 K	316.77 ± 0.07	0.13 ± 0.02	$\sim 3 \times 10^{-51}$–0.05	MOKE	[456]
1 ML Fe/W(1 1 0)	[1 $\bar{1}$ 0]	223	0.134 ± 0.003	0[k]–0.04	SPLEED	[458]
20 ML Au/3.4 ML Fe/GaAs(1 0 0)-(2×6)	[1 1 0]	254.8	0.26 ± 0.02	0.003–0.1	MOKE	[472]
Fe (bulk)	⟨1 0 0⟩	1044 ± 2	0.38	—		[238]
Fe (bulk)[e]	⟨1 0 0⟩	1044 ± 2	0.389 ± 0.005	—	BM	[442]
2 ML Co/Cu(1 0 0)	In-plane ⟨1 1 0⟩	325[f]	0.24 ± 0.01	0.04–0.3	MOKE	[473, 474]
1 ML Co/Cu(1 1 1)		434	1/8[g]	0.006–0.6	TOM	[453]
1.0 ML Co/Cu(1 1 1)	In-plane[h]	207	0.15 ± 0.08	n.a.	MOKE	[257]
1.1; 1.3 ML Co/Cu(1 1 1)	In-plane[h]	283; 380	0.28 ± 0.09	n.a.	MOKE	[257]
1.5; 1.7 ML Co/Cu(1 1 1)	In-plane[h]	460; 500	0.15 ± 0.08	n.a.	MOKE	[257]
2.5–7 ML Co_1Ni_9/Cu(0 0 1)		200–500	0.25 ± 0.05	n.a.	MOKE	[256]
7–9 ML Co_1Ni_9/Cu(0 0 1)		500–550	0.38 ± 0.05	n.a.	MOKE	[256]
fcc Co (bulk)	⟨1 1 1⟩	1388 ± 2	0.42	—		[238]
fcc Co (bulk)[e]	⟨1 1 1⟩	1382.15	0.435 ± 0.025		BM	[442]
3–6.2 ML Ni/Cu(0 0 1)	In-plane	210–388	0.23 ± 0.05	0.003–0.5	MOKE	[256, 257]
7.2–16 ML Ni/Cu(0 0 1)	PMA	425–540	0.41 ± 0.04	0.003–0.5	MOKE	[256, 257]
1.6 ML Ni/Cu(1 1 1)		319	0.56 ± 0.05	0.03–0.7	MOKE	[475]
5 ML Ni/Cu(1 1 1)		507	0.50 ± 0.02	0.004–0.3	MOKE	[475]
2.3; 2.8 ML Ni/Cu(1 1 1)		380; 409	0.24 ± 0.07	0.01–0.3	MOKE	[476]
8 ML Ni/Cu(1 1 1)		580	0.32 ± 0.09	0.01–0.3	MOKE	[476]
1.8–7.3 ML Ni(1 1 1)/Cu(1 1 1)	In-plane[h]	197–519	0.30 ± 0.07	n.a.	MOKE	[257]
10.5–16.7 ML Ni(1 1 1)/Cu(1 1 1)	In-plane[h]	559–603	0.49 ± 0.08	n.a.	MOKE	[257]

Table 3. (Continued).

System	MA	T_c (K)	β	Δt	Technique	References
7.5 ML Ni(1 1 1)/W(1 1 0)	$[\bar{1}\,1\,0]^i$	512	0.29 ± 0.06	0.005–0.05	FMR	[477]
12.3 ML Ni(1 1 1)/W(1 1 0)	$[\bar{1}\,1\,0]^i$	583	0.32 ± 0.04	0.003–0.04	FMR	[477]
19.7 ML Ni(1 1 1)/W(1 1 0)	$[\bar{1}\,1\,0]^i$	596	0.34 ± 0.04	0.003–0.04	FMR	[477]
2–4 ML Ni(1 1 1)/W(1 1 0)	$[\bar{1}\,1\,0]^i$	325–435	0.13 ± 0.06	0.01–0.2	FMR	[255]
10–20 ML Ni(1 1 1)/W(1 1 0)	$[\bar{1}\,1\,0]^i$	557–596	0.33 ± 0.04	0.002–0.06	FMR	[255]
Ni (bulk)	⟨1 1 1⟩	627.4 ± 0.3	0.38		—	[238]
Ni (bulk)[e]	⟨1 1 1⟩	627.4	0.378 ± 0.004		BM	[442]
Ni (bulk)	⟨1 1 1⟩	630	0.38 ± 0.04	0.005–0.1	FMR	[477, 478]
Ni (bulk)	⟨1 1 1⟩	635.0 ± 0.5	0.395 ± 0.010		VSM	[479]
300 Å Gd(0001)/W(1 1 0)		290.0 ± 0.1	0.375 ± 0.006	0.003–0.1	MOKE	[454]
Gd (bulk)[e]		293.3 ± 0.1	0.381 ± 0.015		BM	[442]
50 Å Tb(0001)/W(1 1 0)		249.96	0.348 ± 0.01	0.0002–0.02	ECM	[463]

[a] Some reports do not find magnetism in this system [480–482].
[b] Only the top surface layer is ferromagnetic [464].
[c] In-plane magnetization for films grown and measured at room temperature; films grown and measured at 100 K show PMA [483].
[d] The authors fit their data to the Ising expression for the saturation magnetization $M_s = [1 - \sinh^{-4}(2J/k_BT)]^{1/8}$, extracting the critical temperature. Using a power law they obtain, from the remanence magnetization variation with temperature, $T_c = 423$ K and $\beta = 0.265$.
[e] Fe/Ag(1 1 1): in-plane magnetization and weak in-plane surface anisotropy [324].
[f] Estimated from the reported error in temperature. The last data point before T_c seems to lie at $t = 8 \times 10^{-9}$.
[g] M–T is fitted using a Gaussian distribution of T_c's due to size distribution of the Fe stripes.
[h] Values selected by Kaul [442] as most representative for these systems.
[i] For deposition temperatures below 275 K; a drastic drop in T_c is observed for films deposited at higher temperatures even though the critical exponent is not significantly affected. The value of β quoted is from a film deposited at 325 K with $T_c = 250$ K.
[j] Fe/Ag(1 0 0): strong perpendicular surface anisotropy [324].
[k] In-plane anisotropy, but strong PMA surface anisotropy.
[l] From [460].

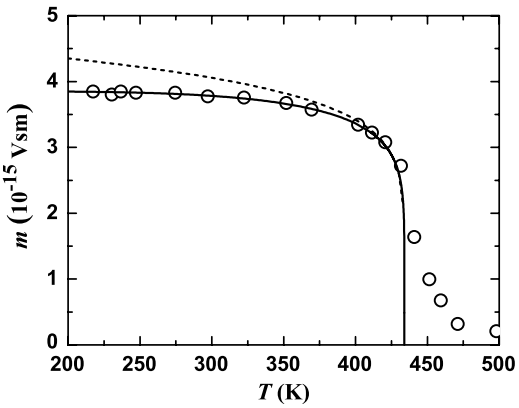

Figure 6. Variation of the saturation magnetic moment of a pseudomorphic Co/Cu(1 1 1) monolayer near the Curie temperature; the solid line is the 2D Ising variation of the magnetization $M(T) = [\sinh^{-4}(0.88137T_c/T)]^{1/8}$ [424, 485], with $T_c = 434$ K determined from data up to 430 K; dashed curve is the power expansion of the magnetization near the critical point, $M(T) = 1.22(1 - T/T_c)^{1/8}$. The tail above the critical temperature is attributed to the effect of structural imperfections of the film. (Adapted from [453].)

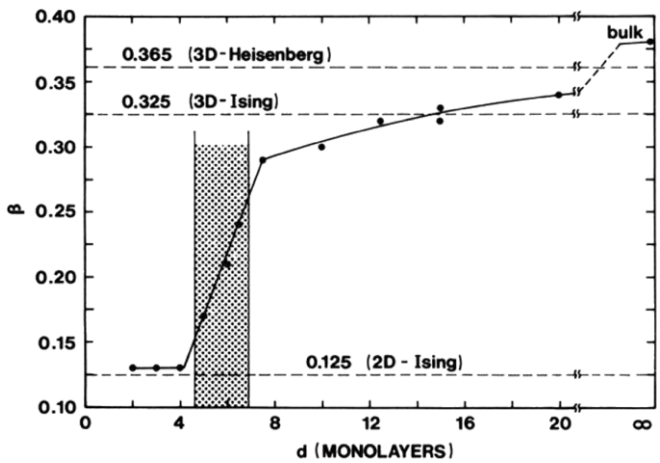

Figure 7. Variation of the critical exponent β for Ni(1 1 1)/W(1 1 0) films as a function of thickness showing the 2D to 3D crossover. The error bars in β are of the order of 0.05 [255]. Reprinted with permission from Y Li and K Baberschke 1992 Dimensional crossover in ultrathin Ni(1 1 1) films on W(1 1 0) *Phys. Rev. Lett.* **68** 1208 Copyright (1992) by the American Physical Society.

indicates that capping layers do generally strongly affect the magnetism of thin films [496]. A more subtle effect of the capping layer has been put in display by the observation of oscillations in the critical temperature of Fe/Cu(0 0 1) [497] and Co/Cu(0 0 1) [495] with increasing Cu capping layer thickness (see figure 8, where the monotonic decrease in the critical temperature with Cu capping layer thickness was subtracted to extract the oscillatory component), results which have been replicated by *ab initio* calculations [498–501]. This effect is similar in nature to the observation of oscillations in the Curie temperature of Ni in 7.3 Å Ni/Au multilayers

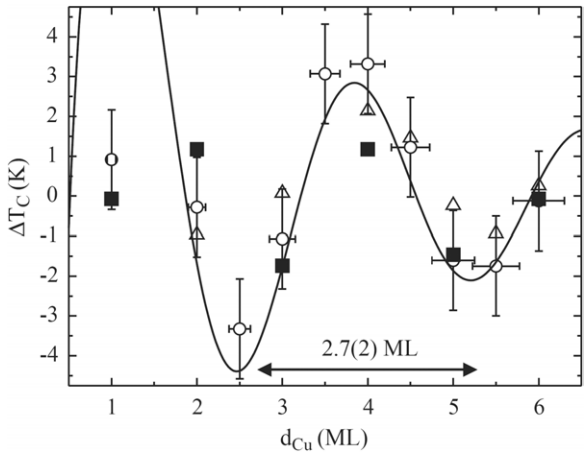

Figure 8. Oscillation of the Curie temperature as a function of the Cu capping layer thickness in Co/Cu(0 0 1) films after subtraction of a monotonic decrease in the critical temperature with Cu capping layer thickness; open symbols are experimental data (circles and triangles are for a 2.2 ML and 2.5 ML Co films, respectively) [495] and solid squares are theoretical values [498]. Reprinted from C Rüdt, A Scherz and K Baberschke 2005 Oscillatory Curie temperature in ultrathin ferromagnets: experimental evidence *J. Magn. Magn. Mater.* **285** 95. Copyright (2005), with permission from Elsevier.

as a function of the Au interlayer thickness by Bayreuther *et al* [502]. This oscillatory behaviour in the strength of the exchange interaction is yet another manifestation of quantum well effects in sandwiched itinerant systems [99, 502]. The effect of exchange coupling between magnetic layers was also addressed by Donath *et al* [503], who determined the variation in T_c of a 4 Å thin Fe film separated by a Ta layer from a thick magnetic film (5 Å Fe/NiFe), for Ta thicknesses of 3, 5 and 7 Å. The critical temperature is observed to increase with increasing coupling strength in a fashion that is consistent with the theory of phase transitions in quasi-2D systems (where a linear variation of the 2D critical temperature with spacer layer thickness is inferred); similar results are obtained for Co/Cu/Ni/Cu(0 0 1) exchange coupled trilayers [504]. Also, the 3D–2D crossover with decreasing interlayer coupling observed in (3 Å Fe/Ag) multilayers, manifested in the change of the *M*–*T* curves from a linear to a $T^{3/2}$ variation [270–272], can be seen in the same light. More recently, a systematic study of the effect of interlayer exchange coupling on the critical temperature of Ni in Co/Ni/Cu/Cu(0 0 1) structures by Scherz *et al* [505,506] demonstrates that the effect of interlayer coupling is that of enhancing spin–spin correlations near the critical temperature of Ni, increasing its critical temperature by 30–70 K for the range of Ni thicknesses studied, from 2–6 ML; the effect of the spin–spin correlations is also manifested in the presence of a tail in the *M*–*T* curve which is absent in the *M*–*T* curve of the Ni film alone, pointing to the importance of enhanced spin fluctuations in 2D coupled films. The results of this study also indicate that the effect of interlayer coupling cannot be described by an effective static exchange field arising from adjacent magnetic layers. Oscillations in the Curie temperature with interlayer spacer thickness have been observed in polycrystalline (7.3 Å Ni/Au) multilayers [502] and in Co/Cu/Ni/Cu(0 0 1) trilayers [505, 507], where T_c is found to oscillate with the same periodicity as that of the RKKY oscillation period of the interlayer coupling. Experimental work on the critical behaviour of Co/Ni bilayers [493, 494, 508, 509] shows that the two components of the system undergo one phase transition at the same critical temperature, which lies in between the values found for a Ni or Co film with the total thickness of the bilayer (a similar result was found for CoNi alloys [257]) [510]. We refer to Farle [191] and Baberschke *et al* [173, 511] for detailed discussions of the effect of interlayer coupling on the critical properties of ferromagnetic layered systems.

An issue which has drawn much interest is the so-called reorientation phase transition, which occurs when the perpendicular magnetic anisotropy is compensated by in-plane anisotropies as the film thickness or temperature is varied. It has been suggested that, at this particular point, the cancellation in anisotropies will drive the system from an Ising to an isotropic *XY* system, which in 2D should be non-magnetic at finite temperatures [512]. Several experiments have been performed motivated by this suggestion [222, 375, 513–515], but the results seem inconclusive due to the difficulty in distinguishing domain formation from the absence of ferromagnetic order. An identical anomaly is found when an applied magnetic field is made to counterbalance exactly the anisotropy field; in such a case, we are confronted with a first order phase transition [247, 516–519], and it is likely that the character of the above mentioned reorientation phase transitions is identical. It is not clear, however, whether these magnetic instabilities do correspond to a *XY* magnetic system (which is expected not to be magnetically ordered at finite temperatures) and some studies do suggest that the system simply breaks into very fine magnetic domains [220, 520–525]. Also puzzling are the results by Elmers *et al* [526] for Fe islands on a 1 ML Fe/W(1 1 0), showing non-magnetic behaviour, even though the system is magnetic for coverages above and below that particular coverage range. This was attributed to frustration of long range order perhaps due to indirect interactions of electronic origin between double layer islands, mediated by the surrounding monolayer and its W substrate.

3.1. The thickness dependent phase transition

The thickness dependent phase transition at fixed temperature has been much less studied than the corresponding temperature dependent transition. In the case of a percolation transition at a critical thickness t_c exchange interactions develop in the film due to the physical (site) percolation of islands. Such a transition is difficult to observe for two reasons. Firstly, the true geometric percolation transition applies strictly at 0 K only; secondly, the combination of STM and magnetic measurements are required *in situ*. The percolation problem can be described by the Potts model introduced earlier, and its critical behaviour is independent of the type of percolation processes involved (site or bond) and the type of lattice [435, 527]. For a 2D square lattice with site percolation the thickness at which percolation occurs corresponds to a coverage of 59%, i.e. an incomplete film of thickness 1 ML. Near the percolation critical point, the magnetic order

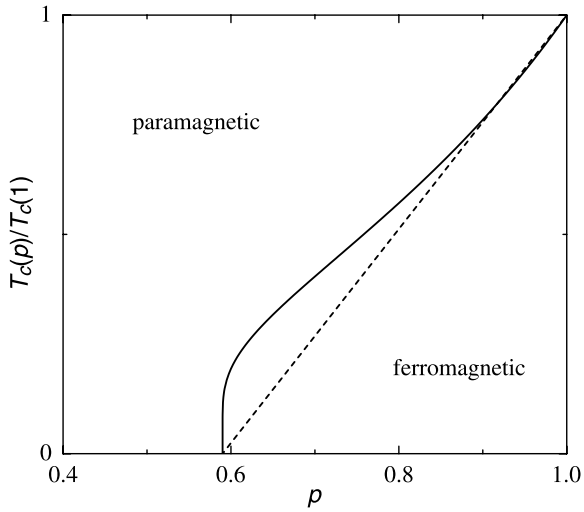

Figure 9. Schematic phase diagram of 2D Ising (solid line) and XY (dashed line) site-percolating ferromagnet (with $p_c = 0.59$). $T_c(p)/T_c(1)$ is the normalized critical temperature and p is the percolation concentration.

parameters are described by scaling relations in terms of the concentration or coverage p:

$$P_\infty \sim (p_c - p)^{\beta_p}, \tag{32}$$

$$\chi \sim (p_c - p)^{-\gamma_p}, \tag{33}$$

$$\xi \sim (p_c - p)^{-\nu_p}, \tag{34}$$

where p_c is the critical coverage, P_∞ is the number of sites (or bounds) in the finite cluster; in diluted magnetic systems it is proportional to the magnetization at $T = 0$ [435]. The percolation critical exponents for two dimensions are $\beta_p = 0.139$, $\gamma_p = 2.43$ and $\nu_p = 1.33$ [435, 527]. The critical percolation coverage for site processes in 2D lattices with first neighbour interactions is, for a honeycomb lattice (3 nearest neighbours) $p_c = 0.70$, for a square lattice (4 nearest neighbours) $p_c = 0.59$ and for a triangular lattice (6 nearest neighbours) $p_c = 0.5$ [435].

The problem at hand closely resembles the problem of dilute magnetism, where the onset of ferromagnetic order is induced by a percolative mechanism. Here, two critical processes occur simultaneously, the onset of ferromagnetic order and the geometrical percolative process, with their associated and distinct critical behaviour. Figure 9 shows a schematic phase diagram of 2D Ising and XY magnetic systems; at $T = 0$ we have the pure percolation process at $p = p_c$, with critical exponents given by (32)–(34). At finite temperatures, thermal as well as configurational processes occur; referring to figure 9, we can distinguish three situations: (i) for $p < p_c$, as the temperature is lowered, the correlation length increases but remains finite; (ii) at $p = p_c$ the correlation length increases with decreasing temperature, and diverges at $T = 0$; (iii) for $p > p_c$, the correlation length diverges when the temperatures approaches $T_c(p)$ from above and there is a magnetic phase transition with critical exponents that may differ from the $p = 1$ values, and which may be denoted by their dependence on p, that is $\beta(p)$, $\nu(p)$, etc. Close to p_c one may write

$$T_c(p) \sim (p - p_c)^{1/\phi}; \tag{35}$$

for Heisenberg and XY magnets in 3D; for Ising systems (2D, 3D), a similar expression applies but with the temperature replaced by a relevant *thermal variable* $\tilde{T} = \exp\{2J/k_B T\}$ [435]:

$$\tilde{T}_c(p) \sim (p - p_c)^{1/\phi_t}, \tag{36}$$

where the ϕ are called *crossover* exponents. Stinchcombe [435] used the following argument in relating the crossover exponents to the critical exponents at the percolation transition: considering a crossover induced by adding to the Hamiltonian of the system an extra term g, say caused by randomness in our case. For $g = 0$, the correlation length behaves as in (31), $\xi \sim (T - T_c)^{-\nu}$; when $g \neq 0$, homogeneity relationships imply that the correlation length scales as [412]

$$\xi \sim (T - T_c)^{-\nu} f(g(T - T_c)^{-\phi_g}), \tag{37}$$

where $f(T)$ is some homogeneous function and ϕ_g is the crossover exponent for the field g; therefore, the field g influences ξ when $g(T - T_c)^{-\phi_g} \sim 1$, that is, within a temperature range defined by

$$(T - T_c)_g \sim g^{1/\phi_g} \tag{38}$$

and near the percolation threshold, $g \sim p - p_c$,

$$\xi \sim (T - T_c)^{-\nu_t} \sim (p - p_c)^{-\nu_t/\phi_g} \equiv (p - p_c)^{-\nu_p}, \tag{39}$$

where now ν_t is the critical exponent at $p - p_c$. It follows then that

$$\phi_g = \nu_t/\nu_p. \tag{40}$$

For the Ising case, the expression for the correlation length is identical if one uses the relevant thermal variable introduced above and the relation between the exponents remains unchanged. The values for ν_t corresponding to the ordered system at $p = p_c$ are in general different from the ν values for $p = 1$. For the Ising systems it is found that $\nu_t = \nu_p$ ($= 4/3$ for the 2D Ising system) while calculations yield $\nu_t = 0.92$ for the 2D XY model ($\nu_p = 4/3$, as mentioned before) [435]. We have therefore

$$\phi_{2D}^{I} = 1 \quad (\text{2D Ising}), \tag{41}$$

$$\phi_{2D}^{XY} = 0.69 \quad (\text{2D XY}), \tag{42}$$

so that a different crossover behaviour is expected for the 2D Ising and XY systems (see figure 9).

Bensch *et al* [472] have studied the critical behaviour of thin Fe/GaAs films and in particular the onset of ferromagnetism as a function of temperature and film thickness. The critical exponent for the magnetization, $\beta = 0.26$, is close to the 2D XY value of 0.23. The variation of T_c with Fe film coverage is ascribed to a percolation process and, assuming film thickness proportional to the film coverage, results in $\phi_{exp}^{Fe} = 0.837(3)$, which the authors relate to a 2D XY behaviour, see figure 10. The critical thickness for

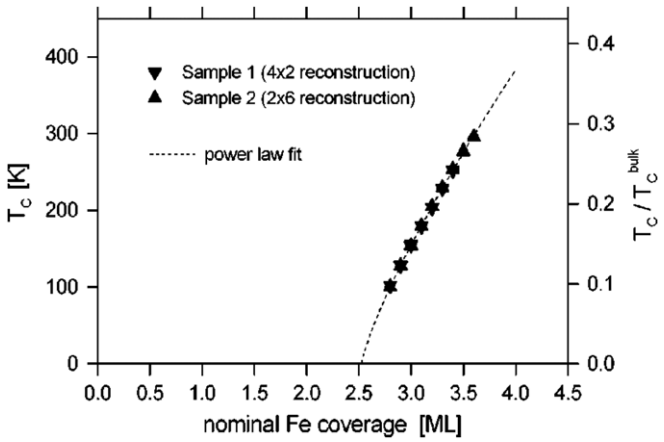

Figure 10. Variation of the critical temperature with nominal Fe film coverage, deposited on GaAs(0 0 1) substrates with surface reconstructions as labelled in the figure. Dotted line is a power law fit to the experimental data [472]. Reused with permission from F Bensch, G Garreau, R Moosbühler, G Bayreuther and E Beaurepaire 2001 *J. Appl. Phys.* **89** 7133. Copyright 2001, American Institute of Physics.

percolation was estimated at $t_p^{Fe} = 2.5$ ML. As mentioned above, it is known that the Fe/GaAs(0 0 1) develops strong in-plane uniaxial magnetic anisotropies at small Fe thicknesses [326,486–490], which would be expected to render this system more akin to a 2D Ising system; also, strictly speaking, relations (41)–(42) are only valid at $p = p_c$.

Assuming proportionality between coverage and thickness the magnetization develops with thickness according to a power law of the form

$$M \sim (1 - t/t_c)^{\beta_p}. \tag{43}$$

In practice perfect layer-by-layer growth is almost never observed. For Co/Cu(0 0 1) for example, some second layer growth occurs before the completion of the first layer [528–530] (depending on evaporation rate, see section 6.4). Thus islands form and it is the critical concentration of islands rather than the concentration of atoms which determines the percolation transition. The thickness of the islands can significantly exceed 1 ML but due to the strong exchange coupling across the film each island acts as a single 'giant spin'. On the other hand, until recently, it was supposed that a single monolayer would always constitute a 2D ferromagnetic system. This distinction provides an important example of how the nanoscale morphology of the film holds the key to understanding the magnetic properties of monolayer-thick films.

In thin magnetic layers, this geometry-related phase transition corresponds to the physical coalescence of the magnetic islands, or clusters, in the initial states of growth before a continuous magnetic film is formed. Accordingly, for small film thickness, the behaviour of the magnetic susceptibility measured at 0 K may be divided into four regimes: (i) in the initial stages the magnetic islands have not developed long range order and are non-magnetic: the magnetic susceptibility is therefore very small. (ii) At a later stage, the islands may be large enough to exhibit ferromagnetism, and at the transition thickness (which may exceed 1 ML if growth does not occur layer-by-layer), the susceptibility becomes very large. If this happens before physical percolation (for instance, if the growth mode is granular and the islands form sufficiently large 3D magnetic particles) then the behaviour of the magnetic susceptibility should be characteristic of the ferromagnetic phase transition. This has been identified in 1–3 ML Co/Cu(0 0 1) films, where magnetic order is observed before island percolation; at the critical coverage the Curie temperature increases abruptly by more than 100 K, perhaps indicative of a dimensional crossover [531]. (iii) If, however, magnetic order does not set in before physical percolation, and magnetic order appears as a consequence of the setting in of long range spin correlations, then the magnetic susceptibility should be characteristic of a (site) percolation transition. (iv) Another possible regime corresponds to the case where percolation occurs without ferromagnetic ordering; while this situation could occur in principle, in practice most continuous monolayer-thick magnetic films have been found to develop magnetic order, which is attributed to the presence of magnetic anisotropies, as discussed in the previous section. At finite temperatures, there is the added complication that before coalescence the islands may be superparamagnetic, and the system exhibits a magnetic susceptibility higher than that of the non-magnetic system, but still very small; the sudden increase in size that occurs upon island percolation suddenly drives the system into a stable ferromagnetic phase, with a divergence in the magnetic susceptibility at the transition film coverage. The critical coverage at which ferromagnetic order sets in will vary with the temperature, but the critical behaviour of the percolation process is expected to remain the same as at 0 K.

In table 4 we list results from the published literature. We see that the value for the critical exponent γ_p determined experimentally for all the systems studied is very close to the expected theoretical value ($\gamma_p = 2.43$), even though one may expect the growth modes to be considerably different for the Co/Cu(0 0 1), Co/Cu(1 1 0) or Fe/InAs(0 0 1) systems. This may be intuitively expected, since the mechanism for percolation is identical in all cases. The values for the critical percolation threshold do not correspond to an effective coverage, since islands more than one monolayer in thickness are probably formed before full coverage, and in the case of the Fe/InAs one cannot exclude yet the possibility of reaction at the interface and reduced moment in the first Fe atomic layers [532–534] (see section 5.5). In figure 11 we show the variation of the magnetic susceptibility for Co/Cu(1 1 0) as a function of Co thickness and STM images depicting the evolution of the Co islands with increasing film thickness, showing that even after deposition of a thickness equivalent to four monolayers, the Cu(1 1 0) substrate is not fully covered yet [535]. Other reports have addressed the percolation nature of the onset of magnetism in thin films; Elmers *et al* [457] were able to determine the percolation threshold for Fe grown on W(1 1 0) at room temperature, where the film grows by nucleation and island growth, at a coverage of 0.6 (measured at temperatures down to 115 K), very close to the value predicted

Table 4. Experimental values for the critical coverage t_c and the critical susceptibility exponent γ_p in ferromagnetic films (T_m is the measurement temperature).

System	t_c (ML)	γ_p	T_m (K)	References
Co/Cu(0 0 1)	1.3 ± 0.3	2.40 ± 0.07	300	[536]
Co/Cu(1 1 0)	4.6 ± 1.2	2.39 ± 0.08	300	[535, 537]
Fe/W(1 1 0)	0.59 ± 0.01	—	115–300	[457]
Fe/InAs(0 0 1)	3.5 ± 0.3	2.21 ± 0.25	300	[538]
Fe/GaAs(0 0 1)	2.5	—	100–300	[472]

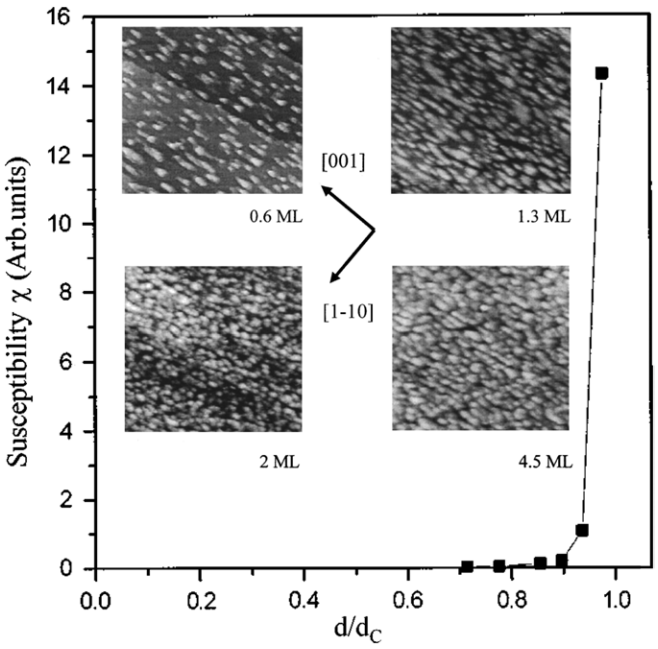

Figure 11. Variation of the magnetic susceptibility for Co/Cu(1 1 0) as a function of Co thickness (normalized to the percolation thickness, $d_c = 4.6 \pm 1.2$ ML) and STM images depicting the evolution of the Co islands with increasing film thickness [535]. Reprinted with permission from S Hope, M Tselepi and E Gu, T M Parker and J A C Bland 1999 Two-dimensional percolation phase transition in ultrathin Co/Cu(1 1 0) *J. Appl. Phys.* **85** 6094. Copyright 1999, American Institute of Physics.

for a 2D square lattice; this fits well with the STM images they present, where for a coverage of 0.53 (just below percolation) each island is seen to have roughly four close neighbours. As discussed before, Bensch *et al* [472] report on Fe films grown on GaAs(0 0 1) for two Ga rich surface reconstructions, (4×2) and (2×6), and relate the onset of magnetism in this system to a percolation process which is insensitive to the surface reconstruction (figure 10).

3.2. Finite size effects

In the previous section we mentioned that in real systems the critical transition is often smeared due to the finite size of the sample as reflected, for instance, in a tail above T_c in the M–T plots or in shifts in the maximum of the response functions of the system [262, 539–542]. This effect can be readily understood as a result of the sensitivity of the long ranged correlation length near the critical point to the system boundaries. The physical boundaries effectively act as a cut-off length to the correlation length. One expects, therefore, a strong dependence of the critical phase transition as one, or more, of its dimensions is reduced, one important example of which is the large change in the critical temperature with varying film thickness observed in the systems listed in table 3. This variation of the critical temperature with size is discussed next in more detail.

A simple argument based on the mean field theory approximation can be used to estimate the variation in T_c due to the change in the mean coordination number with increasing film thickness [543]. Mean field theory predicts that $k_B T_c = z J_0$, where z is the lattice coordination number and J_0 is the exchange integral; for a system with free surfaces, the mean coordination number is then reduced from 6 (for a simple cubic lattice) to $6 - 2/N$, where N is the number of layers, hence, expressing the variation of T_c in the form

$$\epsilon_N \equiv 1 - T_c(N)/T_c = c_0 N^{-\lambda}, \tag{44}$$

this simple argument predicts $\lambda = 1$. However, scaling arguments and series expansions suggest $\lambda = 1/\nu$, where ν is the critical exponent for the correlation length [262, 541, 544, 545], and experimental values yielding $\lambda = 1.33 \pm 0.13$ for relatively thick (20–1300 nm) Ni films seem to support this result, since $1/\nu = 1.43$ for bulk Ni [261]. For very thin films, it is found that (44) is not followed accurately [256, 257] and instead the alternative expression has been suggested [543, 546]

$$\epsilon_N = c_0 (N - N')^{-\lambda}, \tag{45}$$

where N' is a fixed 'shift' parameter which is introduced to provide some account of higher order N-dependent corrections (this expression is asymptotically equivalent to (44)). One may expect these expressions to be valid for films that grow in a layer-by-layer mode, or for films above full coverage, where other factors that also affect the onset of ferromagnetic order, including percolation and lateral size effects, do not contribute to variations in the critical temperature.

In 2D systems, finite size effects are also present when the lateral size is constrained, such as in islands or stripes. For instance, before physical percolation during film growth, the Curie temperature may increase as the island size increases, as described for the thickness dependent phase transition in section 3.1. One example of the effect of the finite width in Fe stripes on the critical behaviour of Fe/W(1 1 0) films is given by Elmers *et al* [457], where they show experimentally the onset of rounding effects due to the finite size of the sample (and in particular on the change on T_c with terrace size; see also [458]). Another example of size effects in 2D corresponds to the critical behaviour of the XY system, which develops a

Table 5. Experimental values for the shift exponent reported in the literature.

System	N (ML)	C_0	N'	λ	References
Fe(1 1 0)/W(1 1 0)[a]	0–1	0.018	0	1.03 ± 0.14	[457]
Co/Cu(1 0 0)	1–2	1.82	1.0	1.02[b]	[257]
Co_1Ni_9/Cu(1 0 0)	2–9	6.16	0.9 ± 0.2	1.39 ± 0.08[b]	[256, 257]
Co_1Ni_3/Cu(1 0 0)	2–5	7.31	1.0	1.49[b]	[256, 257]
Co_1Ni_1/Cu(1 0 0)	2–4	4.58	1.0	1.66[b]	[256, 257]
Ni/Cu(1 0 0)	3–16	4.62	1.1 ± 0.2	1.25 ± 0.07[b]	[256, 257]
Ni/Cu(1 0 0)	4–26	5.2 ± 4	0	1.42[b]	[552]
Ni/Cu(1 1 1)	1–8	2.1	0	1.48 ± 0.20[b]	[475]
Ni/Cu(1 1 1)[c]	1–10	2.30	0	1.44 ± 0.20[b]	[476]
Ni/Cu(1 1 1)[c]	1–10	1.03	0.6	1.01[b]	[476]
Ni/Cu(1 1 1)[c]	1–10	1.08	−0.4	1.04	[476]
Ni(1 1 1)/W(1 1 0)	7.5–20	2.8 ± 1.0	0	1.42 ± 0.30	[477]
Ni(1 1 1)/W(1 1 0)	5–20	2.7 ± 0.5	0	1.4 ± 0.1	[255]
Ni(1 1 1)/Re(0 0 0 1)	4–50	1.9 ± 0.5	0	1.27 ± 0.20	[553]
Ni (poly)	20–1300 nm	11.1 ± 0.6	0	1.33 ± 0.13	[261]
Ni (poly)	5–35 nm	8.9	0	1.30 ± 0.10[b]	[475, 554]
Ni/Ag (poly)	2.5–13.5	1.58 ± 0.03	0	0.63 ± 0.02	[502]
$Ni_{48}Fe_{52}$(1 1 1)/Cu(1 1 1)	0.9	0.594	0.58		[132]
Gd(0 0 0 1)/W(1 1 0)	5–100	7.0	0	1.59	[448]

[a] T_c for 1 ML was used to normalize $T_c(\theta)$ where θ is the film coverage.
[b] The expression used to fit the data was $T_c/T_c(N) - 1 = C_0(N - N')^{-\lambda}$.
[c] The values quoted for this system correspond to alternative fits to the same data.

non-zero critical temperature as a consequence of the cut-off in spin excitations imposed by the lateral boundaries [431, 432].

In table 5 we list the results of experimental studies where the shift exponent was estimated. We see that the value of λ spreads over a wide range, from the mean field value $\lambda = 1$ and $\lambda = 1/\nu_{2D} = 1$ to that given by $\lambda = 1/\nu_{3D} = 1.59$. For instance, in studies where the thickness was limited to a single monolayer (Fe/W(1 1 0) [457] and Co/Cu(1 0 0) [257]), the value of the shift exponent is close to that expected to a 2D Ising system. For several of the Ni systems, the value is close to $1/\nu = 1.43$ quoted above for bulk Ni. It is possible that the spread in values is due to differences in film morphology and growth conditions (see sections 6.4 and 6.5).

A 2D to 3D dimensionality crossover has also been observed in the character of the magnetization dependence with temperature at low temperatures, appearing as deviations from the bulk $T^{3/2}$ Bloch's behaviour to a quadratic temperature dependence at an intermediate temperature range, which has been attributed to the presence of an energy gap in the spin-wave spectrum introduced by the limited number of degrees of freedom in the finite system (see however [547]); such effects have been observed in small ferromagnetic clusters [548–550] (where size effects are found to lead to a deviation from the usual $T^{3/2}$ Bloch's law to a T^2 dependence) and in thin Fe/Au/GaAs(0 0 1) films in the thickness range from 20 to 200 nm [551], where a cut off in the spin wave spectrum in the direction perpendicular to the film plane leads to a deviation from a T^2 to a $T^{3/2}$ dependence on the temperature.

In short, the thickness variation of the critical temperature in thin magnetic films can be attributed to three factors: (i) reduction in the relative weight of the low coordination surface atoms as the thickness of the film increases, leading to an increase in T_c towards the bulk value; (ii) variation of T_c due to percolation, as discussed in the previous section; (iii) variation of T_c due to the presence of islands with effective thickness larger than the single monolayer, yielding an 'average' critical temperature higher than the expected for a monolayer film, or from the expected percolation variation [447, 448]. It is clear from the above discussion that the change in T_c depends strongly on the growth mode of the magnetic film; the percolation process yields a strong variation of T_c until full film coverage is achieved, and one may expect this process to dominate in films that grow in 3D (island) mode. Above full coverage, such variation should cease, but the second process described above may still lead to a strong variation of the critical temperature if islands with varying thicknesses develop. Finally, for thicker films, the third process may come into play, at least while the thickness is comparable to, or smaller than, the lateral correlation length.

4. The exchange constant

A very important parameter in magnetism, and in micromagnetics in particular, is the exchange constant A, introduced in section 1.1, which is a measure of the interaction strength between adjacent spins due to the exchange interaction. A is a phenomenological parameter that reflects the magnetic symmetry of the system (in the general case a tensor, but a scalar for cubic systems) [555–557], which can be related to the microscopic parameters of the system, for instance, the exchange integral in the Heisenberg model of ferromagnetism. The current interest in magnetic thin films and nanostructures makes it essential to understand how the exchange constant is modified by reduced dimensions and by the presence of interfaces. However, the exchange constant is a very difficult parameter to access experimentally and has been estimated for thin magnetic films in a limited number of studies, such that one must rely on values determined for the bulk. For this reason, we first review the experimental results for

the bulk before considering the determination of the exchange constant in thin films. The estimate of the exchange constant is done by indirect means which involve the assumption of specific models for magnetic order. Since the exchange constant relates to the energy cost involved in non-collinear orientations of neighbouring spins, its experimental estimate requires the determination of energies associated with non-uniform spin states. Three general processes can be envisaged for such an estimate [556,557], (i) the crude process of relating the exchange energy to the thermal excitation energy which destroys the magnetic order in the system (it is crude because the vanishing of magnetic order in magnetic systems arises not just from Stoner excitations but also from the excitation of short spin-waves, which are not taken into account in the mean field theory expressions); (ii) from the measurement of spin-waves or quantities that can be related to them (for instance, variation of the magnetization at low temperatures), i.e. from the value of the stiffness constant D. (iii) From measurements of the domain wall energy or domain wall width.

The expression for the exchange energy, as used in micromagnetics, assumes a continuum approximation and also that the angle of the magnetization changes slowly over atomic distances. With these conditions, it is straightforward to relate the exchange constant with the exchange integral of the Heisenberg exchange energy, $-J_{ij}\boldsymbol{S}_i \cdot \boldsymbol{S}_j$, for cubic (Bravais) lattices, assuming nearest neighbour interactions [556,557]:

$$A = \frac{1}{2g\mu_B} M_0(2JSa^2), \tag{46}$$

where g is the Landé factor, M_0 the saturation magnetization at 0 K and a the lattice constant. For the ideal hcp lattice this expression is still valid if $2a^2$ is replaced by $4a^2$, where a is the basal lattice constant. The quantity in parentheses, $D = 2JSa^2$, is the spin wave stiffness constant, which is given more generally by [558]

$$D = \tfrac{1}{3} z\rho^2 J^{(2)} S \tag{47}$$

to take into account interactions beyond first neighbours, where ρ is the nearest neighbour distance, z is the coordination number (number of nearest neighbours) and

$$J^{(n)} = \frac{1}{z}\sum_r J(\boldsymbol{r})(r/\rho)^n \tag{48}$$

is the nth spatial moment of the exchange integral [559].

From the mean field theory of ferromagnetism, the relation between J and T_c is [560,561]

$$k_B T_c = \tfrac{2}{3} zS(S+1)\sum_r J(\boldsymbol{r}) = \tfrac{2}{3} zS(S+1)J^{(0)}. \tag{49}$$

For nearest neighbour interactions, $J^{(0)} = J$, and the estimate of the exchange integral would be, in principle, identical to that determined from the stiffness constant, D. However, not only the exchange interaction extends beyond first neighbours in 3d metals [562], but also the mean field theory neglects the effects of correlations (i.e. spin waves) close to the critical point, and is therefore likely to underestimate the value of J from T_c.

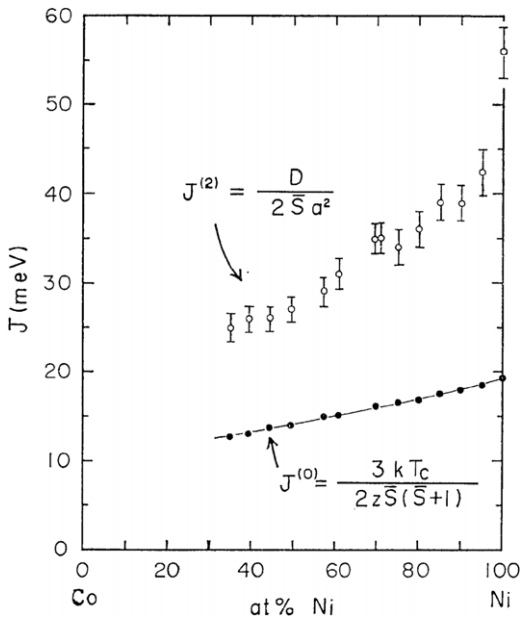

Figure 12. Variation of $J^{(0)}$ and $J^{(2)}$ for bulk Ni–Co alloys determined from analysis of M–T curves estimated from bulk magnetometry. Reproduced from [563] with permission from the Physical Society of Japan.

As an example, figure 12 shows the variation of $J^{(0)}$ and $J^{(2)}$ for Ni–Co alloys determined experimentally by Maeda *et al* [559, 563] from the analysis of M–T curves, demonstrating the large discrepancy between these two quantities. The S factor in (46) and (47) and the $S(S+1)$ factor in (49) are reminders that these expressions are derived for an Heisenberg ferromagnet, but an extension to itinerant systems may be obtained by replacing gS and $g\sqrt{S(S+1)}$ by the number of effective Bohr magnetons. We have, in particular, $A = M_0 D/(2g\mu_B)$. Estimates for D and A determined from the critical temperature using the mean field expression for the exchange integral are given in table 6 for bulk Fe, Co, Ni and $Ni_{80}Fe_{20}$, where we have used bulk values for the Landé, or g-factor. The g-factor is the constant of proportionality (in the general case, a tensor) between the magnetic moment and the total angular momentum (in units of $\hbar$):

$$\boldsymbol{\mu} = -g\mu_B \boldsymbol{J}, \tag{50}$$

and for the free electron is equal to 2 to within $\alpha/2\pi$, where $\alpha = e^2/\hbar c \approx 1/137$ is the fine-structure constant ($g = 2.002\,319\,304\,3622$). For itinerant electrons in 3d transition ferromagnets, the g-factor is slightly larger than 2 [238, 564], reflecting the fact that the magnetic moment still has an orbital momentum component in addition to the spin momentum. While the orbital contribution is small (of the order of 4–10%), due to the near quenching of the orbital momentum, this contribution is responsible for the magnetocrystalline anisotropy, via the spin–orbit coupling. An important expression due to Kittel [565] relates the orbital and spin components of the magnetic moment, μ_L and μ_S, respectively:

$$(g-2)/2 = \mu_L/\mu_S. \tag{51}$$

Table 6. Estimates of the exchange constant A from the Curie temperature (the value for the Curie temperature of hcp Co is an estimate [568]). z is the coordination number (number of nearest neighbours). Values of M_0, g and T_c for Fe, hcp Co and Ni are taken from [238]. RT values for a are from [569] except where noted.

System	a (Å)	z	M_0 (emu cm^{-3})	g	T_c (K)	D (meV Å^2)	A (μerg cm^{-1})
bcc Fe	2.866	8	1752	2.091	1044	260	1.88
fcc Co	3.544[a]	12	1471[b]	2.08[c]	1388	380	2.32
hcp Co	2.501	12	1446	2.187	1360	570	3.25
fcc Ni	3.524	12	510	2.183	627	610	1.23
fcc $Ni_{80}Fe_{20}$	3.540[d]	12	878[d]	2.163[e]	843[f]	470	1.64

[a] [571].
[b] Estimated from the mass magnetization [574].
[c] From [572].
[d] [570].
[e] From [559].
[f] From [573].

This expression suggests that for ultrathin films the large modifications in the orbital moment due to the break in symmetry at the interface may lead to sizeable changes in the g-factor. More extended discussions of the g-factor in 3d ferromagnetic thin films have been given by Farle [191], Baberschke [566] and by Pelzl *et al* [567].

A more accurate estimate of the exchange constant is obtained from the experimental value of the stiffness constant. In the above expressions J and D are the values at 0 K, but these expressions remain formally valid above 0 K if the temperature dependence is incorporated in J and D [558]. In particular,

$$A(T) = M_s(T, 0)D(T)/(2g\mu_B), \tag{52}$$

where $M_s(T, 0)$ is the saturation magnetization at temperature T and zero applied field. The effect of thermal excitations is to add a term that depends on the temperature as a result of magnons (occupation of excited energy levels and Boson statistics) and multi-magnon scattering processes [558]. The detailed temperature variation depends on the particular model: in the localized model the leading term for D is in $T^{5/2}$ while in the itinerant model an additional term in T^2 is expected due to interactions between spin waves and excited electrons [558, 575, 576].

The bulk stiffness constant has been determined using a number of experimental techniques, including spin wave resonance measurements on thin films, neutron scattering, Brillouin light scattering and bulk magnetometry. The spin wave resonance data were mostly collected until the early 1960s and are regarded as superseded by values obtained from neutron scattering measurements [238] (Döring [556] provides a table of exchange constants obtained by spin wave resonance measurements for Ni, Fe and Co, while Maeda *et al* [559] gives an overview for NiFe alloys). To date, the neutron data are still considered to provide the best estimates available.

Neutron scattering measurements have the ability to probe the magnon dispersion relation up to fairly large wave vector values up to the Brillouin zone boundary, and therefore to yield reliable numbers for the stiffness constant. The triple axis neutron spectrometry technique allows the measurement of the dispersion relation along different crystallographic directions, and where such detailed studies were conducted, they show (to within the degree of accuracy available in such experiments) that the spin wave energy dispersion is identical along the three principal crystal directions for the cubic phases of Fe [577–580], Ni [581, 582] and Co [583]. We list in table 7 the values for D obtained by neutron scattering experiments in 3d metals and alloys; overall, the values reported for the stiffness constant vary considerably, and this dispersion could be related to a certain extent to the sample quality (for example, large single crystal bcc Fe samples are difficult to make since other crystalline phases are known to coexist in bulk crystals; the bcc phase can be stabilized by the addition of small amounts of Si, but the magnetic properties are slightly modified [579, 580, 584]). Most neutron scattering measurements date from the 1960s, on bulk samples, and correspond to the coefficient affecting the quadratic dependence of the energy dispersion with magnon wave vector. A thorough discussion of these data in relation to the stiffness constant in Fe, Co and Ni is given by Wohlfarth [238], who tabulates values for the stiffness constant for Fe, Co and Ni from the neutron data; Winsor [585] also provides a useful overview of neutron scattering results on itinerant magnets up to the same date. Here we mention briefly the more recent measurements only.

Mitchell and Paul [586] determined the dispersion curve for Ni at low temperatures, where Stoner excitations have been frozen out; they find $D = 400 \pm 20$ meV Å^2 at 1.2 K, and no significant changes up to room temperature. They suggest that their data, corresponding to the excitation of low energy spin waves, are to be preferred to previous neutron data obtained by excitation of high energy spin waves, where a deviation from the quadratic dispersion relation results in overestimated stiffness constants. Measurements of the stiffness constant by neutron inelastic scattering by Hennion *et al* [587] of fcc NiFe alloys of varying compositions suggest that the stiffness constant varies little with temperature up to room temperature; they found that D decreases steadily with increasing Fe content, from a value of approximately 500 meV Å^2 for pure Ni down to 150 meV Å^2 for $Ni_{40}Fe_{60}$ (see figure 13).

The spin wave excitation spectrum of bulk bcc Fe (stabilized with 12% Si) was determined by Yethiraj *et al* [590] at relatively high wave vector, and they obtain a spin-wave dispersion that is in good agreement with previous neutron scattering results, with $D = 230$ meV Å^2. In this study, the authors confirm early observations relating to the intensity loss

Table 7. Experimental values of the stiffness constant from neutron scattering measurements. TA—triple axis neutron spectrometry; DM—neutron diffraction method; SAS—small angle neutron scattering; NIS—neutron inelastic scattering.

Material	*t*	*D* (meV Å^2)	*T* (K)	Method	References
bcc Fe	Bulk	330 ± 10	0[a]	TA	[577]
bcc Fe	Bulk	310 ± 10	0[a]	SAS	[596]
bcc Fe	Bulk	310 ± 15	10	NIS	[597]
bcc Fe	Bulk	310	RT	SAS	[598]
bcc Fe	Bulk	280 ± 10	295	TA	[577]
bcc Fe	Bulk	280 ± 10	295	TA	[577]
bcc Fe	Bulk	250 ± 20	300	SAS	[596]
bcc Fe	Bulk	280 ± 10[b]	295	TA	[578]
bcc Fe	Bulk	280	RT	TA	[579]
bcc Fe	Bulk	280	295	TA	[580]
bcc Fe(12% Si)	Bulk	230	RT	INS	[590]
fcc $Co_{92}Fe_8$	Bulk	370 ± 40	295	TA	[583]
fcc $Co_{92}Fe_8$	Bulk	384	RT	NIS	[599]
fcc $Co_{92}Fe_8$	Bulk	380	295	DM	[577]
hcp Co	Bulk	490 ± 20	295	DM	[600]
hcp Co	Bulk	437 ± 20	295	NIS	[601]
hcp Co	Bulk	510[b]	295	TA	[577]
hcp Co	Bulk	478 ± 10[c]	295	NIS	[591]
hcp Co	Bulk	410 ± 12[d]	295	NIS	[591]
nc-hcp Co	Bulk	500 ± 20	295	SAS	[592, 593]
fcc $Ni_{95}Co_5$	Bulk	485 ± 15	4	TA	[602]
fcc $Ni_{95}Co_5$	Bulk	430 ± 15	293	TA	[602]
fcc $Ni_{90}Co_{10}$	Bulk	550 ± 40	RT	TA	[603]
fcc $Ni_{83}Co_{17}$	Bulk	536 ± 30	RT	TA	[603]
fcc $Ni_{79}Co_{21}$	Bulk	560 ± 30	RT	TA	[603]
fcc $Ni_{79}Co_{21}$	Bulk	380 ± 15	293	TA	[602]
fcc $Ni_{69}Co_{31}$	Bulk	565 ± 30	RT	TA	[603]
fcc $Ni_{50}Co_{50}$	Bulk	590 ± 50	RT	TA	[603]
fcc $Ni_{50}Co_{50}$	Bulk	375 ± 15	293	TA	[602]
fcc Ni	Bulk	400 ± 20	1.5	TA	[586]
fcc Ni	Bulk	555	4.2	TA	[594]
fcc Ni	Bulk	525 ± 15	4.2	NIS	[587]
nc-fcc Ni	Bulk	450 ± 10	5	SAS	[592, 593]
p-fcc Ni	Bulk	415 ± 30	0[a]	SAS	[604]
fcc Ni	Bulk	400 ± 16	97	TA	[586]
fcc Ni	Bulk	340	295	DM	[605]
fcc Ni	Bulk	391	RT	NIS	[599]
fcc Ni	Bulk	370	295	DM	[577]
fcc Ni	Bulk	400	295	TA	[595]
fcc Ni	Bulk	430	RT	TA	[581]
fcc Ni[e]	Bulk	455[b]	295	TA	[606]
fcc Ni	Bulk	460 ± 15	293	NIS	[587]
fcc Ni	Bulk	446 ± 29	RT	TA	[588]
fcc Ni	Bulk	461 ± 30	RT	TA	[603]
fcc Ni	Bulk	433	RT	TA	[582]
fcc Ni	Bulk	400 ± 12	295	TA	[586]
nc-fcc Ni	Bulk	370 ± 20	295	SAS	[592, 593]
cw-fcc Ni	Bulk	400 ± 10	295	SAS	[592, 593]
fcc Ni	Bulk	280	635	TA	[594]
fcc $Ni_{95}Fe_5$	Bulk	400 ± 10	4.2	NIS	[587]
fcc $Ni_{95}Fe_5$	Bulk	365 ± 10	293	NIS	[587]
fcc $Ni_{95}Fe_5$	Bulk	423 ± 39	RT	TA	[588]
fcc $Ni_{86}Fe_{14}$	Bulk	349 ± 15	RT	TA	[588]
p-fcc $Ni_{80}Fe_{20}$	Bulk	415 ± 30	0[a]	SAS	[604]
fcc $Ni_{80}Fe_{20}$	Bulk	250 ± 15	295	DM	[589]
fcc $Ni_{75}Fe_{25}$	Bulk	349 ± 18	RT	TA	[588]
fcc $Ni_{66}Fe_{34}$	Bulk	309 ± 10	85	TA	[588]
fcc $Ni_{66}Fe_{34}$	Bulk	292 ± 27	RT	TA	[588]
fcc $Ni_{60}Fe_{40}$	Bulk	250 ± 10	4.2	NIS	[587]
fcc $Ni_{60}Fe_{40}$	Bulk	235 ± 10	293	NIS	[587]
p-fcc $Ni_{50}Fe_{50}$	Bulk	240 ± 20	0[a]	SAS	[604]

Table 7. (Continued).

Material	t	D (meV Å^2)	T (K)	Method	References
fcc $Ni_{50}Fe_{50}$	Bulk	245 ± 15	295	DM	[577, 589]
fcc $Ni_{50}Fe_{50}$	Bulk	200 ± 5	4.2	NIS	[587]
fcc $Ni_{50}Fe_{50}$	Bulk	200 ± 5	293	NIS	[587]
fcc $Ni_{50}Fe_{50}$	Bulk	191 ± 10	RT	TA	[588]
fcc $Ni_{40}Fe_{60}$	Bulk	160 ± 5	4.2	NIS	[587]
fcc $Ni_{40}Fe_{60}$	Bulk	140 ± 5	293	NIS	[587]
fcc $Ni_{39}Fe_{61}$	Bulk	121 ± 23	RT	TA	[588]
fcc $Ni_{32}Fe_{68}$	Bulk	70 ± 5	293	NIS	[587]

[a] Extrapolated value.
[b] Value tabulated in [238] for D at RT.
[c] In the basal plane.
[d] From graphical data given in [594] and [595].
[e] Along the c direction.

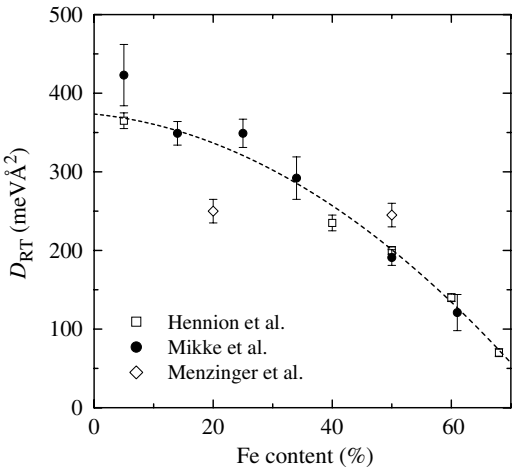

Figure 13. Room temperature variation of the exchange stiffness of NiFe alloys as determined from neutron scattering. Data collected from Hennion *et al* [587], Mikke *et al* [588] and Menzinger *et al* [589]. The dashed line is a guide to the eye.

at high magnon energies, which is associated with excitations into the Stoner continuum, a hallmark of an itinerant magnetic system.

Perring *et al* [591] measured the spin-wave dispersion curve of hcp Co along the basal plane as well as along the c direction for momentum transfer values that extend almost up to the Brillouin zone boundary. Their results show that the dispersion relation is quadratic over this extended q range (suggesting that higher order correction terms in q, which are included in some studies, may not be warranted, as noted also by Windsor [585]). The value for D along the c direction, 478 ± 10 meV Å^2, is slightly larger than that along the basal plane, 410 ± 12 meV Å^2.

More recent measurements of the exchange constant have been performed using small angle neutron scattering (SANS) on polycrystalline Ni and Co samples [592, 593]. The method used relies on the presence of non-uniform magnetic anisotropy in such samples due to the presence of randomly oriented crystallites. The samples consist of high purity electrodeposited Ni and Co films (100–300 μm thick) and a cold-worked Ni polycrystalline reference sample. The exchange constant values obtained for these samples are identical to that of other polycrystalline or single crystal samples (see table 7 for the corresponding stiffness constant values). These authors suggest that with this technique they are able to probe the nanocrystalline exchange constant and conclude that A is not affected by the presence of grain boundaries and that no anisotropies in the exchange energy are present (as expected for this high symmetry crystals) but it is not clear why these results should be distinct from other measurements of polycrystalline samples, since this technique does not probe locally the magnetic properties of the nanocrystals, but give instead an average over many such crystallites.

Another method for extracting the stiffness constant is from the Bloch $T^{3/2}$ law for the temperature variation of the magnetization at low temperatures, since the coefficient affecting the $T^{3/2}$ term is related to the stiffness constant; for an Heisenberg ferromagnet [556, 558],

$$\frac{M(T) - M_0}{M_0} = \frac{g\mu_B \zeta(3/2)}{M_0} \left(\frac{k_B T}{4\pi D}\right)^{3/2} + O(T^{5/2}), \quad (53)$$

where M_0 is the saturation magnetization at $T = 0$ K, D is the zero temperature stiffness constant and $\zeta(3/2) = 2.612\,375\,349$. However, this method of determining the stiffness constant is less simple than the previous expression would suggest; since most magnetization measurements involve the application of a magnetic field, the energy gap in the spin wave energy dispersion needs to be taken into account (this results in a slightly more complex version of (53)); also, the variation of $M(T, H)$ includes terms other than due to spin waves, such as defects, inclusions, anisotropy distribution in polycrystalline samples, and magnetic susceptibility, each with different H dependences [607]; in addition, the temperature dependence may arise both from $M(T)$ and $D(T)$, with powers that may depend on the specific origin of the magnetic order (while at the same time being difficult to distinguish between those different terms, to within the experimental error bars) [607, 608]. All these factors make the analysis of the magnetization data subject to serious difficulties. Values for the (0 K) stiffness constant determined with this method are listed in table 8. It is seen that where a simple estimate of D from the $a_{3/2}$ coefficient is made, the agreement with the neutron data (at low temperatures or extrapolated to $T = 0$)

Table 8. Experimental values of the stiffness constant determined from the temperature coefficient $a_{3/2}$ of the Bloch $T^{3/2}$ law. This method estimates D extrapolated to $T = 0$. MF—magnetic flux measurement; BM—bulk magnetometry; NMR—nuclear magnetic resonance spectroscopy; VSM—vibrating sample magnetometry.

Material	t	$a_{3/2}$ (10^{-6} K$^{-3/2}$)	D (meV Å^2)	Method	References
bcc Fe	Bulk	3.1 ± 0.2	304 ± 13	MF	[611]
bcc Fe[a]	Bulk	—	310 ± 10[b]	BM	[607]
p-bcc Fe	Powder	2.94 ± 0.06	316 ± 5	NMR	[576, 612]
bcc Fe	Bulk	3.4 ± 0.3	286 ± 17	BM	[609, 613]
bcc Fe	Bulk	3.61 ± 0.07	274 ± 4	BM	[610]
hcp Co	Powder	3.3	344	NMR	[614]
hcp Co	Bulk	∼1.5	∼580	BM	[609]
p-fcc $Ni_{35}Co_{65}$	Bulk	3.2 ± 0.3	390 ± 20	BM	[563]
p-fcc $Ni_{40}Co_{60}$	Bulk	3.3 ± 0.3	390 ± 20	BM	[563]
p-fcc $Ni_{50}Co_{50}$	Bulk	3.8 ± 0.3	380 ± 20	BM	[563]
p-fcc $Ni_{61}Co_{39}$	Bulk	4.4 ± 0.5	380 ± 20	BM	[563]
p-fcc $Ni_{70}Co_{30}$	Bulk	4.9 ± 0.4	380 ± 20	BM	[563]
p-fcc $Ni_{81}Co_{19}$	Bulk	6.3 ± 0.7	340 ± 20	BM	[563]
p-fcc $Ni_{90}Co_{10}$	Bulk	7.9 ± 0.7	330 ± 20	BM	[563]
p-fcc $Ni_{96}Co_4$	Bulk	8.7 ± 0.5	320 ± 20	BM	[563]
fcc Cu/$Ni_{84}Co_{16}$/Cu/Si(0 0 1)	165 nm	—	403 ± 40	SQUID	[615]
fcc Cu/$Ni_{50}Co_{50}$/Cu/Si(0 0 1)	175 nm	—	541 ± 60	SQUID	[615]
fcc Ni	Bulk	6.0 ± 1.2	450 ± 60	VSM	[616]
fcc Ni	Bulk	7.5 ± 0.2	397 ± 7	MF	[611]
fcc Ni	Bulk	7.8 ± 1.1	378 ± 35	VSM	[617]
p-fcc Ni	∼2 μm	7.56	400	BM	[559]
fcc Ni	Bulk	—	362 ± 1[b]	BM	[606]
fcc Ni	Bulk	—	472 ± 16[c]	BM	[606]
p-fcc Ni	Bulk	7.6 ± 0.7	390 ± 25	BM	[563]
p-fcc ^{61}Ni	Bulk	—	398 ± 4	NMR	[576, 608]
fcc Ni	Bulk	6.6 ± 0.6	422 ± 25	BM	[609, 613]
fcc Ni	Bulk	6.84	413	BM	[610]
fcc Cu/Ni/Cu/Si(0 0 1)	220 nm	—	450 ± 55	SQUID	[615]
fcc $Ni_{79}Fe_{21}$	Bulk	7.6 ± 0.1	288 ± 3	MF	[618]

[a] Value of D corresponds to an average over several samples, including polycrystalline and single crystal specimens; the value for D was found to be identical in all instances.
[b] D in (53) was assumed to have an additional T^2 term.
[c] In addition to a T^2 term in D, a T^2 term for $M(T)$ in (53) was also assumed.

is poor; the values for Fe determined by Pauthenet [609, 610] from the $a_{3/2}$ coefficient are smaller than the neutron values (∼310 meV Å^2 at $T = 0$ K), while those obtained from a more detailed studies which consider a T^2 term in $D(T)$ yield values that are very close to the neutron results [607, 611] (this point is made by Aldred and Froehle [607], who consider several T dependences in $D(T)$ and $M(T)$). The case of Ni is complicated by the relatively small exchange splitting ($\Delta \sim$ 300 meV [178]), which makes Stoner excitations as important as the thermal excitation of spin waves at temperatures close to RT, making high order temperature corrections to $D(T)$ and $M(T)$ necessary in order to obtain meaningful values for the $a_{3/2}$ coefficient [608, 611]. If the value ∼540 meV Å^2 is taken for D_0 from the neutron measurements, then one may say that the values for D_0 obtained from the $a_{3/2}$ coefficient are slightly underestimated, but other values for D_0 from neutron measurements could be cited to suggest a better agreement with the values listed in table 8 for Ni.

More recently, some attempts have been made to measure the stiffness constant in thin films. A systematic study of the exchange constant of bcc Fe/GaAs(0 0 1) and bcc Fe/GaAs(0 1 1) deposited at 150 °C as a function of film thickness (2–117 nm) using Brillouin light scattering has been reported by Hicken *et al* [249]; the exchange constant can be accurately determined only if at least one volume spin wave mode is observed, which correspond in this case to films with thicknesses above 14 nm, and these are the values listed in table 9. Within this thickness range, a significant reduction in the stiffness constant with decreasing thickness is observed; in particular, the stiffness constant for the 117 nm film, $D = 260$ meV Å^2, is found to be very close to the bulk value determined from neutron scattering measurements.

Several studies have focused on the experimental determination of the stiffness constant of Co. Karanikas *et al* [619] used BLS to determine the stiffness constant of a 375 Å bcc Co/GaAs(0 0 1) film, $D = 340 \pm 40$ meV Å^2, suggesting that their results are compatible with a localized model of ferromagnetism from comparison with the stiffness constant of hcp Co. However, they compare their result with those of bulk samples, while an identical BLS study by Vernon *et al* [620]

Table 9. Experimental values of the stiffness constant for thin films (t is the film thickness). BLS—Brillouin light scattering spectroscopy. SP-EELS—spin-polarized electron energy loss spectroscopy. FMR—ferromagnetic resonance. SWR—spin wave resonance.

Material	Phase	t	D (meV Å^2)	T (K)	Method	References
Fe/GaAs(0 0 1)	bcc	117 nm	260	RT	BLS	[249]
Fe/GaAs(0 0 1)	bcc	52 nm	300	RT	BLS	[249]
Fe/GaAs(0 0 1)	bcc	44 nm	170	RT	BLS	[249]
Fe/GaAs(0 0 1)	bcc	14 nm	160	RT	BLS	[249]
Fe/1 ML Co/Cu(0 0 1)	fcc	3 ML	154	RT?	SP-EELS	[624, 626]
Co/Al_2O_3	p-hcp	100 nm	340 ± 75	RT	BLS	[620]
Co(0 0 0 1)	hcp	100 nm	435 ± 35	RT	BLS	[572]
Cr/Co(1 0 1 0)/Cr(2 1 1)/MgO(1 1 0)	hcp	50 nm	460 ± 70	RT	BLS	[621]
Co	p-hcp	30 nm	436 ± 44	RT	BLS	[633]
Co	p-hcp	60 nm	520.5	RT	BLS	[634]
Co(0 0 0 1)/W(1 1 0)	hcp	8 ML	370 ± 25	RT?	SP-EELS	[625]
Co/GaAs(0 0 1)	bcc	37.5 nm	340 ± 40	RT	BLS	[619]
Co(1 0 0)	bcc	21.6 nm	428 ± 22	RT	BLS	[572]
Co(1 1 0)	bcc	20.2 nm	430 ± 22	RT	BLS	[572]
Co/Cu(0 0 1)	fcc	8 ML	390 ± 25[a]	RT?	SP-EELS	[623]
Co/Cu(0 0 1)	fcc	2.5, 5 ML	390 ± 25[a]	RT?	SP-EELS	[624]
Au/Co/C(0 0 1)	fcc	131.2 nm	250 ± 30	RT	FMR	[635]
Co(1 0 0)	fcc	105 nm	466 ± 16	RT	BLS	[572]
Co(1 1 0)	fcc	115 nm	466 ± 16	RT	BLS	[572]
$Cu/Ni_{84}Co_{16}/Cu/Si(0\,0\,1)$	fcc	165 nm	379	RT	SWR	[615]
$Cu/Ni_{50}Co_{50}/Cu/Si(0\,0\,1)$	fcc	175 nm	379	RT	SWR	[615]
Cu/Ni/Cu/Si(0 0 1)	fcc	220 nm	392	RT	SWR	[615]

[a] Assuming $a = a^{Cu}$.

yield a very similar value for a 1000 Å hcp Co film, $D = 340 \pm 75$ meV Å^2. In fact, in a later study by Liu *et al* [572], a comparison between the exchange stiffness of the hcp, bcc and fcc phases of Co suggest no significant differences in the experimental values, $D \approx 435$ meV Å^2, and the authors conclude that the itinerant picture of magnetism describes their findings better. The BLS study of Grimsditch *et al* [621] on b-axis oriented 50 nm hcp Co(1 0 1 0)/Cr(2 1 1)/MgO(1 1 0) yielded a stiffness constant $D = 460 \pm 70$ meV Å^2, a value which is slightly larger than those reported in the previous BLS studies; these authors suggest that one source of this discrepancy may originate from pinning effects, which modify the location of the surface antinodes of the standing spin waves thereby changing their effective wavelength; since in BLS the spin wave frequencies depend on Dq^2, this leads to a decrease in the value extracted for D. The effect of surface anisotropies on the determination of the stiffness constant by spin wave resonance has been addressed by Talagata *et al* [615], who find that the stiffness constant values determined by this technique are reduced compared with estimates from bulk magnetometry; these results suggest that standing waves in resonance experiments are more influenced by surfaces than travelling spin waves in the bulk magnetometry measurements of the same films.

Spin-polarized electron energy loss spectroscopy (SP-EELS) has been shown recently to provide a surface sensitive tool for measuring spin excitations from magnetic surfaces, capable of probing wave vectors across the Brillouin zone [622]. SP-EELS measurements of fcc Co/Cu(0 0 1) films, 2.5, 5 and 8 ML thick have been reported by Vollmer *et al* [623,624], who estimated the value of the exchange integral by fitting the magnon dispersion data using a localized Heisenberg Hamiltonian, obtaining $JS = 15$ meV for all Co thicknesses. From this value, and taking the in-plane lattice constant of Co the same as the Cu substrate due to lattice matching in this thickness range, one estimates the stiffness constant as $D = 390 \pm 25$ meV Å^2. Measurements of 8 ML hcp Co(0 0 0 1)/W(1 1 0) by the same group [625] yielded a value of JS identical to that of fcc Co, to within the error bars, a result in agreement with the BLS results of Liu *et al* [572]; from the value of JS one estimates a stiffness constant value of 370 ± 25 meV Å^2, which is indeed close to the value for fcc Co, to within the accuracy of the measurements. A plot of these data is shown in figure 14 for the 8 ML fcc and hcp Co. SP-EELS measurements on 3 ML fcc Fe/1 ML Co/Cu(0 0 1) structure did not follow a dispersion relation like that of Co, but required the assumption of an enhanced exchange coupling at the surface, twice that of the bulk layers [624, 626]. From the value of $JS = 5.8$ meV Å^2 we estimate a stiffness constant $D \sim 154$ meV Å^2.

An alternative method of estimating the exchange constant is from the experimental determination of the domain wall energy and domain wall width. This method has been applied often to amorphous materials with uniaxial anisotropies, for which the expressions for the Bloch domain wall width and energy are simple [557], but some results have been obtained for ferromagnetic transition metals. For instance, Hemenger and Wiek [627] have used this method to estimate the exchange energy constant of Ni films (20 nm thick) as 0.46×10^{-6} erg cm^{-1} using Lorentz microscopy. More recently, estimates of the exchange constant of monolayer-thin bcc Fe/W(1 1 0) stripes have been obtained from measurements of

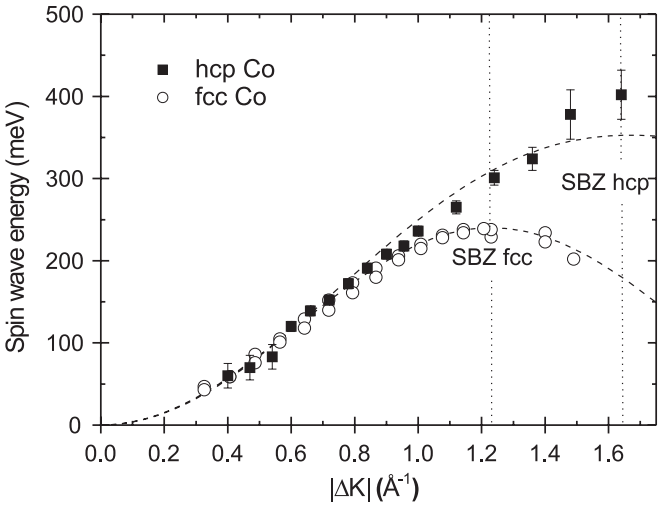

Figure 14. Magnon dispersion curves for 8 ML fcc Co (empty circles) and for 8 ML hcp Co (filled squares) as obtained from SP-EELS. Dashed lines are the acoustic magnon mode calculated using a nearest-neighbour Heisenberg model, while dotted lines denote the surface Brillouin zone for the two crystals [625]. Reprinted with permission from M Etzkorn, P S A Kumar, W Tang, Y Zhang and J Kirschner 2005 High-wave-vector spin waves on W(1 1 0) *Phys. Rev.* B **72** 184420. Copyright (2005) by the American Physical Society.

the domain wall width and wall energy [628–630]. Such two-dimensional Fe wires have a very strong uniaxial anisotropy along the direction perpendicular to the wire axis (due to the Fe/W(1 1 0) lattice mismatch), and are observed to form magnetic domains along the direction along the wire length [628–630]. For a 1 ML Fe film the wall width was determined as 0.6 ± 0.2 nm from SP-STM images taken at 14 K, while the wall energy was determined from susceptibility measurements above the film Curie temperature; the exchange constant is estimated by the product of these two quantities as $(0.4 \pm 0.2) \times 10^{-6}$ erg cm^{-1} [628, 629]. The validity of expressions based in a continuum model for such small wall widths, and the assumption of independence of A on temperature, are debatable. Such sharp domain walls for the monolayer wire are energetically more favourable than extended domain walls since for such thicknesses the exchange and anisotropy energies dominate over the magnetostatic energy [631]. For 2 ML Fe/W(1 1 0) stripes, the exchange constant has been determined from measurements of the profile of 360° walls as a function of applied field using SP-STM at 14 K [630]. The value obtained was 1.82×10^{-6} erg cm^{-1}, almost an order of magnitude larger than for the 1 ML Fe stripes. Although suggestive of a reduced exchange constant for the 'one-dimension' like system, there is the possibility that micromagnetics may be reaching its limit of validity in these systems. In general, one expects that, in comparison with bulk materials, atomically thin narrow nanowires may present new and exciting properties, such as effects due to quantum confinement and strongly modified electronic properties [632].

We finish our survey of the exchange constant in ferromagnetic transition metals with a brief overview of theoretical estimates for the exchange constant. This is a difficult problem since it requires the *ab initio* calculation of excited states of the system and approximative schemes need to be implemented in order to tackle the numerical problem; usually, one starts by solving the ground state problem to obtain the low excitation energy spectrum and then proceed by incorporating additional methods to obtain the finite temperature properties; one complication is the long-range character of the RKKY magnetic interaction in metallic systems which adds to the complexity and this factor has been argued to be underestimated in some studies [636, 637]. Detailed descriptions of finite temperature magnetism from an *ab initio* perspective have been given in the excellent accounts of Staunton [69], Kübler [77, 638] and Bihlmayer [76], which also include extended discussions of the magnon spectra of the 3d ferromagnets. In view of the complications inherent in these calculations, we do not attempt a very exhaustive review of the work published on this problem.

Liechtenstein *et al* [562, 639] have calculated values for the exchange interaction parameters for Fe and Ni within the local spin-density approach, and provide estimates for the stiffness constant and Curie temperatures (see table 10); they suggest that interactions from the larger distances become negligible due to the oscillating character of the RKKY interactions (a point also made by Antropov *et al* [640, 641], who realize that the value for the stiffness constant is closer to the experimental values if exchange between the three nearest neighbours only is taken into account; also Spišák and Hafner [642] suggest that the value of the stiffness constant rapidly converges with the interaction distance) but this has been disputed by more recent theoretical work that suggests the need to calculate the stiffness constant over longer distances [623]. Finite temperature calculations of the magnetic properties of Fe, Co and Ni using a simplified model for itinerant magnets combined with Monte Carlo simulations were reported by Rosengaard and Johnsson [643]. The results for the stiffness constants (at 0 K) and Curie temperatures are listed in table 10 and the results are in relatively good agreement with experimental values. Pajda *et al* [636] have calculated the spin wave stiffness constant and Curie temperatures of Fe, fcc Co and Ni using the non-relativistic spin-polarized Green function technique within the tight binding muffin-tin orbital method. They neglect Stoner excitations in calculating the excitation spectrum, which is a good approximation for ferromagnets with large exchange splitting, but not for Ni [644]. The Curie temperatures they obtain (using the Green function random phase approximation) is 950, 1311 and 350 K for Fe, Co and Ni respectively, while the respective experimental values are 1044, 1388, 627 K [238]; while the agreement for Fe and Co is good indeed, that of Ni is underestimated by almost a factor of 2. The obtained values for the stiffness constant are given in table 10, and while the values for Fe and Co are close to the experimental values, the value for Ni is grossly overestimated; this again is attributed to the neglect of Stoner excitations. Another study by Halilov *et al* [645, 646], yielding similar results, uses the spin-density functional theory to calculate the magnon spectra of Fe, Co and Ni and the respective Curie temperatures, but they do not provide values for the stiffness constants. In another study by Brown *et al* [647], also using the local density functional

Table 10. Theory values of the stiffness constant reported in the literature. LSD—local spin-density approximation; TB—tight binding approximation; RPA—random phase approximation; TB-LMTO—tight binding linear muffin-tin orbital approximation; LMTO+MC—linear muffin-tin orbital approximation and Monte Carlo; ASW—augmented spherical wave approximation; DLM-MFT—magnetic force theorem using disordered local moment reference states; FM-MFT—magnetic force theorem using ferromagnetic reference states; FBT—fluctuating band theory; GF—Green's function.

Material	t	D (meV Å^2)	T_t (K)	Method	References
bcc Fe	Bulk	560	1051	FBT+GF	[656]
bcc Fe	Bulk	294	1200	LSD	[639]
bcc Fe	Bulk	313	1260	TB	[657]
bcc Fe	Bulk	423	1078	LSD	[562]
bcc Fe(1 0 0)	1 ML	210	—	RPA	[658]
bcc Fe	Bulk	214	—	LSD	[659]
bcc Fe	Bulk	—	1037	LSD	[645, 646]
bcc Fe	Bulk	247	1060	LMTO+MC	[643]
bcc Fe	Bulk	280	1050	LSD	[660]
bcc Fe	Bulk	135	—	LSD	[647]
bcc Fe	Bulk	355	—	ASW	[638]
bcc Fe	Bulk	250 ± 7	950	TB-LMTO	[636]
bcc (1 1 0) Fe [1 0 0]	1 ML	382	—	RPA	[655]
bcc (1 1 0) Fe [0 1 $\bar{1}$]	1 ML	192	—	RPA	[655]
bcc Fe/W(1 1 0) [1 0 0]	1 ML	400	—	RPA	[655]
bcc Fe/W(1 1 0) [0 1 $\bar{1}$]	1 ML	107	—	RPA	[655]
bcc Fe	Bulk	187	1053	LSD	[661]
bcc Fe	Bulk	313	1190	DLM-MFT	[648]
bcc Fe	Bulk	322	550	FM-MFT	[648]
hcp Co	Bulk	620	—	RPA	[662]
hcp Co	Bulk	712	—	LDA	[572]
fcc Co	Bulk	360	—	LSD	[659]
fcc Co	Bulk	808	—	LDA	[572]
fcc Co	Bulk	—	1250	LSD	[645, 646]
fcc Co	Bulk	502	1080	LMTO+MC	[643]
fcc Co	Bulk	610	1500	LSD	[660]
fcc Co	Bulk	255	—	LSD	[647]
fcc Co	Bulk	535	—	ASW	[638]
fcc Co	Bulk	663 ± 6	1311	TB-LMTO	[636]
fcc Co/Cu(0 0 1)	8 ML	510	—	RPA	[650]
fcc Co/Cu(0 0 1)	8 ML	238.7	—	RPA	[651]
fcc Co	Bulk	520	1350	DLM-MFT	[648]
fcc Co	Bulk	480	1120	FM-MFT	[648]
bcc Co	Bulk	764	—	LDA	[572]
fcc Ni	Bulk	662	290	FBT+GF	[656]
fcc Ni	Bulk	386	380	LSD	[639]
fcc Ni	Bulk	537	425	LSD	[562]
fcc Ni	Bulk	690	—	RPA	[658]
fcc Ni(1 0 0)	1 ML	377	—	RPA	[658]
fcc (1 0 0) Ni	1 ML	470	—	RPA	[649]
fcc (1 1 0) Ni [1 1 1]	1 ML	685	—	RPA	[649]
fcc (1 1 1) Ni	1 ML	350	—	RPA	[649]
fcc Ni	Bulk	527	—	LSD	[659]
fcc Ni	Bulk	—	430	LSD	[645, 646]
fcc Ni	Bulk	739	510	LMTO+MC	[643]
fcc Ni	Bulk	740	406	LSD	[660]
fcc Ni	Bulk	480	—	LSD	[647]
fcc Ni	Bulk	790	—	ASW	[638]
fcc Ni	Bulk	756 ± 29	350	TB-LMTO	[636]
fcc Ni	Bulk	1796	820	DLM-MFT	[648]
fcc Ni	Bulk	541	320	FM-MFT	[648]

approximation, the stiffness constant is calculated for Fe, Co and Ni, but the values are grossly underestimated (see table 10); they attribute this to the adiabatic approximation used in the calculations. Values obtained in other studies are given in table 10. More recently, Shallcross *et al* [648] calculated the stiffness constant using a perturbative approach based on the magnetic force theorem (MFT) [638] using both a ferromagnetic (FM) and disordered local moment (DLM) reference states (simply speaking, the first method approaches the problem from the low temperature end while the second

Table 11. Estimates for the room temperature stiffness constant D and exchange constant A from the neutron data.

Material	M_s^{RT} (emu cm^{-3})	D_{RT} (meV Å^2)	A_{RT} (μerg cm^{-1})
Fe	1714[a]	280 ± 10	1.98
Co (fcc)	1445[b]	500 ± 20	3.00
Co (hcp)	1422[a]	500 ± 20	2.81
Ni	484.1[a]	450 ± 20	0.86
$Ni_{80}Fe_{20}$	813[c]	330 ± 20	1.07

[a] From [569].
[b] From [574, 663].
[c] From [570].

method applies to the high temperature region). The values obtained are listed in table 10; it is found that the DLM–MFT approach yields better estimates for the Curie temperatures while using the ferromagnetic reference state yields more accurate results for the low energy excitations, such as magnon spectra.

While all the previous studies deal with 3D systems, some studies have tackled the problem of calculating the spin wave dispersion curves in thin films; the report by Tovar Costa *et al* [649] deals with the spin wave excitation spectrum of a Ni monolayer for the three high symmetry orientations (1 0 0), (1 1 0) and (1 1 1), and they find that while the spin wave spectrum is isotropic for the (1 0 0) and (1 1 1) surface, it is highly anisotropic for the (1 1 0) surface due the asymmetry in the crystalline structure of this plane, consisting of weakly interacting linear chains of nearest neighbours, making it relatively easy to excite long wavelength spin waves propagating perpendicularly to the chains. In addition, contrary to what is expected from a Heisenberg model, they find that the exchange interaction decreases with increasing number of nearest neighbours. Costa *et al* [650] have considered the case of 8 ML Co/Cu(0 0 1), and the value they obtain for the stiffness constant, 510 meV Å^2, is in good agreement with the value obtained by Liu *et al* [572] for ~20 nm Co, 466 meV Å^2, and in fair agreement with the results of Vollmer *et al* [623]; according to their calculations, the stiffness constant is found to attain the bulk value at around 4 ML. In a subsequent publication, the same authors considered a modified value for the intra-Coulomb interaction U within the 3d shell to improve the predictions of the random phase approximation (RPA) calculations [651]. By taking a slightly lower value for U (from 1 to 0.85 eV) they obtain a better agreement with the experimental results of Vollmer *et al* [623], obtaining a stiffness constant $D = 390$ meV Å^2 when fitting their numerical data to the same Heisenberg model used by Vollmer *et al* [623]; the wave vector range probe by SP-EELS is rather high compared with the low energy excitations where a quadratic wave vector dependence may be expected; in fact, a value $D = 238.7$ meV Å^2 is obtained at low q from the numerical results. The spin dynamics of bulk Fe and ultrathin Fe(0 0 1) films was studied within the same empirical tight binding formalism by Tang *et al* [584]; they considered two models for bulk Fe according to different tight binding parameters available in the literature, model A (from a compilation from Papaconstantopoulos [652]) and model B (from values provided by Cooke *et al* [653, 654]), yielding slightly different values for the stiffness constant: $D = 230$ meV Å^2 for model A and $D = 289$ meV Å^2 for model B, demonstrating the sensitivity of the spin dynamics of Fe to the details of the underlying band structure. Muniz and Mills [655] studied the case of Fe(1 1 0) monolayers, free standing and on a W(1 1 0) substrate; in both cases they found that the dispersion curve is anisotropic, the stiffness constant being larger along the [1 0 0] direction while the effect of the W substrate is mostly to reduce the stiffness constant along the [0 1 $\bar{1}$] direction.

This survey of the experimental and theoretical reports on the exchange constant and stiffness constant suggest that many gaps remain in our understanding of these crucial parameters, both quantitatively and qualitatively. In fact, the large dispersion of values reported for D implies that a standard value cannot be invoked for the transition metals and alloys. The neutron data, which are believed to be the most reliable, are still marred by large error bars, and are not reproducible for different samples, data analysis or experimental procedures (the results for Fe seem to be the less problematic). The other methods used to determine the stiffness constant involve too many parameters or rely on assumptions which limit their dependability; at best, they either give credence to the neutron data, or otherwise suggest limitations in the model employed to analyse the system under discussion. The results in thin film systems are still too scarce to allow a broader perspective, especially since additional parameters are introduced into the equation. A tentative list for values of D and A from the neutron data is given in table 11.

5. Absolute magnetic moments

The magnetic moment is the most fundamental quantity in magnetism and yet very difficult to measure experimentally in the case of thin films. Magnetic order corresponds to the microscopic ordering (over macroscopic distances) of the electron angular momentum, be it the localized atomic orbital and spin moment and/or the spin moment of itinerant band electrons. Due to the Pauli exclusion principle, electrons with antisymmetric wavefunctions and same spin have vanishing probability density as they approach each other [186, 664]; this results in spin states with more extended overlap of the atomic orbitals, where the decrease in Coulomb repulsion outweighs the increase in kinetic energy. The magnitude of the magnetic moment depends, on the one hand, on the magnitude of the angular moment (particularly for localized systems) and on the

Table 12. Experimental room temperature (E) and calculated (C) ground state values of the electronic contributions to the bulk and surface total magnetic moment in μ_B/atom of Fe, Co and Ni.

System	3d (spin)	3d (orbital)	4s	Meth.	References
bcc Fe (bulk)	2.27	0.12	−0.21	E	[670, 671]
bcc Fe (bulk)	2.18	0.05	−0.04	C	[672, 673]
bcc Fe(0 0 1)	2.87	0.12	0.00	C	[672, 673]
hcp Co (bulk)	1.86	0.13	−0.28	E	[674]
hcp Co (bulk)	1.58	0.09	−0.07	C	[672, 673]
hcp Co(0001)	1.75	0.11	−0.07	C	[672, 673]
fcc Ni (bulk)	0.656	0.055	−0.105	E	[675, 676]
fcc Ni (bulk)	0.55	0.04	−0.04	C	[672, 673]
fcc Ni(0 0 1)	0.59	0.06	−0.03	C	[672, 673]

other on the spin imbalance between majority and minority electron bands (itinerant magnetism). For the 3d transition metals the orbital moment is quenched by the strong crystal field and the magnetic moment is mostly due to the electron spin as a result of the electron band splitting (there is, however, a small orbital contribution to the magnetic moment which is responsible for the magnetocrystalline anisotropy through the spin–orbit coupling [664], see table 12). For the 4f series, the orbital moment is not quenched, and the main contribution to the magnetic moment comes from the atomic angular moment. Additionally, the mechanisms responsible for the magnetic order are different: while for the 3d direct exchange leads to ferromagnetic order, for the rare earths there is a strong RKKY exchange interaction term [178].

Due to changes in electronic structure in reduced dimensions, the magnetic moment does not necessarily scale with the volume of the system. In fact, it is expected that as the physical dimensions of the system are reduced, the break in symmetry induces a localization of the wavefunction of those atoms closest to the interface [186, 192]. While the effect of this symmetry break on the magnetic anisotropy is very pronounced, the effect on the magnetic moment is in general smaller and more difficult to observe. Also, metastable crystal structures can be stabilized as thin films or small particles, which often exhibit magnetic moments which are different from those corresponding to the bulk equilibrium phase. We can therefore distinguish several mechanisms that can lead to a change in the magnetic moment in thin films: (i) break in symmetry and consequent orbital localization effects; (ii) electronic interaction (hybridization) between the atoms of the magnetic layer with those of the adjacent interface layers (substrate or overlayer), which may lead to electron exchange processes that enhance or reduce the magnetic moment; (iii) changes in the atomic cell volume which may change the imbalance of spin up and down density of states (DOS); (iv) occurrence or stabilization of other crystalline and magnetic phases with magnetic ordered states and moments distinct from that of the equilibrium phase. To the extent that it is possible to separate these effects we shall consider each in turn by considering some examples extracted from published theoretical *ab initio* calculations. Such studies have become in the last two decades an important tool for the understanding of the mechanisms responsible for the macroscopic behaviour of magnetism in thin films at the microscopic level [70, 71, 74, 75, 665–669].

5.1. Break of symmetry and interface moments

The break of symmetry at the surface or interface is at the origin of important changes in the electronic structure of the atomic orbitals along the direction perpendicular to the interface as compared with the bulk, resulting in strong surface anisotropies (as first pointed out by Néel [199, 200], based on symmetry arguments) and enhanced magnetic moments. These changes in anisotropy and magnetic moment can be understood as the result of localization and band narrowing of the atomic orbitals of the interface atoms, leading to a larger density of states at the Fermi level and enhanced spin imbalance [677, 678]. In the 2D limit, even some non-magnetic metallic systems have been predicted to become magnetic [71, 679], although this has not been fully confirmed by experiment [410]. Atomic surface relaxations can lead to further changes in the surface magnetic moment as compared with the unrelaxed surface; for instance, inward relaxation in V and Cr tend to diminish the surface magnetic moment [71, 680] and downward relaxation of the surface layer in 1 ML Fe/W(1 1 0) leads to a strong reduction of the Fe magnetic moment [681, 682]. The increase in the magnetic moment as the symmetry of the system is reduced is borne by the results of *ab initio* calculations of the electronic configuration of slabs of atoms, of free standing atomic layers and linear chains of atoms, which approach, in this order, the magnetic moment of the isolated atom as determined assuming Hund's rules, table 13. One result that comes out of these calculations is that interface effects are confined to, at most, 5 ML from the interface. This is in agreement with x-ray absorption spectra results on Ni/Cu(0 0 1) [258, 259, 683] and Co/Cu(0 0 1) [683] thin films, which suggest that the electronic structure does not change significantly for thicknesses above 2–5 ML, and also with the crossover from 2D to 3D behaviour at a thickness of around 7 ML [255–257] (see section 3).

The role of charge redistribution at the surface on the magnitude of the magnetic moment can be appreciated by comparing the bulk and surface decomposition of the magnetic moment into its orbital and spin components (see table 12). We see that while both spin and orbital components of the magnetic moment are enhanced at the surface, the effect is much more pronounced for the orbital component [709],

Table 13. Calculated magnetic moments for 3d transition metals (values in μ_B/atom). The 'bulk' value refers to the magnetic moment of the atoms at the centre of the slab used in the calculations while the atomic magnetic moment was calculated from Hund's rules assuming that the orbital moment is quenched, as in the solid. FLAPW—full-potential linearized augmented plane wave approximation; LCAO—linear combination of atomic orbitals; LMTO—linear muffin-tin orbitals; GF—Green function method; ASA—atomic sphere approximation; LAPW—linearized augmented plane wave approximation.

System	Bulk	Surface	ML	Chain	Atom	Method	References
bcc Cr(0 0 1)[a]	0.89	2.49	4.12[b]	—	4	FLAPW	[688]
bcc Cr(0 0 1)[a]	0.23	2.61	—	—	4	TB-LMTO	[689]
bcc Cr(0 0 1)[a]	0.95	2.80	—	—	4	FLAPW	[690]
bcc Cr(1 1 0)[a]	0.21	1.39	—	—	4	TB-LMTO	[689]
bcc Fe(0 0 1)	2.15	3.01	—	—	4	LCAO	[691]
bcc Fe(0 0 1)	2.25	2.98	3.20[b]	3.36[c]	4	FLAPW	[260]
bcc Fe(0 0 1)	2.18	2.87	—	—	4	LMTO	[672,673]
bcc Fe(0 0 1)	2.24	2.97	3.10[d]	—	4	TB-LMTO	[689,692]
bcc Fe(0 0 1)	2.32	3.01	—	—	4	FLAPW	[690]
bcc Fe(0 0 1)	2.33	3.12	—	—	4	LMTO	[693]
bcc Fe(0 0 1)	2.22	2.97	—	—	4	GF	[694]
bcc Fe(0 0 1)	2.28	3.04	3.17	—	4	LMTO-ASA	[695]
bcc Fe(1 1 0)	2.22	2.65	—	—	4	FLAPW	[696]
bcc Fe(1 1 0)	2.24	2.57	—	—	4	TB-LMTO	[689,692]
bcc Fe(1 1 0)	2.24	2.57	—	—	4	GF	[694]
bcc Fe(1 1 1)	2.00	2.60	—	—	4	FLAPW	[697]
bcc Fe(1 1 1)	2.23	2.92	—	—	4	GF	[694]
fcc Fe(1 0 0)[a]	1.78	2.59	—	—	4	TB-LMTO	[689]
fcc Fe(1 1 1)[a]	1.76	2.30	—	—	4	TB-LMTO	[689]
hcp Co(0 0 0 1)	1.64	1.76	—	—	3	FLAPW	[698]
hcp Co(0 0 0 1)	1.61	1.70	—	—	3	TB-LMTO	[689,692]
hcp Co(0 0 0 1)	1.58	1.75	—	—	3	LMTO	[672,673]
hcp Co(0 0 0 1)	1.57	—	1.87	—	3	LMTO	[699]
hcp Co(0 0 0 1)	1.75	1.95	—	—	3	LMTO	[693]
fcc Co(0 0 1)	1.65	1.86	—	—	3	FLAPW	[700]
fcc Co(0 0 1)	1.64	1.84	—	—	3	TB-LMTO	[689,692]
fcc Co(0 0 1)	1.65	1.84	—	—	3	GF	[694]
fcc Co(1 1 0)	1.65	1.90	—	—	3	GF	[694]
fcc Co(1 1 1)	1.64	1.72	—	—	3	TB-LMTO	[689,692]
fcc Co(1 1 1)	1.64	1.72	—	—	3	GF	[694]
bcc Co(0 0 1)	1.76	1.94	2.12	—	3	FLAPW	[701]
bcc Co(1 1 0)	1.74	1.94	—	—	3	TB-LMTO	[689]
bcc Co(0 0 1)	1.73	1.94	—	—	3	GF	[694]
bcc Co(1 1 0)	1.76	1.82	—	—	3	FLAPW	[702]
bcc Co(1 1 0)	1.74	1.78	—	—	3	TB-LMTO	[689]
bcc Co(1 1 0)	1.74	1.78	—	—	3	GF	[694]
bcc Co(1 1 1)	1.74	2.01	—	—	3	GF	[694]
fcc Ni(0 0 1)	0.69	0.73	0.86	1.07[c]	2	LAPW	[677]
fcc Ni(0 0 1)	0.56	0.68	0.85[e]	—	2	FLAPW	[703]
fcc Ni(0 0 1)	0.61	0.65	0.95	—	2	LAPW	[704]
fcc Ni(0 0 1)	0.64	0.69	—	—	2	TB-LMTO	[689]
fcc Ni(0 0 1)	0.56	0.66	—	—	2	FLAPW	[690]
fcc Ni(0 0 1)	0.54	0.44	—	—	2	LCAO	[705]
fcc Ni(0 0 1)	0.56	0.74	—	—	2	TB	[706]
fcc Ni(0 0 1)	0.64	0.69	—	—	2	GF	[692]
fcc Ni(0 0 1)	0.55	0.59	—	—	2	LMTO	[672,673]
fcc Ni(0 0 1)	0.64	0.82	—	—	2	LMTO	[693]
fcc Ni(0 0 1)	0.65	0.69	—	—	2	GF	[694]
fcc Ni(0 0 1)	0.62	0.71	0.82	—	2	LMTO-ASA	[695]

Table 13. (Continued).

System	Bulk	Surface	ML	Chain	Atom	Method	References
fcc Ni(0 0 1)	0.60	0.62	—	—	2	TB-LMTO	[707]
fcc Ni(1 1 0)	0.62	0.70	0.96	—	2	LAPW	[677]
fcc Ni(1 1 0)	0.65	0.77	—	—	2	GF	[694]
fcc Ni(1 1 1)	0.63	0.62	—	—	2	TB-LMTO	[689]
fcc Ni(1 1 1)	0.56	0.65	—	—	2	TB	[706]
fcc Ni(1 1 1)	0.58	0.63	—	—	2	FLAPW	[708]
fcc Ni(1 1 1)	0.63	0.62	—	—	2	GF	[692]
fcc Ni(1 1 1)	0.64	0.62	—	—	2	GF	[694]
bcc Ni(0 0 1)	0.485	0.74	0.93	—	2	LMTO-ASA	[695]

[a] Antiferromagnet.
[b] From [685].
[c] From [684].
[d] From [686].
[e] From [687].

although its contribution to the total magnetic moment is much smaller. However, since it is this component that is responsible for magnetic anisotropies, the implications of surface effects on the magnetic anisotropies in thin films can be readily understood. The fourth column of this table lists the value of the s–p contribution to the magnetic moment (*diffuse magnetism* [673]); neutrons are not sensitive to this contribution, and in table 12 it has been determined by subtracting the moment obtained from neutron diffraction from that obtained by ordinary magnetometry; it is the contribution associated with the s–p band electrons, which are polarized antiparallel to the total moment in Fe, Co and Ni.

It is noteworthy to point out here the results of first principles calculations by Nakamura *et al* [710] for the magnetic spin structure of a magnetic vortex core of an Fe dot, which predicts an orbital magnetic moment per Fe atom at the centre of the vortex larger than that in the ferromagnetic dot, pointing to the importance of coupling between the spin density and the orbital motion in structures with non-uniform magnetic configurations.

5.2. Interface magnetic moment: effect of the substrate and overlayer

The experimental realization of ultrathin films in the monolayer range requires the presence of a substrate upon which the magnetic layer is deposited. In the case of epitaxial growth, the deposited atoms grow in registry with the substrate due to atomic bonding, thereby reducing the surface energy [711–715]. Epitaxial growth tends to occur when the lattice mismatch between the substrate and the deposited material is small, as the elastic energy competes with the surface energy. Since most materials have distinct equilibrium lattice constants, epitaxy leads to strained ultrathin films with lattice constants that differ from the bulk equilibrium value (at least during the initial stages of growth). In general, this leads to a lattice structure with a symmetry lower than the bulk system (the equilibrium out-of-plane lattice constant, which is under no strain and is therefore able to adjust itself to minimize the elastic energy, assumes a value that acts to keep the primitive volume cell approximately constant and equal to the bulk equilibrium value [716–718]; this suggests that even in the atomic limit, Hooke's law is approximately valid). In some instances it is possible to stabilize crystalline phases which are not found in nature at normal temperature and pressure in bulk [719] (examples are fcc Co grown on the Cu(0 0 1) surface [720, 721] and bcc Co/GaAs(0 1 1) [722, 723]).

When a different species comes into contact with the magnetic film, chemical interaction in the form of electronic bonding (through electron charge transfer) takes place and affects, in general, the magnetic moment amplitude. This change depends on the atomic elements involved and the process is very similar to that involved in the magnetism of metallic alloys (orbital hybridization) [694, 729, 748, 749] and leads to plots identical to the Slater–Pauling curves of bulk alloys [694, 729, 737, 750], see figure 15. In tables 14, 15, 16 we list the calculated values of the interface magnetic moments of Fe, Co and Ni, respectively, in contact with different substrate materials. These calculations correspond to ground state (0 K) properties and assume perfect, flat, interfaces. For the listed values, it is seen that the interface moment of Fe is always enhanced with respect to the bulk value when in contact with Cu, Pd, Ag and Au (for the case of thicker fcc Fe/Cu(1 0 0), ferromagnetic coupling is predicted for the surface and subsurface layers while deeper layers couple antiferromagnetically [727, 751]; other more complex configurations have been suggested [728]). For fcc Co/Cu, the interface moment is enhanced for the single monolayer, but according to Niklasson *et al* [694], the interface moment of a semi-infinite Co layer in contact with Cu is slightly reduced with respect to the bulk. This suggests that the enhancement observed for the thin Co films on Cu is related to the reduced thickness of the Co film and that the enhancement due to the break of symmetry at the Co/Cu interface is partly cancelled out by orbital hybridization. Capping 1 ML Co with Cu leads to a strong reduction of the Co moment to near zero, according to the results of Szunyogh *et al* [737]. For Ni monolayer films on Cu and Au, the magnetic moment is strongly reduced, while it is enhanced when in contact with Pd and Ag. This trend in the magnetic moment can be compared with the change in the magnetic moment of alloys, as shown in table 4.2 of Stoner [749].

In addition to affecting the magnetic moment of the magnetic layers, contact with non-magnetic layers has been

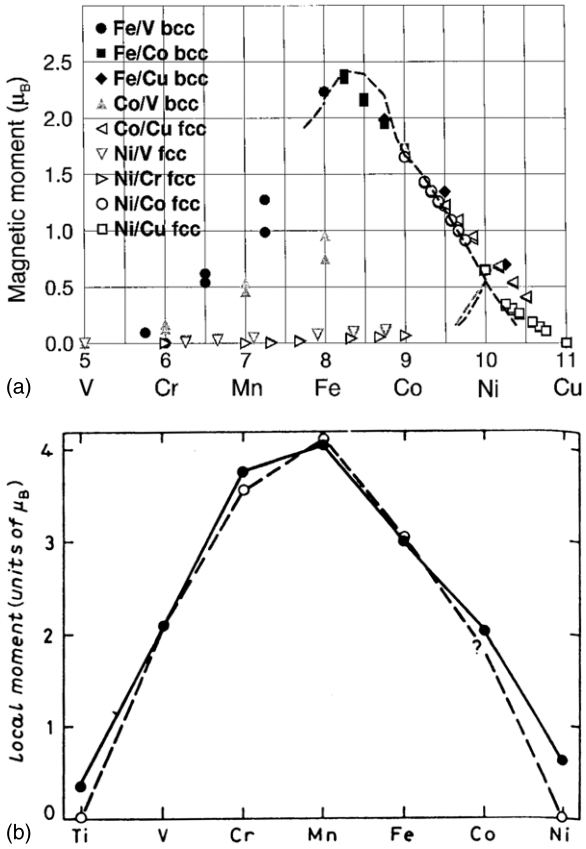

Figure 15. Slater–Pauling curves for (*a*) the average interface moments for different interfaces (symbols); lines correspond to experimental data for FeV, FeCo, CoNi and NiCr alloys [694]; (*b*) magnetic moment of 3d transition metals monolayers on Ag(0 0 1) for ferromagnetic (full circles) and antiferromagnetic (open circles) configurations [729]. Reprinted with permission from (a) A M N Niklasson, B Johansson and H L Skriver 1999 Interface magnetism of 3d transition metals *Phys. Rev.* B **59** 6373. Copyright (1999) by the American Physical Society; (b) S Bluegel and P H Dederichs 1989 Enhanced magnetic moments in bcc Fe films *Europhys. Lett.* **9** 597.

found to induce a spin polarization in the interface atoms of the latter. While these effects are generally observed in the results of *ab initio* calculations, they tend to be small and difficult to observe experimentally. However, evidence for spin polarization of Cu in Co/Cu [752, 753] and Fe/Cu multilayers [753, 754], of Ag and W in NiFe/Ag and W/Fe multilayers, respectively [755], of Au in Au/Fe [756] and Au/Co multilayers [757], of V in V/Fe multilayers [758, 759] and of Pd in Pd(1 1 1)/Ni(1 1 1) films [760], among others [761] have been obtained experimentally. It is noteworthy that most of these measurements were performed using XMCD.

5.3. Variation of the magnetic moment with volume and strain

Given the sensitivity of magnetism to the details of the band structure near the Fermi level, it is not surprising that the magnetic moment should be very sensitive to the interatomic spacing. Magnetic order in 3d transition metals is a result of a competition between the exchange interaction (due to the Coulomb repulsion and the Pauli exclusion principle) that favours a state with the highest number of electrons with the same spin and the kinetic energy that increases when promoting same spin electrons into unoccupied levels higher in energy. In normal metals the second term outweighs the first, but in 3d transition metals the existence of a very large DOS at the Fermi energy issuing from the narrow 3d bands favours magnetically ordered states [762,763]. On the other hand, the kinetic energy is inversely proportional to the volume and can be reduced by lattice dilatation [71, 176].

An increase in the atomic spacing leads in general not only to band narrowing but also to a reduction in the atomic overlapping and a weakening of the (direct exchange) magnetic coupling. Conversely, a more compact atomic arrangement would lead to broader electron bands and an increase in the Fermi energy (larger kinetic energy), reducing the energy gain from the exchange interaction and reducing the band splitting (and the magnetic moment). In other words, one expects a certain range of atomic volumes where magnetic phases are stable. This can be observed in the calculated energy of several cubic crystal phases of 3d transition metals (Fe, Co, Ni, Pd and Mn) [764–771]. These local density approximation (LDA) calculations show that while the magnetic moment in the equilibrium crystal phases varies slowly with the atomic volume, metastable crystal phases in general exhibit a more unstable magnetic phase diagram. For example, fcc Fe is found to be non-magnetic at the equilibrium lattice constant, bcc Ni just barely magnetic and fcc Co is magnetic at the total energy minimum; however, a 5% expansion in the fcc lattice of Fe is found to bring the system into a magnetic state, while a 4% contraction of the fcc Co lattice brings the system into a non-magnetic phase. This is illustrated in figure 16 from calculations of the crystal energy and magnetic moment of fcc and bcc phases of bulk Fe against the atomic volume performed by Herper *et al* [772] obtained from full-potential augmented plane wave (FLAPW) calculations within the generalized gradient approximation (GGA) framework. It is worth noting that the local density approximation fails to predict the ground state of Fe [771–773], indicating that LDA does not properly account for the correlations in Fe [771]. We note that these variations in the magnetic moment refer to hydrostatic changes in volume and are distinct from the moment variation with in-plane strain which occurs in epitaxial thin films.

The pressure dependence of the magnetic moment in bulk samples has been measured and available experimental results are listed in table 17. The value $-\kappa_m/\kappa_T$ gives the relative change in the magnetic moment with relative change in volume with respect to the equilibrium value; it is surprisingly very similar for all the crystal structures (bcc Fe, hcp Co, fcc Ni) and of the order of 0.5. Hence, for these systems, a relative change in volume of 1%, gives a relative change in the magnetic moment of approximately 0.5%. It implies that increasing the lattice cell volume leads to an increase in the magnetic moment, as expected from band narrowing effects.

It is often possible to extract $-\kappa_m/\kappa_T$ from first principle reports of the magnetic properties of transition metal elements, since often part of the calculation consists of determining the equilibrium lattice constant and the respective magnetic

Table 14. Calculated magnetic moments for Fe on different non-magnetic substrates (values in μ_B/atom). The 'bulk' value refers to the magnetic moment of the atoms at the centre of the slab used in the calculations and s.i. stands for semi-infinite layers. LSD—local spin-density approximation; LMTO—linear muffin-tin orbitals; ASA—atomic sphere approximation; TB—tight binding; FLAPW—full-potential linearized augmented plane wave approximation; SCLOM—self-consistent local orbital method; (L)APW+lo—full-potential partial linearized augmented plane wave with local orbitals method.

Substrate	Phase	Bulk	Interface	t (ML)	Method	References
Cu(0 0 1)	fcc	2.332	2.936	1	LSD	[693]
Cu(0 0 1)	fcc	2.25	2.69	1	LSD	[724]
Cu(0 0 1)	fcc	2.12	2.33	1	LMTO-ASA	[725]
Cu(0 0 1)	fcc	2.24	2.71	1	TB-LMTO	[726]
Cu(0 0 1)	fcc	—	2.85	1	FLAPW	[685, 727]
Cu(0 0 1)	fcc	—	2.65	11	LSD	[728]
Cu(0 0 1)	fcc	—	2.79	1	LSD	[728]
Cu(0 0 1)	bcc	2.253	2.636	s.i.	LMTO	[694]
Cu(1 1 0)	bcc	2.241	2.472	s.i.	LMTO	[694]
Cu(1 1 1)	bcc	2.276	2.553	s.i.	LMTO	[694]
Pd(0 0 1)	bcc	—	3.19	1	FLAPW	[667, 729, 730]
Ag(0 0 1)	bcc	—	3.01	1	FLAPW	[667, 729, 730]
Ag(0 0 1)	bcc	—	2.96	1	FLAPW	[685]
Ag(0 0 1)	bcc	2.2	3.0	1	SCLOM	[731]
Ag(0 0 1)	bcc	—	3.0	1	FLAPW	[679]
Au(0 0 1)	bcc	—	2.97	1	FLAPW	[732]
Au(0 0 1)	bcc	2.24	3.01	1	LSD	[733]
W(1 1 0)	bcc	—	2.18[a]	1	FLAPW	[681]
W(1 1 0)	bcc	2.2	2.56	1	(L)APW+lo	[734]

[a] Fe atoms allowed to relax.

Table 15. Calculated magnetic moments for Co on different non-magnetic substrates (values in μ_B/atom). The 'bulk' value refers to the magnetic moment of the atoms at the centre of the slab used in the calculations. LSD—local spin-density approximation; FLAPW—full-potential linearized augmented plane wave approximation; LDA+U—local density approximation plus total energy functional; LMTO—linear muffin-tin orbitals; GF—Green function method.

Substrate	Phase	Bulk	Interface	t (ML)	Method	References
Cu(0 0 1)	fcc	1.753	2.111	1	LSD	[693]
Cu(0 0 1)	fcc	1.64	1.79	1	LSD	[724]
Cu(0 0 1)	fcc	—	1.90	1	FLAPW	[735]
Cu(0 0 1)	fcc	—	1.817	3	LDA+U	[736]
Cu(0 0 1)	fcc	—	1.67	1	LSDA	[737]
Cu(0 0 1)	fcc	1.678	1.634	s.i.	LMTO	[694]
Cu(0 1 1)	fcc	1.676	1.620	s.i.	LMTO	[694]
Cu(1 1 1)	fcc	1.674	1.622	s.i.	LMTO	[694]
Cu(1 1 1)		1.72	1.79	1	GF	[738]
Pd(0 0 1)	fcc	—	2.12	1	FLAPW	[667, 729, 730]
Pd(1 1 1)		—	1.88	1	FLAPW	[739]
Ag(0 0 1)	fcc	—	2.03	1	FLAPW	[667, 729, 730]
Ag(0 0 1)	fcc	—	2.0	1	FLAPW	[679]
Pt(1 1 1)		—	1.84	1	FLAPW	[739]

moment. Values extracted from a selection of reports are given in table 18. The numerical results are of the same order of magnitude as the experimental values, but the dispersion between the results of different studies is quite pronounced.

At the Curie temperature, large changes in volume are observed for Fe, Co, Ni and alloys, associated with the magnetic phase transition to a paramagnetic state [570, 777]. The empirical behaviour of the volume variation can be understood in terms of the qualitative Bethe curve, which relates the energy of magnetization to the atomic radius [570, 778], while within the local density functional approximation an expansion of the atomic volume is found when comparing unpolarized with spin-polarized band structure calculations (the spin splitting of the electron bands causes an enhanced population of antibonding majority spin states at the top of the band and a reduction of the bonding and non-bonding spin states at the bottom and middle of the minority spin band, leading to weaker bonding) [76]. However, calculations based on the Stoner band model fail to predict the correct magnitude of the effect, and when neutron scattering measurements were initially reported suggesting the presence of spin waves at temperatures well beyond the Curie temperature in Fe and Ni [580,594, 779–782], it was suggested that the magneto-volume changes at the critical point could be explained by assuming that localized magnetic moments remain in the paramagnetic phase and that band splittings do not collapse at the critical temperature (in contradistinction to what band theory posits), but are stabilized by local magnetic order [657, 783–788]. This would agree, at first sight, with the large values for the exchange splitting predicted [238] and measured [789] for

Table 16. Calculated magnetic moments for Ni on different non-magnetic substrates (values in μ_B/atom). The 'bulk' value refers to the magnetic moment of the atoms at the centre of the slab used in the calculations. LAPW—linearized augmented plane wave approximation; TB—tight binding; SCLO—self-consistent local orbital method; LSD—local spin-density approximation; SPR-LMTO—spin-polarized relativistic linear muffin-tin orbitals; LMTO-ASA—linear muffin-tin orbitals atomic sphere approximation; LMTO—linear muffin-tin orbitals; GF—Green function method; FLAPW—full-potential linearized augmented plane wave approximation.

Substrate	Phase	Bulk	Interface	t (ML)	Method	References
Cu(0 0 1)	fcc	0.62	0.37	1	LAPW	[687]
Cu(0 0 1)	fcc	0.62	0.39	1	LAPW	[740]
Cu(0 0 1)	fcc	0.55	0.48	1	TB	[706]
Cu(0 0 1)	fcc	0.55	0.37	5	TB	[706]
Cu(0 0 1)	fcc	—	0.24	1	SCLO	[741]
Cu(0 0 1)	fcc	0.638	0.537	1	LSD	[693]
Cu(0 0 1)	fcc	0.71	0.48	5	SPR-LMTO	[742]
Cu(0 0 1)	fcc	0.59	0.00	1	LMTO-ASA	[743]
Cu(0 0 1)	fcc	0.667	0.469	s.i.	LMTO	[694]
Cu(0 0 1)	fcc	0.57	0.369	3	GF	[744, 745]
Cu(0 0 1)	fcc	—	0.544	1	FLAPW	[746]
Cu(0 0 1)	fcc	—	0.503	4	FLAPW	[746]
Cu(1 1 0)	fcc	0.661	0.422	s.i.	LMTO	[694]
Cu(1 1 0)	fcc	0.57	0.272	3	GF	[744, 745]
Cu(1 1 1)	fcc	0.56	0.09	1	TB	[706]
Cu(1 1 1)	fcc	0.56	0.38	5	TB	[706]
Cu(1 1 1)	fcc	0.58	0.34	1	FLAPW	[708]
Cu(1 1 1)	fcc	0.647	0.463	s.i.	LMTO	[694]
Cu(1 1 1)	fcc	0.57	0.341	3	GF	[744, 745]
Pd(0 0 1)		—	0.89	1	FLAPW	[667, 729, 730]
Ag(0 0 1)		—	0.65	1	FLAPW	[667, 729, 730]
Ag(0 0 1)		—	0.57	1	FLAPW	[747]
Ag(0 0 1)		—	0.7	1	FLAPW	[679]
Au(0 0 1)		0.59	0.49	1	LMTO-ASA	[743]

3d transition metals: 1.5 eV for Fe, 1.1 eV for Co and 0.3 eV for Ni. However, later neutron scattering experiments revealed limitations in the interpretation of the earlier neutron data and concluded that no spin waves could be detected above the Curie temperature [780, 790–793]. The idea that local moments are present in the paramagnetic state of the ferromagnetic transition metals would explain many of the localized-moment properties exhibited by these materials. In the spin fluctuation theory [794, 795], the magnetic moment in itinerant systems is carried by spin density, and macroscopic magnetic properties arise as a consequence of thermodynamic fluctuations in the magnetization [796, 797]. Such spin fluctuations are also present above the Curie temperature and give rise to significant modifications to the magnetic behaviour of the system; while such formalism is more appropriate for weak ferromagnetism, it nevertheless emphasizes the role of short-range magnetic correlations in determining the magnetic behaviour above the critical point. Measurements of the temperature variation of the exchange splitting of Ni by spin-resolved inverse photoemission show that the exchange splitting closely follows the magnetization curve [185, 798], suggesting indeed that the spin bands collapse at the Curie temperature, as assumed in the Stoner band model [178, 185].

As an aside, we note that often the variation in magnetization with temperature $M(T)$ is reported in the literature, while what is effectively measured is a variation in the mass magnetization $\sigma(T)$ with temperature. This is because most magnetometry measurements are performed at constant pressure, since it is experimentally very difficult to keep the sample volume constant. $M(T)$ is the most interesting quantity because it is a relevant quantity used in the theory of solids, but the error of assuming a constant lattice constant from room temperature down to 0 K is only a few tenths of a per cent point (for Fe, the lattice constant changes by 0.17% from 0 K up to RT [799]). Close to the critical temperature other factors may also contribute, such as changes in T_c with volume [570, 573] (this correction is particularly important for Ni near T_c [800, 801]). A thermodynamic expression relating the temperature variation of $M(T)$ at constant volume to the temperature variation of $\sigma(T)$ at constant pressure is given by

$$\left(\frac{\partial\sigma}{\partial T}\right)_V = \left(\frac{\partial\sigma}{\partial T}\right)_P + \alpha\sigma_0\frac{\kappa_m}{\kappa_T}, \tag{54}$$

where $\kappa_T = -(1/V)(\partial V/\partial P)_T$ is the isothermal compressibility, $\kappa_m = \sigma_0^{-1}(\partial\sigma/\partial P)_T$ is the isothermal magnetization compressibility, $\alpha = (1/V)(\partial V/\partial T)_P$ is the coefficient of thermal expansion and σ_0 is the mass magnetization at 0 K. The left-hand side of the previous equation can be written as $(1/\rho)(\partial M/\partial T)_V$, where $\rho = \rho(T)$ is the mass density. Assuming the last term of (54) constant in temperature, it follows that

$$M_V(T) = \rho(T)\sigma_P(T) + \alpha\sigma_0\frac{\kappa_m}{\kappa_T}\rho(T)T, \tag{55}$$

which can be used to convert mass magnetization to volume magnetization if the other parameters are known.

In epitaxial thin films the strain exerted by the substrate still allows the film to relax along the out-of-plane direction,

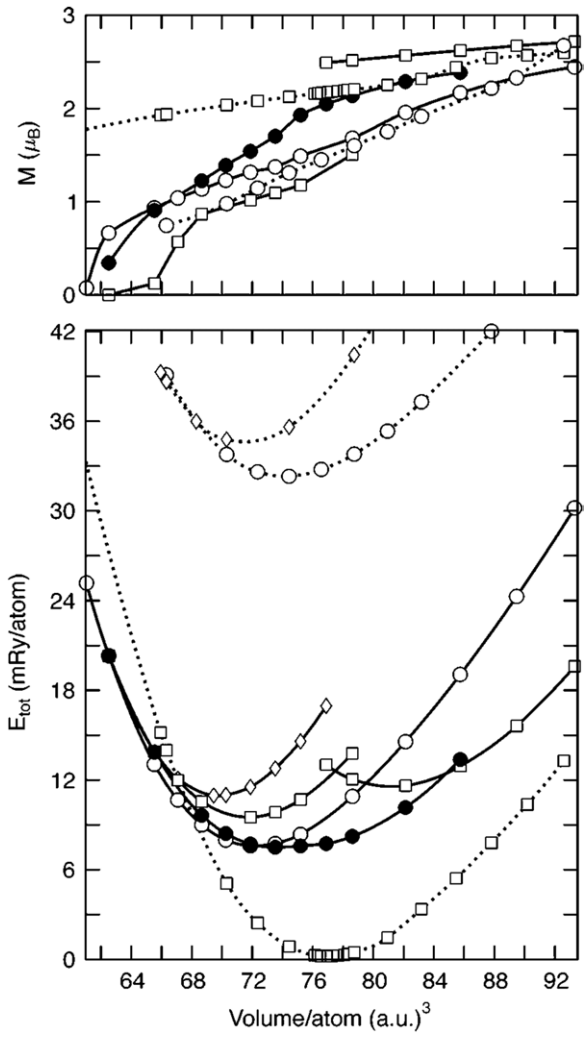

Figure 16. First principles calculations of the variation of the magnetic moment per atom (upper panel) and total energy per atom (lower panel) as a function of the atomic volume for bcc Fe (dotted lines) and fcc Fe (full lines) for different magnetic configurations: non-polarized (diamonds), ferromagnetic (squares), antiferromagnetic-I (open circles) and antiferromagnetic double layer (filled circles) [772]. Here, the atomic unit (a.u.) volume is that contained in one Bohr radius ($a_0 = 0.529\,177\,208$ Å) cubed. Reprinted with permission from H C Herper, E Hoffmann and P Entel 1999 *Ab initio* full-potential study of the structural and magnetic phase stability of iron *Phys. Rev.* B **60** 3839. Copyright (1999) by the American Physical Society.

where no stress is present. Usually it attains a value that tends to keep the equilibrium atomic volume approximately constant [716–718]; this has the effect of distorting the crystal lattice (usually reducing the space symmetry of the magnetic film), leading to significant changes in the magnetic anisotropies but the changes in the magnetic moment are usually less dramatic. The issue of the variation of the magnetic moment with different tensile and compressive strains has been addressed theoretically by considering distortions to the equilibrium lattice, e.g. by Peng and Jansen [773], Fox and Jansen [806] and Herper *et al* [772] for the face centred tetragonal and trigonal Fe, by Fox and Jensen for trigonal and tetragonal Co [805] and by Jansen [807] for tetragonal Ni. Peng and Jansen [773] have studied the evolution of the electronic structure of the face centred tetragonal Fe for several c/a ratios of the tetragonal lattice constants to include both the fcc and bcc phases. They find that the fcc is the state of lowest energy, in contrast to the fact that the low temperature equilibrium phase of Fe is the bcc phase, again pointing to the difficulty of LDA to predict the properties of Fe. The fcc phase lies in a low magnetic moment in the volume-c/a phase diagram, while the bcc point lies in a high magnetic moment region, which is fairly insensitive both to uniform volume variations and to tetragonal distortions.

5.4. Metastable magnetic and crystalline phases

While the ground state crystalline and magnetic ordering are intimately related, the effect of thermal excitations adds an extra layer of complexity that leads to the presence of different crystallographic and magnetic equilibrium states. Since the relatively localized 3d bands actively participate in chemical bonding (i.e. the equilibrium lattice structure) and are largely responsible for the magnetic properties of the 3d transition metals, such strong correlation between magnetism and structure is to be expected, beyond the arguments related to volume and exchange energy. In bulk materials, this results in a phase diagram with a rich variety of crystalline and magnetic phases as a function of temperature (and pressure), as listed in table 19 for Fe, Co and Ni.

The crystalline phase diagram of Fe is the more varied of the 3d ferromagnetic transition metals [799]. Fe orders in the bcc structure for temperatures up to $T_{\alpha\to\gamma} = 1183$ K (α-Fe), at which point it changes to the fcc γ phase; it reverts to the bcc (δ) phase at temperatures above $T_{\gamma\to\delta} = 1663$ K up to the melting temperature [799]. α-Fe is ferromagnetic below $T_c = 1044$ K [238], above which it reverts to a paramagnetic state [808] up to $T_{\alpha\to\gamma}$ at which point it transforms to the paramagnetic γ-Fe phase. The δ-Fe phase is also paramagnetic [809]. Fcc γ-Fe is believed to be an antiferromagnet at 0 K with a small magnetic moment (0.5–0.7 μ_B/atom), which is thermally excited to a high magnetic moment (2.8 μ_B/atom) paramagnetic state at higher temperatures by a Schottky type excitation process [810–812]. Fcc Fe has been stabilized at room temperature as precipitates in a Cu matrix [810, 813–816], in multilayers [817] or by epitaxial growth on fcc surfaces (see section 5.5). At high pressures, bulk Fe stabilizes in the paramagnetic ϵ hcp phase [799, 809], but thin film hcp Fe films have been observed at atmospheric pressure upon deposition on KCl or NaCl followed by irradiation with He ions [818] and has since been observed in Fe/Ru and Fe/Re superlattices [819, 820].

Bulk Co exhibits only two stable crystal phases, both close packed [799]. The low temperature equilibrium structure of Co is the ferromagnetic α hcp phase, which transforms to the ferromagnetic fcc β phase at 710 K [409]. The β-Co phase, which becomes paramagnetic at 1388 K in the bulk, has a slightly larger magnetic moment per atom than the hcp phase [574, 663]. Another Co phase observed experimentally is the bcc phase, first grown as thin films in polycrystalline Co/Cr multilayers [821] and epitaxially on GaAs [722, 723, 822]; this system will be considered in more detail in section 5.6.

Table 17. Pressure dependence of the magnetic moment of Fe, Co and Ni. The value of 9.804 m s^{-2} for the standard acceleration of gravity was used for unit conversion to cgs. Values for σ_0 (the mass magnetization at 0 K) are from [238], while the values for the isothermal compressibility $\kappa_T = -V^{-1}(\partial V/\partial P)_T$ are those used in the cited reports for the determination of $\kappa_m = \sigma_0^{-1}(\partial\sigma/\partial P)_T$. The quantity calculated in the 5th column is the relative change in magnetic moment with relative change in volume with respect to the equilibrium values, $-\kappa_m/\kappa_T = (\partial(\sigma/\sigma_0)/\partial(V/V_0))_T$. ΔP is the experimental pressure range investigated.

System	σ_0 (emu g^{-1})	κ_T (μbar^{-1})	κ_m (μbar^{-1})	$-\kappa_m/\kappa_T$	ΔP (kbar)	References
bcc Fe	221.71	0.612	−0.316	0.516	0.4	[774]
p-bcc Fe	221.71	0.598	−0.310	0.518	11	[775]
hcp Co	162.55	0.539	−0.218	0.404	4.6	[776]
p-fcc Ni	58.57	0.542	−0.296	0.546	0.4	[774]
p-fcc Ni	58.57	0.539	−0.243	0.451	11	[775]

Table 18. Bulk theoretical ground state values for κ_m and $-\kappa_m/\kappa_T = \partial(\sigma/\sigma_0)/\partial(V/V_0)$.

System	a_0 (Å)	μ_0/atom (μ_B)	κ_T (μbar^{-1})	κ_m (μbar^{-1})	$-\kappa_m/\kappa_T$	References
bcc Fe	2.79	2.15	0.461	−0.49	—	[802]
bcc Fe	2.86	2.153	—	−0.525	0.86	[768]
bcc Fe	2.76	2.100	0.376	−0.305	0.81	[771]
bcc Fe	2.76	2.06	0.417	−0.343	0.82	[769]
bcc Fe	2.83	2.136	—	−0.612	1.00	[764]
bcc Fe	2.87	2.05	—	−0.582	0.95	[773]
bcc Fe	2.25	2.17	0.575	−0.421	0.73	[772]
bcc Fe	2.84	2.17	0.538	−0.397	0.74	[803]
hcp Co	2.50[a]	1.60	0.452	−0.172	0.38	[803]
fcc Co	3.46	1.56	0.417	−0.71	—	[802]
fcc Co	3.50	1.560	—	−0.175	—	[804]
fcc Co	3.50	1.531	—	−0.378	0.70	[764]
fcc Co	3.52	1.51	0.422	−0.190	0.45	[805]
fcc Co	3.53	1.64	0.463	−0.231	0.50	[803]
bcc Co	2.80	1.655	—	−0.143	—	[804]
bcc Co	2.82	1.62	0.398	−0.177	0.44	[805]
bcc Co	2.82	1.73	0.478	−0.230	0.48	[803]
fcc Ni	3.47	0.59	0.441	−0.21	—	[802]
fcc Ni	3.52	0.62	0.503	−0.282	0.56	[803]
bcc Ni	2.80	0.53	0.510	−0.338	0.66	[803]

[a] $c/a = 1.62$.

Bulk Ni is fcc for all temperatures, but other phases have been synthesized as thin films and nano-crystallites, namely, in the hcp [799] and bcc phases [799, 823–825] (see section 5.7).

As already suggested, many of these crystal phases can be induced at normal pressure and temperature when grown as thin films or as small nanocrystals [719]. These structures are interesting in that they may exhibit properties which could be of technological interest and also because they provide model systems on which to test our current understanding of the fundamental relations linking magnetism to the electronic structure of metals. In the following sections 5.5–5.7 we shall briefly overview the magnetic moments of the 3d transition metals Fe, Co and Ni for the crystal phases that have been stabilized as thin films. Although much work has been devoted to this challenging problem, many issues remain open, partly as a consequence of the sensitivity of the magnetism of thin films to structural properties, such as interface reaction and roughness, presence of impurities or adsorbates, film morphology and strain. On the other hand, the experimental difficulty of accurately measuring the magnetic moment of thin films also prevents some of these questions from being answered more conclusively, even though several techniques have been developed exclusively for the measurement of the magnetic properties of thin films and interfaces, such as polarized neutron reflectometry (PNR) and x-ray magnetic circular dichroism (XMCD).

The magnetic moments of ultrathin Fe, Co and Ni films have been studied for a range of interface materials and for different crystallographic phases and orientations. These structures are often grown by atom deposition from the vapour phase onto the substrate in ultrahigh vacuum conditions by heteroepitaxy [83, 96, 831–834]. This is possible for a range of systems that exhibit a close crystallographic lattice match between the substrate and the film. These films are single crystalline, as opposed to the polycrystalline films that result from evaporation onto an amorphous or polycrystalline surface or when the lattice mismatch is too large to allow epitaxy or when still the metal film does not interact (bond) with the substrate. Epitaxial films have a much larger crystallite size and a preferential crystal orientation, although some degree of mosaicity (deviation from the ideal crystallographic structure) is always present in macroscopic films. They therefore exhibit less structural defects than polycrystalline films and have an effective magnetic anisotropy, which is usually averaged out (and therefore absent) in polycrystalline films. Needless to say, the magnetic properties depend sensitively on the preparation conditions, since contaminants can change the magnetic and/or structural properties of thin films and mask

Table 19. Crystal phases for Fe, Co and Ni. Data are representative of the bulk crystal and are collected from [573] except for those indicated in footnotes. NM—non-magnetic.

Element	phase	T (K)	P (bar)	a (Å)	c (Å)	μ_0/atom (μ_B)
α-Fe	bcc	293	1	2.866	—	2.226[a]
γ-Fe	fcc	1183	1	3.647	—	AF[b]
δ-Fe	bcc	1663	1	2.932	—	NM
ϵ-Fe	hcp	296	1.3×10^5	2.468	3.956	NM
α-Co	hcp	296	1	2.507	4.070	1.729[a]
β-Co	fcc	296	1	3.545	—	1.75[c]
Co	bcc	300	1	2.82[d]	—	1.50[e]
β-Ni	fcc	296	1	3.524	—	0.619[a]
Ni	hcp	296	1	2.50	4.05	
Ni	bcc	296	1	2.78	—	NM[f]

[a] [609, 613, 828].
[b] [810–815].
[c] [574, 663].
[d] [722, 723, 826, 827].
[e] [619] at room temperature.
[f] Theory [764, 829, 830].

the intrinsic properties of the system under study. In particular, it is important to rule out the possibility of chemical reaction or interdiffusion between the magnetic film and the substrate. For example, one of the motivations behind the study of the Fe system on Ag and Cu substrates was the possibility of growing high quality, optically flat films (with an interface roughness of ∼15 Å and correlation lengths of the order of 200 Å for continuous Fe films [268, 835]) with limited interdiffusion at the interface [514, 836, 837] (although with quite complex structural changes for the case of Fe/Cu [514, 836, 838–843], and for Fe grown on Ag (0 0 1) single crystals complete coverage of the substrate is achieved only for films thicker than ∼5 ML, as deduced from the appearance of RHEED oscillations at this stage of growth [823]).

5.5. *Magnetic moments of thin Fe films*

Fe thin films in the bcc phase have been grown as a single crystal in many (suitably prepared) substrates, such as Ag(0 0 1) [78, 845–848], MgO(0 0 1) [849–851], Au(0 0 1) [321, 469, 852, 853], Pt(0 0 1) [854], Cr(0 0 1) [854, 855], W(1 1 0) [273, 447, 856], W(1 0 0) [856, 857], GaAs(0 0 1) [486, 487, 858–861], GaAs(1 1 0) [862–864], Ge(0 0 1) [142, 865–868], Ge(1 1 1) [869, 870] and ZnSe [871–875] and when conditions for epitaxial growth are not met, it grows in a bcc polycrystalline form. A systematic study of the magnetic moment of bcc Fe/Ag(0 0 1) in contact with different materials, Ag, Au, Cu, Pd and Ni, was conducted by Bland *et al* [268, 876–879] (this study on high quality samples with flat interfaces clarified an earlier report of a strongly reduced magnetic moment for Fe/Ag(0 0 1) films [880, 881], where the large interface roughness affected the deduced magnetic moment from PNR due to large diffuse scattering). In all cases the magnetic moment per atom of Fe is found to be significantly enhanced with respect to the bulk value, in agreement with ferromagnetic resonance (FMR) measurements performed on the same samples [268, 878, 879]. For the Ag/5.5 ML Fe/Ag(0 0 1) sandwich, Ohnishi *et al* [882] predicted a moment of 0.08 μ_B/atom for the interface Ag layer and a layer averaged moment per Fe atom of 2.4 μ_B/atom; while Ag polarization was too small to be measured, the value for Fe is close to that observed experimentally, $\mu^{Fe} = 2.58 \pm 0.09$ μ_B/atom. The interface moment of Fe in contact with Au is not significantly different from that of the Ag/Fe/Ag structure. The Pd/Fe sample exhibits the largest net moment, although an interface moment for the Pd layer could not be excluded from the PNR data. Polarization of the Pd atoms at the Pd/Fe interface has been reported using other techniques, such as VSM (vibrating sample magnetometry) [883], BLS (Brillouin light scattering), FMR (ferromagnetic resonance) [884], SQUID [885] and XMCD [886]. For the Cu/Fe system, the moment of bcc Fe is still enhanced, in agreement with the results of *ab initio* calculations of Niklasson *et al* [694]. A summary of the results is presented in figure 17, where the magnetic moment per atom of Fe is plotted against the Fe thickness. It is seen that the experimental values are in general higher than the predicted values for the 5–6 ML thick films, but that good agreement is obtained for the 10 ML film [268]. This was attributed to the effect of interface roughness on reducing the effective local coordination of Fe atoms at the interface, leading to further enhancement of the magnetic moment. Detailed measurements of the variation of the magnetic moment of 1 and 4 ML Fe(1 1 0)/Au(1 1 1) were performed by Lugert *et al* [276], showing a large enhancement of the ground state moment of Fe, of 2.95 μ_B/atom and 2.56 μ_B/atom for the 1 ML and 4 ML films, respectively.

The Fe/W system is a particularly interesting one in that the difference in surface energies strongly favours Fe wetting of the W surface [83], such that relatively smooth epitaxial Fe films can be produced, despite the large misfit strain between these systems of $\eta = (a^W - a^{Fe})/a^{Fe} = 10.4\%$, where $a^W = 3.165$ Å and $a^{Fe} = 2.866$ Å.[9] The

[9] An alternative definition for the lattice mismatch is also used, $\tilde{\eta} = (a^f - a^s)/a^s = -\eta(a^s/a^f)$, where a^s and a^f are the lattice constant of the substrate and film systems, respectively [83, 887–889]. The expression in the main text has the advantage that the film strain is then given by $\epsilon = \eta$, by definition [712, 890], although experimentally the alternative definition is more convenient.

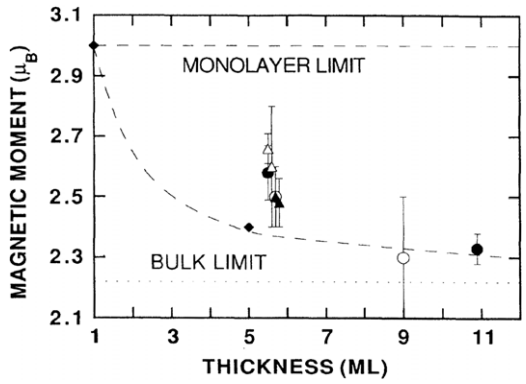

Figure 17. Values for the layer averaged moment per bcc Fe atom deduced from PNR measurements [268], compared with the predicted values [882] for the layer averaged moment of a 1 ML Fe/Ag(0 0 1) and 5 ML Fe/Ag shown as solid diamonds [268]. The Fe/Ag data are shown as full circles, the Cu/Fe as solid triangles and the Pd/Fe as open triangles. The dashed line is a guide to the eye. Reprinted with permission from J A C Bland, C Daboo, B Heinrich, Z Celinski and R D Bateson 1995 Enhanced magnetic moments in bcc Fe films *Phys. Rev.* B **51** 258. Copyright (1995) by the American Physical Society.

evolution of the Fe film growth has been studied in detail with STM for various deposition temperatures [891–895] and shows that at room temperature the first monolayer grows by nucleation and expansion of monolayer islands till near coalescence, when double layer islands nucleate; at an elevated temperature, growth proceeds by step flow [891, 892]. Pseudomorphic growth is attained up to 1 ML for the (1 1 0) surface [174, 891–893, 896] and up to 3 ML for Fe/W(1 0 0) [174, 203, 897]. The presence of a large strain strongly modifies the magnetic properties of monolayer-thick Fe films, including magnetic anisotropies [174], domain walls and critical behaviour, as discussed earlier (sections 3 and 4). Pasyuk *et al* [898] have measured the room temperature magnetic moment of a 6 Å epitaxial bcc Fe(1 1 0) film buried between W(1 1 0) layers using PNR and determined the temperature dependence of the magnetization using SQUID magnetometry to determine the absolute ground state magnetic moment of the Fe film. The value obtained, 2.1 μ_B/atom, slightly reduced compared with the bulk value (2.226 μ_B/atom), is in agreement with theoretical calculations predicting slightly reduced moments for a monolayer of Fe(1 1 0) on W(1 1 0) due to hybridization effects [681] but not with previous experimental results obtained by conversion electron Mössbauer spectroscopy on a Fe/W(1 1 0) monolayer capped with Ag, where an enhanced magnetic moment of $\mu_0 = 2.53$ μ_B/atom was observed [899] (a slight reduction was also predicted upon Ag capping [681]). More recent *ab initio* calculations by Andersen and Hübner [734] suggest instead that the moment of 1 ML Fe/W(1 1 0) is enhanced with respect to the bulk value, from 2.2 μ_B/atom to 2.56 μ_B/atom. Other substrates have been used for the epitaxial growth of thin Fe films; in particular, MgO(1 0 0) (where a bulk magnetic moment was found, irrespective of the film thickness [900]) and V(1 1 0) where a reduction of the magnetic moment is observed for an uncapped 6 Å Fe film measured using an *in situ* PNR set-up [901, 902].

Due to the importance that the interface between magnetic films and semiconductors holds for the development of the emerging field of spintronics [17–20, 142, 143], there is a growing interest in the characterization of ferromagnetic/semiconductor heterostructures. Spintronics device performance is expected to depend sensitively on the interface quality [144–147], and since epitaxial films are more likely to meet the required quality standards, much attention has been devoted to the study of metal/semiconductor epitaxy and to interface magnetic moments. One promising candidate is Fe, which has been shown to grow epitaxially on GaAs(1 0 0) [486, 487, 858–861, 912] and GaAs(1 1 0) [862–864, 912] substrates (see Wastlebauer and Bland [489] for a review of the magnetic properties of Fe grown on GaAs and on other related semiconductor substrates). Initial reports seemed to indicate the presence of Fe magnetic dead layers at the semiconductor interface, attributed to the formation of Fe arsenides [486, 912, 913]; however, later reports, while suggesting strong reductions in the magnetic moment in As rich surfaces [914, 915], showed an almost bulk-like interface moment [146, 487, 916], or at most only slightly reduced [917–919] moments, for Fe films grown on the As depleted GaAs(0 0 1)-$p(4 \times 6)$ reconstructed surface. Theoretical *ab initio* studies of Fe thin films on GaAs surfaces by Mirbt *et al* [920] confirm the sensitivity of the Fe magnetic moment to the particular GaAs surface arrangement; in particular, due to the lower binding energy of Fe–As with respect to Ga–As and Ga–Fe, the lowest energy configuration for an Fe atom at the As terminated surface is to replace Ga positions, with the Ga atom being displaced to an interstitial position. The magnetic moment of Fe is relatively unaffected by neighbouring Ga atoms, but strongly reduced if the number of As neighbours is larger or equal to two due to strong pd hybridization. This study also confirms the tendency of As segregation into the Fe film and its surface, as observed experimentally [920–922]. Figure 18(*a*) shows the values for the magnetic moments reported for Fe/GaAs(0 0 1), not included in table 20.

A closely related system is Fe/InAs(0 0 1), which has been the focus of large interest recently as a more promising alternative to Fe/GaAs(0 0 1) for applications. This is due to the smaller energy band gap of InAs, which favours the formation of ohmic contacts with Fe [931–933]; a more significant spin–orbit interaction in InAs quantum wells (the Rashba spin–orbit term, caused by the macroscopic electric field of the quantum well potential, is negligible in GaAs quantum wells compared with k^3 splitting originating from the lack of inversion symmetry in zinc-blende structures [934–936], while it is important in InAs quantum well structures [937–939]), allowing in principle a better control of spin currents in the proposed spin-polarized field effect transistor [940]; InAs has a higher carrier mobility [941, 942] and Fe/InAs(0 0 1) has a lower interfacial reactivity compared with Fe/GaAs and Fe/InP [532, 943]. Despite its larger lattice mismatch compared with the Fe/GaAs(0 0 1) system, Fe grows epitaxially on InAs(0 0 1) in a three-dimensional (island) mode [930–932, 944]. As in the case of Fe/GaAs(0 0 1), we expect the properties of thin Fe/InAs(0 0 1) films to depend sensitively upon the substrate preparation and growth conditions. In fact, growth at elevated

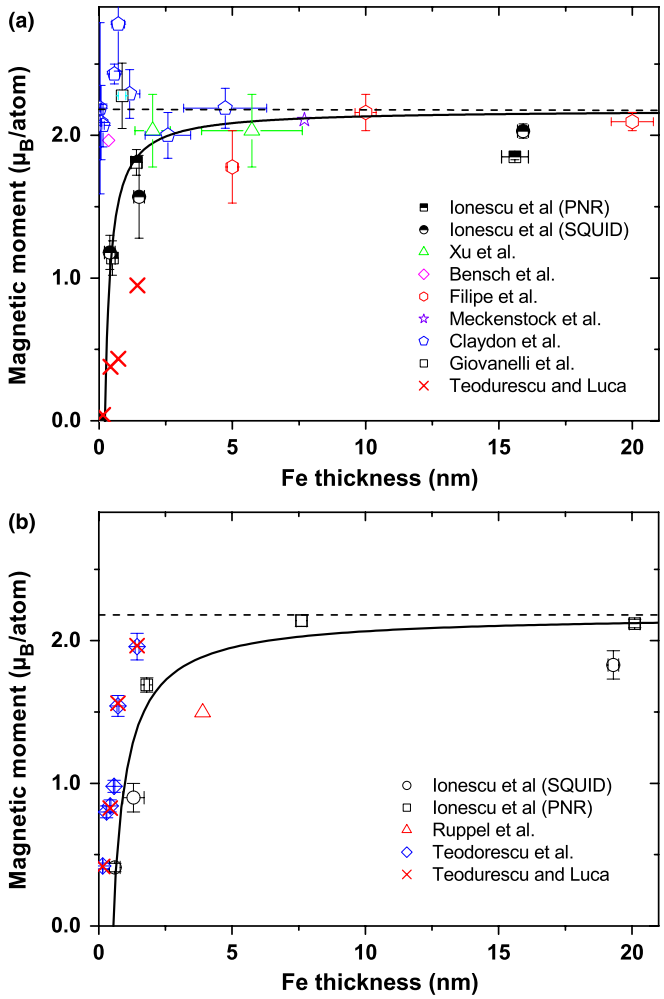

Figure 18. Room temperature magnetic moment of (*a*) Fe/GaAs(0 0 1) and (*b*) Fe/InAs(0 0 1) films as a function of Fe film thickness. Data collected from Ionescu *et al* [923, 924], Xu *et al* [487], Bensch *et al* [472], Filipe *et al* [915], Meckenstock *et al* [925], Claydon *et al* [926, 927], Giovanelli *et al* [922, 928], Teodurescu and Luca [929], Teodurescu *et al* [532, 533] and Rupel *et al* [930].

temperatures (∼175 °C) is found to be more favourable for epitaxy than growth at lower temperatures (RT) [932, 945]. XPS studies by Teodurescu *et al* [532, 533, 945] for films grown at 175 °C show that while In diffusion is unimportant, As does diffuse into the Fe film and a monolayer of As is believed to float over the Fe film and act as a surfactant promoting the epitaxial growth of Fe (the same study suggests that Fe/InAs(0 0 1) grows initially in island mode and reverts to layer-by-layer growth mode for thicknesses above a few monolayers). This is also observed for Fe films grown at room temperature [930, 933], but with the Fe growth proceeding in a three-dimensional mode and, in addition, the study of Schieffer *et al* [933] found evidence for significant substrate disruption, with In atoms segregating into the Fe film and its surface; their results did not depend on the InAs(0 0 1) surface preparation (either by sputtering and annealing cycles or MBE-prepared surfaces). In addition, a recent comparative study of the Fe/InAs(0 0 1) interface for two growth temperatures (23 and 175 °C) by Uoh *et al* [534] suggests that while growth at elevated temperatures does promote Fe epitaxy, this is at the cost of increased reaction at the interface and a larger diffusion of As over the Fe film. However, despite these complications, it appears that the magnetic moment of Fe grown on InAs(0 0 1) is fairly robust; for Fe/InAs(0 0 1) thin films grown at 175 °C, XMCD results suggest that the equivalent of the 0.7 ML Fe interface layer reacts with InAs and is magnetically inert, while an intermediate FeAs compound layer with a low magnetic moment (1.0 μ_B/atom) exists up to 3 ML and thicker films attain bulk magnetic moments [532, 533]. An enhancement of orbital magnetization of three times the bulk value is observed for films up to 10 ML [532, 533, 946], as also observed in Fe/GaAs(0 0 1) films [926, 947], which could be explained if the majority E state (formed by linear combinations of d wavefunctions with quantum numbers $m_l = \pm 2$ and 0) is empty such that the total orbital moment arises from the minority spin DOS only [948]. Ruppel *et al* [930] have measured the magnetic moment of a 3.9 nm Fe/InAs(0 0 1) film grown at RT with SQUID magnetometry at 5 K, obtaining a magnetization of $(1.2 \pm 0.3) \times 10^3$ emu cm^{-3} (1.52 μ_B/atom), which is reduced compared with the bulk value (2.226 μ_B/atom); their XPS study also suggests the formation of an FeAs interface layer, which they assume to be responsible for the reduction in the Fe magnetic moment. More recent experimental results have been performed using PNR and SQUID techniques [923, 924] showing that the room temperature magnetic moment of Fe is bulk-like above 5 nm thickness and is reduced at lower thicknesses; by assuming a surface and bulk moment contribution to the total moment, a magnetic dead layer of 3.7 ML is obtained; this thickness coincides with STM and MOKE results showing that ferromagnetic order is a consequence of island coalescence at around this thickness value [538] (see section 3.1). This is in slight disagreement with the results of Teodorescu *et al* [532, 533], which suggest that a 1 ML film is already magnetically active (under a field of 400 Oe); this could be due to different surface preparation and growth conditions that may have resulted in smoother surfaces for the samples prepared by Teodorescu *et al* [532, 533]. In fact, when all results for the magnetic moment of Fe/InAs(0 0 1) available in the literature are plotted together, it is observed that they seem to be in good agreement, in spite of the different sample preparations and measurement techniques (see figure 18(b)). Few theoretical studies have been performed for this system; Sacharow *et al* [949] have studied the magnetic and electronic properties of an Fe monolayer on InAs(1 1 0) using the density functional approximation (FLAPW). They find that the Fe layer retains not only its structural integrity but also a large spin polarization value of 80%; at first sight, this seems to be in disagreement with the experimental results mentioned above, but one must bear in mind that the calculations correspond to the ground state, to a different InAs surface plane and do not consider the experimental complications related to surface conditions, although their structural results are found to be in good agreement with experimental STM studies of Fe/InAs(1 1 0) [950].

Bulk fcc Fe has a room temperature lattice constant $a^{\text{fcc Fe}} = 3.59$ Å [207, 815, 840, 951, 952], which is very close

Table 20. Values for the magnetic moment of Fe thin films for different interface materials. Thickness in ML unless specified otherwise; PNR—polarized neutron reflection; TM—torsion magnetometry; SQUID—superconducting quantum interference device magnetometry; XMCD— x-ray magnetic circular dichroism spectroscopy; AGFM—alternating gradient force magnetometer; VSM—vibrating sample magnetometry; CEMS—conversion electron Mössbauer spectroscopy. $\langle D \rangle$ is the average particle diameter.

Sample	Phase	μ^{Fe}/atom (μ_B)	T (K)	Tech.	References
20 Au/7 Ag/5.5 Fe/Ag(0 0 1)	bcc	2.58 ± 0.09	4	PNR	[268, 876–879]
20 Au/7 Ag/10.9 Fe/Ag(0 0 1)	bcc	2.33 ± 0.05	4	PNR	[268, 876–879]
52 Au/5.7 Fe/Ag(0 0 1)	bcc	2.5 ± 0.1	4	PNR	[268, 876–879]
20 Au/9 Fe/Ag(0 0 1)	bcc	2.3 ± 0.2	4	PNR	[268, 876–879]
20 Au/7 Cu/5.8 Fe/Ag(0 0 1)	bcc	2.48 ± 0.08	4	PNR	[268, 876–879]
42 Au/8 Cu/5.7 Fe/Ag(0 0 1)	bcc	2.5 ± 0.1	4	PNR	[268, 876–879]
20 Au/7 Pd/5.6 Fe/Ag(0 0 1)	bcc	2.66 ± 0.05	4	PNR	[268, 876–879]
42 Au/7 Pd/5.7 Fe/Ag(0 0 1)	bcc	2.6 ± 0.2	4	PNR	[268, 876–879]
24 Au/3 Ni/5 Fe/Ag(0 0 1)	bcc	2.6 ± 0.1[a]	4	PNR	[268, 876–879]
1 Fe(1 1 0)/Au(1 1 1)	bcc	2.89	0	SQUID	[276]
4 Fe(1 1 0)/Au(1 1 1)	bcc	2.56	0	SQUID	[276]
200 Å Au/4 Å Fe/MgO(0 0 1)	bct	0 (2.2 ± 0.2)	RT (40)	PNR	[900]
200 Å Au/6 Å Fe/MgO(0 0 1)	bct	<0.5 (2.2 ± 0.2)	RT (40)	PNR	[900]
200 Å Au/8 Å Fe/MgO(0 0 1)	bct	2.0 (2.2 ± 0.2)	RT (40)	PNR	[900]
Ag/1 Fe/W(1 1 0)	bcc	2.53 ± 0.12	0	CEMS, TM	[447]
100 Å W/6 Å Fe/W(1 1 0)[b]	bcc	1.80 ± 0.05	RT	PNR	[898]
70 Å Au/Fe/140 Å Ni/SiO_2[c]	bcc	$\sim$2.1	RT	PNR	[898]
6 Å Fe(1 1 0)/V(1 1 0)[d]	bcc	0	80	PNR	[901, 902]
$\sim$60 FeÅ/$(C_8H_8)_n$-poly	bcc	2.07	n.a.	XMCD	[320]
70 Å Au/Fe/140 Å Ni/SiO_2[e]	fcc	$\sim$0.2	RT	PNR	[903]
10 Å Fe/V(1 1 0)		1.3	80	PNR	[903]
19.5 Å Fe/V(1 1 0)		1.8	110, 300	PNR	[903]
2.9 Å Fe/Cu(1 1 1)	fcc	0.6	0	TM	[904]
6.5 Fe/Cu(0 0 1)	fcc	0.3	5	SQUID	[905]
6.5 Fe/$Cu_{80}Au_{20}$(0 0 1)	fcc	2.0	5	SQUID	[905]
3.4 Fe/Cu(0 0 1)	bct	3.56 ± 0.70	n.a.	XMCD	[906]
3.8 Fe/Cu(0 0 1)	bct	3.71 ± 0.75	n.a.	XMCD	[906]
1–4 Fe/Cu(0 0 1)	bct	2.8 ± 0.15[f]	110	XMCD	[907]
5–10 Fe/Cu(0 0 1)	bct	0.8 ± 0.15[f]	110	XMCD	[907]
1–4 Fe/Co(0 0 1)	bct	3.2 ± 0.15	110	XMCD	[907]
5–10 Fe/Co(0 0 1)	bct	1.2 ± 0.15	110	XMCD	[907]
(0 0 0 1)[4–12 Å Fe/4–52 Å Ru]$_N$	hcp	2.1	4.2	SQUID	[819, 908]
(1 0 2)[7.5 Å Fe/3.5–18 Å Ru]$_{20}$	hcp	0	RT	XMCD	[909]
[8 Å Fe/9-35 Å Re]$_N$	hcp	2.2	RT	XMCD	[820]
poly-[0.7–4.7 nm Fe/4.0 nm Ru]$_8$	hcp	2.66	RT	AGFM	[910]
$Fe_{75}C_{20}$ particles, $\langle D \rangle = 4$ nm	hcp	1.65	0	VSM	[911]

[a] $\mu^{Ni} = 0.6 \pm 0.1\ \mu_B$/atom.
[b] 100 Å W/6 Å Fe(1 1 0)/550 Å W/Al_2O_3(1 1 $\bar{2}$ 0); $\mu^{Fe} = 2.1 \pm 0.1\ \mu_B$/atom at 0 K, extrapolated from SQUID data.
[c] $t^{Fe} = 49, 53, 84, 87$ Å; $\mu^{Ni} \approx 0.5\ \mu_B$/atom.
[d] *In situ* PNR.
[e] $t^{Fe} = 7, 13, 17, 24, 26$ Å; $\mu^{Ni} \approx 0.5\ \mu_B$/atom.
[f] Spin moment only.

to the lattice constant of Cu (lattice mismatch $\tilde{\eta} = -0.6\%$) and in fact the fcc phase of Fe has been stabilized in fcc surfaces such as Cu(0 0 1) [269, 836, 838, 953–957], Cu(0 1 1) [838, 958], Cu(1 1 1) [838, 904, 957, 959–961], Cu(3 1 1) [962], fcc Co(0 0 1) [963, 964], Ni(0 0 1) [817, 963], $Cu_{1-x}Au_x$(0 0 1) [960], $Cu_{1-x}Au_x$(1 1 1) [905], C(0 0 1) [965] and Pd(0 0 1) [966]. As mentioned before, the fcc phase of Fe shows several competing magnetic phases in close proximity, and one may expect the magnetism of this crystalline phase to be particularly unstable [716]. For instance, Marcus and Moruzzi [766] find that a 5% expansion in the fcc lattice of Fe from the equilibrium position favours a ferromagnetic state, a result which is consistent with other *ab initio* calculations [771, 772, 967, 968]. It turns out, indeed, that the results concerning the exact structure and magnetism of fcc Fe thin films have been surrounded by controversy, with divergent interpretations of the experimental results being proposed, particularly for Fe films grown on Cu(0 0 1) substrates. It emerges that there is a strong correlation between film morphology and magnetism, with different magnetic phases being associated with different

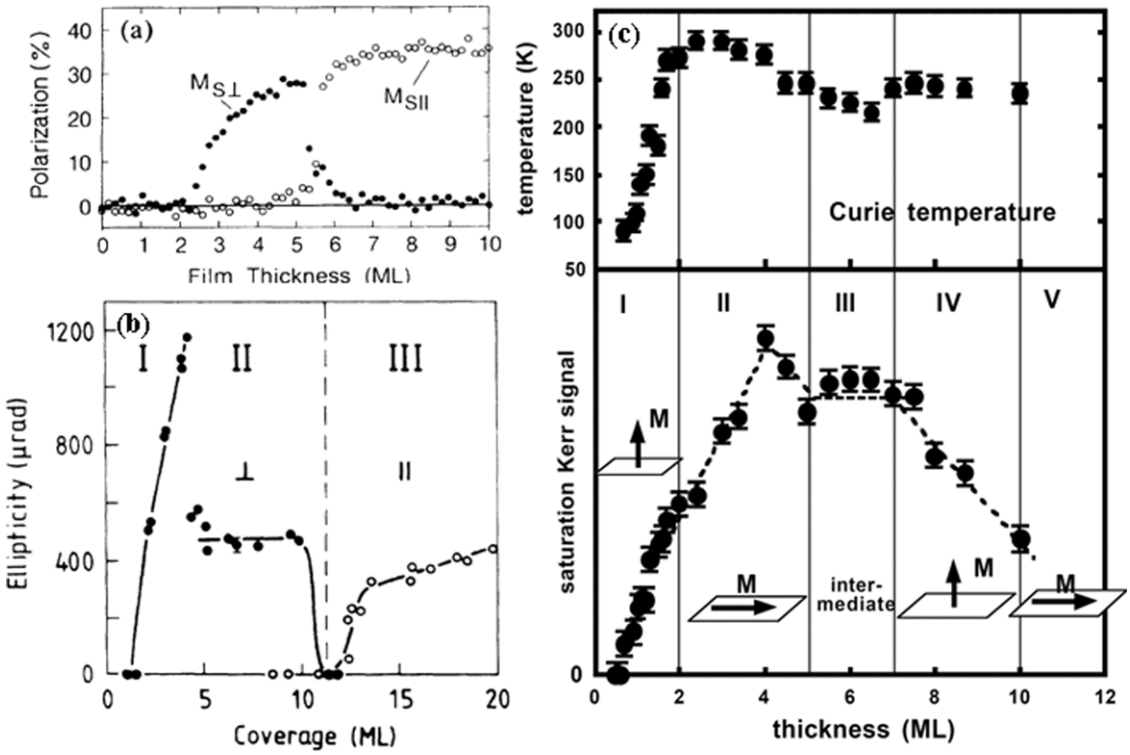

Figure 19. (*a*) Variation of the perpendicular and parallel component to the film of the spin polarization of fcc Fe/Cu(0 0 1) films grown at 90 K and annealed at 300 K (measurements at 175 K, adapted from [973]). (*b*) Thickness dependence of the longitudinal (∥) and polar (⊥) Kerr ellipticities at saturation extrapolated to 0 K for fcc Fe/Cu(0 0 1) films grown at 300 K (adapted from [464]). (*c*) Variation of the Curie temperature (top panel) and saturation Kerr signal (bottom panel) versus thickness of fcc Fe/Cu(0 0 1) films deposited by pulsed-laser deposition (adapted from [957]). Reprinted with permission from R Allenspach and A Bischof 1992 Magnetization direction switching in Fe/Cu(1 0 0) epitaxial films: temperature and thickness dependence *Phys. Rev. Lett.* **69** 3385. Copyright (1992) by the American Physical Society; from J Thomassen, F May, B Feldmann, M Wuttig and H Ibach 1992 Magnetic live surface layers in Fe/Cu(1 0 0) *Phys. Rev. Lett.* **69** 3831. Copyright (1992) by the American Physical Society; and from J Shen, Z Gai and J Kirschner 2004 Growth and magnetism of metallic thin films and multilayers by pulsed-laser deposition, *Surf. Sci. Rep.* **52** 163. Copyright (2004), with permission from Elsevier.

stages of the film growth and with different sample growth conditions (such as growth temperature [836, 838, 843, 956, 969, 970], the presence of adsorbates [464, 836, 971] and the growth technique [957]) yielding fcc Fe films with disparate morphologies and magnetic properties [394]. The available literature suggests the separation of fcc Fe films into three groups, depending on the growth temperature for films grown by MBE [394, 969] and between films grown by MBE and laser ablation [394, 957]. Fe films grown at low temperatures by MBE (100–200 K) and subsequently annealed to room temperature are ferromagnetic and exhibit a spin-reorientation transition at about 5 ML from a perpendicularly magnetized state to a state of in-plane magnetization [513, 516, 839, 843, 952, 969, 972, 973]. This behaviour is illustrated in figure 19(*a*) from the results of Allenspach and Bischof [973], which shows the variation of the parallel and perpendicular spin polarization components (proportional to the spontaneous magnetization) with Fe thickness; below 2 ML no magnetic signal is observed, which is attributed to a reduced Curie temperature [514]. Fe films grown at room temperature by MBE, however, are fct and ferromagnetic below ∼5 ML (in this thickness range the Fe film is ferromagnetic with dominant perpendicular magnetic anisotropy), change to a relaxed fcc phase in the range between 5 and 11 ML, which is non-magnetic in the bulk of the film but has a single magnetic layer at the surface, and for thicknesses above 11 ML, it reverts gradually to the bcc phase [207, 269, 464, 716, 905, 952, 956, 964, 974–981], see figure 19(*b*) (fcc Fe films grown on fcc Co(0 0 1) and Ni(0 0 1) surfaces are found to exhibit similar magnetic and structural behaviour [963, 964, 977, 978, 982, 983]). Indeed, Müller *et al* [716, 952] argued that below 5 ML, the Fe films grown at both low and room temperature are in the same ferromagnetic state, in an expanded fct structure with an atomic volume of the order of 12.1 $Å^3$, favouring ferromagnetism; for larger thicknesses, the RT deposited films have a relaxed fcc structure in the bulk of the film and an expanded ferromagnetic surface layer which solely contributes to the magnetic signal for films up to 10 ML thick, while for films deposited at low temperatures, the Fe films revert to the bcc(1 1 0) phase. However, later STM results seem to suggest instead that the low thickness range consists of a mixture of fcc and bcc phases, where the magnetic response arises from the bcc component [984]. Ellerbrock *et al* [976] have compared the magnetic properties of 3 and 7 ML fcc Fe/Cu(0 0 1) films grown both at 90 K and RT using Mössbauer spectroscopy and found that for both growth temperatures, the 3 ML Fe films are expanded fct ($c/a > 1$) in a high-spin state and the same result is found for the 7 ML film grown at low temperature; however, for the 7 ML Fe film

grown at RT, they found that the film is paramagnetic at 300 K and exhibits low-spin antiferromagnetism (with a sublattice magnetic moment smaller than 0.7 μ_B/per atom) at 45 K in the film interior. Qian *et al* [981] and Amemiya *et al* [985] suggest that this antiferromagnetism is of the spin-density wave type. Mössbauer spectroscopy results by Keavney *et al* [905] for 6.5 ML fcc Fe(0 0 1)/40 ML $Cu_{1-x}Au_x$(0 0 1) multilayers, where the interior 2.5 ML layer is composed of ^{57}Fe and therefore detected in Mössbauer spectroscopy, suggest the simultaneous presence of high- and low-spin fcc phases and attribute the increase in the average magnetic moment with the lattice constant (via x, from 0.3 μ_B/atom for $x = 0$ to 2.0 μ_B/atom for $x = 0.2$ [816,905]) to an increase in the high-spin moment population, rather than to an increase in the atomic moment of Fe, as expected from *ab initio* calculations (while not finding evidence for the presence of a bcc Fe phase in their structures). Dunn *et al* [906] have reported enhanced orbital and spin moments for 3.4 and 3.8 ML fct Fe/Cu(0 0 1) films grown at 120 K measured by XMCD, which are compared with values for 19 and 25 ML bcc films exhibiting moments close to the bulk bcc Fe. Schmitz *et al* [907] measured the magnetic moment (at 110 K) of fcc Fe/Cu(0 0 1) and fcc Fe/Co(0 0 1) films grown at room temperature; they find a spin moment of 3.0 μ_B/atom for Fe/Co(0 0 1) and 2.8 μ_B/atom for Fe/Cu(0 0 1) for thicknesses of 1–4 ML, while between 5 and 10 ML the average spin moment is 1.1 and 0.8 μ_B/atom for Fe/Co(0 0 1) and Fe/Cu(0 0 1), respectively, with the surface region being ferromagnetically ordered. Escorcia-Aparicio *et al* [978] studied the effect of roughness and growth temperature on the magnetic phase transition of fcc Fe/Co(0 0 1) and suggest that the differences observed between the low temperature and RT growth may be due to roughness in the film deposited at low temperatures. More recently, it has been shown that pulsed-laser deposition (PLD) can yield metallic films with improved surface morphology [957,961] and, in particular, Fe/Cu(0 0 1) films grown using this method (at room temperature) are found to grow in an almost ideal two-dimensional mode up to 10 ML, beyond which they revert to the bcc phase accompanied with surface roughening [986, 987]. Weinelt *et al* [988] have suggested that the high thermal energy characteristic of atom beams in PLD leads to enhanced surface mobility upon adsorption and intermixing and incorporation of Cu on the fcc Fe film, thus leading to a stabilization of the fcc Fe structure [394]; experimental results for thermally deposited 6-8 ML Fe/Cu(0 0 1) films also show significant intermixing within the four interface layers [989]. The magnetic properties are also found to be distinct from the MBE grown films: films between 0–2 ML and 7–10 ML are magnetized out of plane, while films 2–5 ML and beyond 10 ML (where the structure is dominated by the bcc phase) are magnetized in-plane, see figure 19(*c*) [957, 987]. The exact magnetic evolution underpinning these transitions remains unclear; for small thicknesses (much smaller than the light attenuation length), the saturation Kerr signal is approximately proportional to the magnetization (barring additional magneto-optic contributions that may arise in ultrathin films with modified spin–orbit coupling) and therefore the constant slope below 4 ML suggests that the films are uniformly magnetized while the plateau between 5 and 7 ML could indicate the presence of only three ferromagnetically active layers, but the complicated structural transformations occurring simultaneously with the magnetic transitions do not allow for definite conclusions [957, 987, 988].

The hexagonal closed packed (hcp) phase of Fe is the equilibrium phase of Fe at pressures above ∼130 kbar [990] and was first observed by Bancroft *et al* [991]. It is believed to be the phase present in the Earth's core and its magnetic properties are important for the understanding of Earth's geomagnetism, in particular, the dynamo causing Earth's magnetic field [992–994]. The ground state of ϵ-Fe is found to be non-magnetic, according to several Mössbauer studies [990, 995–1000] (Gilder and Glen [1001] suggest that ϵ-Fe micrometre-sized particles are either paramagnetic or ferromagnetic at room temperature, based on the observation of particle motion subjected to an external magnetic field). *Ab initio* calculations also suggest that at high pressures hcp Fe is non-magnetic [772, 803, 1002–1011], but for the pressure range close to the α–ϵ transition, several studies predict that antiferromagnetic configurations may be lower in energy [772, 1003, 1006–1008, 1010, 1011] (this has been suggested to be related to the observation of superconductivity in hcp Fe within a small pressure range between 150 and 300 kbar [1011–1016]). As a function of the unit cell volume, hcp Fe has a stable non-magnetic configuration for volumes below 10.8 Å^3 per atom, with a minimum at 10.3 Å^3, which is also close to the energy minimum for the antiferromagnetic configuration; for larger atomic volumes, antiferromagnetic states are lower in energy (several have been considered, from commensurate to incommensurate configurations [1010, 1011]) up to 12.2 Å^3 per atom, above which a high-spin ferromagnetic state is that of lower energy; the energy curve for this state has a minimum at around 12.2 Å^3 per atom and is therefore a metastable energy state [772, 1003, 1006, 1008] (these studies assume c/a close to the ideal hcp value, $\sqrt{8/3}$). Earlier work on hcp FeRu, FeOs and FeMn alloys suggested that hcp Fe may order antiferromagnetically [1017–1019], as also suggested by band structure calculations (the atomic volume of Fe in these alloys is of the order of 11.6 Å^3 [1018]). Part of the motivation for these *ab initio* studies was the experimental observation of ferromagnetic hcp Fe in Fe/Ru superlattices [819, 1020], where the estimated Fe atomic volume is much larger than the high pressure volume of hcp Fe. hcp Fe can be stabilized at NPT (normal pressure and temperature) as monolayer-thick films in Ru(0 0 0 1), Ir(1 1 1) and Rh(1 1 1) substrates [1021–1025], in superlattices involving Ir, Ru and Re spacer layers [819, 820, 908–910, 1020, 1026–1028] or yet as small particles (with a rather large C content of ∼20%) [911]. The results by Maurer *et al* [819, 908, 1020] suggest the Fe to be in the hcp phase with a volume cell of 12.8 ± 0.2 Å^3 per atom (that of high pressure hcp Fe is 11.3 Å^3) and SQUID magnetometry and Mössbauer spectroscopy suggest the hcp Fe to be ferromagnetic above 4 ML, with a magnetic moment of 2 μ_B/atom [1020, 1029]. However, results on the Fe/Ru superlattices have proven to be controversial, both regarding the exact atomic stacking of the Fe atoms (Baudelet *et al* [1030] suggested the packing to be closer to a bcc packing, while later studies have disputed

this conclusion [1031]; Spišák *et al* [1032, 1033] also suggest the distorted bcc structure to be lower in energy, from their results of *ab initio* calculations on Fe/Ru multilayers) and the existence of ferromagnetism (some studies found the hcp Fe phase to be non-magnetic [909]); additional complications are interdiffusion at the Fe/Ru interface [908, 1023, 1026], the spin polarization of Ru in contact with Fe [909, 1034] and differences in magnetic and structural properties resulting from different growth conditions [1025, 1026, 1031]. *Ab initio* calculations of hcp Fe/Ru multilayers confirm the strong hybridization at the interface, suppressing ferromagnetism for the monolayer Fe/Ru superlattice [1007] or resulting in a antiferromagnetic state for a single Fe monolayer on Ru(0 0 0 1) [1035], but that does not lead to a significant reduction of the magnetic moment of Fe for thicker films (i.e. to dead layers) [1007, 1032, 1033, 1035–1037]. Andrieu *et al* [1026, 1028] suggest that Fe/Ru(0 0 0 1) and Fe/Ir(1 1 1) films are hcp up to 4 ML and that no magnetic moment is detected at temperatures down to 4 K; above this thickness a magnetic moment of 1.5 μ_B/atom at room temperature for additional layers develops, which they relate to the relaxation of the Fe layer to the bcc phase; they obtain $c = 4.15, 4.20$ Å, and $a = 2.706, 2.715$ Å for Fe/Ru and Fe/Ir superlattices, respectively (the latter values also correspond to the nearest neighbour distance of bulk Ru and Ir). Perhaps less controversial is a recent report [820] showing that hcp Fe in Fe/Re multilayers with an atomic volume of 14.57 Å^3 is ferromagnetic with a magnetic moment that is identical to that of bcc Fe, as deduced from the XMCD data; since Fe and Re are immiscible, this results in sharp interfaces therefore minimizing the problem of hybridization effects. These results are in agreement with *ab initio* calculations of hcp Fe/Re multilayers reported by Zenia *et al* [1038, 1039]. The above experimental results are summarized in table 20.

5.6. *Magnetic moments of thin Co films*

hcp Co is the low temperature equilibrium phase of Co and hcp films can be grown epitaxially on a variety of substrates, including Au(1 1 1), Pt(1 1 1), Ag(1 1 1), Pd(1 1 1) and W(1 1 0) [1040, 1041]. The magnetic moment of hcp Co(0 0 0 1)/W(1 1 0) films was measured by Fritzsche *et al* [1041] using torsion oscillation magnetometry at room temperature. They observed a linear variation of the magnetic moment with the film thickness, which crosses the abscissa at 0.18 nm, suggesting the presence of 0.9 magnetically dead layers. Studies of the magnetic moment of Co films sandwiched between Pd layers, using PNR magnetometry, have been reported by Pasyuk *et al* [1042, 1043], where an enhanced moment of 1.84 μ_B/atom is obtained, compared with the bulk value of 1.73 μ_B/atom (no information about the crystalline structure of the Co film and the temperature of measurement is given). Beauvillain *et al* [1044] have also obtained an induced interfacial magnetic moment of 1.2 ± 0.6 μ_B per interface atom at the Pd/Co interface in the $t^{Co} = 0$ limit in Au/hcp Co/Pd/Au structures using SQUID and alternating gradient force magnetometry. These results are in agreement with numerical calculations that predict an enhanced moment for this system [730, 739, 1045].

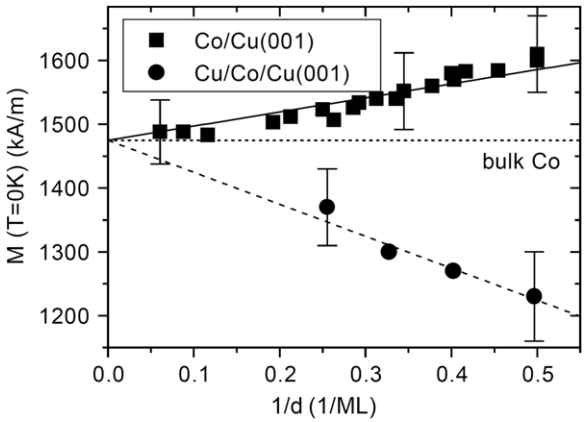

Figure 20. Variation of the magnetization of Co/Cu(0 0 1) and 5 ML Cu/Co/Cu(0 0 1) films as a function of inverse thickness [292]. Reprinted with permission from A Ney, P Poulopoulos and K Baberschke 2001 Surface and interface magnetic moments of Co/Cu(0 0 1) *Europhys. Lett.* **54** 820.

The fcc phase of Co can be stabilized in the thin film form when grown on Cu [132, 1046–1048], Ni(0 0 1) [1049–1051], C(0 0 1) [635] or MgO(0 0 1) [849] surfaces, for example. PNR results for the Cu/Co/Cu system have shown that the magnetic moment of Co is essentially bulk-like [1052–1059]. XMCD measurements have shown that the surface Co moment is enhanced in the Co/Cu(0 0 1) system [494, 1060] while adding a Cu overlayer has the effect of reducing the Co Curie temperature [492, 494, 509]. *In situ* SQUID magnetometry has been successfully used to measure the absolute moment of ultrathin fcc Co/Cu(0 0 1) films by Ney *et al* [290–292] where they found an enhanced Co magnetic moment of 1.87(3) μ_B/atom for a 2 ML Co/Cu(0 0 1) film from the bulk value of 1.69(1) μ_B/atom [290]. The effect of adding a 5 ML Cu overlayer is to reduce the total magnetic moment [292], which is attributed to a reduced interface Co moment, see figure 20. These results are in agreement with *ab initio* studies indicating surface moment enhancement of Co(0 0 1) (see section 5.1) and the study of Niklasson *et al* [694] which suggests a reduction in the Co moment at the Co/Cu(0 0 1) interface (see section 5.2). Another system that has been studied extensively is the Co/Ni system, for which a strong perpendicular magnetic interface anisotropy has been predicted [1061] for the (1 1 1) orientation, while for the (1 0 0) orientation the perpendicular anisotropy is overwhelmed by a strain and magnetostatic contribution from the Co layer [1049–1051, 1062, 1063]. Lauhoff *et al* [1056] have performed PNR measurements on a Cu/9 Å Co/50 Å Ni/Cu/Si(0 0 1) structure to find that the magnetic moment of the Co layer, $\mu^{Co} = 1.70 \pm 0.20$ μ_B/atom, was essentially bulk-like. For this particular system, the magnetic moment is predicted not to change significantly across the Co/Ni interface [694, 750], as the PNR results seem to confirm [1055–1059]. The magnetic moment of fcc Co/Ag(0 0 1) films has been studied using neutron reflection and shows that for 1 and 2 ML Co films the magnetic moment is enhanced relative to the bulk value, but that the moment decreases rapidly as the thickness increases, an effect that was attributed to strain-induced disorder in the Co films [1064, 1065].

Table 21. Values for the magnetic moment of Co thin films for different interface materials. Thickness in ML unless specified otherwise. PNR—polarized neutron reflection; SQUID—superconducting quantum interference device magnetometry; VSM—vibrating sample magnetometry; FMR—ferromagnetic resonance; BLS—Brillouin light spectroscopy; XMCD—x-ray magnetic circular dichroism spectroscopy; AGFM—alternating gradient force magnetometer. $\langle D \rangle$ is the average particle diameter.

Sample	Phase	μ^{Co}/atom (μ_B)	T (K)	Tech.	References
1450 Å $Co_{81}Cr_{19}$/quartz	hcp, poly	0.6[a]		PNR	[1066]
70 Å Pd/21 Å Co/345 Å Pd/215 Å Au/Si(0 0 1)[b]	hcp?	1.84	RT?	PNR	[1042, 1043]
∼60 CoÅ/$(C_8H_8)_n$-poly	hcp 1.70	n.a.	XMCD		[320]
42 Å Cu/10 Co/Cu(0 0 1)	fcc	1.8 ± 0.5	4	PNR	[1052, 1054]
40 Å Cu/18 Å Co/Cu(0 0 1)		1.8 ± 0.3	4	PNR	[1053]
40 Å Cu/2 Co/Cu(0 0 1)	fcc	2.1 ± 0.3	4	PNR	[1053]
222 Å Ag/2 Co/222 Å Ag/GaAs(0 0 1)	fcc	2.10 ± 0.15	5	PNR	[880]
222 Å Ag/1 Co/222 Å Ag/GaAs(0 0 1)	fcc	2.15 ± 0.2	5	PNR	[1064]
125 Å Ag/2 Co/Ag(0 0 1)	fcc	2.05 ± 0.15	5	PNR	[1064]
230 Å Ag/3 Co/230 Å Ag/GaAs(0 0 1)	(fcc)	1.65 ± 0.15	5	PNR	[1064]
160 Å Ag/5 Co/Ag(0 0 1)	(fcc)	0.45 ± 0.1	5	PNR	[1064]
45 Å Cu/9 Å Co /50 Å Ni/Cu/Si(0 0 1)	fcc	1.70 ± 0.20	RT	PNR	[1056, 1057]
40 Å Cu/23 Å Co/10 Å Cu/53 Å Ni/Cu/Si(0 0 1)	fcc	1.57 ± 0.08	RT	PNR	[1058]
2 Co/Cu(0 0 1)	fcc	1.91 ± 0.06	0	SQUID	[290–292]
3 Co/Cu(0 0 1)	fcc	1.46 ± 0.09	0	SQUID	[290–292]
5 Cu/2 Co/Cu(0 0 1)	fcc	1.67 ± 0.07	0	SQUID	[290–292]
5 Cu/3 Co/Cu(0 0 1)	fcc	1.32 ± 0.07	0	SQUID	[290–292]
93 Å Cu/9 Å Co/830Å Cu/Si(0 0 1)	fcc	1.78 ± 0.14	RT	PNR	[1059]
93 Å Cu/9 Å Co/62 Å Ni/830 Å Cu/Si(0 0 1)	fcc	1.71 ± 0.23	RT	PNR	[1059]
24 Å Au/102-1313 Å Co/C(0 0 1)	fcc	1.26 ± 0.13	RT	SQUID	[635]
2.1 ML Co/Cu(0 0 1)	fcc	2.02 ± 0.15	40	XMCD	[494]
$[21$ Å Co/5 Å Cr$]_N$	bcc	1.55[c]	RT	VSM	[821]
275 Å Co/GaAs(011)	bcc	1.53	RT	VSM	[722]
275 Å Co/GaAs(011)	bcc	1.5	RT	FMR	[822, 1067]
200, 357 Å Co/GaAs(011)	bcc	1.50	RT	BLS	[619]
80 Å Au/100 Å Co/GaAs(0 0 1)	bcc	1.40 ± 0.05[d]	300	PNR	[1068]
$[t_{Fe}$ Fe/t_{Co} Co$]_N$[e]	bcc	1.58	10	SQUID	[1069]
10 Å CoO/30 Å Co/GaAs(0 0 1)	bcc	1.2[f]	300	PNR	[1070]
$[t_{Fe}$ Fe/t_{Co} Co$]_N$[g]	bcc	1.71	RT	VSM	[1071]
$\langle D \rangle = 1.5 \pm 0.1$ nm particles	bcc	1.94 ± 0.05[h]	5	SQUID	[1072]
$\langle D \rangle = 1.9 \pm 0.1$ nm particles	bcc	1.83 ± 0.05[h]	5	SQUID	[1072]
36 Å Co/Ge(1 0 0)	bcc	1.53	RT	XMCD	[1073]
300 Å $Ni_{80}Fe_{20}$/80 Å Co/180 Å Mo/Al_2O_3(1 1 0 0)	poly?	1.5 ± 0.2		PNR	[1074]

[a] $\mu_{bulk} = 0.5\ \mu_B$/atom.
[b] Also with Si(1 0 0)-H and SiO_2 substrates.
[c] With $a = 2.77$ Å.
[d] $\mu^{Co} = 1.7\ \mu_B$/atom (centre), $\mu^{Co} = 1.0\ \mu_B$/atom (interface).
[e] $15 < t_{Co} < 25$ Å, $8 < t_{Fe} < 107$ Å; $a = 2.825$ Å.
[f] $\mu^{Co} = 1.7\ \mu_B$/atom (centre); $\mu^{Co} = 0.8\ \mu_B$/atom (interface).
[g] $6 < t_{Co} < 42$ Å, $14 < t_{Fe} < 55$ Å.
[h] Saturation moment at 5 T.

The experimental discovery of the bcc phase of Co in polycrystalline Co/Cr multilayers [821][10] and in epitaxial Co films grown on GaAs(0 1 1) [722] has led to much theoretical interest in this magnetic phase of Co [701, 770, 804, 805, 1077–1085]. Earlier studies suggested that the bcc phase was a metastable phase of the energy diagram [804], while later calculations suggest instead that this phase is probably stabilized by interactions with the substrate and/or by defects but is energetically unstable [1084, 1086], even if allowing for tetragonal distortions [805, 1085]. More recently, epitaxial body centred tetragonal (bct) Co has been grown on Ag(0 0 1) [880], Pt(0 0 1) [1087], Pd(0 0 1) [1088], Fe(0 0 1) [1089–1093], Cr(0 0 1) [1094], Cr(1 1 0) [1095–1097], FeAl(0 0 1) [1098], TiAl(0 1 0) [1099], W(0 0 1) [1100, 1101], W(1 1 1) [1102], Au(0 0 1) [1103], GaAs(1 1 0) [723, 822, 1104, 1105], GaAs(0 0 1) [1104, 1106, 1107] and in τ-MnAl/Co multilayers [1108]. Earlier estimates of the magnetic moment of bcc Co/GaAs(0 0 1) suggested an average magnetic moment of around 1.5 μ_B/atom [619, 722, 822, 1067], smaller than the bulk

[10] This result was later questioned by Stearns *et al* [1075], who did not find evidence for the presence of the bcc Co phase in Co/Cr multilayers, but again this study disagrees with the results of Metoki *et al* [1076], where the Co layer in Co/Cr multilayers was found to change to a bcc phase with decreasing thickness due to epitaxial strain.

moment of fcc or hcp Co. However, it was recognized that strong interdiffusion at the interface [1104] was responsible for a large reduction of the average magnetic moment. In fact, PNR results showed that the magnetic moment of polycrystalline Co/GaAs was strongly reduced at the interface (down to 0.8 μ_B/atom) while it was essentially (hcp) bulk-like at the centre of the film (1.7 μ_B/atom) [1109]; similar results were found in bcc Co/GaAs(0 0 1) samples [1068], where a magnetic moment per atom at the centre of the film of 1.7 μ_B/atom was found, similar to the theoretically predicted values [770, 804, 1077, 1079, 1080, 1082]. These studies suggest a reaction depth of around 20–50 Å, which are compatible with independent TEM [1107] and STM [1110] observations and consistent with the observation of interface reaction in Co/GaAs pairs [1104, 1111]. Recently, more systematic studies of the growth and evolution of the crystal phases of Co grown on GaAs(0 0 1) have been made available, and some discrepancies have been found with respect to the maximum bcc Co thickness achievable. Mangan *et al* [1112] report the observation of epitaxial bcc Co up to 8 nm thick and up to 15 nm in a polycrystalline fashion, with hcp domains starting to develop above this thickness (although they also report that for a 87.5 nm Co film, the bcc Co layer was only 4–5 nm thick; this may be due to the effect of the hcp overlayer, which may induce a reversion of part of the bcc film to hcp [1091], see below). On the other hand, Wu *et al* [1106, 1113] report that while Co grows in the bcc phase on GaAs(0 0 1)-$p(4 \times 2)$ for thicknesses up to 2 nm, above this thickness hcp domains develop which become dominant for thicknesses beyond ∼6 nm; they have cast doubt on the possibility that the Co/GaAs(0 0 1) films reported in [1068, 1114, 1115] (10–20 nm thick) are bcc. Wieldraaijer *et al* [1093] mention that they failed to replicate layers of bcc Co as thick (10–20 nm) as reported in earlier studies [1068]; Blundell *et al* [1070] report that for Co thicknesses above 3 nm deposited on GaAs(0 0 1)-$p(4 \times 2)$, hcp domains start to develop. Coincidentally, the typical thickness range for bcc Co epitaxy observed for growth on other substrates is around 1–3 nm: 1.5 nm [1090, 1091], 2.0 nm [1093], 2.1 nm (which is extended to 5 nm if O is used as a surfactant) [1092] for growth on Fe surfaces, 2 nm for Fe/Co multilayers [1069, 1116], smaller than 1.7 nm for τMnAl/Co superlattices [1108, 1117], at least 3 nm for Co/Pt(0 0 1) [1087], 2.8 nm for Co/Cr(1 0 0) [1094], 1.3 nm for Co/FeAl(0 0 1) [1098], up to at least 1.6 nm for Co/Au(0 0 1) [1103], but larger than 4.5 nm for Co/Pd(0 0 1) [1088] and 6 nm for Co/Cr(1 1 0) [1095, 1096]. It may be possible that the different substrate preparations and growth conditions may be responsible for the divergent results reported by the different groups, but a perusal of the GaAs substrate preparation steps and sample growth details, to the extent that they are reported, does not show any obvious clue about the origin of the discrepancies in the reported values for bcc Co grown on GaAs. It has also been realized that the deposition of an overlayer on bcc Co has a significant effect upon the crystal structure of the Co underlayer; Gazzadi and Valeri [1091] have found that the overgrowth of an hcp Co layer results in a thinner bcc Co layer than initially determined during the growth stage, and Wieldraaijer *et al* [1093] observed that while capping the bcc Co with Fe or Al_2O_3 preserves the bcc phase, a Cu film causes a transformation into an fcc or hcp phase; in Fe/Co multilayers, it is observed that the bcc thickness limit is extended compared with the Co open surface by a factor of 2, from 1 to 2 nm [1116, 1118]. A study of epitaxial Co/Ge(1 0 0) [1073] also suggests that Co grows in the bcc phase up to 3 nm thickness, although the evidence given is rather circumstantial, based as it is on similarities to a previous work on Co/GaAs and a more direct determination of the crystalline phase of the Co film is warranted. We have nevertheless listed the value of the magnetic moment for this system in table 21, 1.53 μ_B/atom, obtained from XMCD; it is reported that an intermixed region of 4.8 Å exists at the Co/Ge interface, and it is not clear how this may affect the value of the magnetic moment. It is possible that the reduction observed may be due to a decrease in magnetic polarization in this intermixed region. The magnetic moment of bcc Co across the Co/Fe(1$\bar{1}$0) interface in multilayer structures of the form (2 nm Co/1–4 nm Fe)$_{10}$/20 nm Fe/GaAs(1$\bar{1}$0) has been determined experimentally by means of perturbed angular correlation (PAC) spectroscopy by Swinnen *et al* [1119–1122]. In this technique, trace amounts of diamagnetic atoms are implanted across the magnetic structure and modifications in the hyperfine field are used as probes of the local magnetic field, allowing the determination of the magnetization profile across the interface. These authors observe a decaying oscillation in the interface magnetic moment away from the interface towards the bulk values, similar to the so-called Friedel oscillation, and the Fe moment is significantly enhanced at the interface (in agreement with XMCD results on bcc CoFe alloys and Co/Fe multilayers [1123]) while the Co moment appears strongly reduced. These results have been disputed by Šljivančanin and Vukajlović [1124, 1125], who do not theoretically reproduce such oscillations at the bcc Fe/Co interface from tight binding LMTO first principle calculations, but rather a monotonic variation of the moment of Fe and Co towards the bulk value. Also relevant to this discussion is the study of fine particles by Respaud *et al* [1072], which are confirmed to be in the bcc phase from the results of high resolution TEM and wide angle x-ray scattering measurements. Ensembles of particles with average diameters of 1.5 and 1.9 nm exhibit a saturation magnetic moment per atom of 1.94 ± 0.05 μ_B/atom and 1.83 ± 0.05 μ_B/atom, respectively, at 5 K and 5 T (at 35 T the saturation moment increases to 2.1 ± 0.1 μ_B/atom for the 1.5 nm diameter nanoparticles). This is significantly higher than the predicted magnetic moment of bcc Co, which the authors attribute to surface effects. Makhlouf *et al* [1126] had earlier reported on the magnetic properties of bcc Co nanoparticles (6 nm average diameter): their results suggest a magnetic moment for the bcc phase which is 40% smaller than the magnetic moment of the fcc Co particles (obtained upon annealing the bcc particles; the size of the fcc particles are, however, much larger). Despite the increasing number of studies reporting the observation of the bcc Co phase, surprisingly little details have been given to the magnetic properties of this system, and this is particularly true of the magnetic moment. It is fair to say that an accurate determination of the magnetic moment of bcc Co would benefit from additional work.

5.7. Magnetic moments of thin Ni films

An early observation of the enhanced surface orbital spin moment in Ni(1 1 0) using magnetic circular dichroism was reported by van der Laan *et al* using the surface sensitivity of core-level photoemission spectroscopy (CDXPS) [1127]. In this study, the Ni 3p core-level photoemission peak dependence on the light helicity showed a dichroic amplitude signal significantly larger than that expected for Ni based on the calculated spectra using an Anderson impurity model, indicating a much larger orbital spin moment at the Ni(1 1 0) surface compared with the bulk value by about 10%. Although very qualitative, this result demonstrated the effect of symmetry breaking on the surface layer of Ni. Later developments in this technique have made it a powerful tool in the investigation of the spin and orbital contributions to the total moment of surface layers, yielding information about both surface magnetic moments and anisotropies [186, 192, 193, 315, 1128]. Oscillations in the ground state ($T = 0$ K) magnetic moment of Ni were observed in 7.3 Å Ni/Au multilayers as a function of interlayer thickness up to about 15% around its mean value of $\approx 0.36\ \mu_B$/atom, significantly reduced compared with the bulk value [502]. These oscillations were also correlated with oscillations found in the remanent magnetization, the effective spin-wave parameter (prefactor to the $T^{3/2}$ term of Bloch's temperature variation of the saturation magnetization) and the Curie temperature and are attributed to the effect of oscillatory interlayer coupling, which also modulates the strength of the exchange interaction across the Ni layers.

The study of the magnetic moment of thin fcc Ni films, particularly for the Ni/Cu interface, has been considered in some detail by several authors [294, 311, 744, 1129–1132] fuelled in large measure by the discrepancy in the reported observation of the Ni magnetic moment with the film thickness, see figure 21. The particular interest in Ni/Cu(0 0 1) resides in the unusual magnetic properties of this system, exhibiting dominant perpendicular magnetic anisotropy over the thickness range from 15 to 120 Å, which manifests itself in a state of perpendicular magnetization at remanence (see section 6.5). Reduced magnetic moments at the Cu/Ni interface have been predicted by numerical calculations, due to sp–d hybridization at the interface between the Ni and Cu orbitals (significant only within the first two interface layers) [693, 742–746, 1133]. Experimentally a large reduction in the moment of Ni has been observed for films grown on Cu/Si(0 0 1) substrates [191, 494, 1129–1132], larger than that predicted by interface hybridization effects and also not explainable by interdiffusion at the Ni/Cu interface [1130, 1134, 1135]. In particular, it is observed that the magnetic moment of Ni increases with thickness but in a thickness range where the interface effects are expected not to contribute much to a variation in the magnetic moment [1129–1131]. An identical reduction in the magnetic moment of Ni films grown on 200 nm Cu/Si(0 0 1) substrates has been reported independently by Gubbiotti *et al* [1132]; in this study, the thicker Cu buffer layer is expected to result in better Cu crystal quality [1130, 1136]. This reduction in the moment of Ni films grown on Cu/Si(0 0 1) has been attributed to strain in the Ni layer, which has the effect of decreasing the magnetic moment per atom of Ni. This is also suggested by experiments where the Cu overlayer in a Cu/Ni/Cu(0 0 1) structure is varied, which show that the sample with the thicker Cu overlayer exhibits a smaller magnetic moment; this is concomitant with an increase in the Ni strain (observed in identical structures), see figure 22 [1137]. A variation in the magnetic moment of Ni with strain has been predicted theoretically but is too small to account for the experimental results [742, 807]. Although Wu *et al* [1138] present a variation in the magnetic moment per Ni atom which is consistent with the variation reported in [1137], the calculations refer to uniform expansions of the fct primitive cell along the *c*-axis; in practice it is the in-plane lattice constant of Ni that is changed while the out-of-plane lattice parameter is free to adjust to the value that minimizes the free energy of the system (usually tending to keep the volume of the primitive cell approximately constant). However, high precision magnetometry studies on 4 ML to bulk Ni/Cu(0 0 1) films using an *in situ* SQUID technique and XMCD have not corroborated this large decrease in the magnetic moment of Ni with thickness, except for a reduced moment at the Ni/Cu interface [294]; in this case a Cu(0 0 1) single crystal is used and it is argued that the strain in the Ni films is reduced as compared with the case of the Ni films grown on Cu/Si(0 0 1), where the strain in the Cu layer could be only partially relaxed; x-ray diffraction results indicate, however, that the Cu buffer layer is fully relaxed [718, 1137, 1139]. In addition, roughness has also been suggested to contribute to a significant reduction in the magnetic moment of Ni films, due to a reduction in the coordination number of the Ni atoms [1140, 1141], but the origin of the discrepancy still remains unsolved. We have compiled in table 22 a list of values for the magnetic moment of fcc Ni films as reported in the literature.

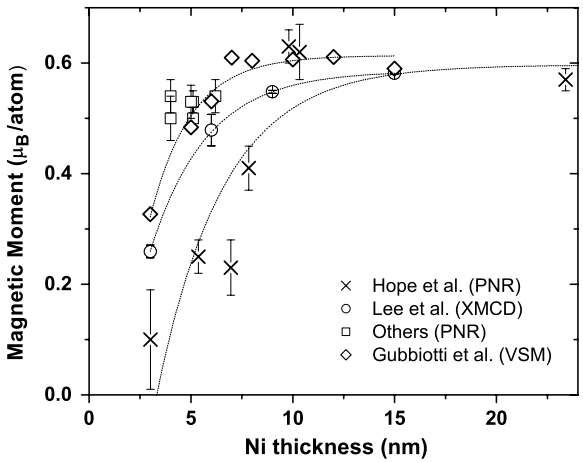

Figure 21. Room temperature variation of the Ni magnetic moment per atom as a function of the film thickness in Cu/Ni/Cu/Si(0 0 1) samples reported in the literature: Hope *et al* [1129], Lee *et al* [1129, 1130], Gubbiotti *et al* [1132] and others [1056, 1059, 1137, 1142]. Dotted lines are guides to the eye.

The bcc phase of Ni is not usually found in nature, but it was shown by Moruzzi *et al* [764, 766, 829, 1150] that it corresponds to a metastable phase with an equilibrium lattice constant of $a_{\mathrm{eq}}^{\mathrm{bcc\,Ni}} = 2.78$ Å, with a nearby non-magnetic-to-ferromagnetic transition with increasing atomic volume (see

Table 22. Values for the magnetic moment of Ni thin films for different interface materials. Thickness in ML unless specified otherwise. PNR—polarized neutron reflection; XMCD—x-ray magnetic circular dichroism spectroscopy; FMR—ferromagnetic resonance; SP-ARPES—spin-polarized angular-resolved photoemission spectroscopy; VSM—vibrating sample magnetometry; SQUID—superconducting quantum interference device magnetometry.

Sample	Phase	μ^{Ni} (μ_{B}/atom)	T (K)	Tech.	References
Cu/3–30 nm Ni/Cu/Si(0 0 1)-H	fcc	[a]	RT	PNR	[1129, 1130, 1132]
20 Å Cu/51 Å Ni/500 Å Cu/Si(0 0 1)	fcc	0.50 ± 0.02[b]	RT	PNR	[1142]
20 Å Cu/51 Å Ni/770 Å Cu/Si(0 0 1)	fcc	0.53 ± 0.02[c]	RT	PNR	[1142]
50 Å Cu/40 Å Ni/Cu/Si(0 0 1)	fcc	0.54 ± 0.03	RT	PNR	[1137]
180 Å Cu/40 Å Ni/Cu/Si(0 0 1)	fcc	0.45 ± 0.03	RT	PNR	[1137]
45 Å Cu/50 Å Ni/Cu/Si(0 0 1)	fcc	0.53 ± 0.03	RT	PNR	[1056–1058]
45 Å Cu/9 Å Co/50 Å Ni/Cu/Si(0 0 1)	fcc	0.57 ± 0.03	RT	PNR	[1056–1058]
45 Å Cu/23 Å Co/10 Å Cu/50 Å Ni/Cu/Si(0 0 1)	fcc	0.50 ± 0.04	RT	PNR	[1056–1058]
[23-30 Å Ni(0 0 1)/12 Å Fe(0 0 1)]$_{20}$	fct	0.69	RT	XMCD	[1143]
93 Å Cu/62 Å Ni/Cu/Si(0 0 1)	fcc	0.54 ± 0.03	RT	PNR	[1059]
93 Å Cu/9 Å Co/62 Å Ni/Cu/Si(0 0 1)	fcc	0.50 ± 0.05	RT	PNR	[1059]
4 Ni/Cu(0 0 1)	fcc	0.3 ± 0.1	40	XMCD	[494]
4-bulk Ni/Cu(0 0 1)	fcc	0.61 ± 9	40	SQUID	[294]
1.4–2.6 Co/11-14 Ni/Cu(0 0 1)	fcc	0.65	RT	XMCD	[521]
3 nm Au/6 nm Ni/Fe(0 0 1)	bcc	0.4	RT	FMR	[1144]
30 Au/3 bcc Ni/5 Fe/Ag(0 0 1)	bcc	0.55	4	PNR	[877]
Ni(4–8)/Fe(0 0 1)	bcc	0.4 ± 0.45	RT	SP-ARPES	[824]
[8 Ni (1 1 0)/2 Fe(1 1 0)]$_{25}$	bcc	0.69	RT	VSM	[1145]
1 Ni/Fe(0 0 1)	bcc	0.33 ± 0.12	RT	XMCD	[1146]
2 Ni/Fe(0 0 1)	bcc	0.29 ± 0.12	RT	XMCD	[1146]
4 Ni/Fe(0 0 1)	bcc	0.43 ± 0.12	RT	XMCD	[1146]
5 Ni/Fe(0 0 1)	bcc	0.39 ± 0.10	RT	XMCD	[1147]
[3.3 Ni(0 0 1)/Fe(0 0 1)]$_{10}$	bcc	0.8[d]	4.5	VSM, SQUID	[1148]
$\langle D \rangle \sim 3$ nm particles (L1)	bcc	(1.848 emu g^{-1})	RT	VSM	[825]
[0.5 Å Ni(0 0 1)/12 Å Fe(0 0 1)]$_{20}$	bcc	1.1	RT	XMCD	[1143]
[3–16 Å Ni(0 0 1)/12 Å Fe(0 0 1)]$_{20}$	bcc	0.85	RT	XMCD	[1143]
2 nm Au/<2.5 nm Ni/GaAs(0 0 1)	bcc	0.52 ± 0.08	5	SQUID	[1149]

[a] A variation in the Ni moment per atom with thickness is reported.
[b] 0.55 ± 0.03 (XMCD).
[c] 0.58 ± 0.03 (XMCD).
[d] Assuming bulk magnetic moment for Fe.

also [830]); for $a^{\mathrm{bcc\ Ni}} = 2.78$ Å, the magnetic moment of Ni is predicted to be around 0.41 μ_{B}/atom [829], and given the small lattice mismatch between the equilibrium lattice constant of bcc Ni (2.78 Å) and that of bcc Fe (2.866 Å), $\tilde{\eta} = -3.0\%$, it may be expected that bcc Ni could be grown on Fe(0 0 1). This Ni phase was indeed obtained by means of molecular beam epitaxy by Heinrich *et al* [823, 1144, 1151–1153] and Wang *et al* [1150, 1154]. These experimental results suggest that bcc Ni can be grown homomorphically on the bcc Fe(0 0 1) surface up to 3–6 ML, depending on substrate conditions; above this thickness the lattice constant expands by ≈2% and develops a $c(2 \times 2)$ surface reconstruction [823, 1154]. According to Heinrich *et al* [823], the unreconstructed (strained) bcc Ni films are presumed non-magnetic, while the reconstructed $c(2 \times 2)$ (assumed to correspond to the equilibrium bcc Ni) is magnetic with a four-fold in-plane magnetic anisotropy and a magnetic moment of ≈ 0.4 μ_{B}/atom (for a 6 nm bcc Ni/Fe(0 0 1) film, determined from FMR data [1144]). This is not the behaviour expected from the results of the theoretical calculations of Moruzzi *et al* [764, 829] (using band theory for a rigid lattice), unless the calculated value for the equilibrium lattice constant of bcc Ni is underestimated. Work on Ni/Fe multilayers by Kamada *et al* [1148, 1155] suggests that for a [3.3 ML bcc Ni/13 ML Fe]$_{10}$ structure, the in-plane bcc Ni lattice is in registry with that of Fe, $a = 2.86$ Å, while the out-of-plane lattice constant is stretched to $c = 2.70$ Å, whereby the Ni unit cell is bct with $c/a = 0.94$; if one assumes that this contraction is such as to keep the volume of the equilibrium unit cell unchanged, then these values would give an equilibrium value of 2.81 Å for the lattice constant of bcc Ni. These authors also note that the $c(2 \times 2)$ diffraction pattern observed for thicker Ni films does not correspond to a correct $c(2 \times 2)$ structure. Perhaps motivated by these results, Mijiritskii *et al* [1156] have suggested, based on a detailed study of the angle dependence of the RHEED patterns, that this apparent surface reconstruction corresponds instead to the fcc Ni phase consisting of a mosaic of four different Ni(1 1 0) domains (a possibility also considered by Heinrich *et al* [1153]) and that at the thickness where these extra diffraction patterns appear, a bcc-Ni-to-fcc-Ni martensitic transformation takes place (they also relate this transformation to the decrease in the period of the RHEED oscillations observed during growth by Heinrich *et al* [823, 1157]). In the light of these later results, it is possible that the Ni in the structures reported by Gutierrez *et al* [1158] for a [Fe/14 Å Ni] multilayer, where 'weak reconstruction features were apparent', may have been,

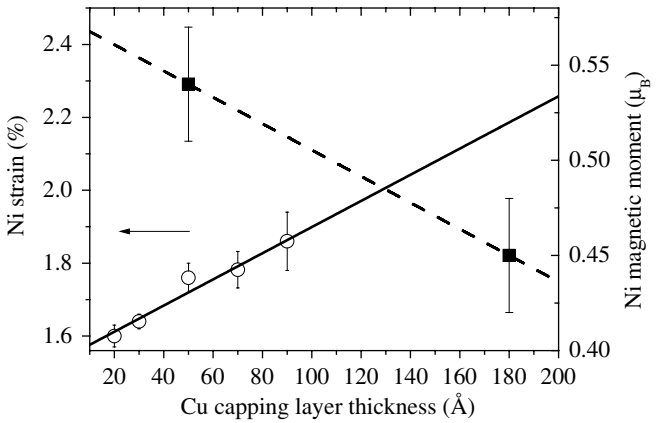

Figure 22. Room temperature variation of the Ni magnetic moment (PNR) and strain (grazing incidence x-ray diffraction) in the Ni layer in Cu/Ni/Cu/Si(0 0 1) structures for different values of the Cu overlayer thickness. The strain in the Ni films for exact lattice matching to the Cu is 2.5% [1137]. Reprinted from C A F Vaz, G Lauhoff, J A C Bland, B D Fulthorpe, T P A Hase, B K Tanner, S Langridge and J Penfold 2001 Effect of the Cu capping thickness on the magnetic properties of thin Ni/Cu(0 0 1) films *J. Magn. Magn. Mater.* **226–30** 1618. Copyright (2001), with permission from Elsevier.

in fact, fcc Ni. Heinrich *et al* also reported that bcc Ni can be grown on Ag(0 0 1) [823], although the growth is more three-dimensional, and on Au(0 0 1) [1144], as also observed by Kamada and Matsui [1155] who report the growth of bcc Ni on Au(0 0 1) up to 5 ML. Bland *et al* [877] have carried out PNR measurements on a 30 ML Au/3 ML bcc Ni/5 ML Fe/Ag(0 0 1) and found that the data are consistent with the magnetic moment for Fe of 2.2 μ_B/atom per atom and the magnetic moment per Ni atom of at least 0.55 μ_B/atom; FMR results on similar structures were found to be in agreement with the PNR results [341]. Other studies on this system have been reported by Brookes *et al* [824], who found that 4–8 ML bcc Ni films on Fe(0 0 1) are ferromagnetic and estimated the magnetic moment per atom as 0.4 ± 0.45 μ_B/atom, from their spin-polarized angle-resolved photoexcitation emission spectroscopy (SP-ARPES) results. Wieczorek *et al* [1145] studied bcc Ni(1 1 0) in Fe/Ni multilayers (deposited on an epitaxial Ag base layer) for Ni thicknesses up to 8 ML. In this study, RHEED data along the ⟨11⟩ azimuth suggest that the Ni in-plane lattice spacing follows that of Fe with an expansion of 5%, while XRD data suggest that the perpendicular lattice spacing follows that of Fe with an expansion of 1.5%, in qualitative agreement with the results of Heinrich *et al* [823] for the 'reconstructed' Ni but at variance with the results of Kamada *et al* [1148, 1155] for bcc Ni. From their VSM data, we may infer a RT magnetization of 462 emu cm^{-3} for the 8 ML bcc Ni film, which yields an atomic moment of the order of 0.60 μ_B/atom assuming a unit cell volume of 1.12 $(a_{eq}^{bcc\ Ni})^3$. This suggests an enhanced magnetic moment relative to the magnetic moment of fcc Ni. Such an enhancement in the magnetic moment of bcc Ni in contact with Fe(0 0 1) has been predicted by Lee *et al* [1159, 1160] by means of a self-consistent, fully relativistic, FLAPW method; for the bcc Ni monolayer a magnetic moment of 0.86 μ_B/atom is predicted, while for a 2 ML bcc Ni (with the out-of-plane Ni spacing set to that of fcc Ni), the averaged magnetic moment of the two layers drops to 0.69 μ_B/atom (the magnetic moment of Fe is also significantly enhanced at the interface). Paduani [830] studied the electronic and magnetic properties of bcc FeNi alloys based on a non-relativistic spin-polarized method in the LSD approximation; the results predict a magnetic moment per Ni atom of 0.74 μ_B/atom for a 1ML bcc Ni embedded in a bcc Fe matrix; for a 3 ML bcc Ni they found for the magnetic moment of Ni at the centre a value of 1.14 μ_B/atom, which is surprisingly large. Shawagfeh and Khalifeh [695] have also performed first principle calculations (LMTO-ASA) to determine the electronic and magnetic properties of Ni/Fe(0 0 1) overlayers; from the energy calculation of bulk bcc Ni, they obtained an equilibrium lattice constant of 2.79 Å and a Ni magnetic moment of 0.585 μ_B/atom at the equilibrium lattice constant, in good agreement with the calculations of other authors [764, 766, 803, 829, 830, 1150]. For a bcc Ni layer sandwiched between bcc Fe, they found a Ni magnetic moment of 0.89 μ_B/atom for the thick Fe slabs (7 to 11 ML), while for the bcc Ni bilayer, the magnetic moment of Ni is 0.76 μ_B/atom at the surface layer and 0.59 μ_B/atom at the interface. Vogel *et al* [1146, 1147] performed XMCD studies on 1–5 ML bcc Ni/Fe(0 0 1), showing that the bcc Ni films are ferromagnetic at room temperature, but with magnetic moments per atom (measured at remanence) that are much smaller than that of bulk fcc Ni (and therefore not enhanced at the Fe interface); the average magnetic moment is estimated as 0.3 ± 0.1 μ_B/atom, which does not vary with thickness in the 1–5 ML range, within error. Kamada *et al* [1148], whose work we have referred to above, have also studied the magnetic properties of bcc Ni/Fe multilayers; from bulk magnetometry measurements (VSM and SQUID) they estimate the magnetic moment of bcc Ni as 0.8 μ_B/atom at 4.5 K assuming a bulk magnetic moment for Fe; they also perform *ab initio* calculations to determine both the change in the magnetic moment of bcc Ni as a function of the volume of the tetragonal $c/a = 0.94$ bct unit cell (they obtain a magnetic moment of 0.35 μ_B/atom at the experimental value of $V = 22.1$ Å^3, while the energy minimum is at $V \approx 20.3$ Å^3, corresponding to a magnetic moment of 0.12 μ_B/atom) and the Ni and Fe interface moments. They found that both the Ni and Fe magnetic moments are enhanced at the interface, in agreement with the results of Lee *et al* [1159, 1160]; the magnetic moment of Ni they obtain from the calculations is 0.65 μ_B/atom for the interface Ni atoms and 0.43 μ_B/atom for the centre Ni atoms. Another study of bcc $[Ni/Fe]_{20}$ multilayers, in the range 0–30 Å of Ni (Fe thickness set to 12 Å), reported by Lin *et al* [1143] shows that Ni is bct for thicknesses up to 16 Å, with $c/a \approx 0.99$, $c = 2.80$ Å and $a = 2.86$ Å; the value of a is identical to the lattice constant of bcc Fe, and the out-of-plane lattice constant is contracted with respect to the in-plane component, but less than that reported in the study by Kamada *et al* [1148, 1155]; these values yield a unit cell atomic volume of 22.90 Å^3 and a lattice constant of 2.84 Å assuming the atomic volume of the unstrained unit cell with the same volume. MOKE measurements suggest that the easy direction axes of bcc Ni are along the ⟨1 0 0⟩ directions, but since the Ni is ferromagnetically coupled with the Fe layer, this property is that of the Ni/Fe bilayer. XMCD

data suggest that for the 0.5 Å Ni sample, the Ni magnetic moment is 1.1 μ_B/atom decreasing to 0.85 μ_B/atom for 3 Å Ni and remaining constant up to 16 Å. The large moment observed for the thinner Ni layer is attributed to the effect of interdiffusion at the Ni/Fe interface (estimated at ≈ 3 Å) and is therefore more akin to a FeNi alloy; for thicker Ni films, in the fct phase, the magnetic moment is estimated as 0.69 μ_B/atom. In this study the XMCD spectra were calibrated against the published spectra for Ni and systematic errors associated with the magnetic moments thus obtained were estimated to be smaller than 20%. More recently, Tang *et al* [1149, 1161] have reported the growth of bcc Ni on GaAs(0 0 1) up to 2.5 nm; the RHEED patterns suggest the growth to be three-dimensional, and they find a magnetic anisotropy constant of 4.0×10^4 erg cm^{-3} (easy magnetic axes along the in-plane ⟨1 0 0⟩ directions). From SQUID magnetometry, a magnetic moment of 0.52 ± 0.08 μ_B/atom at 5 K is found. The synthesis of bcc Ni nanoparticles has also been reported, e.g. by Kim *et al* [825]. These authors provide only general information about the structure and magnetism of the Ni nanoparticles, but for their sample L1, with an average size of the order of 3 nm, a very small magnetization is measured, which suggests a magnetic moment per atom much smaller than that of fcc Ni (to which the particles revert upon annealing). Although such small particles may be expected to be superparamagnetic, the powder was pressed for the measurements, which may be sufficient for the establishment of intercluster magnetic order; the field cooled *M–T* curves presented do not show the behaviour typical of a superparamagnetic system [1162, 1163].

6. Magnetic anisotropies

The magnetic anisotropy is another key parameter of magnetic materials. It is a relativistic manifestation of the coupling between the electron spin and the orbital moment (spin–orbit coupling). Hence, modifications in the electronic structure at surfaces and interfaces are expected to lead to changes in the magnetic anisotropy. These local interface effects can give rise to striking magnetic behaviour in ultrathin magnetic films, such as interface induced perpendicular magnetic anisotropy, first shown experimentally by Gradmann and Müller [79] in $Ni_{48}Fe_{52}$(1 1 1) thin films. Typically, interface magnetic anisotropies are of the order of 0.1–1 erg cm^{-2} [81, 84, 132, 133, 201]. In this section we consider some examples as prototypical of the changes that arise as a consequence of the presence of an interface. The published literature addressing the magnetic behaviour of thin magnetic films is vast and for concreteness we consider only three representative cases, the fcc phases of Fe, Co and Ni epitaxial films deposited on Cu(0 0 1) surfaces. The case of thin fcc Fe films, stabilized in fcc (0 0 1) surfaces such as Cu(0 0 1), has been addressed in section 5.5; since the equilibrium state of this system is believed to lie at the boundary between non-magnetic and ferromagnetic order, the intricate magnetic ordering and magnetic anisotropy behaviour of this system are inextricably linked to its complex crystalline structure (a result of the metastability of the fcc state) and illustrate the extent to which these aspects are interrelated. We discuss next the magnetic anisotropy of ultrathin fcc Co(0 0 1) films to illustrate the sensitivity of magnetism to structural factors such as strain, surface morphology and surfactants. In section 6.5 we consider the unusual magnetic anisotropy behaviour of the Ni/Cu system in order to illustrate the key role of strain in determining magnetic properties and the influence of film structure and surface morphology.

Central to an understanding of the role of the interface in modifying the magnetic properties of ultrathin films and nanostructures, and the magnetic anisotropy in particular, is a detailed knowledge of the interface structure at the atomic and nanometre scale, in addition to the crystallographic structure and chemical composition. This includes structural contributions, such as strain, chemical intermixing and surface morphology (including atomic steps, islands, ridges, roughness, etc) and the effects of adsorbates, which can significantly modify the intrinsic electronic properties of the interface [205, 208, 393, 716, 1164–1166]. One important conclusion is that the magnetic anisotropy is particularly sensitive to atomic scale order at the interface and reflects the local symmetry 'felt' by the magnetic atoms.

6.1. Phenomenology

The break of symmetry at the interface introduces lower order anisotropy terms, as first pointed out by Néel [199, 200]. To second order of approximation, the surface anisotropy is given by [83]

$$E_s = K_s \cos^2\theta + K_{s,p} \sin^2\theta \cos^2\phi, \qquad (56)$$

where θ and ϕ are the polar and azimuthal angles of the magnetization vector with respect to the direction perpendicular to the surface, respectively. The first term is the out-of-plane surface anisotropy and, following Néel's notation, it favours perpendicular anisotropy for negative values of the constant K_s. This has the advantage that it is consistent with the fact that the magnetostatic energy, which is positive definite, also appears positive in this notation [83]. The second term corresponds to an in-plane surface anisotropy, which must be considered in lower symmetry surfaces, e.g., fcc(1 1 0), bcc(1 1 0), etc.

Based on a phenomenological pair-bonding model of magnetic anisotropies, Néel deduced expressions for the surface anisotropy for some crystallographic surfaces, in terms of elastic and magnetostriction coefficients, since magnetostatic and magnetoelastic effects are expected to play a crucial role in determining the surface anisotropy [284]. The estimates for the uniaxial surface anisotropies based on these expressions are not accurate and in some instances give erroneous values for the sign of the surface anisotropy, but the model provides nevertheless a qualitative description of the origin of surface magnetic anisotropies. Recently, Bayreuther *et al* [1167] have suggested that the failure could be due to the fact that such estimates fail to take into account atomic surface relaxations, which are expected to critically affect the atomic coupling constants; likewise, such changes are expected to be less severe for the case of fourth-order in-plane anisotropies, and these authors show that Néel's model

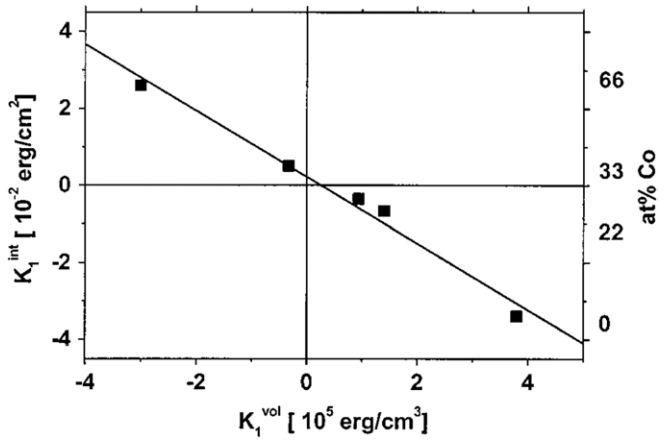

Figure 23. Relation between the fourth-order interface magnetic anisotropy constant for a range of epitaxial Fe and FeCo alloy films (K_1^{int}) and their respective fourth-order bulk anisotropy constant (K_1^{vol}). The sign of K_1^{int} and K_1^{vol} is opposite to each other and the slope corresponds to the critical thickness for the in-plane easy axis reorientation of the magnetization. The scale on the right indicates the Co content of the CoFe alloy from which the data point is obtained [1167]. Reused with permission from G Bayreuther, M Dumm, B Uhl, R Meier and W Kipferl 2003 *J. Appl. Phys.* **93** 8230. Copyright 2003, American Institute of Physics.

can account for the variation of the in-plane cubic surface anisotropy of Fe and FeCo alloys, namely, the experimental observation that the ratio between the in-plane surface and volume fourth-order anisotropy constants is constant for Fe and CoFe films, see figure 23. Victora and MacLauren [1168] also obtained good agreement between Néel's model and the magnetic anisotropies of Co/Pd superlattices, while Chuang *et al* [204] have used Néel's model to calculate expressions for step anisotropies in vicinal surfaces, which are in agreement with experimental results for Co/Cu(1 1 13) and bcc Fe on vicinal W(0 0 1) surfaces. A more elaborate model based on the effective ligand interaction has been developed by Wang *et al* [1169], while Bruno [1170] has calculated perturbatively the magnetic anisotropy of (0 0 1), (1 1 0) and (1 1 1) monolayers within the tight binding approach, demonstrating the close relationship between magnetic anisotropy and the orbital magnetic moment. For more quantitative estimates of the surface anisotropy contribution to the total anisotropy of monolayer-thin films, first principles calculations are necessary and are now available for a wide range of systems [68, 75, 665, 669, 673, 692, 693, 699, 703, 706, 724, 741, 1168, 1171].

The effective uniaxial anisotropy perpendicular to the plane of a thin film can be written as

$$K_{u,eff} = 2\pi D_m M_s^2 + K_u + 2K_s/t, \qquad (57)$$

where the first term is the magnetic dipolar energy contribution [84, 218], K_u is the magnetocrystalline energy contribution from the bulk of the film and the last term is the surface magnetic anisotropy energy contribution. D_m is the out-of-plane demagnetizing factor and is $\approx$1 for thin films, but in general is a function of the film thickness; for an undistorted fcc (0 0 1) film, it has been calculated to vary as $D = 1-0.2338/n$, where $n > 1$ is the film thickness in monolayers [529] (see also [566, 1172–1174]). It follows from the previous expression that for small thicknesses the bulk contribution can be overwhelmed by the surface term, and when the latter is negative, a state of perpendicular magnetic anisotropy may ensue. Examples where this occurs include $Ni_{48}Fe_{52}$(1 1 1) [79], Co/Au(1 1 1) [220, 221] and Fe/Ag(0 0 1) [222].

One important contribution to the magnetic anisotropy of epitaxial ultrathin films arises from strain, via magnetoelastic coupling [174, 194, 197, 201, 224, 1175–1179]. Strain contributes to the elastic energy of the system, and for a uniformly strained system this term scales with the volume. Beyond a *critical coherence thickness*, t_c, misfit dislocations set in order to relieve strain, which then decreases approximately with the reciprocal of the thickness [1051, 1176, 1180–1182] (deviations from this variation have been suggested in the literature [224, 718, 1183]). If we consider again only the perpendicular uniaxial anisotropy, $K_{u,eff}$ becomes

$$K_{u,eff} = 2\pi M_s^2 + K_u + B_{me}\epsilon + 2K_s/t, \qquad (58)$$

where ϵ is the strain and B_{me} is the magnetoelastic coupling coefficient, which is sometimes written as composed of a bulk and surface contribution, $B_{me} = B_v + B_s/t$ [197, 1182, 1184–1186]. Magnetoelastic anisotropy energies have been found to be different from the bulk for several systems, such as in polycrystalline NiFe/Ag/Si, FeNi/Cu/Si thin films [1187], Ni/Ag multilayers [1188] and Ni/Cu/Si(0 0 1) films [1189].

The magnetization spin-reorientation transition observed in many ultrathin films, whereby the magnetization easy axis switches from out-of-plane to in-plane with film thickness, can be understood easily as a consequence of the competition between the surface and volume terms in (57). At a critical thickness t_{SRT},

$$t_{SRT} = -2K_s/(2\pi M_s^2 + K_u), \qquad (59)$$

$K_{u,eff}$ changes sign from positive to negative: for thicknesses below t_{SRT} the spins prefer to lie along the surface normal, while for larger thicknesses the spins lie in-plane. This description ignores the effect of higher order anisotropies; when higher order anisotropies of appropriate sign are present, as in Co(0 0 0 1)/Au(1 1 1) [220], for example, a canted state can arise [217, 220, 496, 1190–1193].

The simplified expressions given above suffice for a broad understanding of the magnetic behaviour exhibited by ultrathin films and are used in the following sections to describe the magnetic anisotropies of thin Fe, Co and Ni films.

6.2. *Effect of temperature*

The temperature dependence of the magnetic anisotropy is an important aspect of the behaviour of magnetic systems and has been widely studied in bulk systems as well as in ultrathin films. For localized spin systems, a reasonably well-established understanding of the physical processes and a microscopic description of the temperature variation of the magnetic anisotropy has long been available [1194];

within the context of the single-ion interaction pair model (with Hamiltonian $H = -\sum_i D\vec{S}_{zi}^2$), a relation between the temperature dependent magnetic anisotropy and magnetization has been derived at low temperatures, as [1194]

$$\kappa_l(T)/\kappa_l(0) = [M_s(T)/M_s(0)]^{l(l+1)/2}, \qquad (60)$$

where $\kappa_l(T)$ is the coefficient affecting the magnetic anisotropy energy expansions (2) and (3) when expressed in terms of the spherical harmonic combinations $\Upsilon_l = \sum_m a_l^m Y_l^m(\vec{\alpha})$, dictated by the crystal symmetry [191,1194]. For temperatures close to the critical temperature, the exponent in (60) is expected to be equal to l and for other types of interactions the temperature range of validity for the previous expression is reduced to lower temperatures [1194]. The magnetoelastic energy terms follow the same expression [1194], which is expected since the magnetoelastic energy also originates from spin–orbit coupling. The above expression arises from a thermal average of the spin deviations (magnons) away from the easy magnetic direction and may be less suitable for itinerant ferromagnets. However, the general dependence seems to hold, as found experimentally in several magnetic thin film systems [1196–1198], although with an exponent that cannot be calculated simply from the previous expression. In this respect, recent developments in theoretical *ab initio* calculation methods have made possible the study of the magnetocrystalline anisotropy temperature dependence in metallic magnets, including thin films [1199–1202], and important developments are expected in this area in the near future.

An aspect which we wish to discuss here relates to the thickness dependence of the magnetic anisotropy, which is often determined experimentally at constant temperature. As described in section 3.2, the Curie temperature depends strongly on the film thickness for monolayer-thick films; for example, the magnetic anisotropy of a film barely magnetic at room temperature yields a value for the magnetic anisotropy that may be strongly reduced compared with equivalent measurements at low temperatures or compared with a film only slightly thicker. One way to circumvent this 'artefact' is to plot the anisotropy values as a function of the reduced temperature T/T_c [191,1195], since in magnetic systems this reduced temperature can be seen as a scaled temperature [1203] (for the 2D Ising system, the thermal variable is $\tilde{T} = \exp\{2J/k_BT\}$, as mentioned in section 3.1). Using this insight, Farle *et al* [191,1195] have shown how apparent scatter in the data at small thicknesses when plotted at constant temperature falls into the same linear curve when plotted against the reduced temperature. This is illustrated in figure 24, showing the variation of the perpendicular magnetic anisotropy constant of Co/Cu(1 1 1) with the reduced temperature after size effect corrections to the critical temperature (the actual temperature range extends from ~160 to 300 K) [1195]; it shows that the temperature dependence of the anisotropy constant becomes particularly pronounced for the thinnest films, demonstrating the importance of plotting the anisotropy constants with the film thickness at a constant reduced temperature. Experimentally, this procedure is cumbersome, and most often data at a fixed temperature are presented; in such cases, only the thicker data points, for which the Curie temperature approaches that of the bulk, or is much larger than the temperature of measurement, should be considered in the data analysis. The dependence of the critical temperature on the film thickness can be obtained from studies of the shift exponent, discussed in section 3.2 and presented in table 5 for selected systems.

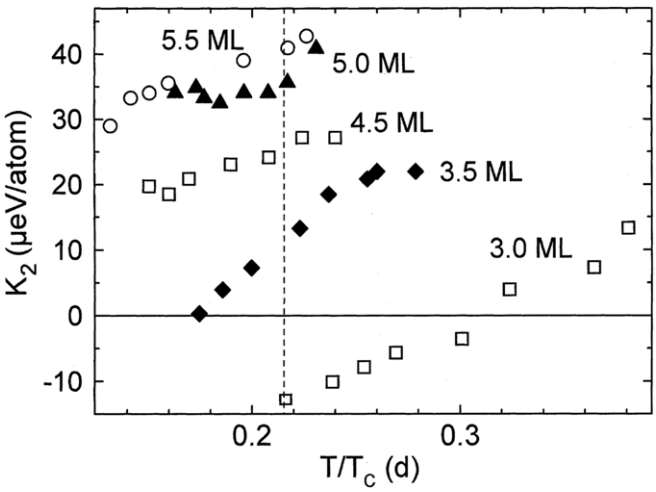

Figure 24. Variation of the perpendicular magnetic anisotropy constant of Co/Cu(1 1 1) with the reduced temperature after size effect corrections to the critical temperature. The 3 ML data point under the dashed line has been extrapolated [1195]. Reprinted from M Farle, W Platow, E Kosubek and K Baberschke 1999 Magnetic anisotropy of Co/Cu(1 1 1) ultrathin films *Surf. Sci.* **439** 146. Copyright (1999), with permission from Elsevier.

6.3. fcc Fe/Cu(0 0 1)

The magnetic properties of this system have been largely presented in section 5.5, where we emphasized the strong correlation between magnetism and crystal structure. There we saw how the intricate and coincident structural and magnetic evolutions exceedingly complicate our understanding of the magnetic anisotropies in this system. In figure 19 we reproduced the typical magnetic evolution observed for fcc Fe/Cu(0 0 1) films grown under different conditions and growth techniques. Broadly speaking, one can distinguish a state of perpendicular magnetization at low Fe thicknesses, up to a critical thickness that depends on the film morphology and/or structure, beyond which the magnetization switches to the in-plane direction (spin-reorientation transition). Given the coincidence of structural modifications with the changes in the magnetic state of these films, the separation between intrinsic magnetocrystalline anisotropies and extrinsic anisotropic contributions remains an open challenge.

6.4. fcc Co/Cu(0 0 1)

In contrast, the Co/Cu(0 0 1) system is relatively well behaved, and has been considered a model system for the study of magnetic phenomena, exhibiting no strong structural, magnetic and chemical instabilities. Indeed, the Co/Cu system has been one of the most extensively investigated magnetic thin

film systems, and our current understanding of nanomagnetism owes much to such work. Several reviews of the magnetic anisotropies of Co/Cu(0 0 1) are available in the literature [83, 84, 171].

The lattice mismatch between fcc Co and Cu(0 0 1) is $\tilde{\eta} = -1.66\%$, and Co grows in registry with the Cu(0 0 1) substrate (in a face centred tetragonal structure) for thicknesses below $t_c \approx 26$ Å (or 15 ML) [720, 721, 1204], beyond which misfit dislocations set in to relax film strain. Co and Cu have a very limited equilibrium miscibility at each end of the composition range at low temperatures (the miscibility of Cu in Co is 0.2% at 400°C [1205]) [1206] and Cu surface segregation is limited in the range below 100 °C [838, 1207–1210] to 250 °C [1211–1213]. Interface interdiffusion in submonolayer Co coverages has been identified in STM studies of Co/Cu(0 0 1) grown at room temperature [1214] and also confirmed in other reports [838, 1213–1216]. Above 2 ML, Co grows in an almost layer-by-layer mode at room temperature [528, 529, 1046, 1211, 1214, 1217, 1218]; below this thickness a layer-by-layer growth mode is observed at low deposition rates, ~0.003 ML s^{-1}, while double layer growth is observed at higher rates, ~0.3 ML s^{-1} [1214, 1219], in agreement with the results of molecular dynamics simulations at 310 K which predict bilayer island formation at high deposition rates, attributed to an upward interlayer transport mechanism at the island edges [1220]. Other studies report the formation of double Co islands before completion of the first monolayer at deposition rates between 0.003 and 0.02 ML s^{-1} [528, 530, 531, 838, 1218]. The sensitivity of the Co surface morphology to the growth conditions is likely the reason for the discrepancy in the magnetic behaviour reported for submonolayer-thick films [838]. A striking example of this sensitivity is the sudden jump in the Curie temperature in Co/Cu(0 0 1) films at 1.8 ML thickness, corresponding to physical coalescence of the Co islands [531]; at this particular thickness, the critical behaviour of the Co film depends sensitively on thermal treatment and time, due to changes in the film morphology. Despite such complications, the equivalent of a single monolayer of Co on Cu(0 0 1) is ferromagnetic, albeit with a reduced Curie temperature [531, 1046, 1212, 1221–1223].

Several studies of the magnetic anisotropies of fcc Co/Cu(0 0 1) have been reported in the literature [171, 267, 529, 1204, 1224, 1225]. One detailed study of the evolution of the magnetic anisotropies of fcc Co/Cu(0 0 1) thin films with thickness (both at room temperature and at 77 K) is that of Kowalewski *et al* [1226]. The results for the uniaxial out-of-plane and four-fold in-plane anisotropy constant variation with thickness at both temperatures are reproduced in figure 25 and the values in the insets show the anisotropy constants extracted from fits to the data to expressions of the form given in (57). In both cases, the variation with thickness is due to the surface contribution to the magnetic anisotropy energy; the values obtained for the uniaxial perpendicular anisotropy constants for fcc Co/Cu(0 0 1) are +0.508 erg cm^{-2} at 77 K and +0.263 erg cm^{-2} at 300 K (our sign convention), favouring in-plane magnetization, while the value for the four-fold in-plane surface anisotropy is smaller by two orders of magnitude, expressing the much larger interruption in the crystal potential along the out-of-plane direction. At large thickness the anisotropy constants converge to the volume values, which for the uniaxial term arise from the magnetostatic and magnetoelastic energy contributions; the values given in figure 25 correspond to the magnetoelastic energy term only and issue from the strain in the Co film. This strain leads to a tetragonal distortion in the crystal structure, which results in a reduced symmetry and in much larger anisotropies than those corresponding to the cubic magnetocrystalline anisotropy. It turns out that phenomenological estimates of the magnetoelastic energy based on classical elastic theory are sufficient to explain the size of the anisotropies observed; for the (0 0 1) cubic surface under a *biaxial* strain ϵ, the magnetoelastic anisotropy can be expressed as [174, 1177, 1178, 1226]

$$K_{ME} = B_{me}\epsilon = \tfrac{3}{2}c_{11}\left(1 + \frac{2c_{12}}{c_{11}}\right)\lambda_{100}\epsilon, \qquad (61)$$

where c_{11} and c_{12} are the elastic moduli and λ_{100} is the (0 0 1) film magnetostriction coefficient. If the bulk magnetostriction coefficient is used, then the expression for the magnetoelastic anisotropy becomes

$$K_{ME} = \tfrac{3}{2}\left(1 + \frac{2c_{12}}{c_{11}}\right)(c_{11} - c_{12})\lambda_{100}^{bulk}\epsilon. \qquad (62)$$

Assuming a fully strained Co film, $\epsilon = -\tilde{\eta}$, where $\tilde{\eta} = a_{Co}/a_{Cu} - 1$ is the lattice mismatch, and using room temperature bulk values for the elastic moduli and for the magnetostriction coefficient, $c_{11} = 2.42 \times 10^{12}$ erg cm^{-3}, $c_{12} = 1.60 \times 10^{12}$ erg cm^{-3} [1227, 1228] and $\lambda_{100} = 1.33 \times 10^{-4}$ [239], one obtains $K_{ME} = 6.31 \times 10^{6}$ erg cm^{-3}, not far from the experimental value; for comparison, *ab initio* calculations of the magnetoelastic energy of the Co monolayer on Cu(0 0 1) by Shick *et al* [1177] yields a volume magnetoelastic energy of 15.63×10^{6} erg cm^{-3}. The four-fold volume anisotropy constant agrees well with the bulk magnetocrystalline anisotropy constant of fcc Co, $K_1 = 1.2 \times 10^{6}$ erg cm^{-3} [239]. The systematic study of the variation of the magnetic anisotropies of fcc Co/Cu(011) with thickness by Hillebrands *et al* [1229] is also particularly instructive. Of relevance in the context of the effect of the magnetoelastic contribution to the magnetic anisotropy of fcc Co(0 0 1) is the work on Co/Ni/Cu(0 0 1) structures by Vaz *et al* [1051, 1063], where use was made of the fact that in the incoherent growth regime of Ni, the partially relaxed Ni lattice can be used as a template for growth of differently strained fcc Co films, and which allows the separation of magnetocrystalline and magnetoelastic contributions to the bulk anisotropy terms. Due to the biaxial strain induced by the lattice mismatch in the (0 0 1) surface plane, the out-of-plane anisotropy is expected to be strongly modified due to magnetoelastic coupling. The study of the perpendicular magnetic anisotropy of fcc Co(0 0 1) with strain shows that the second order anisotropy constant is significant and changes in an opposite fashion compared with the first order anisotropy constant such that the effective magnetoelastic contribution cannot be made to favour a state of perpendicular magnetization. For fcc Co films grown on

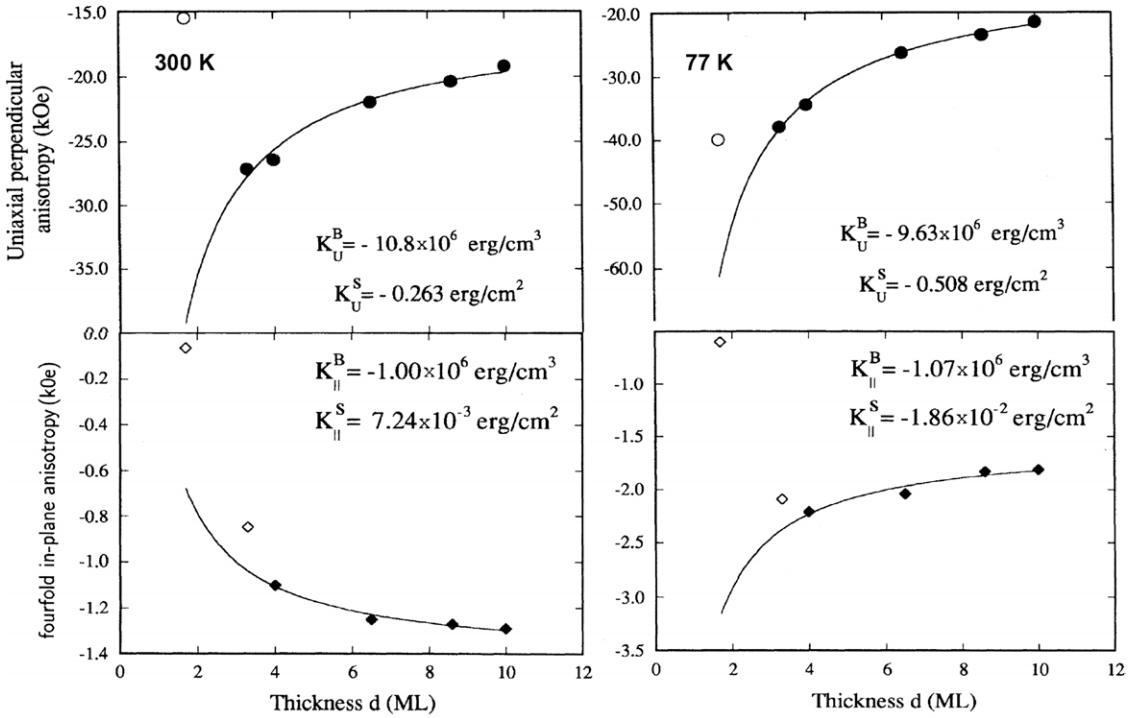

Figure 25. Variation of the uniaxial out-of-plane (top) and four-fold in-plane (bottom) magnetic anisotropy of Co/Cu(0 0 1) films as a function of thickness at room temperature (left) and 77 K (right) (adapted from [1226]). Empty symbols indicate data points not included in the fits due to reduced Curie temperature and a not well-defined strain in the film. The sign convention for the anisotropy constants is opposite the one adopted here. Reprinted with permission from M Kowalewski, C M Schneider and B Heinrich 1993 Thickness and temperature dependence of magnetic anisotropies in ultrathin fcc Co(0 0 1) structures *Phys. Rev.* B **47** 8748. Copyright (1993) by the American Physical Society.

slightly miscut Cu(0 0 1) surfaces, Weber *et al* [1204] have shown that the critical coherence thickness for the onset of misfit dislocations at ∼15 ML correlates with changes in the magnetic anisotropy, in this case attributed to a directional relaxation of the lattice strain due to the stepped surface.

In figure 25, it is observed that for the smallest Co thicknesses (open symbols) the data points deviate from the expect variation, while the deviation is less severe for the measurements at 77 K, an effect attributed to a reduced Curie temperature and a not well-defined strain in the film [1226]. The Curie temperature may be also reduced for films up to 6 ML thickness, but corrections are difficult to implement in Co due to the high Curie temperature of films thicker than about 2 ML (measurements of the variation of T_c with Co thickness are not possible without causing structural modifications in the Co film at high temperatures). The importance of taking into account the effect of temperature and the variation of the Curie temperature with film thickness has been demonstrated for ultrathin Co/Cu(1 1 1) films by Farle *et al* [1195], who showed that the correct sign and amplitude of the interface anisotropy constant can only be obtained by considering the implicit variation in the reduced temperature with film thickness, see figure 26; for films thicker than 6 ML, the surface anisotropy reverses sign, due to the occurrence of structural transformation in the film [1195, 1223]. Hence, magnetic surface anisotropies obtained from measurements at constant temperature are reliable only for films sufficiently thick so that variations in the critical temperature with thickness are negligible; structural changes that could modify the interface anisotropies also need to be ruled out.

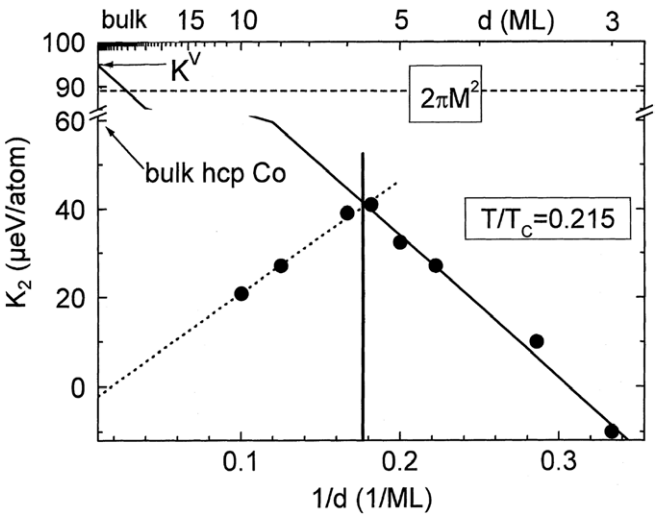

Figure 26. Variation of the perpendicular magnetic anisotropy constant of Co/Cu(1 1 1) with film thickness at a constant reduced temperature $T/T_c = 0.215$ [1195]. Reprinted from M Farle, W Platow, E Kosubek and K Baberschke 1999 Magnetic anisotropy of Co/Cu(1 1 1) ultrathin films *Surf. Sci.* **439** 146. Copyright (1999), with permission from Elsevier.

The presence of a non-magnetic overlayer exerts a strong effect on the magnetic anisotropy of thin ferromagnetic films through interfacial hybridization [737, 1044, 1230–1232],

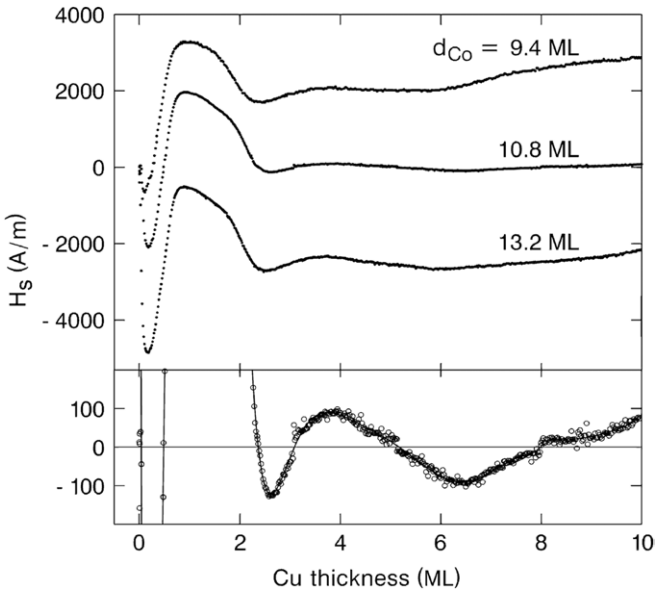

Figure 27. Variation of the 'shift field' (a measure of the magnetic anisotropy) with Cu capping layer in fcc Co films grown on a 3.4° miscut Cu(0 0 1) surface, for different Co film thicknesses, t_{Co} [1225]. (The shift field is the coercivity of the symmetric minor loops observed along the intermediate magnetic axis, measured with respect to the zero field.) Reprinted with permission from W Weber, A Bischof, R Allenspach, Ch Wursch, C H Back and D Pescia 1996 Oscillatory magnetic anisotropy and quantum well states in Cu /Co /Cu(1 0 0) films *Phys. Rev. Lett.* **76** 3424. Copyright (1996) by the American Physical Society.

quantum confinement effects (quantum well states) [1225] or strain [198, 1137, 1204], resulting in changes in the amplitude of the magnetic anisotropy and in the magnetization switching behaviour [138, 1040, 1044, 1231–1236]. When interfacial hybridization effects dominate, the modification in magnetic anisotropy should be maximal at full surface coverage, i.e. about 1 ML thickness. This is the case for the effect of Cu, Pd, Ag, Au and Pt capping layers on the interface anisotropy of hcp Co(0 0 0 1) films exhibiting dominant perpendicular magnetic anisotropy reported by Kohlhepp *et al* [1040], Beauvillain *et al* [1044, 1232] and Engel *et al* [1231, 1237, 1238], showing that strong anisotropy changes occur for approximately 1 ML capping layer thickness. The role of quantum well states was demonstrated by Weber *et al* [1225] in Cu/Co/Cu(0 0 1) (using slightly miscut Cu single crystals) who observed a periodic oscillation in the magnetic anisotropy as a function of the Cu capping layer, see figure 27. Changes in the band structure from quantum well states [92–99, 102–104] modify the magnetic anisotropy via spin–orbit coupling, but with a characteristic oscillation period that need not coincide with that observed for interlayer coupling [1048, 1239–1245] since the electronic states affecting the magnetic anisotropy issue from the entire Brillouin zone, unlike the exchange coupling which is governed by states at the Fermi surface [1225]. The observed period of the oscillation (3–4 ML) is independent of the Co film thickness, and for a 10.8 ML Co film, the anisotropy easy axis is found to oscillate between the [1 $\bar{1}$ 0] and [1 1 0] directions, as shown in figure 27. Strain induced by the overlayer can also modify the magnetic anisotropy, in particular for partially relaxed magnetic films, as the strain in the overlayer may be transmitted to the magnetic film with increasing capping layer thickness. This is observed as a monotonic change in the coercive field with increasing Cu capping layer in Ni/Cu(0 0 1) and Co/Cu(0 0 1) systems for Cu thicknesses well beyond film coverage [198, 1137].

Another key ingredient for the understanding of the magnetic behaviour of thin films is the effect of surface morphology, in particular atomic steps and other surface defects. A series of studies addressing this problem was carried out by Weber *et al* [138, 1204, 1233] on deliberately miscut Cu(0 0 1) crystal substrates. For a 1.6° miscut sample, the initial step anisotropy favours spin alignments parallel to the step edges. However, minute coverages of non-magnetic metals cause a 90° switching of the Co spins from an alignment along the steps to one perpendicular to them. Further deposition of the non-magnetic metal (Cu, Ag) or even O_2 caused the Co spins to reorient again to become aligned parallel to the step edges. The view that the origin of the behaviour is due to the atomic steps is supported by STM studies which show that the Cu tends to preferentially adsorb at the step edges [1246]. With increasing coverage, Cu growth occurs on terraces and the step geometry is recovered with a concurrent reappearance of step-induced magnetic anisotropy. *Ab initio* calculations also found that submonolayer amounts of Cu on Co/Cu(0 0 1) change dramatically the electronic and magnetic properties of the system [1247] due to hybridization of Co and Cu d electrons when Cu forms a wire structure next to a Co step at the surface. It is remarkable that such small coverages of a non-magnetic material can have such a strong effect [1247]. Subsequent studies used the linear part of the magnetic hysteresis loops associated with two fold anisotropy induced by the steps to determine the thickness dependence of the uniaxial anisotropy. Evidence of oscillatory (1 ML period) anisotropy was found in this way [1204, 1249], attributed to the periodic variations of the film morphology alternating between filled and incompletely filled atomic layers, which leads to an oscillatory relaxation of the lattice constant of the topmost surface layer [1204, 1248].

Adsorbates have also been shown to lead to drastic changes in the magnetic anisotropy of ultrathin films. Exposure of Co films grown on stepped Cu(0 0 1) surfaces to 20 L (1 L = 10^{-6} Torr s) oxygen leads to a switching in the easy magnetization axis; the observation of a $c(2\times2)$ reconstruction in the O exposed surface indicates that O adsorbs on the terraces, and therefore the change in anisotropy is likely due to a hybridization or bonding process [138]. Trace amounts of CO have the effect of switching the magnetic easy axis of Co/Cu(1 1 0) thin films from the [0 0 1] direction to [1 $\bar{1}$ 0] [139, 140, 1250]. This effect was observed while Co(1 1 0) was exposed to residual gases in a 10^{-10} mbar ultrahigh vacuum and confirmed by exposure to the equivalent of 0.08 ML of CO adsorbed to the surface, see figure 28; that such minute amounts of CO are able to so drastically modify the magnetic anisotropy of the whole Co film suggest that the CO adsorbs at specific sites in the surface, such as steps, which could strongly alter the strength of the step anisotropy. In fact, unlike the Co/Cu(0 0 1) system, Co/Cu(1 1 0) grows in a three-dimensional (3D) mode,

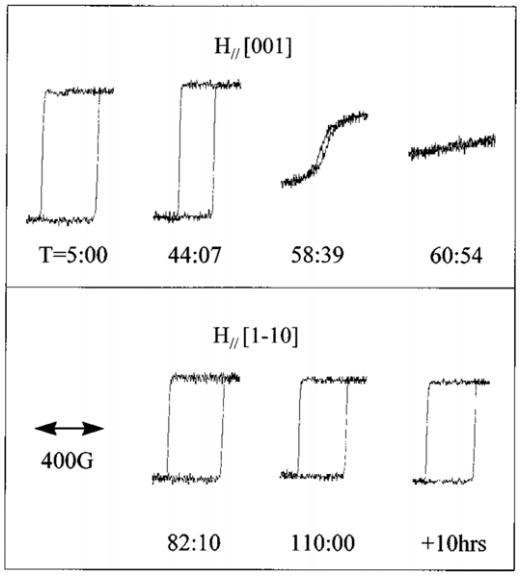

Figure 28. Time evolution of the hysteresis loops of a 6 ML Co/Cu(1 1 0) film after deposition, showing the switch in the magnetic easy axis from the [0 0 1] direction to the [1 $\bar{1}$ 0] direction due to exposure to trace amounts of residual CO [1250]. Reprinted with permission from S Hope, E Gu, M Tselepi, M E Buckley and J A C Bland 1998 Dynamic evolution of the magnetic anisotropy of ultrathin Co/Cu(1 1 0) films *Phys. Rev.* B **57** 7454. Copyright (1998) by the American Physical Society.

with elongated islands (oriented along the [0 0 1] direction, according to Hope *et al* [1250], or along the [1 $\bar{1}$ 0] direction, according to Fassbender *et al* [1251]); Co/Cu(1 1 0) films below 5 nm have a dominant uniaxial anisotropy with easy magnetization axis along the [0 0 1] direction, attributed to the effect of strain due to the lattice mismatch in the low symmetry (1 1 0) surface plane of Cu [1229, 1251–1253]. For thicknesses above 5 nm the uniaxial anisotropy vanishes and the [1 1 1] direction becomes the magnetic easy axis, as in bulk fcc Co. The effect of O and N adsorbates on the Cu(0 0 1) substrate is also found to affect the magnetic properties of Co films up to 12 ML in thickness [1254].

Atomic step-induced magnetic anisotropies have been investigated by other groups and extensive results for bcc Fe films have been reported by Albrecht *et al* [202], for example. In particular, the group of Gradmann has also related step-induced moments to step-induced anisotropies and shown that enhanced moments occur for Fe moments at atomic steps on roughened surfaces [1255]. The Strasbourg theory group have made extensive predictions of the magnitudes of magnetic moments at atomic steps [71]. It should be noted that the step-induced uniaxial anisotropy easy axis can lie either along the steps or perpendicular to the steps. The latter case has been identified for Fe/W(1 1 0) structures [203], whereas the former case applies for Co films on deliberately stepped Cu(1 1 13) surfaces up to ∼16 ML thickness [1225, 1256]. This behaviour can be thought of as analogous to the surface anisotropy at planar interfaces in ultrathin films which can be positive or negative in sign. As in Néel's model of surface anisotropies, the origin of step-induced anisotropy is due to the reduced symmetry of the atoms at the step edges. It is clear that there is considerable future scope for combining experimental and theoretical studies to relate step moments and anisotropies quantitatively.

On a larger scale, interface and surface roughness is also widely recognized to result in extra magnetostatic energy via the so-called 'orange-peel' effect [1257], resulting, for example, in changes in the perpendicular magnetic anisotropy [1258–1262], extra anisotropy terms in surfaces with directional morphology [1258, 1263–1266] and additional magnetic coupling in multilayer systems [1267–1276]. Another roughness contribution to the magnetic anisotropy of epitaxial ultrathin films covering a randomly corrugated substrate surface has been suggested, whereby the magnetization is expected to follow the roughness profile, reducing the magnetostatic energy contribution, but giving rise to an additional magnetic anisotropy contribution due to the tilting away from the magnetization easy axis [1277–1279]. In measurements of the magnetic anisotropy, unless the applied magnetic field completely saturates the sample magnetization (which may require fields of the order of a few tesla for 3d transition ferromagnets), a residual ripple in the magnetization will contribute to the magnetic anisotropy. Such contribution has been identified in fcc Co films grown on rough Cu(0 0 1) template layers [1278, 1279].

Studies of the film thickness dependence of the magnetic anisotropy have now been carried out for a wide range of epitaxial systems. Such investigations reveal a highly sensitive dependence of the magnetic anisotropy on the growth conditions and film morphology. As such studies increase in sophistication it is now becoming clear that the structure at the atomic level has a profound influence on the observed anisotropy behaviour and where STM studies are providing important insights.

6.5. fcc Ni/Cu(0 0 1)

The early studies of the magnetic properties of epitaxial Ni/Cu(0 0 1) showed an intriguing behaviour for the magnetic anisotropy evolution as a function of the Ni film thickness: while below ∼1.5 nm the magnetization was found to lie in the plane of the film, indicating dominant in-plane anisotropy, above this thickness a sudden reorientation of the magnetic easy axis was observed along the out-of-plane direction, indicating a dominant perpendicular magnetic anisotropy (PMA); for thicknesses above ∼12 nm the perpendicular magnetic anisotropy fades gradually and in-plane magnetization ensues [223, 224, 1182, 1280–1282]. (Ni films as thick as 200 nm are also reported to exhibit perpendicular magnetic anisotropy, with perpendicular domains capped by closure domains [1283].) Such a large range of dominant perpendicular magnetic anisotropy observed for this material spurred much interest, partly motivated by the possibility of applications in perpendicular recording media. In this context it is worth noting that the first report of PMA of Ni/Cu(0 0 1) by Chang [1280] employed epitaxial Cu buffer layers deposited on Si(0 0 1), a method for obtaining Cu(0 0 1) single crystalline surfaces followed by several research groups.

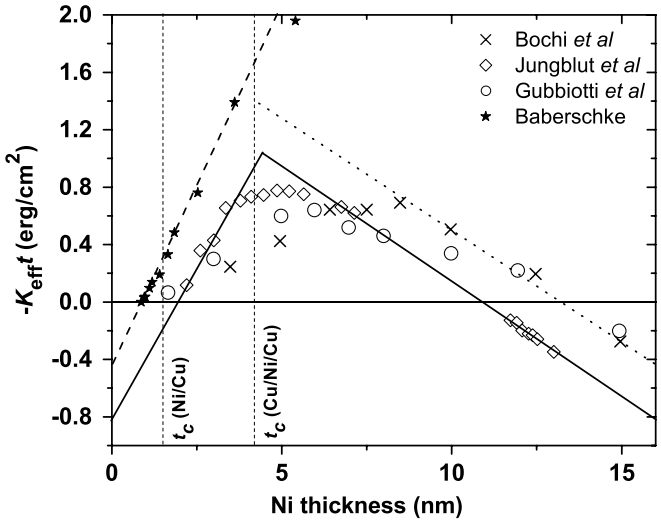

Figure 29. Room temperature variation of the magnetic anisotropy of Ni/Cu(0 0 1) as determined experimentally by several groups: Jungblut *et al* [1281], Bochi *et al* [1182, 1183], Gubbiotti *et al* [1132] and Baberschke [460]. Lines are linear fits to the data.

Ni(0 0 1) has a relatively small lattice mismatch $\tilde{\eta} = -2.5\%$ with Cu(0 0 1), and it is found experimentally that Ni(0 0 1) films grow homoepitaxially on Cu(0 0 1) up to a coherence thickness of approximately 15 Å [717, 1281, 1284], after which misfit dislocations set in to relief strain. Several reports have demonstrated that Ni grows layer by layer on Cu(0 0 1) single crystals at room temperature with no interdiffusion [257, 1285–1289], although some evidence of limited intermixing at the interface has been reported in a 1.1 ML Ni/Cu(0 0 1) film grown at room temperature [1135]. Better Ni films, with less roughness, improved layer-by-layer growth and larger coherent growth thickness (due to a decrease in the interface energy compared with the bare Cu surface [75]), can be grown using oxygen as a surfactant [1140, 1290, 1291]. While Cu(0 0 1) single crystals, after suitable preparation, offer the best surfaces, several studies have been performed on epitaxial Cu(0 0 1)/Si(0 0 1) buffer layers [223,224,1182,1183,1292], after the demonstration that crystalline Cu(0 0 1) can be grown epitaxially on H-passivated Si(0 0 1) [1293, 1294]. One major advantage of using this approach is that of opening the possibility of combining magnetic metal systems with semiconductors, which is key to the integration of magnetism into current microelectronic technology; also, high quality Si surfaces are widely available and its surface preparation is relatively simple. One concern is the reaction at the Cu/Si interface as expected for the Cu–Si system and observed experimentally [1295–1297] (although disparate results have been reported [1298–1302]). Fairly good surfaces require the growth of relatively thick Cu buffer layers, from 100 to 200 nm, yielding surface roughnesses in the sub-nanometre range [1130, 1136, 1139]. Such extra surface disorder may promote interdiffusion at the Cu/Ni interface, but the experimental evidence points to the absence of significant intermixing [1134].

The evolution of the magnetic anisotropy of Ni/Cu with Ni thickness was studied by several authors and in figure 29 we show the results obtained by several groups. Differences that need to be taken into account include the absence [460] or presence [1132, 1182, 1183, 1281] of a Cu capping layer, growth on a Cu(0 0 1) single crystal [460, 1281] or a Cu(0 0 1) buffer layer [1132, 1182, 1183] and whether the measurements were corrected for variations in the Curie temperature [460]. The latter corrections are important for films thinner than 16 Å (9 ML) for uncapped Ni films (see table 5), where the Curie temperature deviates by more than 20% from that of the bulk; for Cu capped films such corrections are likely to be important for thicker Ni films. Broadly speaking, one finds a dominant PMA for an intermediate thickness range from approximately 2 to 12 nm ($K_{\rm eff}t < 0$) [460, 1132, 1182, 1183, 1281]. Using our sign convention, the positive value of $K_{\rm eff}t$ at $t = 0$ indicates that the effective surface anisotropy favours in-plane magnetization, while the initial negative slope indicates that the effective volume anisotropy favours perpendicular magnetic anisotropy: the magnetostatic energy favours in-plane magnetization, but is overwhelmed by the magnetoelastic energy, which favours PMA [1288]. With increasing thickness, the sign of $K_{\rm eff}t$ changes from positive to negative and PMA ensues. Beyond a certain Ni thickness, the slope of $K_{\rm eff}t$ becomes positive, indicating that the volume term increasingly favours a state of in-plane magnetization. This is due to the fact that, above a critical Ni thicknesses, misfit dislocations set in to relax strain, and the magnetoelastic energy no longer scales with the sample volume. In this regime, the film strain varies approximately as $\epsilon = -\tilde{\eta}t_{\rm c}/t$ [1176]. Because of this inverse dependence on the film thickness, the magnetoelastic anisotropy due to strain above $t_{\rm c}$ behaves as an effective surface anisotropy. Extrapolation of this part of the curve to $t = 0$ yields, all other factors constant, $2K_{\rm s} - B_{\rm me}\tilde{\eta}t_{\rm c}$, from which the magnetoelastic coefficient or $t_{\rm c}$ could be determined. Beyond around 12 nm, the magnetostatic energy becomes dominant and a state of in-plane magnetization sets in. The Ni thickness range over which perpendicular anisotropy dominates is determined, therefore, by a fine balance between elastic and surface bonding on the one hand, which determine the range of coherent growth before dislocations set in to relief strain, and on the other hand, by magnetoelastic, magnetostatic and magnetic anisotropy energies.

The magnetic behaviour described above follows closely that described by (58) or, taking into account explicitly the change due to strain relaxation above the critical coherence thickness:

$$K_{\rm u,eff} = \begin{cases} 2\pi M_{\rm s}^2 + B_{\rm me}\epsilon + 2K_{\rm s}/t, & t \leqslant t_{\rm c} \\ 2\pi M_{\rm s}^2 + (B_{\rm me}\epsilon_0 t_{\rm c} + 2K_{\rm s})/t, & t > t_{\rm c}. \end{cases} \quad (63)$$

While Ni films are found to grow coherently on Cu(0 0 1) single crystals up to a critical thickness of $t_{\rm c} \approx 15$ Å [717,1281,1284], for Cu/Ni/Cu(0 0 1) $t_{\rm c}$ is extended to ≈42 Å [1281]. This difference in $t_{\rm c}$ explains partly the horizontal shift observed in the data sets shown in figure 29. The expression above predicts a sharp peak at $t_{\rm c}$, but the transition from the fully strained to the partially relaxed regime may be less abrupt than assumed; in fact, deviations from the $1/t$ strain variation have been reported [224, 718, 1183, 1204]. This may also result in a non-linear variation in $tK_{\rm u,eff}$ for large Ni thicknesses and the data shown in figure 29 may suggest this issue to be more significant

for the Ni films grown on Cu(0 0 1) buffer layers. Another issue relates to the difference between the magnetoelastic anisotropy obtained from the slope below t_c and from extrapolation to zero of the curve above t_c, where the latter procedure yields a larger value. This may be related to a slight reduction in the Ni magnetization at small Ni thicknesses, as shown in figure 21 (corrections due to reduced Curie temperature are less significant for the Ni thickness range shown in the graph, although this is no longer the case for films thinner than 8 Å, see [460]). Surface magnetoelastic terms have been suggested to contribute to the magnetic anisotropy [224, 1177, 1182, 1183], but this remains controversial; we note that such contribution would add to the surface anisotropy term below t_c; above t_c, the contribution to the total energy would be expected to become small, given the expected $1/t^2$ dependence associated with this surface term.

The in-plane magnetization found for Ni thicknesses below 2.5 nm has been interpreted in two ways: (i) due to a positive surface magnetic anisotropy at the Ni/Cu interface which favours a state of in-plane magnetization at small thicknesses [460, 566, 1190, 1281, 1303, 1304], an interpretation supported by band structure calculations which predict a positive K_s (in our notation) for Ni/Cu(0 0 1) [75, 742, 1305]; (ii) due to a large positive surface magnetoelastic coupling energy [224, 1182, 1183].

Experimental evidence of a negative K_s was initially suggested from the magnetic anisotropy behaviour of $Ni/Cu_{1-x}Ni_x/Cu(0\,0\,1)$, which shows a variation in the critical thickness for the onset of PMA that varies with x [224]. It was therefore suggested that different interfaces led to different surface magnetic anisotropies while it was assumed that differences in the lattice mismatch do not effect the PMA as expected from the Mathews–Blakeslee model [196, 1181]—which predicts that the misfit strain in the Ni film is independent of the lattice mismatch to the underlayer in the incoherent regime. However, the results of Lauhoff *et al* [1306, 1307] on $Ni/Cu/Ni_{60}Cu_{40}/Cu(0\,0\,1)$ films suggest that changes in surface anisotropies are not significant while strain is responsible for the change in the magnetic anisotropy. Indeed, it is found that on changing the Ni/Cu interface to $Ni/Ni_{60}Cu_{40}$ while keeping the Ni film under the same strain (by interposing a 1 nm thick Cu layer between Ni and $Ni_{60}Cu_{40}$), one finds no significant changes in the M–H characteristics. Conversely, when keeping the same interface but modifying the strain (by varying the thickness of the same Cu spacer layer), large modifications in the M–H loops are observed (figure 30), confirming that the dominant term for the perpendicular anisotropy arises from strain [1305–1307].

Indirect evidence that strain is the main origin of PMA in this system comes from the measurements of the coercive field. It is well known that defects and dislocations in magnetic single crystals increase the coercive field. O'Brien and Tonner [1282, 1303] have observed a rapid increase in the coercive field when $t > t_c$, i.e. as the strain starts to relax, as shown in figure 31. Vaz *et al* [198, 1137] studied the effect of the Cu capping layer thickness on the coercive field, strain and magnetic moment for 3 nm Au/t^{Cu} Cu/4 nm Ni/100 nm Cu/Si(0 0 1) films, with t^{Cu} = 2–18 nm (figure 22). Both

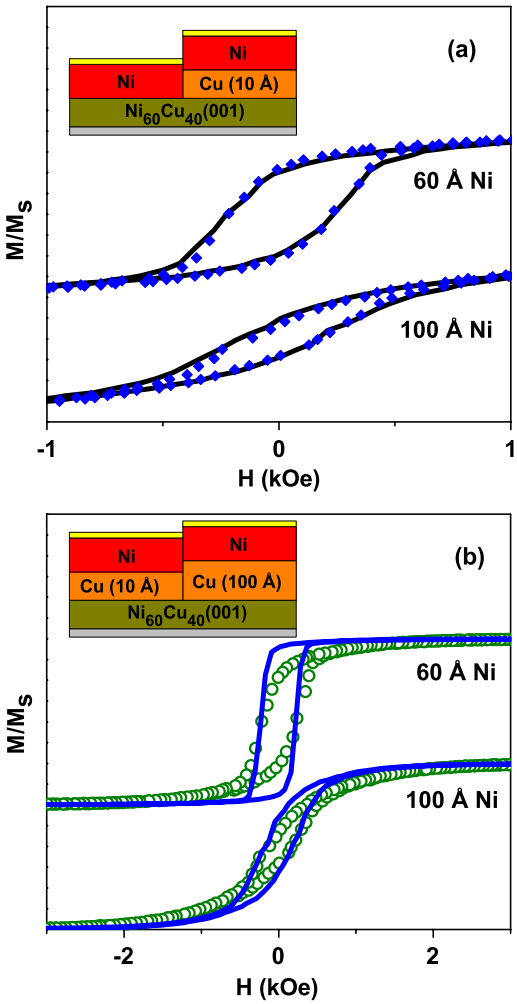

Figure 30. Out-of-plane magnetization curves for fcc Ni films embedded in $Cu/Ni/Cu(t)/Ni_{60}Cu_{40}/Cu/Si(0\,0\,1)$ structures demonstrating the effect of strain and interface on the magnetic anisotropy of Ni [1307]. (*a*) Identical strain, different interface: Ni/Cu ($t = 0$ nm, diamonds) and $Ni/Ni_{60}Cu_{40}$ ($t = 1$ nm, solid line). (*b*) Same interface, different strain: $t = 1$ nm (circles) and $t = 10$ nm (solid line). The lattice mismatch between Ni and bulk $Ni_{60}Cu_{40}$ is $\tilde{\eta} = -1.1\%$ [1205].

the coercive field and the strain are found to increase with increasing Cu capping layer thickness. The magnetization reversal process in Ni/Cu(0 0 1) films has been shown to take place by domain wall motion [1136] and the coercive field for this reversal process has been shown to increase linearly with strain for this process [748].

The effect of an overlayer on the perpendicular magnetic anisotropy of Ni/Cu(0 0 1) has also been addressed. Cu has the effect of increasing the range over which PMA dominates, from 40 Å for the uncapped system [1282, 1288, 1308] to 140 Å [224, 257], while Fe does not seem to change the magnetization direction for Ni thicknesses up to 10 ML [1303], but Co overlayers [1050, 1051, 1063, 1303] or spacer layers in a multilayer system [1049] drastically reduce the PMA, mainly due to the additional magnetostatic energy contribution from the Co films [1055]. For $Ni_{80}Fe_{20}$ a similar effect is observed although the transition to in-plane magnetization occurs at larger thicknesses [1309].

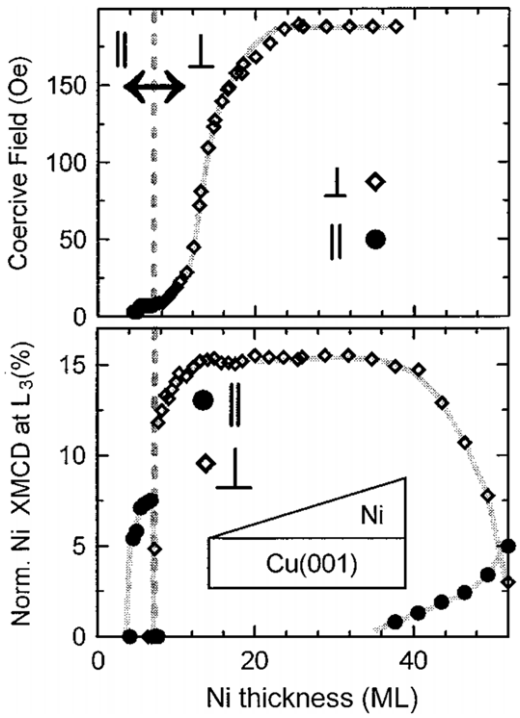

Figure 31. Variation of the coercive field (top) and remanent magnetization (bottom) as a function of Ni film thickness [1303]. Reused with permission from W L O'Brien and B P Tonner 1996 *J. Appl. Phys.* **79** 5623. Copyright 1996, American Institute of Physics.

7. Conclusions

The study of magnetic phenomena at the nanoscale presents a plethora of research possibilities, and the work reviewed here is but a modest testimony to its vibrancy and to the intellectual stimulation it provides to both experimental and theoretical physicists and to technologists. We have chosen to focus in this review on some of the fundamental aspects of thin film magnetism, in particular, key magnetic properties such as magnetic moments, two-dimensional phase transitions, exchange constants and magnetic anisotropies, and to suggest that despite a good deal of work already accomplished, much still remains to be clarified and understood. This is partly due to the fact that several physical mechanisms contribute to determine such properties and their separation is difficult. We also show that *ab initio* band structure calculations have brought an invaluable contribution to our understanding of interfacial magnetism and of magnetism at the nanoscale, and as device dimensions shrink to the nanoscale, there is an increasing recognition of the importance of knowing the modified magnetic parameters (exchange, magnetic moments and anisotropies) in computing magnetic properties, e.g. domain structure and dynamics of spin reversal.

Space and time limitations have imposed strict bounds to the material we were able to present in detail. We trust, however, that our exposition may illustrate some of the fundamental aspects that govern the magnetic behaviour of ultrathin films. In particular, we aimed at highlighting the link between magnetic properties such as magnetic moments, anisotropies and critical behaviour. The availability of appropriate experimental tools is also very important in this context, and this paper also aimed at illustrating the vast array of techniques that have been employed in the study of the magnetism of thin films.

The connection between magnetic properties and the interface structure at the atomic scale has also been emphasized. For example, as discussed in this paper, the presence of atomic steps and submonolayer overlayers can have surprisingly large effects on the magnetic behaviour. Epitaxial systems will continue to be of great value in the subject of ultrathin film and interface magnetism for the insights they provide into the effect of crystallographic structure, strain and well-defined interfaces on magnetic properties. As the results discussed here show, careful studies of such systems have recently advanced considerably our understanding of interface anisotropies and the origin of the interface in giving rise to enhanced moments, for example. The connection between ground state properties, e.g. magnetic moments and magnetic anisotropies, will require much further work in which experimental studies and theoretical modelling of realistic interface structures and strained layers will need to progress in parallel. We are only at the beginning of a fully quantitative understanding of these effects.

Many interesting predictions are already available for the magnetic properties of nanoscale particles and clusters which will require yet further advancement in experimental probes of magnetism. Presently, laterally defined nanostructures prepared by advanced lithographic and pattern transfer techniques, for example, are already playing a key role in magnetism studies, with many new phenomena to be discovered in the near future. Such studies require an even better understanding of interface physics, much as thin film magnetism has required good understanding of the bulk properties of materials.

Acknowledgments

The authors wish to express their gratitude to Jayong Lee for his help in the initial stages of this project and to the authors who kindly permitted their work to be reproduced here. The authors are particularly indebted to R Allenspach and K Baberschke for insightful comments on parts of the manuscript. The comments and suggestions provided by the anonymous referees, which have led to many improvements to the original manuscript, are also duly acknowledged. This work was made possible through the financial support of the EPSRC (UK).

References

[1] Arthur J R 2002 *Surf. Sci.* **500** 189
[2] Bland J A C and Heinrich B (ed) 1994 *Ultrathin Magnetic Structures: I* (Berlin: Springer)
[3] Heinrich B and Bland J A C (ed) 1994 *Ultrathin Magnetic Structures: II* (Berlin: Springer)
[4] Bland J A C and Heinrich B (ed) 2005 *Ultrathin Magnetic Structures: III* (Berlin: Springer)
[5] Heinrich B and Bland J A C (ed) 2005 *Ultrathin Magnetic Structures: IV* (Berlin: Springer)

[6] Baibich M N, Broto J M, Fert A, Nguyen Van Dau F, Petroff F, Etienne P, Creuzet G, Friederich A and Chazelas J 1988 *Phys. Rev. Lett.* **61** 2472
[7] Binasch G, Grünberg P, Saurenbach F and Zinn W 1989 *Phys. Rev.* B **39** 4828
[8] Nielsen J W 1979 *Annu. Rev. Mater. Sci.* **9** 87
[9] Bowen M *et al* 2001 *Appl. Phys. Lett.* **79** 1655
[10] Parkin S S P, Kaiser C, Panchula A, Rice P M, Hughes B, Samant M and Yang S H 2004 *Nat. Mater.* **3** 862
[11] Yuasa S, Nagahama T, Fukushima A, Suzuki Y and Ando K 2004 *Nat. Mater.* **3** 868
[12] Hillebrands B and Ounadjela K (ed) 2002 *Spin Dynamics in Confined Magnetic Structures: I* (*Topics in Applied Physics* vol 83) (Berlin: Springer)
[13] Hillebrands B and Ounadjela K (ed) 2003 *Spin Dynamics in Confined Magnetic Structures: II* (*Topics in Applied Physics* vol 87) (Berlin: Springer)
[14] Hillebrands B and Thiaville A (ed) 2006 *Spin Dynamics in Confined Magnetic Structures: III* (*Topics in Applied Physics* vol 101) (Berlin: Springer)
[15] Tserkovnyak Y, Brataas A, Bauer G E W and Halperin B I 2005 *Rev. Mod. Phys.* **77** 1375
[16] Gallagher W J and Parkin S S P 2006 *IBM J. Res. Dev.* **50** 5
[17] Prinz G A 1995 *Phys. Today* **48** (4) 58
[18] Prinz G A 1998 *Science* **282** 1660
[19] Wolf S A, Awschalom D D, Buhrman R A, Daughton J M, von Molnár S, Roukes M L, Chtchelkanova A Y and Treger D M 2001 *Science* **294** 1488
[20] Žutić I, Fabian J and Das Sarma S 2004 *Rev. Mod. Phys.* **76** 323
[21] Xu Y B and Thompson S M (ed) 2006 *Spintronic Materials and Technology* (London: Taylor and Francis)
[22] Maekawa S (ed) 2006 *Concepts in Spin Electronics* (Oxford: Oxford University Press)
[23] Wolf S A, Chtchelkanova A Y and Treger D M 2006 *IBM J. Res. Dev.* **50** 101
[24] Berger L 1978 *J. Appl. Phys.* **49** 2156
[25] Berger L 1984 *J. Appl. Phys.* **55** 1954
[26] Freitas P P and Berger L 1985 *J. Appl. Phys.* **57** 1266
[27] Berger L 1992 *J. Appl. Phys.* **71** 2721
[28] Salhi E and Berger L 1994 *J. Appl. Phys.* **76** 4787
[29] Berger L 1996 *Phys. Rev.* B **54** 9353
[30] Marrows C H 2005 *Adv. Phys.* **54** 585
[31] Kohno H and Tatara G 2006 *Spintronic Materials and Technology* ed Y B Xu and S M Thompson (London: Taylor and Francis) p 225
[32] Sun J Z 2006 *IBM J. Res. Dev.* **50** 81
[33] Kläui M, Vaz C A F, Bland J A C, Wernsdorfer W, Faini G, Cambril E and Heyderman L J 2003 *Appl. Phys. Lett.* **83** 105
[34] Tsoi M, Fontana R E and Parkin S S P 2003 *Appl. Phys. Lett.* **83** 2617
[35] Yamaguchi A, Ono T, Nasu S, Miyake K, Mibu K and Shinjo T 2004 *Phys. Rev. Lett.* **92** 077205
[36] Vernier N, Allwood D A, Atkinson D, Cooke M D and Cowburn R P 2004 *Europhys. Lett.* **65** 526
[37] Kläui M, Vaz C A F, Bland J A C, Wernsdorfer W, Faini G, Cambril E, Heyderman L J, Nolting F and Rüdiger U 2005 *Phys. Rev. Lett.* **94** 106601
[38] Kläui M, Jubert P O, Allenspach R, Bischof A, Bland J A C, Faini G, Rüdiger U, Vaz C A F, Vila L and Vouille C 2005 *Phys. Rev. Lett.* **95** 026601
[39] Laufenberg M, Bührer W, Bedau D, Melchy P E, Kläui M, Vila L, Faini G, Vaz C A F, Bland J A C and Rüdiger U 2006 *Phys. Rev. Lett.* **97** 046602
[40] Wegrowe J E, Kelly D, Jaccard Y, Guittienne P and Ansermet J P 1999 *Europhys. Lett.* **45** 626
[41] Myers E B, Ralph D C, Katine J A, Louie R N and Buhrman R A 1999 *Science* **285** 867
[42] Katine J A, Albert F J, Buhrman R A, Myers E B and Ralph D C 2000 *Phys. Rev. Lett.* **84** 3149
[43] Albert F J, Katine J A, Buhrman R A and Ralph D C 2000 *Appl. Phys. Lett.* **77** 3809
[44] Grollier J, Cros V, Hamzic A, George J M, Jaffrès H, Fert A, Faini G, Youssef J B and Legall H 2001 *Appl. Phys. Lett.* **78** 3663
[45] Kiselev S I, Sankey J C, Krivorotov I N, Emley N C, Schoelkopf R J, Buhrman R A and Ralph D C 2003 *Nature* **425** 380
[46] Tsoi M, Sun J Z and Parkin S S P 2004 *Phys. Rev. Lett.* **93** 036602
[47] Tsoi M, Sun J Z, Rooks M J, Koch R H and Parkin S S P 2004 *Phys. Rev.* B **69** 100406
[48] Rippard W H, Pufall M R, Kaka S, Russek S E and Silva T J 2004 *Phys. Rev. Lett.* **92** 027201
[49] AlHajDarwish M, Kurt H, Urazhdin S, Fert A, Loloee R, W P Pratt J and Bass J 2004 *Phys. Rev. Lett.* **93** 157203
[50] Zimmler M A, Özyilmaz B, Chen W, Kent A D, Sun J Z, Rooks M J and Koch R H 2004 *Phys. Rev.* B **70** 184438
[51] Krivorotov I N, Emley N C, Garcia A F, Sankey J, Kiselev S I, Ralph D C and Buhrman R A 2004 *Phys. Rev. Lett.* **93** 166603
[52] Covington M, AlHajDarwish M, Ding Y, Gokemeijer N J and Seigler M A 2004 *Phys. Rev.* B **69** 184406
[53] Kiselev S I, Sankey J C, Krivorotov I N, Emley N C, Garcia A G F, Buhrman R A and Ralph D C 2005 *Phys. Rev.* B **72** 064430
[54] Tulapurkar A A, Suzuki1 Y, Fukushima A, Kubota H, Maehara H, Tsunekawa K, Djayaprawira D D, Watanabe N and Yuasa S 2005 *Nature* **438** 339
[55] Rippard W H, Pufall M R, Kaka S, Silva T J, Russek S E and Katine J A 2005 *Phys. Rev. Lett.* **95** 067203
[56] Deac A, Lee K J, Liu Y, Redon O, Li M, Wang P, Nozières J P and Dieny B 2006 *Phys. Rev.* B **73** 064414
[57] Acremann Y, Strachan J P, Chembrolu V, Andrews S D, Tyliszczak T, Katine J A, Carey M J, Clemens B M, Siegmann H C and Stöhr J 2006 *Phys. Rev. Lett.* **96** 217202
[58] Ravelosona D, Mangin S, Lemaho Y, Katine J A, Terris B D and Fullerton E E 2006 *Phys. Rev. Lett.* **96** 186604
[59] Beach G S D, Knutson C, Nistor C, Tsoi M and Erskine J L 2006 *Phys. Rev. Lett.* **97** 057203
[60] Ozatay O, Emley N C, Braganca P M, Garcia A G F, Fuchs G D, Krivorotov I N, Buhrman R A and Ralph D C 2006 *Appl. Phys. Lett.* **88** 202502
[61] Woltersdorf G, Mosendz O, Heinrich B and Back C H 2007 *Phys. Rev. Lett.* **99** 246603
[62] Zhu J G and Zheng Y 2002 *Spin Dynamics in Confined Magnetic Structures: I* (*Topics in Applied Physics*) ed B Hillebrands and K Ounadjiela (Berlin: Springer) p 289
[63] Arrott A S 2005 *Ultrathin Magnetic Structures: IV* ed B Heinrich and J A C Bland (Berlin: Springer) p 101
[64] Kronmüller H 2007 in Kronmüller and Parkin [181] p 703
[65] Krakauer H, Posternak M and Freeman A J 1979 *Phys. Rev.* B **19** 1706
[66] Wimmer E, Krakauer H, Weinert M and Freeman A J 1981 *Phys. Rev.* B **24** 864
[67] Skriver H L 1984 *The LMTO Method* (*Solid-State Sciences* vol 41) (Berlin: Springer)
[68] Gay J and Richter R 1986 *Phys. Rev. Lett.* **56** 2728
[69] Staunton J B 1994 *Rep. Prog. Phys.* **57** 1289
[70] Freeman A J and Wimmer E 1995 *Annu. Rev. Mater. Sci.* **25** 7
[71] Dreyssé H and Demangeat C 1997 *Surf. Sci. Rep.* **28** 65
[72] Argaman N and Makov G 2000 *Am. J. Phys.* **68** 69

[73] Vega A, Parlebas J C and Demangeat C 2003 *Handbook of Magnetic Materials* ed K H J Buschow (Amsterdam: Elsevier) p 199
[74] Wu R, Yang Z and Hong J 2003 *J. Phys.: Condens. Matter* **15** S587
[75] Wu R 2007 in Kronmüller and Parkin [181] p 425
[76] Bihlmayer G 2007 in Kronmüller and Parkin [181] p 1
[77] Kübler J 2007 in Kronmüller and Parkin [181]
[78] Jonker B T, Walker K H, Kisker E, Prinz G A and Carbone C 1986 *Phys. Rev. Lett.* **57** 142
[79] Gradmann U and Müller J 1968 *Phys. Status Solidi* **27** 313
[80] Gradmann U and Müller J 1968 *J. Appl. Phys.* **39** 1379
[81] Gradmann U 1986 *J. Magn. Magn. Mater.* **54–57** 733
[82] Carcia P F 1988 *J. Appl. Phys.* **63** 2055
[83] Gradmann U 1993 *Handbook of Magnetic Materials* vol 7 ed K H J Buschow (Amsterdam: Elsevier) p 1
[84] Johnson M T, Bloemen P J H, der Broeder F J A and de Vries J J 1996 *Rep. Prog. Phys.* **59** 1409
[85] Naganuma H, Sato K and Hirotsu Y 2002 *J. Appl. Phys.* **100** 074914
[86] He K, Ma L Y, Ma X C, Jia J F and Xue Q K 2006 *Appl. Phys. Lett.* **88** 232503
[87] Winkelmann A, Przybylski M, Luo F, Shi Y and Barthel J 2006 *Phys. Rev. Lett.* **96** 257205
[88] Dho J and Hur N H 2007 *J. Magn. Magn. Mater.* **318** 23
[89] Richter H J 2007 *J. Phys. D: Appl. Phys.* **40** R149
[90] Parkin S S P, More N and Roche K P 1990 *Phys. Rev. Lett.* **64** 2304
[91] Unguris J, Celotta R J and Pierce D T 1991 *Phys. Rev. Lett.* **67** 140
[92] Edwards D M, Mathon J, Muniz R B and Phan M S 1991 *Phys. Rev. Lett.* **67** 493
[93] Hathaway K B 1994 *Ultrathin Magnetic Structures: II* ed B Heinrich and J A C Bland (Berlin: Springer) p 45
[94] Fert A and Bruno P 1994 *Ultrathin Magnetic Structures: II* ed B Heinrich and J A C Bland (Berlin: Springer) p 82
[95] Li D, Pearson J, Mattson J E, Bader S D and Johnson P D 1995 *Phys. Rev.* B **51** 7195
[96] Himpsel F J, Ortega J E, Mankey G J and Willis R F 1998 *Adv. Phys.* **47** 511
[97] Stiles M D 1999 *J. Magn. Magn. Mater.* **200** 322
[98] Altmann K N, O'Brien W, Seo D J, Himpsel F, Ortega J, Naermann A, Segovia P, Mascaraque A and Michel E G 1999 *J. Electron Spectrosc. Relat. Phenom.* **101–103** 367
[99] Himpsel F J 1999 *J. Phys.: Condens. Matter* **11** 9483
[100] Qiu Z Q and Smith N V 2002 *J. Phys.: Condens. Matter* **14** R169
[101] Yu D H and Donath M 2003 *Europhys. Lett.* **63** 729
[102] Stiles M D 2005 *Ultrathin Magnetic Structures: III* ed J A C Bland and B Heinrich (Berlin: Springer) p 99
[103] Stiles M D 2006 *Nanomagnetism* ed D L Mills and J A C Bland (Amsterdam: Elsevier) p 51
[104] Edwards D M and Umerski A 2007 in Kronmüller and Parkin [181] p 487
[105] Tsang C, Fontana R E, Lin T, Heim D E, Speriosu V S, Gurney B A and Manson M L 1994 *IEEE Trans. Magn.* **30** 3801
[106] Abarra E N, Inomata A, Sato H, Okamoto I and Mizoshita Y 2000 *Appl. Phys. Lett.* **77** 2581
[107] Fullerton E E *et al* 2000 *Appl. Phys. Lett.* **77** 3806
[108] Iwasaki S 2003 *IEEE Trans. Magn.* **39** 1868
[109] Richter H J 1999 *J. Phys. D: Appl. Phys.* **32** R147
[110] Richter H J 1999 *J. Phys. D: Appl. Phys.* **32** 3092
[111] Moneck M, Zhu J G, Che X, Tang Y, Lee H J, Zhang S, Moon K S and Takahashi N 2007 *IEEE Trans. Magn.* **43** 2127
[112] Che X, Tang Y, Lee H J, Zhang S, Moon K S, Kim N Y, Hong S Y, Takahashi N, Moneck M and Zhu J G 2007 *IEEE Trans. Magn.* **43** 2292
[113] White R, Newt R and Pease R 1997 *IEEE Trans. Magn.* **33** 990
[114] Todorovic M, Schultz S, Wong J and Scherer A 1999 *Appl. Phys. Lett.* **374** 2516
[115] Haginoya C, Koike K, Hirayama Y, Yamamoto J, Ishabashi M, Kitakami O and Shimada Y 1999 *Appl. Phys. Lett.* **75** 3159
[116] Hughes G F 2001 *The Physics of Ultra-high-Density Magnetic Recording* ed M L Plumer *et al* (Berlin: Springer) p 205
[117] Terris B D and Thomson T 2005 *J. Phys. D: Appl. Phys.* **38** R199
[118] Richter H *et al* 2006 *IEEE Trans. Magn.* **42** 2255
[119] Li S P, Lew W S, Bland J A C, Lopez-Diaz L, Vaz C A F, Natali M and Chen Y 2002 *Phys. Rev. Lett.* **88** 087202
[120] Li S P, Lew W S, Bland J A C, Lopez-Diaz L, Natali M, Vaz C A F and Chen Y 2002 *Nature* **415** 600
[121] Bland J A C, Lew W S, Li S P, Lopez-Diaz L, Vaz C A F, Natali M and Chen Y 2002 *J. Phys. D: Appl. Phys.* **35** 2384
[122] Ruigrok J J M, Coehoorn R, Cumpson S R and Kesteren H W 2000 *J. Appl. Phys.* **87** 5398
[123] Dürr H A and Schneider C M 2007 in Kronmüller and Parkin [181] p 1367
[124] Moodera J, Kinder L, Wong T and Meservey R 1995 *Phys. Rev. Lett.* **74** 3273
[125] Gallagher W J *et al* 1997 *J. Appl. Phys.* **81** 3741
[126] Moodera J S, Nowak J and van de Veerdonk R J M 1998 *Phys. Rev. Lett.* **80** 2941
[127] Miyazaki T and Tezuka N 1996 *J. Magn. Magn. Mater.* **139** L
[128] Bloch F 1930 *Z. Phys.* **61** 206
[129] Mermim N D and Wagner H 1966 *Phys. Rev. Lett.* **17** 1133
[130] Liebermann L, Fredkin D R and Shore H B 1969 *Phys. Rev. Lett.* **22** 539
[131] Liebermann L, Clinton J, Edwards D M and Mathon J 1970 *Phys. Rev. Lett.* **25** 232
[132] Gradmann U 1974 *Appl. Phys.* **3** 161
[133] Gradmann U 1991 *J. Magn. Magn. Mater.* **100** 481
[134] Egelhoff W F Jr, Chen P J, Powell C J, Stiles M D, McMichael R D, Judy J H, Takano K and Berkowitz A E 1997 *J. Appl. Phys.* **82** 6142
[135] Yang D X, Chopra H D, Shashishekar B, Chen P J and Egelhoff W F Jr 2002 *Appl. Phys. Lett.* **80** 2943
[136] Yang D X, Repetski E J, Chopra H D, Chen P J and Egelhoff W F Jr 2003 *J. Appl. Phys.* **93** 8415
[137] Chen J, Drakaki M and Erskine J L 1992 *Phys. Rev.* B **45** 3636
[138] Weber W, Back C H, Ramsperger U, Vaterlaus A and Allenspach R 1995 *Phys. Rev.* B **52** R14400
[139] Hope S, Gu E, Tselepi M and Bland J A C 1997 *Mater. Res. Soc. Symp. Proc.* **475** 143
[140] Hope S, Gu E, Choi B and Bland J A C 1998 *Phys. Rev. Lett.* **180** 1750
[141] Moodera J S and Mathon G 1999 *J. Magn. Magn. Mater.* **200** 248
[142] Prinz G A 1994 *Ultrathin Magnetic Structures: II* ed B Heinrich and J A C Bland (Berlin: Springer) p 1
[143] Ziese M and Thornton M J (ed) 2001 *Spin Electronics* (Berlin: Springer)
[144] Fert A and Jaffres H 2001 *Phys. Rev.* B **64** 184420
[145] Smith D L and Silver R N 2001 *Phys. Rev.* B **64** 045323
[146] Ploog K H, Herfort J, Schönherr H P, Moreno M and Dhar S 2003 *J. Cryst. Growth* **251** 292
[147] Hanbicki A T *et al* 2004 Influence of interface effects on spin injection efficiency in Fe/AlGaAs spin-LEDs

(GF-02) *49th Annual Conf. on Magnetism and Magnetic Materials (Jacksonville, FL, USA)*
[148] Plummer E W, Ismail, Matzdorf R, Melechko A V, Pierce J and Zhang J 2002 *Surf. Sci.* **500** 1
[149] Vaz C A F, Ahn C H and Henrich V E 2008 *Epitaxial Ferromagnetic Films and Spintronic Applications* ed A Hirohata and Y Otani (Trivandrum: Research Signpost) at press
[150] Ziese M, Bollero A, Panagiotopoulos I and Moutis N 2006 *Appl. Phys. Lett.* **88** 212502
[151] Gajek M, Bibes M, Fusil S, Bouzehouane K, Fontcuberta J, Barthélémy A and Fert A 2007 *Nat. Mater.* **6** 296
[152] Laukhin V *et al* 2007 *Phil. Mag. Lett.* **87** 183
[153] Venkatesan T, Kundaliya D C, Wu T and Ogale S B 2007 *Phil. Mag. Lett.* **87** 279
[154] Hochstrat A, Binek C, Chen X and Kleemann W 2004 *J. Magn. Magn. Mater.* **272–276** 325
[155] Borisov P, Hochstrat A, Chen X, Kleemann W and Binek C 2005 *Phys. Rev. Lett.* **94** 117203
[156] Martí X *et al* 2006 *Appl. Phys. Lett.* **89** 032510
[157] Laukhin V *et al* 2006 *Phys. Rev. Lett.* **97** 227201
[158] Qi X, Kim H and Blamire M G 2007 *Phil. Mag. Lett.* **87** 175
[159] Tsymbal E Y and Kohlstedt H 2006 *Science* **313** 181
[160] Velev J P, Duan C G, Belashchenko K D, Jaswal S S and Tsymbal E 2007 *Phys. Rev. Lett.* **98** 137201
[161] Gajek M, Bibes M, Barthélémy A, Bouzehouane K, Fusil S, Varela M, Fontcuberta J and Fert A 2005 *Phys. Rev.* B **72** 020406
[162] Mills D L and Bland J A C (ed) 2006 *Nanomagnetism* (*Contemporary Concepts of Condensed Matter Science*) (Amsterdam: Elsevier)
[163] Dennis C L *et al* 2002 *J. Phys.: Condens. Matter* **14** R1175
[164] Bader S D 2006 *Rev. Mod. Phys.* **78** 1
[165] Kläui M and Vaz C A F 2007 *Handbook of Magnetism and Advanced Magnetic Materials* vol 2 ed H Kronmüller and S Parkin (New York: Wiley) p 879
[166] Martín J I, Nogués J, Liu K, Vicent J L and Schuller I K 2003 *J. Magn. Magn. Mater.* **256** 449
[167] Gijs M A M and Bauer G E W 1997 *Adv. Phys.* **46** 285
[168] Levy P M 1994 *Solid State Physics* vol 47 ed H Ehrenreich and D Turnbull (New York: Academic) p 367
[169] Hirota E, Sakakima H and Inomata K 2002 *Giant Magneto-Resistance Devices* (*Springer Series in Surface Science* no 40) (Berlin: Springer)
[170] Maekawa S and Shinjo T (ed) 2002 *Spin Dependent Transport in Magnetic Nanostructures* (London: Taylor and Francis)
[171] Heinrich B and Cochran J F 1993 *Adv. Phys.* **42** 523
[172] Sander D 2004 *J. Phys.: Condens. Matter* **16** R603
[173] Lindner J and Baberschke K 2003 *J. Phys.: Condens. Matter* **15** R193
[174] Sander D 1999 *Rep. Prog. Phys.* **62** 809
[175] Sander D, Meyerheim H L, Ferrer S and Kirschner J 2003 *Adv. Solid State Phys.* **43** 547
[176] Eastman D E, Janak J F, Williams A R, Coleman R V and Wendin G 1979 *J. Appl. Phys.* **50** 7423
[177] Baberschke K, Donath M and Nolting W (ed) 2001 *Band-Ferromagnetism* (*Lecture Notes in Physics* no 580) (Berlin: Springer)
[178] Stöhr J and Siegmann H C 2006 *Magnetism* (Berlin: Springer)
[179] Awschalom D D, Loss D and Samarth N (ed) 2002 *Semiconductor Spintronics and Quantum Computation* (*Nanoscience and Technology*) (Berlin: Springer)
[180] Hirohata A and Otani Y (ed) 2008 *Epitaxial Ferromagnetic Films and Spintronic Applications* (Trivandrum: Research Signpost) at press
[181] Kronmüller H and Parkin S (ed) 2007 *Handbook of Magnetism and Advanced Magnetic Materials* (Hoboken: Wiley)
[182] Hurd C M 1982 *Contemp. Phys.* **23** 469
[183] Stoner E C 1936 *Proc. R. Soc. A* **154** 656
[184] Stoner E C 1938 *Proc. R. Soc. A* **165** 372
[185] Donath M 2001 *Band-Ferromagnetism* ed K Baberschke *et al* (Berlin: Springer) p 267
[186] Stöhr J 1995 *J. Electron Spectrosc. Relat. Phenom.* **75** 253
[187] Landau L D and Lifshitz E M 1935 *Phys. Z. Sowjetunion* **8** 153
[188] Carr W J Jr 1966 *Encyclopedia of Physics* vol XVIII/2 ed S Flügge (Berlin: Springer) p 274
[189] Kittel C 1987 *Quantum Theory of Solids* 2nd edn (New York: Wiley)
[190] Kanamori J 1963 *Magnetism* vol I ed S Rado (New York: Academic) p 127
[191] Farle M 1998 *Rep. Prog. Phys.* **61** 755
[192] van der Laan G 1998 *J. Phys.: Condens. Matter.* **10** 3239
[193] Stöhr J 1999 *J. Magn. Magn. Mater.* **200** 470
[194] Kittel C 1949 *Rev. Mod. Phys.* **21** 541
[195] Callen E and Callen H B 1965 *Phys. Rev.* A **139** 455
[196] Dodson B W 1991 *J. Cryst. Growth* **111** 376
[197] de Lacheisserie E T 1995 *Phys. Rev.* B **51** 15925
[198] Vaz C A F and Bland J A C 2001 *J. Appl. Phys.* **89** 7374
[199] Néel L 1953 *Comptes Rendus* **237** 1468
[200] Néel L 1954 *J. Phys. Radium* **15** 225
[201] Bruno P and Renard J P 1989 *Appl. Phys.* A **49** 499
[202] Albrecht M, Furubayashi T, Przybylski M, Korecki J, Gradmann U and Harrison W A 1992 *J. Magn. Magn. Mater.* **113** 207
[203] Chen J and Erskine J L 1992 *Phys. Rev. Lett.* **68** 1212
[204] Chuang D S, Ballentine C A and O'Handley R C 1994 *Phys. Rev.* B **49** 15084
[205] Gradmann U, Dürkop T and Elmers H J 1997 *J. Magn. Magn. Mater.* **165** 56
[206] Hyman R A, Zangwill A and Stiles M D 1998 *Phys. Rev.* B **58** 9276
[207] Qiu Z Q and Bader S D 1999 *J. Magn. Magn. Mater.* **200** 664
[208] Choi H J, Kawakami R K, Escorcia-Aparicio E J, Qiu Z Q, Pearson J, Jiang J S, Li D and Bader S D 1999 *Phys. Rev. Lett.* **82** 1947
[209] Bovensiepen U, Choi H J and Qiu Z Q 2000 *Phys. Rev.* B **61** 3235
[210] Rusponi S, Cren T, Weiss N, Epple M, Buluschek P, Claude L and Brune H 2003 *Nat. Mater.* **2** 546
[211] Bisio F, Moroni R and Mattera L 2007 *Phys. Rev.* B **75** 220405(R)
[212] Crangle J and Gibbs M 1994 *Phys. World* (November) 31
[213] Brown W F Jr 1962 *Magnetostatic Principles in Ferromagnetism* (Amsterdam: North-Holland)
[214] Jackson J D 1975 *Classical Electrodynamics* 2nd edn (New York: Wiley)
[215] Mills D L 1989 *Phys. Rev.* B **39** 12306
[216] O'Handley R C and Woods J P 1990 *Phys. Rev.* B **42** 6568
[217] Thiaville A and Fert A 1992 *J. Magn. Magn. Mater.* **113** 161
[218] Corciovei A, Costache G and Vamanu D 1972 *Solid State Phys.* **27** 237
[219] Rado G T and Weertman J R 1959 *J. Phys. Chem. Solids* **11** 315
[220] Allenspach R, Stampanoni M and Bischof A 1990 *Phys. Rev. Lett.* **65** 3344
[221] Pommier J, Meyer P, Pénissard G, Ferré J, Bruno P and Renard D 1990 *Phys. Rev. Lett.* **65** 2054
[222] Qiu Z Q, Pearson J and Bader S D 1993 *Phys. Rev. Lett.* **70** 1006

[223] Bochi G, Hug H J, Paul D I, Stiefel B, Moser A, Parashikov I, Güntherodt H J and O'Handley R C 1995 *Phys. Rev. Lett.* **75** 1839

[224] Bochi G, Ballentine C A, Inglefield H E, Thompson C V, O'Handley R C, Hug H J, Stiefel B, Moser A and Güntherodt H J 1995 *Phys. Rev.* B **52** 7311

[225] Hug H J, Stiefel B, Moser A, Parashikov I, Klicznik A, Lipp D, Güntherodt H J, Bochi G, Paul D I and O'Handley R C 1996 *J. Appl. Phys.* **79** 5609

[226] Kittel C 1996 *Introduction to Solid State Physics* 7th edn (New York: Wiley)

[227] Hubert A and Schäfer R 1998 *Magnetic Domains* (Berlin: Springer)

[228] Vaz C A F, Lopez-Diaz L, Kläui M, Bland J A C, Monchesky T L, Unguris J and Cui Z 2003 *Phys. Rev.* B **67** 140405

[229] Vaz C A F, Lopez-Diaz L, Kläui M, Bland J A C, Monchesky T, Unguris J and Cui Z 2004 *J. Magn. Magn. Mater.* **272–276** 1674

[230] Bruno P 1999 *Phys. Rev. Lett.* **83** 2425

[231] Jubert P O, Allenspach R and Bischof A 2004 *Phys. Rev.* B **69** 220410

[232] Kläui M, Vaz C A F, Rothman J, Bland J A C, Wernsdorfer W, Faini G and Cambril E 2003 *Phys. Rev. Lett.* **90** 097202

[233] Kläui M *et al* 2005 *Appl. Phys. Lett.* **87** 102509

[234] Frenkel J and Dorfman J 1930 *Nature* **126** 274

[235] Néel L 1947 *Comptes Rendus* **224** 1488

[236] Brown W F Jr 1968 *J. Appl. Phys.* **39** 993

[237] Leslie-Pelecky D L and Rieke R D 1996 *Chem. Mater.* **8** 1770

[238] Wohlfarth E P 1980 *Ferromagnetic Materials* vol 1 ed E P Wohlfarth (Amsterdam: North-Holland) p 1

[239] Fujiwara H, Kadomatsu H and Tokunaga T 1983 *J. Magn. Magn. Mater.* **31–34** 809

[240] Hashim I, Joo H S and Atwater H A 1995 *Surf. Rev. Lett.* **2** 427

[241] Hashim I and Atwater H A 1994 *J. Appl. Phys.* **75** 6516

[242] Amulyavichus A and Suzdalev I 1973 *Sov. Phys.—JETP* **31** 261

[243] Wohlfarth E P 1963 *Magnetism* vol III ed G T Rado and H Sulh (New York: Academic)

[244] Bean C P and Livingstone J D 1959 *J. Appl. Phys.* **30** 120S

[245] Bertotti G 1998 *Hysteresis in Magnetism* (San Diego: Academic)

[246] Heinrich B, Cochran J F and Kowalewski M 1998 *Frontiers of Magnetism of Reduced Dimension Systems* (*NATO ASI Series* no 3/49) ed V G Bar'yakhtar *et al* (Dordrecht: Kluwer) p 161

[247] Mills D L 1991 *J. Magn. Magn. Mater.* **100** 515

[248] Mills D L 2007 in Kronmüller and Parkin [181] p 247

[249] Hicken R J, Eley D E P, Gester M, Gray S J, Daboo C, Ives A J R and Bland J A C 1995 *J. Magn. Magn. Mater.* **145** 278

[250] Rado G T and Hicken R J 1988 *J. Appl. Phys.* **63** 3885

[251] Cochran J F and Dutcher J R 1988 *J. Appl. Phys.* **63** 3814

[252] Hillebrands B 1990 *Phys. Rev.* B **41** 530

[253] Erickson R P and Mills D L 1991 *Phys. Rev.* B **43** 10715

[254] Erickson R P and Mills D L 1991 *Phys. Rev.* B **44** 11825

[255] Li Y and Baberschke K 1992 *Phys. Rev. Lett.* **68** 1208

[256] Huang F, Mankey G J, Kief M T and Willis R F 1993 *J. Appl. Phys.* **73** 6760

[257] Huang F, Kief M T, Mankey G J and Willis R F 1994 *Phys. Rev.* B **49** 3962

[258] Srivastava P, Haack N, Wende H, Chauvistré R and Baberschke K 1997 *Phys. Rev.* B **56** R4398

[259] Dhesi S S, Dürr H A, van ver Laan G, Dudzik E and Brookes N B 1999 *Phys. Rev.* B **60** 12852

[260] Ohnishi S, Freeman A J and Weinert M 1983 *Phys. Rev.* B **28** 6741

[261] Lutz H, Gunton J D, Schurmann H K, Crow J E and Mihalisin T 1974 *Solid State Commun.* **14** 1075

[262] Barber M N 1983 *Phase Transitions and Critical Phenomena* vol 8 ed C Domb and J L Lebowitz (London: Academic) p 145

[263] Bruno P 1991 *Phys. Rev.* B **43** 6015

[264] Bruno P 1992 *Mater. Res. Soc. Symp. Proc.* **231** 299

[265] Yafet Y, Kwo J and Gyorgy E M 1986 *Phys. Rev.* B **33** 6519

[266] Bland J A C, Gehring G A, Kaplan B and Daboo C 1992 *J. Magn. Magn. Mater.* **113** 173

[267] Krams P, Lauks F, Stamps R L, Hillebrands B and Güntherodt G 1992 *Phys. Rev. Lett.* **69** 3674

[268] Bland J A C, Daboo C, Heinrich B, Celinski Z and Bateson R D 1995 *Phys. Rev.* B **51** 258

[269] Pescia D, Stampanoni M, Bona G L, Vaterlaus A, Willis R F and Meier F 1987 *Phys. Rev. Lett.* **58** 2126

[270] Gutierrez C J, Qui Z Q, Wieczorek M D, Tang H and Walker J C 1991 *J. Magn. Magn. Mater.* **93** 326

[271] Gutierrez C J, Qui Z Q, Wieczorek M D, Tang H, Walker J C and Mercader R C 1991 *Hyperfine Interact.* **66** 299

[272] Walker J C 1994 *Ultrathin Magnetic Structures: II* ed B Heinrich and J A C Bland (Berlin: Springer) p 328

[273] Przybylski M and Gradmann U 1987 *Phys. Rev. Lett.* **59** 1152

[274] Przybylski M, Kaufmann I and Gradmann U 1989 *Phys. Rev.* B **40** 8631

[275] Lugert G and Bayreuther G 1988 *Phys. Rev.* B **38** 11068

[276] Lugert G, Bayreuther G, Lehner S, Gruber G and Bruno P 1991 *Mater. Res. Soc. Symp. Proc.* **232** 97

[277] Néel L 1949 *Ann. Geophys.* **5** 99

[278] Néel L 1953 *Rev. Mod. Phys.* **25** 293

[279] Brown W F Jr 1959 *J. Appl. Phys.* **30** S130

[280] Aharoni A 1992 *Magnetic Properties of Fine Particles* ed J L Dormann and D Fiorani (Amsterdam: North-Holland)

[281] Siegmann H C and Kay E 1994 *Ultrathin Magnetic Structures: I* ed J A C Bland and B Heinrich (Berlin: Springer) p 152

[282] Chantrell R W and O'Grady K 1994 *Applied Magnetism* (*NATO ASI Series* no Series E 253) ed R Gerber *et al* (Dordrecht: Kluwer) p 113

[283] Tronc E, Prené P, Jolivet J P, d'Orazio F, Lucari F, Fiorani D, Godinho M, Cherkaoui R, Nogués M and Dormann J L 1995 *Hyperfine Interact.* **95** 129

[284] Jacobs I S and Bean C P 1963 *Magnetism* vol III ed G T Rado and H Suhl (New York: Academic) p 271

[285] Camley R E and Barnaś J 1989 *Phys. Rev. Lett.* **63** 664

[286] Dieny B 1992 *J. Phys.: Condens. Matter* **4** 8009

[287] Gurney B A, Speriosu V S, Nozieres J P, Lefakis H, Wilhoit D R and Need O U 1993 *Phys. Rev. Lett.* **71** 4023

[288] Valet T and Fert A 1993 *Phys. Rev.* B **48** 7099

[289] Gurney B, Carey M, Tsang C, Williams M, Parkin S, Fontana R Jr, Grochowski E, Pinarbasi M, Lin T and Mauri D 2005 *Ultrathin Magnetic Structures: IV* ed B Heinrich and J A C Bland (Berlin: Springer) p 149

[290] Ney A, Poulopoulos P, Farle M and Baberschke K 2000 *Phys. Rev.* B **62** 11336

[291] Ney A, Poulopoulos P, Wilhelm F, Scherz A, Farle M and Baberschke K 2001 *J. Magn. Magn. Mater.* **226–230** 1570

[292] Ney A, Poulopoulos P and Baberschke K 2001 *Europhys. Lett.* **54** 820

[293] Ney A, Lenz K, Poulopoulos P and Baberschke K 2002 *J. Magn. Magn. Mater.* **240** 343

[294] Ney A, Scherz A, Poulopoulos P, Lenz K, Wende H, Baberschke K, Wilhelm F and Brookes N B 2001 *Phys. Rev.* B **65** 024411
[295] Wernsdorfer W, Hasselbach K, Mailly D, Barbara B, Benoit A, Thomas L and Suran G 1995 *J. Magn. Magn. Mater.* **145** 33
[296] Wernsdorfer W, Mailly D and Benoit A 2000 *J. Appl. Phys.* **87** 5094
[297] Jamet M, Wernsdorfer W, Thirion C, Mailly D, Dupuis V, Mélinon P and Péez A 2001 *Phys. Rev. Lett.* **86** 4676
[298] Wernsdorfer W 2001 *Adv. Chem. Phys.* **118** 99
[299] Sokolov A, Sabirianov R, Wernsdorfer W and Doudin B 2002 *J. Appl. Phys.* **91** 7059
[300] Mailly D, Chapelier C and Benoit A 1993 *Phys. Rev. Lett.* **70** 2020
[301] Flanders P J and Graham C D 1993 *Rep. Prog. Phys.* **56** 431
[302] Felcher G P, Felici R, Kampwirth R T and Gray K E 1985 *J. Appl. Phys.* **57** 3789
[303] Ankner J F and Felcher G P 1999 *J. Magn. Magn. Mater.* **200** 741
[304] Felcher G P 2000 *J. Appl. Phys.* **87** 5431
[305] Zabel H, Siebrecht R and Schreyer A 2000 *Physica* B **276–278** 17
[306] Zabel H 1994 *Appl. Phys.* A **58** 159
[307] Zabel H, Theis-Bröhl K and Toperverg B P 2007 in Kronmüller and Parkin [181] p 1237
[308] Majkrzak C F 1996 *Physica* B **221** 342
[309] Fermon C, Ott F and Menelle A 1999 *X-Ray and Neutron Reflectivity: Principles and Applications* ed J Daillant and A Gibaud (Berlin: Springer) p 163
[310] Bland J A C 1994 *Ultrathin Magnetic Structures: I* ed J A C Bland and B Heinrich (Berlin: Springer) p 305
[311] Bland J A C and Vaz C A F 2005 *Ultrathin Magnetic Structures: III* ed J A C Bland and B Heinrich (Berlin: Springer) p 233
[312] Schütz G, Wagner W, Wilhelm W, Kienle P, Zeller R, Frahm R and Materlik G 1987 *Phys. Rev. Lett.* **58** 737
[313] Grange W, Kappler J P and Maret M 2002 *Magnetism: Molecules to Materials I: Models and Experiments* ed J S Miller and M Drillon (Weinheim: Wiley-VCH) p 211
[314] Baberschke K 2005 *Phys. Scr.* T **115** 49
[315] Schütz G, Goering E and Stoll H 2007 in Kronmüller and Parkin [181] p 1311
[316] Thole B T, Carra P, Sette F and van der Laan G 1992 *Phys. Rev. Lett.* **68** 1943
[317] Carra P, Thole B T, Altarelli M and Wang X 1993 *Phys. Rev. Lett.* **70** 694
[318] Dürr H A, Guo G Y, van der Laan G, Lee J, Lauhoff G and Bland J A C 1997 *Science* **277** 213
[319] Chen C T, Idzerda Y U, Lin H J, Meigs G, Chaiken A, Prinz G A and Ho G H 1993 *Phys. Rev.* B **48** 642
[320] Chen C T, Idzerda Y U, Lin H J, Smith N V, Meigs G, Chaban E, Ho G H, Pellegrin E and Sette F 1995 *Phys. Rev. Lett.* **75** 152
[321] Moog E R and Bader S D 1985 *Superlatt. Microstruct.* **1** 543
[322] Bader S D 1991 *J. Magn. Magn. Mater.* **100** 440
[323] Bader S D and Erskine J L 1994 *Ultrathin Magnetic Structures: II* ed B Heinrich and J A C Bland (Berlin: Springer) p 297
[324] Qiu Z Q and Bader S D 1998 *Nonlinear Optics in Metals* ed K H Bennemann (Oxford: Oxford University Press) p 1
[325] Florczak J M and Dahlberg E D 1990 *J. Appl. Phys.* **67** 7520
[326] Florczak J M and Dahlberg E D 1991 *Phys. Rev.* B **44** 9338
[327] Bland J A C, Padgett M J, Butcher R J and Bett N 1989 *J. Phys. E: Sci. Instrum.* **22** 308
[328] Sprokel G J 1984 *Appl. Opt.* **23** 3983
[329] Zak J, Moog E R, Liu C and Bader S D 1990 *J. Magn. Magn. Mater.* **89** 107
[330] Zak J, Moog E R, Liu C and Bader S D 1990 *J. Appl. Phys.* **68** 4203
[331] Zak J, Moog E R, Liu C and Bader S D 1991 *Phys. Rev.* B **43** 6423
[332] Višňovský Š 1986 *Czech. J. Phys.* B **36** 625
[333] Višňovský Š 1986 *Czech. J. Phys.* B **36** 835
[334] Višňovský Š 1986 *Czech. J. Phys.* B **36** 1049
[335] Višňovský Š 1986 *Czech. J. Phys.* B **36** 1203
[336] Višňovský Š 2006 *Optics in Magnetic Multilayers and Nanostructures* (Boca Raton, FL: CRC Press)
[337] Sokolov A V 1967 *Optical Properties of Metals* (London: Blackie)
[338] Ebert H 1996 *Rep. Prog. Phys.* **59** 1665
[339] Collins S P, Lovesey S W and Balcar E 2007 *J. Phys.: Condens. Matter* **19** 213201
[340] Heinrich B 1994 *Ultrathin Magnetic Structures: II* ed B Heinrich and J A C Bland (Berlin: Springer) p 195
[341] Celinski Z, Urquhart K B and Heinrich B 1997 *J. Magn. Magn. Mater.* **166** 6
[342] Baberschke K 2007 in Kronmüller and Parkin [181] p 1617
[343] Patton C E 1984 *Phys. Rep.* **103** 251
[344] Cottam M G and Lockwood D J 1986 *Light Scattering in Magnetic Solids* (New York: Wiley)
[345] Bader S D and Erskine J L 1994 *Ultrathin Magnetic Structures: II* ed B Heinrich and J A C Bland (Berlin: Springer) p 222
[346] Hillebrands B and Güntherodt G 1994 *Ultrathin Magnetic Structures: II* ed B Heinrich and J A C Bland (Berlin: Springer) p 258
[347] Carlotti G and Gubbiotti G 1999 *Riv. Nuovo Cimento* **22** 1
[348] Hillebrands B *Light Scattering in Solids: VII* ed M Cardona and G Güntherodt (Springer) p 174
[349] Demokritov S O, Hillebrands B and Slavin A N 2001 *Phys. Rep.* **348** 441
[350] Gubbiotti G, Carlotti G, Nizzoli F, Zivieri R, Okuno T and Shinjo T 2002 *IEEE Trans. Magn.* **38** 2532
[351] Hillebrands B and Hamrle J 2007 in Kronmüller and Parkin [181] p 1566
[352] Falicov L M *et al* 1990 *J. Mater. Res.* **5** 1299
[353] Freeman M R and Choi B C 2001 *Science* **294** 1484
[354] Zhu Y (ed) 2005 *Modern Techniques for Characterizing Magnetic Materials* (Boston: Kluwer Academic)
[355] Binnig G, Quate C F and Gerber C 1986 *Phys. Rev. Lett.* **56** 930
[356] Schirmeisen A, Anczykowski B and Fuchs H 2004 *Applied Scanning Probe Methods* (*Nanoscience and Technology*) ed B Bhushan *et al* (Berlin: Springer) p 3
[357] Morita S, Oyabu N, Nishimoto T, Nishi R, Custance O, Yi I and Sugawara Y 2005 (*NATO Science Series II: Mathematics, Physics and Chemistry* vol 186) ed P M Vilarinho *et al* (Dordrecht: Kluwer) p 173
[358] Grütter P, Mamin H J and Rugar D 1992 in Wiesendanger and Güntherodt [363] p 151
[359] Hug H J *et al* 1998 *J. Appl. Phys.* **83** 5609
[360] Hartmann U 1999 *Annu. Rev. Mater. Sci.* **29** 53
[361] Griffith J E and Kochanski G P 1990 *Annu. Rev. Mater. Sci.* **20** 219
[362] Güntherodt H J and Wiesendanger R (ed) 1992 *Scanning Tunneling Microscopy: I* (*Springer Series in Surface Sciences* no 20) (Berlin: Springer)
[363] Wiesendanger R and Güntherodt H J (ed) 1992 *Scanning Tunneling Microscopy: II* (*Springer Series in Surface Sciences* no 28) (Berlin: Springer)
[364] Wiesendanger R and Güntherodt H J (ed) 1993 *Scanning Tunneling Microscopy III* (*Springer Series in Surface Sciences* no 29) (Berlin: Springer)

[365] Stroscio J A and Kaiser W J (ed) 1993 *Methods of Experimental Physics* vol 27 (Boston: Academic)
[366] Wiesendanger R 1994 *Scanning Probe Microscopy and Spectroscopy* (Cambridge: Cambridge University Press)
[367] Wulfhekel W and Kirschner J 1999 *Appl. Phys. Lett.* **75** 1944
[368] Wiesendanger R and Bode M 2001 *Solid State Commun.* **119** 341
[369] Bode M, Pietzsch O, Kubetzka A and Wiesendanger R 2001 *J. Electron Spectrosc. Relat. Phenom.* **114–116** 1055
[370] Wulfhekel W, Schlickum U and Kirschner J 2006 *Applied Scanning Probe Methods: II* (*Nanoscience and Technology*) ed B Bhushan and H Fuchs (Berlin: Springer) p 121
[371] Wulfhekel W and Kirschner J 2007 *Annu. Rev. Mater. Res.* **37** 69
[372] Schäfer R 2007 in Kronmüller and Parkin [181] p 1513
[373] Scheinfein M R, Unguris J, Kelley M H, Pierce D T and Celotta R J 1990 *Rev. Sci. Instrum.* **61** 2501
[374] Unguris J, Scheinfein M R, Celotta R J and Pierce D T 1990 *Chemistry and Physics of Solid Surfaces: VIII* ed C Domb and M S Green (Berlin: Springer) p 239
[375] Allenspach R 1994 *J. Magn. Magn. Mater.* **129** 160
[376] Oepen H P and Frömter R 2007 in Kronmüller and Parkin [181] p 1488
[377] Schneider C M, Frömter R, Ziethen C, Swiech W, Brookes N B, Schönhense G and Kirschner J 1997 *Mater. Res. Soc. Symp. Proc.* **475** 381
[378] Schönhense G 1999 *J. Phys.: Condens. Matter* **11** 9517
[379] Fischer P *et al* 2001 *Rev. Sci. Instrum.* **72** 2322
[380] Locatelli A, Cherifi K S, Heun S, Marsi M, Ono K, Pavlovska A and Bauer E 2002 *Surf. Rev. Lett.* **9** 171
[381] Scholl A, Ohldag H, Nolting F, Stöhr J and Padmore H A 2002 *Rev. Sci. Instrum.* **73** 1362
[382] Hopster H and Oepen H P (ed) 2005 *Magnetic Microscopy of Nanostructures* (*Nanoscience and Nanotechnology*) (Berlin: Springer)
[383] Kang B S, Kim D H, Anderson E, Fischer P and Cho G 2005 *J. Appl. Phys.* **98** 093907
[384] Chapman J N 1984 *J. Phys. D: Appl. Phys.* **17** 623
[385] Chapman J N and Scheinfein M 1999 *J. Magn. Magn. Mater.* **200** 729
[386] Zweck J and Uhlig T 2007 in Kronmüller and Parkin [181] p 1393
[387] Dunin-Borkowski R E, Mccartney M R, Kardynal B, Parkin S S P, Scheinfein M R and Smith D J 2000 *J. Microsc.* **200** 187
[388] McCartney M R and Smith D J 2007 in Kronmüller and Parkin [181] p 1428
[389] Chang A M, Hallen H D, Harriot L, Hess H F, Kao H L, Kwo J, Miller R E, Wolfe R, van der Ziel J and Chang T Y 1992 *Appl. Phys. Lett.* **61** 1974
[390] Oral A, Bending S J and Henini M 1996 *Appl. Phys. Lett.* **69** 1324
[391] Bending S J 1999 *Adv. Phys.* **48** 449
[392] Dinner R B, Beasley M R and Moler K A 2005 *Rev. Sci. Intrum.* **76** 103702
[393] Bauer E 1999 *J. Phys.: Condens. Matter* **11** 9365
[394] Wuttig M and Liu X 2004 *Ultrathin Metal Films* (*Springer Tracts in Modern Physics* vol 206) (Berlin: Springer)
[395] Hong K and Giordano N 1995 *Phys. Rev.* B **51** 9855
[396] Aumentado J and Chandrasekhar V 1999 *Appl. Phys. Lett.* **74** 1898
[397] Wegrowe J E, Kelly D, Frank A, Gilbert S E and Ansermet J P 1999 *Phys. Rev. Lett.* **82** 3681
[398] Kläui M, Vaz C A F, Wernsdorfer W, Bauer E, Cherifi S, Heun S, Locatelli A, Faini G, Cambril E and Bland J A C 2004 *Physica* B **343** 343
[399] García N, Muñoz M and Zhao Y W 1999 *Phys. Rev. Lett.* **82** 2923
[400] Gabureac M, Viret M, Ott F and Fermon C 2004 *Phys. Rev.* B **69** 100401
[401] Montero M I, Dumas R K, Liu G, Viret M, Stoll O M, Macedo W A A and Schuller I K 2004 *Phys. Rev.* B **70** 184418
[402] Campagna M, Pierce D T, Meier F, Sattler K and Siegmann H C 1976 *Adv. Electron. Electron Phys.* **41** 113
[403] Feder R (ed) 1985 *Polarized Electrons in Surface Physics* (Singapore: World Scientific)
[404] Kisker E 1987 *Metallic Magnetism* (*Topics in Current Physics* no 42) ed H Capellmann (Berlin: Springer) p 57
[405] Johnson P D 1996 *J. Magn. Magn. Mater.* **156** 321
[406] Johnson P D 1997 *Rep. Prog. Phys.* **60** 1217
[407] Johnson P D and Güntherodt G 2007 in Kronmüller and Parkin [181] p 1635
[408] Fisher M E 1967 *Rep. Prog. Phys.* **30** 615
[409] Sucksmith W and Thompson J E 1954 *Proc. R. Soc.* A **225** 362
[410] Siegmann H C 1992 *J. Phys.: Condens. Matter* **4** 8395
[411] Meakin P 1998 *Fractals, Scaling and Growth far from Equilibrium* (Cambridge: Cambridge University Press)
[412] Fisher M E 1974 *Rev. Mod. Phys.* **46** 597
[413] Wilson K G 1979 *Sci. Am.* **241** 140
[414] Fisher M E 1998 *Rev. Mod. Phys.* **70** 653
[415] Stanley E E 1999 *Rev. Mod. Phys.* **71** S358
[416] Ma S K 1976 *Modern Theory of Critical Phenomena* (Reading, MA: Benjamin)
[417] José J V, Kadanoff L P, Kirkpatrick S and Nelson D R 1977 *Phys. Rev.* B **16** 1217
[418] Kosterlitz J M and Thouless D J 1978 *Progress in Low Temperature Physics* vol VII B ed D F Brewer (Amsterdam: North-Holland) p 371
[419] Barber M N 1980 *Phys. Rep.* **59** 375
[420] Landau D P 1999 *J. Magn. Magn. Mater.* **200** 231
[421] Pelissetto A and Vicari E 2002 *Phys. Rep.* **368** 549
[422] Wu F Y 1982 *Rev. Mod. Phys.* **54** 235
[423] Onsager L 1944 *Phys. Rev.* **65** 117
[424] Thompson C J 1988 *Classical Equilibrium Statistical Mechanics* (Oxford: Clarendon)
[425] Wegner F 1967 *Z. Phys.* **206** 465
[426] Hohenberg P C 1967 *Phys. Rev.* **158** 383
[427] Gitterman M and Halpern V H 2004 *Phase Transitions* (New Jersey: World Scientific)
[428] Kosterlitz J M and Thouless D J 1973 *J. Phys. C: Solid State Phys.* **6** 1181
[429] Kosterlitz J M 1974 *J. Phys. C: Solid State Phys.* **7** 1046
[430] Pokrovsky V L 1999 *J. Magn. Magn. Mater.* **200** 515
[431] Bramwell S T and Holdsworth P C W 1993 *J. Appl. Phys.* **73** 6096
[432] Bramwell S T and Holdsworth P C W 1993 *J. Phys.: Condens. Matter* **5** L53
[433] Guillou J C L and Zinn-Justin J 1980 *Phys. Rev.* B **21** 3976
[434] Guillou J C L and Zinn-Justin J 1977 *Phys. Rev. Lett.* **39** 95
[435] Stinchcombe R B 1983 *Phase Transitions and Critical Phenomena* vol 7 ed C Domb and J L Leibowitz (London: Academic) p 151
[436] Kaupužs J 2001 *Ann. Phys., Lpz* **10** 299
[437] Bruce A D and Aharony A 1975 *Phys. Rev.* B **11** 478
[438] Bander M and Mills D L 1988 *Phys. Rev.* B **38** 12015
[439] Erickson R P and Mills D L 1991 *Phys. Rev.* B **43** 11527
[440] Kadanoff L P, Götze W, Hamblen D, Hecht R, Lewis E A S, Palciauskas V V, Rayl M, Swift J, Aspnes D and Kane J 1967 *Rev. Mod. Phys.* **39** 395
[441] Fisher M E and Aharony A 1973 *Phys. Rev. Lett.* **30** 559
[442] Kaul S N 1985 *J. Magn. Magn. Mater.* **53** 5

[443] Rüdt C, Poulopoulos P, Lindner J, Scherz A, Wende H, Baberschke K, Blomquist P and Wäppling R 2002 *Phys. Rev.* B **65** 220404
[444] Kerkmann D, Pescia D and Allenspach R 1992 *Phys. Rev. Lett.* **68** 686
[445] Poulopoulos P, Farle M, Bovensiepen U and Baberschke K 1997 *Phys. Rev.* B **55** R11961
[446] Koch R 1994 *J. Phys.: Condens. Matter* **6** 9519
[447] Gradmann U, Przybylski M, Elmers H J and Liu G 1989 *Appl. Phys.* A **49** 563
[448] Farle M, Baberschke K, Stetter U, Aspelmeier A and Gerhardter F 1993 *Phys. Rev.* B **47** 11571
[449] Przybylski M and Gradmann U 1988 *J. Physique Coll.* **49** C8–1705
[450] Qiu Z Q, Pearson J and Bader S D 1994 *Phys. Rev.* B **49** 8797
[451] Schilbe P, Siebentritt S and Rieder K H 1996 *Phys. Lett.* A **216** 20
[452] Schilbe P and Rieder H 1998 *Europhys. Lett.* **41** 219
[453] Kohlhepp J, Elmers H J, Cordes S and Gradmann U 1992 *Phys. Rev.* B **45** 12287
[454] Farle M, Lewis W A and Baberschke K 1993 *Appl. Phys. Lett.* **62** 2728
[455] Back C H, Würsch C, Kerkmann D and Pescia D 1994 *Z. Phys.* B **96** 1
[456] Back C H, Würsch C, Vaterlaus A, Ramsperger U, Maier U and Pescia D 1995 *Nature* **378** 597
[457] Elmers H J, Hauschild J, Höche H, Gradmann U, Bethge H, Heuer D and Köhler U 1994 *Phys. Rev. Lett.* **73** 898
[458] Elmers H J, Hauschild J and Gradmann U 1996 *Phys. Rev.* B **54** 15224
[459] Landau D P 1976 *Phys. Rev.* B **13** 2997
[460] Baberschke K 1996 *Appl. Phys.* A **62** 417
[461] Elmers H J 1995 *Int. J. Mod. Phys.* B **9** 3115
[462] Rau C, Xing G and Robert M 1988 *J. Vac. Sci. Technol.* A **6** 579
[463] Rau C 1989 *Appl. Phys.* A **49** 579
[464] Thomassen J, May F, Feldmann B, Wuttig M and Ibach H 1992 *Phys. Rev. Lett.* **69** 3831
[465] Liu C and Bader S D 1990 *J. Appl. Phys.* **67** 5758
[466] Liu C and Bader S D 1991 *J. Magn. Magn. Mater.* **93** 307
[467] Rau C, Mahavadi P and Lu M 1993 *J. Appl. Phys.* **73** 6757
[468] Qiu Z Q, Pearson J and Bader S D 1991 *Phys. Rev. Lett.* **67** 1646
[469] Dürr W, Taborelli M, Paul O, Germar R, Gudat W, Pescia D and Landolt M 1989 *Phys. Rev. Lett.* **62** 206
[470] Elmers H J and Hauschild J 1994 *Surf. Sci.* **320** 134
[471] Elmers H J, Hauschild J, Liu G H and Gradmann U 1996 *J. Appl. Phys.* **79** 4984
[472] Bensch F, Garreau G, Moosbühler R, Bayreuther G and Beaurepaire E 2001 *J. Appl. Phys.* **89** 7133
[473] Kuo C C, Lin W C, Chiu C L, Huang H L and Lin M T 2001 *J. Appl. Phys.* **89** 7153
[474] Kuo C C, Chiu C L, Lin W C and Lin M T 2002 *Surf. Sci.* **520** 121
[475] Ballentine C A, Fink R L, Araya-Pochet J and Erskine J L 1989 *Appl. Phys.* A **49** 459
[476] Ballentine C A, Fink R L, Araya-Pochet J and Erskine J L 1990 *Phys. Rev.* B **41** 2631
[477] Li Y, Farle M and Baberschke K 1990 *Phys. Rev.* B **41** 9596
[478] Spörel F and Biller E 1975 *Solid State Commun.* **17** 833
[479] Seeger M, Kaul S N, Kronmüller H and Reisser R 1995 *Phys. Rev.* B **51** 12585
[480] Stampanoni M, Vaterlauss A, Pescia D, Aeschlimann M, Meier F, Dürr W and Blügel S 1988 *Phys. Rev.* B **37** 10380
[481] Stampanoni M 1989 *Appl. Phys.* A **49** 449
[482] Fink R L, Ballentine C A, Erskine J L and Araya-Pochet J A 1990 *Phys. Rev.* B **41** 10175
[483] Liu C and Bader S D 1990 *J. Vac. Sci. Technol.* A **8** 2727
[484] O'Connor D and Stephens C R 1994 *Phys. Rev. Lett.* **72** 506
[485] McCoy B M and Wu T T 1972 *The Two-Dimensional Ising Model* (Cambridge, MA: Harvard University Press)
[486] Krebs J J, Jonker B T and Prinz G A 1987 *J. Appl. Phys.* **61** 2596
[487] Xu Y B, Kernohan E T M, Freeland D J, Ercole A, Tselepi M and Bland J A C 1998 *Phys. Rev.* B **58** 890
[488] Bensch F, Moosbühler R and Bayreuther G 2002 *J. Appl. Phys.* **91** 8754
[489] Wastlbauer G and Bland J A C 2005 *Adv. Phys.* **54** 137
[490] Zakeri K, Kebe T, Lindner J and Farle M 2007 *Superlatt. Microstruct.* **41** 116
[491] Jansen P J, Dreysse H and Bennemann K H 1992 *Surf. Sci.* **269** 627
[492] Schneider C M, Bressler P, Schuster P, Kirschner J, de Miguel J J and Miranda R 1990 *Phys. Rev. Lett.* **64** 1059
[493] May F, Tischer M, Arvanitis D, Dunn J H, Henneken H, Wende H, Chauvistré R and Baberschke K 1997 *J. Physique* IV **7** C2–389
[494] Srivastava P, Wilhelm F, Ney A, Farle M, Wende H, Haack N, Ceballos G and Baberschke K 1998 *Phys. Rev.* B **58** 5701
[495] Rüdt C, Scherz A and Baberschke K 2005 *J. Magn. Magn. Mater.* **285** 95
[496] Baberschke K and Farle M 1997 *J. Appl. Phys.* **81** 5038
[497] Vollmer R, van Dijken S, Schleberger M and Kirschner J 2000 *Phys. Rev.* B **61** 1303
[498] Pajda M, Krudrnovský J, Turek I, Drchal V and Bruno P 2000 *Phys. Rev. Lett.* **85** 5424
[499] Razee S S A, Staunton J B, Szunyogh L and Gyorffy B L 2002 *Phys. Rev. Lett.* **88** 147201
[500] Razee S S A, Staunton J B, Szunyogh L and Györffy B L 2002 *Phys. Rev.* B **66** 094415
[501] Bruno P, Krudrnovský J, Pajda M, Drchal V and Turek I 2002 *J. Magn. Magn. Mater.* **240** 346
[502] Bayreuther G, Bensch F and Kottler V 1996 *J. Appl. Phys.* **79** 4509
[503] Donath M, Scholl D, Siegmann H C and Kay E 1991 *Phys. Rev.* B **43** 3164
[504] Bovensiepen U, Wilhelm F, Srivastava P, Poulopoulos P, Farle M, Ney A and Baberschke K 1998 *Phys. Rev. Lett.* **81** 2368
[505] Scherz A, Sorg C, Bernien M, Ponpandian N, Baberschke K, Wende H and Jensen P J 2005 *Phys. Rev.* B **72** 054447
[506] Sorg C, Scherz A, HWende, Gleitsmann T, Li Z, Rüttinger S, Litwinski C and Baberschke K 2005 *Phys. Scr.* T **115** 638
[507] Ney A, Wilhelm F, Farle M, Poulopoulos P, Srivastava P and Baberschke K 1999 *Phys. Rev.* B **59** R3938
[508] Aspelmeier A, Tischer T, Farle M, Russo M, Baberschke K and Arvanitis D 1995 *J. Magn. Magn. Mater.* **146** 256
[509] Wilhelm F, Bovensiepen U, Scherz A, Poulopoulos P, Ney A, Wende H, Ceballos G and Baberschke K 2000 *J. Magn. Magn. Mater.* **222** 163
[510] Wang R W and Mills D L 1992 *Phys. Rev.* B **46** 11681
[511] Poulopoulos P and Baberschke K 2001 *Band-Ferromagnetism* ed K Baberschke *et al* (Berlin: Springer) p 283
[512] Morr D K, Jensen P J and Bennemann K H 1994 *Surf. Sci.* **307–309** 1109
[513] Pappas D P, Kämper K P and Hopster H 1990 *Phys. Rev. Lett.* **64** 3179
[514] Pappas D P, Brundle C R and Hopster H 1992 *Phys. Rev.* B **45** 8169
[515] Hope S, Choi B C, Bode P J and Bland J A C 2000 *Phys. Rev.* B **61** 5876
[516] Dutcher J R, Cochran J F, Jacob I and Egelhoff W F Jr 1989 *Phys. Rev.* B **39** 10430

[517] Riggs K T, Dahlberg E D and Prinz G A 1990 *Phys. Rev.* B **41** 7088
[518] Hu X and Kawazoe Y 1994 *J. Appl. Phys.* **75** 6486
[519] Kostyuchenko V V and Zvezdin A K 1997 *J. Magn. Magn. Mater.* **155** 445
[520] Arnold C S, Pappas D P and Venus D 1999 *J. Appl. Phys.* **85** 5054
[521] Kuch W, Gilles J, Kang S S, Imada S, Suga S and Kirschner J 2000 *Phys. Rev.* B **62** 3824
[522] Vedmedenko E Y, Oepen H P and Kirschner J 2001 *J. Appl. Phys.* **89** 7145
[523] Bogdanov A N, Rössler U K and Müller K H 2002 *Phys. Status Solidi* a **189** 397
[524] Bauer E, Duden T and Zdyb R 2002 *J. Phys. D: Appl. Phys.* **35** 2327
[525] Zdyb R and Bauer E 2003 *Phys. Rev.* B **67** 134420
[526] Elmers H J, Hauschild J, Fritzsche H, Liu G, Gradmann U and Köhler U 1995 *Phys. Rev. Lett.* **75** 2031
[527] Stauffer D 1979 *Phys. Rep.* **54** 1
[528] Li H and Tonner B P 1990 *Surf. Sci.* **237** 141
[529] Heinrich B, Cochran J F, Kowalewski M, Kirschner J, Celinski Z, Arrott A S and Myrtle K 1991 *Phys. Rev.* B **44** 9348
[530] Schmid A K and Kirschner J 1992 *Ultramicroscopy* **42–44** 483
[531] Bovensiepen U, Poulopoulos P, Platow W, Farle M and Baberschke K 1999 *J. Magn. Magn. Mater.* **192** L386
[532] Teodorescu C M, Chevrier F, Brochier R, Richter C, Heckmann O, Ilakovac V, Padova P D and Hricovini K 2001 *Surf. Sci.* **482–485** 1004
[533] Teodorescu C M, Chevrier F, Brochier R, Richter C, Ilakovac V, Heckmann O, Padova P D and Hricovini K 2002 *Eur. Phys. J.* B **28** 305
[534] Yoh K, Ono H, Sueoka K and Ramsteiner M E 2004 *J. Vac. Sci. Technol.* B **22** 1432
[535] Hope S, Tselepi M, Gu E, Parker T M and Bland J A C 1999 *J. Appl. Phys.* **85** 6094
[536] Schumann F O, Buckley M E and Bland J A C 1994 *Phys. Rev.* B **50** 16424
[537] Gu E, Hope S, Tselepi M and Bland J A C 1999 *Phys. Rev.* B **60** 4092
[538] Tselepi M, Xu Y B, Freeland D J, Moore T A and Bland J A C 2001 *J. Magn. Magn. Mater.* **226–230** 1585
[539] Fisher M E and Ferdinand A E 1967 *Phys. Rev. Lett.* **19** 169
[540] Ferdinand A E and Fisher M E 1969 *Phys. Rev.* **185** 832
[541] Fisher M E and Barber M N 1972 *Phys. Rev. Lett.* **28** 1516
[542] Domb C 1973 *J. Phys. A: Math. Nucl. Gen.* **6** 1296
[543] Allan G A T 1970 *Phys. Rev.* B **1** 352
[544] Binder K and Hohenberg P C 1972 *Phys. Rev.* B **6** 3461
[545] Ritchie D S and Fisher M E 1973 *Phys. Rev.* B **7** 480
[546] Orkoulas G, Panagiotopoulos A Z and Fisher M E 2000 *Phys. Rev.* E **61** 5930
[547] Torre E D, Bennett L H and Watson R E 2005 *Phys. Rev. Lett.* **94** 147210
[548] Merikoski J, Timonen J, Manninen M and Jena P 1991 *Phys. Rev. Lett.* **66** 938
[549] Hendriksen P V, Linderoth S and Lindgard P A 1992 *J. Magn. Magn. Mater.* **104–107** 1577
[550] Bødker F, Mørup S, Oxborrow C A, Madsen M B and Niemantsverdriet J W 1992 *J. Magn. Magn. Mater.* **104–107** 1695
[551] Köbler U and Schreiber R 2006 *J. Magn. Magn. Mater.* **300** 519
[552] Schulz B, Schwarzwald R and Baberschke K 1994 *Surf. Sci.* **307–309** 1102
[553] Bergholz R and Gradmann U 1984 *J. Magn. Magn. Mater.* **45** 389
[554] Araya J and Merlos H 1981 *Cienc. Tec.* **5** 15
[555] Landau L D and Lifshitz E M 1960 *Electrodynamics of Continuous Media* (*Course of Theoretical Physics* vol 8) (Oxford: Pergamon)
[556] Döring W 1966 *Handbuch der Physik* vol XVIII/2 ed S Flügge (Berlin: Springer) p 341
[557] Kronmüller H and Fähnle M 2003 *Micromagnetism and the Structure of Ferromagnetic Solids* (Cambridge: Cambridge University Press)
[558] Lovesey S W 1984 *Theory of Neutron Scattering from Condensed Matter* vol 2 (Oxford: Oxford University Press)
[559] Maeda T, Yamauchi H and Watanabe H 1973 *J. Phys. Soc. Japan* **35** 1635
[560] Vleck J H V 1932 *The Theory of Electric and Magnetic Susceptibilities* 1st edn (London: Oxford University Press) (Reprint, 1966)
[561] Ziman J M 1972 *Principles of the Theory of Solids* 2nd edn (Cambridge: Cambridge University Press) (Reprint, 1999)
[562] Liechtenstein A I, Mryasov O N, Sandratskii L M and Gubanov V A 1991 *Electronic Structure of Solids* ed P Ziesche (New York: Nova Science) p 187
[563] Maeda T, Yamauchi H and Watanabe H 1976 *J. Phys. Soc. Japan* **40** 1559
[564] Stearns M B 1986 *Landolt-Börnstein—Group III: Crystal and Solid State Physics* vol 19a ed H P J Wijn (Berlin: Springer) p 24
[565] Kittel C 1949 *Phys. Rev.* **76** 743
[566] Baberschke K 2001 *Band-Ferromagnetism* ed K Baberschke *et al* (Berlin: Springer) p 27
[567] Pelzl J, Meckenstock R, Spoddig D, Schreiber F, Pflaum J and Frait Z 2003 *J. Phys.: Condens. Matter* **15** S451
[568] Swartzendruber L J 1991 *J. Magn. Magn. Mater.* **100** 573
[569] Lide D R (ed) 1995 *Handbook of Chemistry and Physics* 76th edn (Boca Raton, FL: CRC Press)
[570] Bozorth R M 1951 *Ferromagnetism* (New York: Van Nostrand)
[571] Betteridge W 1979 *Prog. Mater. Sci.* **24** 51
[572] Liu X, Steiner M M, Sooryakumar R, Prinz G A, Farrow R F C and Harp G 1996 *Phys. Rev.* B **53** 12166
[573] Wijn H P J 1991 *Magnetic Properties of Metals: d-Elements, Alloys and Compounds* (*Data in Science and Technology*) (Berlin: Springer)
[574] Myers H P and Sucksmith W 1951 *Proc. R. Soc.* A **207** 427
[575] Herring C 1966 *Magnetism* vol IV ed G T Rado and H Suhl (New York: Academic)
[576] Riedi P C 1977 *Physica* B **91** 43
[577] Shirane G, Minkiewicz V J and Nathans R 1968 *J. Appl. Phys.* **39** 383
[578] Collins M F, Minkiewicz V J, Nathans R, Passell L and Shirane G 1969 *Phys. Rev.* **179** 417
[579] Mook H A and Nicklow R M 1973 *Phys. Rev.* B **7** 336
[580] Lynn J W 1975 *Phys. Rev.* B **11** 2624
[581] Mook H A, Nicklow R M, Thompson E D and Wilkinson M L 1969 *J. Appl. Phys.* **40** 1450
[582] Mook H A and Tocchetti D 1979 *Phys. Rev. Lett.* **43** 2029
[583] Sinclair R N and Brockhouse B N 1960 *Phys. Rev.* **120** 1638
[584] Tang H, Plihal M and Mills D L 1998 *J. Magn. Magn. Mater.* **187** 187
[585] Windsor C G 1977 *Physica* B **91** 119
[586] Mitchell P W and Paul D M 1985 *Phys. Rev.* B **32** 3272
[587] Hennion M, Hennion B, Castets A and Tocchetti D 1975 *Solid State Commun.* **17** 899
[588] Mikke K, Jankowska J and Modrzejewski A 1976 *J. Phys. F: Met. Phys.* **6** 631
[589] Menzinger F, Caglioti G, Shirane G, Nathans R, Pickart S J and Alperin H A 1968 *J. Appl. Phys.* **39** 455
[590] Yethiray M, Robinson R A, Sivia D S, Lynn J W and Mook H A 1991 *Phys. Rev.* B **43** 2565

[591] Perring T G, Taylor A D and Squires G L 1995 *Physica* B **213–214** 348
[592] Michels A, Weissmüller J, Wiedenmann A, Pedersen J S and Barker J G 2000 *Phil. Mag. Lett.* **80** 785
[593] Weissmüller J, Michels A, Barker J G, Wiedenmann A, Erb U and Shull R D 2001 *Phys. Rev.* B **63** 214414
[594] Mook H A, Lynn J W and Nicklow R M 1973 *Phys. Rev. Lett.* **30** 556
[595] Minkiewicz V J, Collins M F, Nathans R and Shirane G 1969 *Phys. Rev.* **182** 624
[596] Stringfellow M W 1968 *J. Phys. C: Solid State Phys.* **1** 950
[597] Loong C K, Carpenter J M, Lynn J W, Robinson R A and Mook H A 1984 *J. Appl. Phys.* **55** 1895
[598] Lowde R D and Umakantha N 1960 *Phys. Rev. Lett.* **4** 452
[599] Pickart S J, Alperin H A, Minkiewicz V J, Nathans R, Shirane G and Steinsvoll O 1967 *Phys. Rev.* **156** 623
[600] Alperin H A, Steinsvoll O, Shirane G and Nathans R 1966 *J. Appl. Phys.* **37** 1052
[601] Dimitrijević Ž, Kraśnicki S, Todorović J and Wanic A 1967 *Physica* **37** 501
[602] Hennion B and Hennion M 1979 *J. Phys. F: Met. Phys.* **9** 557
[603] Mikke K, Jankowska J, Modrzejewski A and Frikkee E 1977 *Physica* B **86–88** 345
[604] Hatherly M, Hirakawa K, Lowde R D, Mallett J F, Stringfellow M W and Torrie B H 1964 *Proc. Phys. Soc.* **84** 55
[605] Riste T, Shirane G, Alperin H A and Pickart S J 1965 *J. Appl. Phys.* **36** 1076
[606] Aldred A T 1975 *Phys. Rev.* B **11** 2597
[607] Aldred A T and Froehle P H 1972 *Int. J. Magn.* **2** 195
[608] Riedi P C 1977 *Phys. Rev.* B **15** 5197
[609] Pauthenet R 1982 *J. Appl. Phys.* **53** 8187
[610] Pauthenet R 1982 *J. Appl. Phys.* **53** 2029
[611] Argyle B E, Charap S H and Pugh E W 1963 *Phys. Rev.* **132** 2051
[612] Riedi P C 1973 *Phys. Rev.* B **8** 5243
[613] Pauthenet R 1982 *C. R. Acad. Sci.* II **295** 1067
[614] Jaccarino V 1959 *Bull. Am. Phys. Soc.* **4** 461
[615] Talagala P, Fodor P S, Haddad D, Naik R, Wenger L E, Vaishnava P P and Naik V M 2002 *Phys. Rev.* B **66** 144426
[616] Foner S and Thompson E D 1959 *J. Appl. Phys.* **30** 229S
[617] Kaul R and Thompson E D 1969 *J. Appl. Phys.* **40** 1383
[618] Argyle B E and Charap S H 1964 *J. Appl. Phys.* **35** 802
[619] Karanikas J M, Sooryakumar R, Prinz G A and Jonker B T 1991 *J. Appl. Phys.* **69** 6120
[620] Vernon S P, Lindsay S M and Stearns M B 1984 *Phys. Rev.* B **29** 4439
[621] Grimsditch M, Fullerton E E and Stamps R L 1997 *Phys. Rev.* B **56** 2617
[622] Etzkorn M, Kumar P S A and Kirschner J 2007 in Kronmüller and Parkin [181] p 1658
[623] Vollmer R, Etzkorn M, Kumar P S A, Ibach H and Kirschner J 2003 *Phys. Rev. Lett.* **91** 147201
[624] Vollmer R, Etzkorn M, Kumar P S A, Ibach H and Kirschner J 2004 *J. Appl. Phys.* **95** 7435
[625] Etzkorn M, Kumar P S A, Tang W, Zhang Y and Kirschner J 2005 *Phys. Rev.* B **72** 184420
[626] Vollmer R, Etzkorn M, Kumar P S A, Ibach H and Kirschner J 2004 *J. Magn. Magn. Mater.* **272–276** 2126
[627] Hemenger P M and Weik H 1965 *J. Appl. Phys.* **36** 1052
[628] Pratzer M, Elmers H J, Bode M, Pietzsch O, Kubetzka A and Wiesendanger R 2001 *Phys. Rev. Lett.* **87** 127201
[629] Pratzer M and Elmers H J 2003 *Phys. Rev.* B **67** 094416
[630] Kubetzka A, Pietzsch O, Bode M and Wiesendanger R 2003 *Phys. Rev.* B **67** 020401
[631] Braun H B 1994 *Phys. Rev.* B **50** 16485
[632] Himpsel F J 1995 *J. Electron Spectrosc. Relat. Phenom.* **75** 187
[633] Yoshihara A, Sato H, Mawatari J, Yoshida K, Kitakami O and Shimada Y 2000 *J. Magn. Magn. Mater.* **221** 261
[634] Kim J G, Han K H, Cho J H and Lee S 2004 *Phys. Status Solidi* b **241** 1718
[635] Wolf J A, Krebs J J and Prinz G A 1994 *Appl. Phys. Lett.* **65** 1057
[636] Pajda M, Krudrnovský J, Turek I, Drchal V and Bruno P 2001 *Phys. Rev.* B **64** 174402
[637] Costa M V T, de Castro Barbosa A C, Muniz R B and d'Albuquerque e Castro J 2001 *Phys. Rev.* B **65** 052401
[638] Kübler J 2000 *Theory of Itinerant Electron Magnetism* (Oxford: Oxford University Press)
[639] Liechtenstein A I, Katsnelson M I, Antropov V P and Gubanov V A 1987 *J. Magn. Magn. Mater.* **67** 65
[640] Antropov V P, Katsnelson M I and Liechtenstein A I 1997 *Physica* B **237–238** 336
[641] Antropov V P, Harmon B N and Smirnov A N 1999 *J. Magn. Magn. Mater.* **200** 148
[642] Spišák D and Hafner J 1997 *J. Magn. Magn. Mater.* **168** 257
[643] Rosengaard N M and Johansson B 1997 *Phys. Rev.* B **55** 14975
[644] Mook H A and Paul D M 1985 *Phys. Rev. Lett.* **54** 227
[645] Halilov S V, Perlov A Y, Oppeneer P M and Eschrig H 1997 *Europhys. Lett.* **39** 91
[646] Halilov S V, Eschrig H, Perlov A Y and Oppeneer P M 1998 *Phys. Rev.* B **58** 293
[647] Brown R H, Nicholson D M C, Wang X and Schulthess T C 1999 *J. Appl. Phys.* **85** 4830
[648] Shallcross S, Kissavos A E, Meded V and Ruban A V 2005 *Phys. Rev.* B **72** 104437
[649] Costa M V T, Muniz R B and d'Albuquerque e Castro J 1995 *J. Phys.: Condens. Matter* **7** 3453
[650] Costa A T Jr, Muniz R B and Mills D L 2004 *Phys. Rev.* B **69** 064413
[651] Costa A T Jr, Muniz R B and Mills D L 2004 *Phys. Rev.* B **70** 054406
[652] Papaconstantopoulos D A 1896 *Handbook of the Band Structure of Elemental Solids* (New York: Plenum)
[653] Cooke J F, Lynn J W and Davis H L 1980 *Phys. Rev.* B **21** 4118
[654] Muniz R B, Cooke J F and Edwards D M 1985 *J. Phys. F: Met. Phys.* **15** 2357
[655] Muniz R B and Mills D L 2002 *Phys. Rev.* B **66** 174417
[656] Wang C S, Prange R E and Korenman V 1982 *Phys. Rev.* B **25** 5766
[657] Luchini M U and Heine V 1989 *J. Phys.: Condens. Matter* 8961
[658] d'Albuquerque e Castro D, Edwards D M and Muniz R B 1991 *J. Magn. Magn. Mater.* **93** 295
[659] Mryasov O N, Freeman A J and Liechtenstein A I 1996 *J. Appl. Phys.* **79** 4805
[660] van Schilfgaarde M and Antropov V P 1999 *J. Appl. Phys.* **85** 4827
[661] Morán S, Ederer C and Fähnle M 2003 *Phys. Rev.* B **67** 012407
[662] Trohidou K N, Blackman J A and Cooke J F 1991 *Phys. Rev. Lett.* **67** 2561
[663] Crangle J 1955 *Phil. Mag.* **46** 499
[664] Jansen H J F 1995 *Phys. Today* **48** (4) 50
[665] Gay J G and Richter R 1994 *Ultrathin Magnetic Structures: I* ed J A C Bland and B Heinrich (Berlin: Springer) p 21
[666] Freeman A J, Wu R, Kim M and Gavrilenko V I 1999 *J. Magn. Magn. Mater.* **203** 1
[667] Asada T, Bihlmayer G, Handschuh S, Heinze S, Kurz P and Bügel S 1999 *J. Phys.: Condens. Matter* **11** 9347
[668] Wu R and Freeman A J 1999 *J. Magn. Magn. Mater.* **200** 498

[669] Wu R 2001 *Band-Ferromagnetism* ed K Baberschke *et al* (Berlin: Springer) p 60
[670] Shull C G and Yamada Y 1962 *J. Phys. Soc. Japan Suppl.* B-III **17** 1
[671] Shull C G 1963 *Electronic Structure and Alloy Chemistry of the Transition Metals* ed P A Beck (New York: Wiley) p 69
[672] Eriksson O, Fernando G W, Albers R C and Boring A M 1991 *Solid State Commun.* **78** 801
[673] Eriksson O, Boring A M, Albers R C, Fernando G W and Cooper B R 1992 *Phys. Rev.* B **45** 2868
[674] Moon R M 1964 *Phys. Rev.* **136** A195
[675] Mook H A 1966 *Phys. Rev.* **148** 495
[676] Brown P J, Deportes J and Ziebeck K R A 1991 *J. Physique* I **1** 1529
[677] Krakauer H, Freeman A J and Wimmer E 1983 *Phys. Rev.* B **28** 610
[678] Freeman A J and Wu R 1991 *J. Magn. Magn. Mater.* **100** 497
[679] Blügel S 1992 *Phys. Rev. Lett.* **68** 851
[680] Moraitis G, Mokrani A, Demangeat C and M'passi-Mabiala B 1996 *Surf. Sci.* **364** 396
[681] Hong S C, Freeman A J and Fu C L 1988 *Phys. Rev.* B **38** 12156
[682] Hong S C, Freeman A J and Fu C L 1988 *J. Physique Coll.* **49** C8–1683
[683] Srivastava P, Wilhelm F, Ney A, Haack N, Wende H and Baberschke K 1998 *Surf. Sci.* **402–404** 818
[684] Weinert M and Freeman A J 1983 *J. Magn. Magn. Mater.* **38** 23
[685] Fu C L, Freeman A J and Oguchi T 1985 *Phys. Rev. Lett.* **54** 2700
[686] Li C and Freeman A J 1991 *Phys. Rev.* B **43** 780
[687] Wang D, Freeman A J and Krakauer H 1981 *Phys. Rev.* B **24** 1126
[688] Fu C L and Freeman A J 1986 *Phys. Rev.* B **33** 1755
[689] Aldén M, Skriver H L, Mirbt S and Johansson B 1994 *Surf. Sci.* **315** 157
[690] Ostroukhov A A, Floka V M and Cherepin V T 1995 *Surf. Sci.* **331–333** 1388
[691] Wang C S and Freeman A J 1981 *Phys. Rev.* B **24** 4364
[692] Alden M, Mirbt S, Skriver H L, Rosengaard N M and Johansson B 1992 *Phys. Rev.* B **46** 6303
[693] Hjortstam O, Trygg J, Wills J M, Johnansson B and Eriksson O 1996 *Phys. Rev.* B **53** 9204
[694] Niklasson A M N, Johansson B and Skriver H L 1999 *Phys. Rev.* B **59** 6373
[695] Shawagfeh N T and Khalifeh J M 2002 *Physica* B **321** 222
[696] Fu C L and Freeman A J 1987 *J. Magn. Magn. Mater.* **69** L1
[697] Wu R and Freeman A J 1993 *Phys. Rev.* B **47** 3904
[698] Li C, Freeman A J and Fu C L 1991 *J. Magn. Magn. Mater.* **94** 134
[699] Daalderop G H O, Kelly P J and Schuurmans M F H 1994 *Phys. Rev.* B **50** 9989
[700] Li C, Freeman A J and Fu C L 1988 *J. Magn. Magn. Mater.* **75** 53
[701] Lee J I, Fu C L and Freeman A J 1986 *J. Magn. Magn. Mater.* **62** 93
[702] Freeman A J and Fu C L 1987 *J. Appl. Phys.* **61** 3356
[703] Wimmer E, Freeman A J and Krakauer H 1984 *Phys. Rev.* B **30** 3113
[704] Jepsen O, Madsen J and Andersen O K 1982 *Phys. Rev.* B **26** 2790
[705] Wang C S and Freeman A J 1980 *Phys. Rev.* B **21** 4585
[706] Tersoff J and Falicov L M 1982 *Phys. Rev.* B **26** 6186
[707] Chakraborty M, Mookerjee A and Bhattacharya A K 2003 *Int. J. Mod. Phys.* B **17** 5839
[708] Fu C L and Freeman A J 1988 *J. Physique* **49** C8-1625
[709] Rodríguez-López J L, Dorantes-Dávila J and Pastor G M 1998 *Phys. Rev.* B **57** 1040
[710] Nakamura K, Ito T and Freeman A J 2003 *Phys. Rev.* B **68** 180404
[711] Bauer E and van der Merwe J H 1986 *Phys. Rev.* B **33** 3657
[712] Marcus P M and Jona F 1995 *Phys. Rev.* B **51** 5263
[713] Thouless M D 1995 *Annu. Rev. Mater. Sci.* **25** 69
[714] Müller B, Fischer B, Nedelmann L, Fricke A and Kern K 1996 *Phys. Rev. Lett.* **76** 2358
[715] Ibach H 1997 *Surf. Sci. Rep.* **29** 193
[716] Heinz K, Müller S and Hammer L 1999 *J. Phys.: Condens. Matter* **11** 9437
[717] Platow W, Bovensiepen U, Poulopoulos P, Farle M, Baberschke K, Hammer L, Walter S, Müller S and Heinz K 1999 *Phys. Rev.* B **59** 12641
[718] Ha K, Ciria M, O'Handley R C, Stephens P W and Pagola S 1999 *Phys. Rev.* B **60** 13780
[719] Prinz G A 1991 *J. Magn. Magn. Mater.* **100** 469
[720] Heckmann O, Magman H, le Fevre P, Chandesris D and Rehr J J 1994 *Surf. Sci.* **312** 62
[721] Cerdá J R, de Andres P L, Cebollada A, Miranda R, Navas E, Schuster P, Schneider C M and Kirschner J 1993 *J. Phys.: Condens. Matter* **5** 2055
[722] Prinz G A 1985 *Phys. Rev. Lett.* **54** 1051
[723] Idzerda Y U, Elam W T, Jonker B T and Prinz G A 1989 *Phys. Rev. Lett.* **62** 2480
[724] Li C, Freeman A J and Fu C L 1990 *J. Magn. Magn. Mater.* **83** 51
[725] dos Santos V and Kuhnen C A 1999 *Thin Solid Films* **350** 186
[726] Lorenz R and Hafner J 1996 *Phys. Rev.* B **54** 15937
[727] Fu C L and Freeman A J 1987 *Phys. Rev.* B **35** 925
[728] Moroni E G, Kresse G and Hafner J 1999 *J. Phys.: Condens. Matter* **11** L35
[729] Blügel S and Dederichs P H 1989 *Europhys. Lett.* **9** 597
[730] Blügel S, Drittler B, Zeller R and Dederichs P H 1989 *Appl. Phys.* A **49** 547
[731] Richter R, Gay J G and Smith J R 1985 *Phys. Rev. Lett.* **54** 2704
[732] Li C, Freeman A J and Fu C L 1988 *J. Magn. Magn. Mater.* **75** 201
[733] Crampin S 1993 *J. Phys.: Condens. Matter* **5** 4647
[734] Andersen T and Hübner W 2006 *Phys. Rev.* B **74** 184415
[735] Wu R and Freeman A J 1996 *J. Appl. Phys.* **79** 6500
[736] Schick A B, Freeman A J and Liechtenstein A I 1998 *J. Appl. Phys.* **83** 7022
[737] Szunyogh L, Újfalussy B, Pustogowa U and Weinberger P 1998 *Phys. Rev.* B **57** 8838
[738] Victora R H and Falicov L M 1983 *Phys. Rev.* B **28** 5232
[739] Wu R, Li C and Freeman A J 1991 *J. Magn. Magn. Mater.* **99** 71
[740] Wang D, Freeman A J and Krakauer H 1982 *Phys. Rev.* B **26** 1340
[741] Huang H, Zhu X and Hermanson J 1984 *Phys. Rev.* B **29** 2270
[742] Guo G Y 1997 *J. Magn. Magn. Mater.* **176** 97
[743] dos Santos V and Kuhnen C A 1999 *Thin Solid Films* **350** 258
[744] Ernst A, van der Laan G, Temmerman W M, Dhesi S S and Szotek Z 2000 *Phys. Rev.* B **62** 9543
[745] Ernst A, Lueders M, Temmerman W M, Szotek Z and van der Laan G 2000 *J. Phys.: Condens. Matter* **12** 5599
[746] Yang Z and Wu R 2001 *Phys. Rev.* B **63** 064413
[747] Hong S C, Freeman A J and Fu C L 1989 *Phys. Rev.* B **39** 5719
[748] Chikazumi S 1997 *Physics of Ferromagnetism* 2nd edn (Oxford: Clarendon)
[749] Stoner E C 1947 *Rep. Prog. Phys.* **11** 43
[750] Šljivančanin Ž V and Vukajlović F R 1998 *J. Phys.: Condens. Matter* **10** 8679

[751] Kraft T, Marcus P M and Scheffler M 1994 *Phys. Rev.* B **49** 11511
[752] Samant M G, Stöhr J, Parkin S S P, Held G A, Hermsmeier B D, Herman F, van Schilfgaarde M, Duda L C, Mancini D C, Wassdahl N and Nakajima R 1994 *Phys. Rev. Lett.* **72** 1112
[753] Pizzini S, Fontaine A, Giorgetti C, Dartyge E, Bobo J F, Piecuch M and baudelet F 1995 *Phys. Rev. Lett.* **74** 1470
[754] Jin Q Y, Xu Y B, Zhai H R, Hu C, Lu M, Bie Q S, Zhai Y, Dunifer G L, Naik R and Ahmad M 1994 *Phys. Rev. Lett.* **72** 768
[755] Jaouen N, Wilhelm F, Rogalev A, Tonnerre J M, Johal T K and van der Laan G 2005 *IEEE Trans. Magn.* **41** 3334
[756] Kobayashi Y, Nasu S, Emoto T and Shinjo T 1994 *Hyperfine Interact.* **94** 2273
[757] Wilhelm F, Angelakeris M, Jaouen N, Poulopoulos P, Papaioannou E T, Mueller C, Fumagalli P, Rogalev A and Flevaris N K 2004 *Phys. Rev.* B **69** 220404
[758] Scherz A, Wende H, Poulopoulos P, Lindner J, Baberschke K, Blomquist P, Wäppling R, Wilhelm F and Brookes N B 2001 *Phys. Rev.* B **64** 180407
[759] Scherz A, Poulopoulos P, Wende H, Ceballos G, Baberschke K and Wilhelm F 2002 *J. Appl. Phys.* **91** 8760
[760] Gradmann U and Bergholz R 1984 *Phys. Rev. Lett.* **52** 771
[761] Wende H, Scherz A, Wilhelm F and Baberschke K 2003 *J. Phys.: Condens. Matter* **15** S547
[762] Slater J C 1936 *Phys. Rev.* **49** 537
[763] Slater J C 1936 *Phys. Rev.* **49** 931
[764] Moruzzi V L, Marcus P M, Schwarz K and Mohn P 1986 *Phys. Rev.* B **34** 1784
[765] Moruzzi V L 1986 *Phys. Rev.* B **57** 2211
[766] Marcus P M and Moruzzi V L 1988 *J. Appl. Phys.* **63** 4045
[767] Moruzzi V L, Marcus P M and Kübler J 1989 *Phys. Rev.* B **39** 6957
[768] Bagayoko D and Callaway J 1983 *Phys. Rev.* B **28** 5419
[769] Hathaway K B, Jansen H J F and Freeman A J 1985 *Phys. Rev.* B **31** 7603
[770] Min B I, Oguchi T and Freeman A J 1986 *Phys. Rev.* B **33** 7852
[771] Wang C S, Klein B M and Krakauer H 1985 *Phys. Rev. Lett.* **54** 1852
[772] Herper H C, Hoffmann E and Entel P 1999 *Phys. Rev.* B **60** 3839
[773] Peng S and Jansen H J F 1990 *J. Appl. Phys.* **67** 4567
[774] Kondorskii E I and Sedov V L 1960 *Sov. Phys.—JETP* **11** 561
[775] Tatsumoto E, Fujiwara H, Tange H and Kato Y 1962 *Phys. Rev.* **128** 2179
[776] Kouvel J S and Hartelius C C 1964 *J. Appl. Phys.* **35** 940
[777] Campbell I A and Creuzet G 1987 *Metallic Magnetism* (*Topics in Current Physics* no 42) ed H Capellmann (Berlin: Springer) p 207
[778] Bethe H 1933 *Handbuch der Physik* ed A G Smekal (Berlin: Springer)
[779] Brown P J, Deportes J, Givord D and Ziebeck K R A 1982 *J. Appl. Phys.* **53** 1973
[780] Steinsvoll O, Majkrzak C F, Shirane G and Wicksted J 1983 *Phys. Rev. Lett.* **51** 300
[781] Uemura Y J, Shirane G, Steinsvoll O and Wicksted J 1983 *Phys. Rev. Lett.* **51** 2322
[782] Brown P J, Capellmann H, Deportes J, Givord D and Ziebeck K R A 1983 *J. Magn. Magn. Mater.* **31–34** 295
[783] Korenman V and Wyman B 1981 *Phys. Rev.* B **24** 5413
[784] Korenman V 1983 *Physica* B **119** 21
[785] Korenman V 1983 *J. Magn. Magn. Mater.* **31–34** 301
[786] Korenman V 1985 *J. Appl. Phys.* **57** 3000
[787] Korenman V 1987 *Metallic Magnetism* (*Topics in Current Physics* no 42) ed H Capellmann (Berlin: Springer) p 109
[788] Mook H A 1983 *J. Magn. Magn. Mater.* **31–34** 305
[789] Eastman D E, Himpsel F J and Knapp J A 1980 *Phys. Rev. Lett.* **44** 95
[790] Steinsvoll O, Majkrzak C F, Shirane G and Wicksted J 1984 *Phys. Rev.* B **30** 2377
[791] Wicksted J, Shirane G and Steinsvoll O 1984 *Phys. Rev.* B **29** 488
[792] Wicksted J, Shirane G and Steinsvoll O 1984 *J. Appl. Phys.* **55** 1893
[793] Wicksted J P, Böni P and Shirane G 1984 *Phys. Rev.* B **30** 3655
[794] Moriya T 1985 *Spin Fluctuations in Itinerant Electron Magnetism* (*Solid-State Sciences* vol 56) (Berlin: Springer)
[795] Moriya T 1991 *J. Magn. Magn. Mater.* **100** 261
[796] Mohn P and Khmelevskyi S 2001 *Band-Ferromagnetism* (*Lecture Notes in Physics* no 580) ed K Baberschke *et al* (Berlin: Springer) p 126
[797] Mohn P 2003 *Magnetism in the Solid State* (*Solid-State Sciences* no 134) (Berlin: Springer)
[798] von der Linden W, Donath M and Dose V 1993 *Phys. Rev. Lett.* **71** 899
[799] Donohue J 1974 *The Structures of the Elements* (New York: Wiley)
[800] Riedi P C 1981 *Phys. Rev.* B **24** 1593
[801] Heller P 1966 *Phys. Rev.* **146** 403
[802] Moruzzi V L, Janak J F and Williams A R 1978 *Calculated Electronic Properties of Metals* (New York: Pergamon)
[803] Guo G Y and Wang H H 2000 *Chin. J. Phys.* **38** 949
[804] Marcus P M and Moruzzi V L 1985 *Solid State Commun.* **55** 971
[805] Fox S and Jansen H J F 1999 *Phys. Rev.* B **60** 4397
[806] Fox S and Jansen H J F 1996 *Phys. Rev.* B **53** 5119
[807] Jansen H, unpublished
[808] Carpenter H and Robertson J M 1939 *Metals* vol II (London: Oxford University Press)
[809] Grigorovich V K 1989 *The Metallic Bond and the Structure of Metals* (Commack: Nova Science)
[810] Abrahams S C, Guttman L and Kasper J S 1962 *Phys. Rev.* **127** 2052
[811] Kaufman L, Clougherty E V and Weiss R J 1963 *Acta Metall.* **11** 323
[812] Weiss R J 1990 *Physics of Materials* (New York: Hemisphere)
[813] Gonser U, Meechan C J, Muir A H and Wiedersich H 1963 *J. Appl. Phys.* **34** 2373
[814] Johanson G J, McGirr M B and Wheeler D A 1970 *Phys. Rev.* B **1** 3208
[815] Ehrhart P, Schönfeld B, Ettwig H H and Pepperhoff W 1980 *J. Magn. Magn. Mater.* **22** 79
[816] Keune W, Ezawa T, Macedo W A A, Glos U, Schletz K P and Kirschbaum U 1989 *Physica* B **161** 269
[817] Edelstein A S, Kim C, Qadri S B, Kim K H, Browning V, Yu H Y, Maruyama B and Everett R K 1990 *Solid State Commun.* **76** 1379
[818] Bykov V N, Zdorovtseva G G, Troyan V A and Khaimovich V S 1972 *Sov. Phys.—Crystallogr.* **16** 699
[819] Maurer M, Ousset J C, Ravet M F and Piecuch M 1989 *Europhys. Lett.* **9** 803
[820] Perjeru F, Schwickert M M, Lin T, Anderson A and Harp G R 2000 *Phys. Rev.* B **61** 4054
[821] Walmsley R, Thompson J, Friedman D, White R M and Geballe T H 1983 *IEEE Trans. Magn.* **19** 1992
[822] Riedi P C, Dumelow T, Rubinstein M, Prinz G A and Qadri S B 1987 *Phys. Rev.* B **36** 4595
[823] Heinrich B, Purcell S T, Dutcher J R, Urquhart K B, Cochran J F and Arrott A S 1988 *Phys. Rev.* B **38** 12879
[824] Brookes N B, Clarke A and Johnson P D 1992 *Phys. Rev.* B **46** 237

[825] Kim H G, Sumiyama K and Suzuki K 1997 *J. Alloys Compounds* **260** 23
[826] Ellis W C and Greiner E S 1941 *Trans. Am. Soc. Met.* **29** 415
[827] Ram S 2001 *Acta Mater.* **49** 2297
[828] Pauthenet R, Picoche J C and Rub P 1982 *C. R. Acad. Sci.* II **295** 331
[829] Moruzzi V L and Marcus P M 1988 *Phys. Rev.* B **38** 1613
[830] Paduani C 2003 *Phys. Status Solidi* b **240** 634
[831] Venables J A, Spiller G D and Handbücken M 1984 *Rep. Prog. Phys.* **47** 399
[832] Zhang Z and Lagally M G 1997 *Science* **276** 377
[833] Eckstein J N 2007 in Kronmüller and Parkin [181] p 1775
[834] Behr G and Löser W 2007 in Kronmüller and Parkin [181] p 1821
[835] Celinski Z, Heinrich B and Cochran J F 1993 *J. Appl. Phys.* **73** 5966
[836] Steigerwald D A, Jacob I and Egelhoff W F Jr 1988 *Surf. Sci.* **202** 472
[837] Xhonneux P and Courtens E 1992 *Phys. Rev.* B **46** 556
[838] Kief M T and Egelhoff W F Jr 1993 *Phys. Rev.* B **47** 10785
[839] Himpsel F J 1991 *Phys. Rev. Lett.* **67** 2363
[840] Wuttig M and Thomassen J 1993 *Surf. Sci.* **282** 237
[841] Thomassen J, Feldmann B and Wuttig M 1992 *Surf. Sci.* **264** 406
[842] Wuttig M, Feldmann B, Thomassen J, May F, Zillgen H, Brodde A, Hannemann H and Neddermeyer H 1993 *Surf. Sci.* **291** 14
[843] Li D, Freitag M, Pearson J, Qiu Z Q and Bader S D 1994 *Phys. Rev. Lett.* **72** 3112
[844] Heinrich B, Celinski Z, Cochran J F, Arrott A S and Myrtle K 1991 *J. Appl. Phys.* **70** 5769
[845] Smith G C, Padmore H A and Norris C 1982 *Surf. Sci.* **119** L287
[846] Stampanoni M, Vaterlauss A, Aeschlimann M and Meier F 1987 *Phys. Rev. Lett.* **59** 2483
[847] Heinrich B, Urquhart K B, Arrott A S, Cochran J F, Myrtle K and Purcell S T 1987 *Phys. Rev. Lett.* **59** 1756
[848] Koon N C, Jonker B T, Volkening F A, Krebs J J and Prinz G A 1987 *Phys. Rev. Lett.* **59** 2463
[849] Sato H, Toth R S and Astrue R W 1964 *Single-Crystal Films* ed M H Francombe and H Sato (Oxford: Pergamon) p 395
[850] Urano T and Kanaji T 1988 *J. Phys. Soc. Japan* **57** 3403
[851] Fahsold G, Priebe A and Pucci A 2001 *Appl. Phys.* A **73** 39
[852] Bader S D and Moog E R 1987 *J. Appl. Phys.* **61** 3729
[853] Paul O, Taborelli M and Landolt M 1989 *Surf. Sci.* **211–212** 724
[854] Daniels B J, Nix W D and Clemens B M 1994 *Thin Solid Films* **253** 218
[855] Theis-Bröhl K, Zoller I, Boödeker P, Schmitte T, Brendel H Z L, Belzer M and Wolf D E 1998 *Phys. Rev.* B **57** 4747
[856] Berlowitz P J and Goodman D W 1988 *J. Vac. Sci. Technol.* A **6** 634
[857] Zhou X L, Yoon C and White J M 1988 *Surf. Sci.* **203** 53
[858] Waldrop J R and Grant R W 1979 *Appl. Phys. Lett.* **34** 630
[859] Kneedler E, Thibado P M, Jonker B T, Bennett B R, Shanabrook B V, Wagner R J and Whitman L J 1996 *J. Vac. Sci. Technol.* B **14** 3193
[860] Thibado P M, Kneedler E, Jonker B T, Bennett B R, Shanabrook B V and Whitman L J 1996 *Phys. Rev.* B **53** R10481
[861] Kneedler E M, Jonker B T, Thibado P M, Wagner R J, Shanabrook B V and Whitman L J 1997 *Phys. Rev.* B **56** 8163
[862] Prinz G A and Krebs J J 1981 *Appl. Phys. Lett.* **39** 397
[863] Prinz G A, Rado G T and Krebs J J 1982 *J. Appl. Phys.* **53** 2087
[864] Qadri S B, Goldenberg M, Prinz G A and Ferrari J M 1985 *J. Vac. Sci. Technol.* B **3** 718
[865] Anderson G W, Ma P and Norton P R 1996 *J. Appl. Phys.* **79** 5641
[866] Ma P and Norton P R 1997 *Phys. Rev.* B **56** 9881
[867] Ma P, Anderson G W and Norton P R 1999 *Surf. Sci.* **420** 134
[868] Tari S, Sporken R, Aoki T, Smith D J, Metlushko V, AbuEl-Rub K and Sivananthan S 2002 *J. Vac. Sci. Technol.* B **20** 1586
[869] Shimizu S and Sasaki N 1996 *Thin Solid Films* **281–282** 46
[870] Chu W, Tsuruta A, Owari M and Nihei Y 2007 *Surf. Sci.* **601** 638
[871] Prinz G A, Jonker B T, Ferrari J J K J M and Kovanic F 1986 *Appl. Phys. Lett.* **48** 1756
[872] Jonker B T, Krebs J J, Prinz G A and Qadri S B 1987 *J. Cryst. Growth* **81** 524
[873] Prinz B T J G A 1991 *J. Appl. Phys.* **69** 2938
[874] Prinz B T J G A and Idzerda Y U 1991 *J. Vac. Sci. Technol.* B **9** 2437
[875] Abad H, Jonker B T, Cotell C M and Krebs J J 1995 *J. Vac. Sci. Technol.* B **13** 716
[876] Bland J A C, Bateson R D, Heinrich B, Celinski Z and Lauter H J 1992 *J. Magn. Magn. Mater.* **104–107** 1909
[877] Bland J A C, Bateson R D, Johnson A D, Heinrich B, Celinski Z and Lauter H J 1991 *J. Magn. Magn. Mater.* **93** 331
[878] Bland J A C, Daboo C, Heinrich B, Celinski Z, Fullerton E E, Ounadjela K and Stoeffler D 1995 *J. Magn. Magn. Mater.* **148** 85
[879] Fullerton E E, Stoeffler, Ounadjela K, Heinrich B, Celinski Z and Bland J A C 1995 *Phys. Rev.* B **51** 6364
[880] Bland J A C, Johnson A D, Norris C and Lauter H J 1990 *J. Appl. Phys.* **67** 5397
[881] Bland J A C, Johnson A D, Lauter H J, Bateson R D, Blundell S J, Shackleton C and Penfold J 1991 *J. Magn. Magn. Mater.* **93** 513
[882] Ohnishi S, Weinert M and Freeman A J 1984 *Phys. Rev.* B **30** 36
[883] den Broeder F J A, Donkersloot H C, Draaisma H J G and de Jonge W J M 1987 *J. Appl. Phys.* **61** 4317
[884] Celinski Z, Heinrich B, Cochran J F, Muir W B, Arrott A S and Kirschner J 1990 *Phys. Rev. Lett.* **65** 1156
[885] Childress J R, Kergoat R, Durand O, George J M, Galtier P, Miltat J and Schuhl A 1994 *J. Magn. Magn. Mater.* **130** 13
[886] Vogel J, Fontaine A, Cross V, Petroff F, Kappler J P and Krill G 1997 *Phys. Rev.* B **55** 3663
[887] Frank F C and van der Merwe J H 1949 *Proc. R. Soc.* A **198** 205
[888] Frank F C and van der Merwe J H 1949 *Proc. R. Soc.* A **198** 216
[889] van der Merwe J H and Ball C A B 1975 *Epitaxial Growth* vol B, ed J W Matthews (New York: Academic) p 493
[890] Matthews J W 1975 *Epitaxial Growth* vol B, ed J W Matthews (New York: Academic) p 559
[891] Bethge H, Heuer D, Jensen C, Reshöft K and Köhler U 1995 *Surf. Sci.* **331–333** 878
[892] Jensen C, Reshöft K and Köhler U 1996 *Appl. Phys.* A **62** 217
[893] Bode M, Pascal R, Dreyer M and Wiesendanger R 1996 *Phys. Rev.* B **54** R8385
[894] Sander D, Skomski R, Schmidthals C, Enders A and Kirschner J 1996 *Phys. Rev. Lett.* **77** 2566
[895] Sander D, Enders A, Schmidthals C, Reuter D and Kirschner J 1998 *Surf. Sci.* **402–404** 351
[896] Gradmann U and Waller G 1982 *Surf. Sci.* **116** 539
[897] Fink R L, Mulhollan G A, Andrews A B, Erskine J L and Walters G K 1991 *J. Appl. Phys.* **69** 4986

[898] Pasyuk V, Grath O F K M, Lauter H J, Petrenko A, Liénard A and Givord D 1995 *J. Magn. Magn. Mater.* **148** 38

[899] Elmers H J, Liu G and Gradmann U 1989 *Phys. Rev. Lett.* **63** 566

[900] Huang Y Y, Liu C and Felcher G P 1993 *Phys. Rev.* B **47** 183

[901] Nawrath T, Fritzsche H and Maletta H 2000 *J. Magn. Magn. Mater.* **212** 337

[902] Nawrath T, Fritzsche H, Klose F, Nowikow J and Maletta H 1999 *Phys. Rev.* B **60** 9525

[903] Li Y, anf F Klose C P, Kapoor J, Maletta H, Mezei F and Riegel D 1996 *Phys. Rev.* B **53** 5541

[904] Kümmerle W and Gradmann U 1977 *Solid State Commun.* **24** 33

[905] Keavney D J, Storm D F, Freeland J W, Grigorov I L and Walker J C 1995 *Phys. Rev. Lett.* **74** 4531

[906] Dunn J H, Arvanitis D and Mårtensson N 1996 *Phys. Rev.* B **54** R11157

[907] Schmitz D, Charton C, Scroll A, Carbone C and Eberhardt W 1999 *Phys. Rev.* B **59** 4327

[908] Maurer M *et al* 1991 *J. Magn. Magn. Mater.* **93** 15

[909] Lin T, Tomaz M A, Schwickert M M and Harp G R 1998 *Phys. Rev.* B **58** 862

[910] Geng K W, He T, Yang G H and Pan F 2004 *J. Magn. Magn. Mater.* **284** 26

[911] Iskhakov R S, Komogortsev S V, Stolyar S V, Prokof'ev D E, Zhigalov V S and Balaev A D 1999 *JETP Lett.* **70** 736

[912] Jantz W, Rupp G, Smith R S, Wettling W and Bayreuther G 1983 *IEEE Trans. Magn.* **MAG–19** 1859

[913] McGuire T R, Krebs J J and Prinz G A 1984 *J. Appl. Phys.* **55** 2505

[914] Gester M, Daboo C, Hicken R J, Gray S J, Ercole A and Bland J A C 1996 *J. Appl. Phys.* **80** 347

[915] Filipe A, Schuhl A and Galtier P 1997 *Appl. Phys. Lett.* **70** 129

[916] Zölfl M, Brockmann M, Köhler M, Kreuzer S, Schweinböck T, Miethaner S, Bensch F and Bayreuther G 1997 *J. Magn. Magn. Mater.* **175** 16

[917] Doi M, Cuenya B R, Keune W, Schmitte T, Nefedov A, Zabel H, Spoddig D, Meckenstock R and Pelzl J 2002 *J. Magn. Magn. Mater.* **240** 407

[918] Cuenya B R, Doi M, Keune W, Hoch S, Reuter D, Schmitte A W T and Zabel H 2003 *Appl. Phys. Lett.* **82** 1072

[919] Giovanelli L, Tian C S, Gastelois P L, Panaccione G, Fabrizioli M, Hochstrasser M, Galaktionov M, Bach C H and Rossi G 2004 *Physica* B **345** 177

[920] Mirbt S, Sanyal B, Isheden C and Johansson B 2003 *Phys. Rev.* B **67** 155421

[921] Schultz B D, Farrell H H, Evans M M R, Lüdge K and Palmstrøm C J 2002 *J. Vac. Sci. Technol.* B **20** 1600

[922] Giovanelli L, Panaccione G, Rossi G, Fabrizioli M, Tian C S, Gastelois P L, Fujii J and Back C H 2005 *Phys. Rev.* B **72** 045221

[923] Ionescu A, Vaz C A F, Laloë J B, van Belle F, Middleton A S, Tselepi M, Wastlbauer G, Bland J A C, Dalgliesh R M and Langridge S 2008, unpublished

[924] Laloë J B, van Belle F, Ionescu A, Vaz C A F, Middleton A, Wastlebauer G, Dalgliesh R, Langridge S and Bland J A C 2006 *IEEE Trans. Magn.* **42** 2933

[925] Meckenstock R, Spoddig D, Himmelbauer K, Krenn H, Doi M, Keune W, Frait Z and Pelzl J 2002 *J. Magn. Magn. Mater.* **240** 410

[926] Xu Y B, Tselepi M, Guertler C M, Wastlbauer G, Bland J A C, Dudzik E and van der Laan G 2001 *J. Appl. Phys.* **89** 7156

[927] Claydon J S, Xu Y B, Tselepi M, Bland J A C and van der Laan G 2004 *Phys. Rev. Lett.* **93** 037206

[928] Giovanelli L, Panaccione G, Rossi G, Fabrizioli M, Tian C S, Gastelois P L, Fujii J and Back C H 2005 *Appl. Phys. Lett.* **87** 042506

[929] Teodorescu C and Luca D 2006 *Surf. Sci.* **600** 4200

[930] Ruppel L, Witte G, Wöll C, Last T, Fischer S F and Kunze U 2002 *Phys. Rev.* B **66** 245307

[931] Xu Y B, Kernohan E T M, Tselepi M, Bland J A C and Holmes S 1998 *Appl. Phys. Lett.* **73** 399

[932] Ohno H, Yoh K, Doi T, Subagyo A, Sueoka K and Mukasa K 2001 *J. Vac. Sci. Technol.* B **19** 2280

[933] Schieffer P, Lépine B and Jézéquel G 2002 *Surf. Sci.* **497** 341

[934] Cardona M, Christensen N E and Fasol G 1988 *Phys. Rev.* B **38** 1806

[935] Eppenga R and Schuurmans M F H 1988 *Phys. Rev.* B **37** 10923

[936] Richards D, Jusserand B, Peric H and Etienne B 1993 *Phys. Rev.* B **47** 16028

[937] Luo J, Munekata H, Fang F F and Stiles P J 1988 *Phys. Rev.* B **38** 10142

[938] Ivanov Y, Kop'ev P S, Suchalkin S D and Ustinov V M 1991 *JETP Lett.* **53** 493

[939] de Andrada e Silva E A, Rocca G C L and Bassani F 1994 *Phys. Rev.* B **50** 8523

[940] Datta S and Das B 1990 *Appl. Phys. Lett.* **56** 665

[941] Holmes S, Stradling R A, Wang P D, Droopad R, Parker S D and Williams R L 1989 *Semicond. Sci. Technol.* **4** 303

[942] Akazaki T, Nitta J, Takayanagi H, Enoki T and Arai K 1994 *Appl. Phys. Lett.* **65** 1263

[943] Damsgaard C D, Gunnlaugsson H P, Weyer G, Hansena J B, Jacobsen C S, Skov J L, Rasmussen I and Mørup S 2006 *Solid State Commun.* **133** 579

[944] Xu Y B, Freeland D J, Tselepi M and Bland J A C 2000 *Phys. Rev.* B **62** 1167

[945] Teodorescu C M, Chevrier F, Richter C, Ilakovac V, Heckmann O, Lechevalier L, Brochier R, Johnson R L and Hricovini K 2000 *Appl. Surf. Sci.* **166** 137

[946] Xu Y B, Tselepi M, Wu J, Wang S, Bland J A C, Huttel Y and van der Laan G 2002 *IEEE Trans. Magn.* **38** 2652

[947] Xu Y B, Tselepi M, Dudzik E, Guertler C M, Vaz C A F, Wastlbauer G, Freeland D J, Bland J A C and van der Laan G 2001 *J. Magn. Magn. Mater.* **226–230** 1643

[948] Eriksson O, Nordström L, Pohl A, Severin L, Boring A M and Johansson B 1990 *Phys. Rev.* B **41** 11807

[949] Sacharow L, Morgenstern M, Bihlmayer G and Blügel S 2004 *Phys. Rev.* B **69** 085317

[950] Morgenstern M, Getzlaff M, Haude D, Wiesendanger R and Johnson R L 2000 *Phys. Rev.* B **61** 13805

[951] Newkirk J B 1957 *Trans. Am. Inst. Min. Metall. Pet. Eng.* **209** 1214

[952] Müller S, Bayer P, Reischl C, Heinz K, Feldmann B, Zilgen H and Wuttig M 1995 *Phys. Rev. Lett.* **74** 765

[953] Jesser W A and Matthews J W 1967 *Phil. Mag.* **15** 1097

[954] Hezaveh A A, Jennings G, Pescia D and Willis R F 1986 *Solid State Commun.* **57** 329

[955] Chambers S A, Wagener T J and Weaver J H 1987 *Phys. Rev.* B **36** 8992

[956] Liu C, Moog E R and Bader S D 1988 *Phys. Rev. Lett.* **60** 2422

[957] Shen J, Gai Z and Kirschner J 2004 *Surf. Sci. Rep.* **52** 163

[958] Pflitsch C, David R, Verheij L K and Franchy R 2001 *Europhys. Lett.* **53** 388

[959] Kümmerle W and Gradmann U 1978 *Phys. Status Solidi* a **45** 171

[960] Gradmann U and Isbert H O 1980 *J. Magn. Magn. Mater.* **15–18** 1109

[961] Zheng M, Shen J, Mohan C V, Ohresser P, Barthel J and Kirschner J 1999 *Appl. Phys. Lett.* **74** 425

[962] Choi B C, Fölsch S, Farle M and Rieder K H 1997 *Phys. Rev.* B **56** 3271
[963] O'Brien W L and Tonner B P 1995 *Phys. Rev.* B **52** 15332
[964] Escorcia-Aparicio E J, Kawakami R K and Qiu Z Q 1996 *Phys. Rev.* B **54** 4155
[965] Pappas D P, Glesener J W, Harris V G, Idzerda Y U, Krebs J J and Prinz G A 1994 *Appl. Phys. Lett.* **64** 28
[966] Boeglin C, Bulou H, Hommet J, Cann X L, Magnan H, Fèvre P L and Chandesris D 1999 *Phys. Rev.* B **60** 4220
[967] Pinski F J, Stauton J, Gyorffy B L, Johnson D D and Stocks G M 1986 *Phys. Rev. Lett.* **56** 2096
[968] Paduani C and da Silva E G 1994 *J. Magn. Magn. Mater.* **134** 161
[969] Giergiel J, Shen J, Woltersdorf J, Kirilyuk A and Kirschner J 1995 *Phys. Rev.* B **52** 8528
[970] Berger A, Feldmann B, Zillgen H and Wuttig M 1998 *J. Magn. Magn. Mater.* **183** 35
[971] Kirilyuk A, Giergiel J, Shen J, Straub M and Kirschner J 1996 *Phys. Rev. Lett.* **54** 1050
[972] Pappas D P, Kämper K P, Miller B P, Hopster H, Fowler D E, Luntz A C, Brundle C R and Shen Z X 1991 *J. Appl. Phys.* **69** 5209
[973] Allenspach R and Bischof A 1992 *Phys. Rev. Lett.* **69** 3385
[974] Macedo W A A and Keune W 1988 *Phys. Rev. Lett.* **61** 475
[975] Schmailzl P, Schmidt K, Bayer P, Döll R and Heinz K 1994 *Surf. Sci.* **312** 73
[976] Ellerbrock R D, Fuest A, Schatz A, Keune W and Brand R A 1995 *Phys. Rev. Lett.* **74** 3053
[977] Kawakami R K, Escorcia-Aparicio E J and Qiu Z Q 1996 *J. Appl. Phys.* **79** 4532
[978] Escorcia-Aparicio E J, Kawakami R K, Choi H J and Qiu Z Q 1997 *J. Appl. Phys.* **81** 4714
[979] Shen J, Mohan C V, Ohresser P, Klaua M and Kirschner J 1998 *Phys. Rev.* B **57** 13674
[980] Platow W, Farle M and Baberschke K 1998 *Europhys. Lett.* **43** 713
[981] Qian D, Jin X F, Barthel J, Klaua M and Kirschner J 2001 *Phys. Rev. Lett.* **87** 227204
[982] Gao X, Salvietti M, Kuch W, Schneider C M and Kirschner J 1998 *Phys. Rev.* B **58** 15426
[983] Gao X, Xu H, Wee A T S, Kuch W, Tieg C and Wang S 2005 *J. Appl. Phys.* **97** 103527
[984] Biedermann A, Tscheließnig R, Schmid M and Varga P 2001 *Phys. Rev. Lett.* **87** 086103
[985] Amemiya K, Kitagawa S, Matsumura D, Abe H, Ohta T and Yokoyama T 2004 *Appl. Phys. Lett.* **84** 936
[986] Shen J, Jenniches H, Mohan C V, Barthel J, Klaua M, Ohresser P and Kirschner J 1998 *Europhys. Lett.* **43** 349
[987] Jenniches H, Shen J, Mohan C V, Manoharan S S, Barthel J, Ohresser P, Klaua M and Kirschner J 1999 *Phys. Rev.* B **59** 1196
[988] Weinelt M, Schwarz S, Baier H, Müller S, Hammer L, Heinz K and Fauster T 2001 *Phys. Rev.* B **63** 205413
[989] Meyerheim H L, Popescu R, Sander D, Kirschner J, Robach O and Ferrer S 2005 *Phys. Rev.* B **71** 035409
[990] Taylor R D, Pasternak M P and Jeanloz R 1991 *J. Appl. Phys.* **69** 6126
[991] Bancroft D, Peterson E L and Minshall S 1956 *J. Appl. Phys.* **27** 291
[992] Williams Q, Jeanloz R, Bass J, Svendsen B and Ahrens T J 1987 *Science* **236** 181
[993] Vočadlo L, de Wijs G A, Gillan M and Price G D 1997 *Faraday Discuss.* **106** 205
[994] Backus G, Parker R and Constable C 1996 *Foundations of Geomagnetism* (Cambridge: Cambridge University Press)
[995] Nicol M and Jura G 1963 *Science* **141** 1035
[996] Pipkorn D N, Edge C K, Debrunner P and Pasquali G D 1964 *Phys. Rev.* **135** A1604
[997] Millet L E and Decker D L 1969 *Phys. Lett.* A **29** 7
[998] Williamson D L, Bukshpan S and Ingalls R 1972 *Phys. Rev.* B **6** 4194
[999] Taylor R D, Cort G and Willis J O 1982 *J. Appl. Phys.* **53** 8199
[1000] Cort G, Taylor R D and Willis J O 1982 *J. Appl. Phys.* **53** 2064
[1001] Gilder S and Glen J 1998 *Science* **279** 72
[1002] Andersen O K, Madsen J, Poulsen U K, Jepsen O and Kollár J 1977 *Physica* B **86–88** 249
[1003] Kübler J 1989 *Solid State Commun.* **72** 631
[1004] Podgórny M and Goniakowski J 1990 *Phys. Rev.* B **42** 6683
[1005] Podgórny M and Goniakowski J 1991 *Nuovo Cimento* D **13** 311
[1006] Goniakowski J 1991 *Phys. Rev.* B **44** 12348
[1007] Knab D and Koenig C 1991 *Phys. Rev.* B **43** 8370
[1008] Asada T and Terakura K 1992 *Phys. Rev.* B **46** 13599
[1009] Paduani C and França F 1995 *J. Magn. Magn. Mater.* **145** 147
[1010] Steinle-Neumann G, Stixrude L and Cohen R E 1999 *Phys. Rev.* B **60** 791
[1011] Thakor V, Staunton J B, Poulter J, Ostanin S, Ginatempo B and Bruno E 2003 *Phys. Rev.* B **67** 180405
[1012] Shimizu K, Kimura T, Furomoto S, Takeda K, Kontani K, Onuki Y and Amaya K 2001 *Nature* **412** 316
[1013] Jaccard D, Holmes A T, Behr G, Inada Y and Onuki Y 2002 *Phys. Lett.* A **299** 282
[1014] Saxena S S and Littlewood P B 2001 *Nature* **412** 290
[1015] Bose S K, Dolgov O V, Kortus J, Jepsen O and Andersen O K 2003 *Phys. Rev.* B **67** 214518
[1016] Jarlborg T 2003 *Physica* C **385** 513
[1017] Ohno H and Mekata M 1971 *J. Phys. Soc. Japan* **31** 102
[1018] Ohno H 1971 *J. Phys. Soc. Japan* **31** 92
[1019] Pearson D I C and Williams J M 1979 *J. Phys. F: Met. Phys.* **9** 1797
[1020] Maurer M, Ousset J C, Piecuch M, Ravet M F and Sanchez J P 1989 *Mater. Res. Soc. Symp. Proc.* **151** 99
[1021] Gao Q J and Tsong T T 1987 *Surf. Sci.* **191** L787
[1022] Egawa C and Iwasawa Y 1988 *Surf. Sci.* **195** 43
[1023] Liu C and Bader S D 1990 *Phys. Rev.* B **41** 553
[1024] Tian D, Li H, Jona F and Marcus P M 1991 *Solid State Commun.* **80** 783
[1025] Korecki J, Przybylski M, Prokop J, Krop K and Auric P 1995 *J. Magn. Magn. Mater.* **140–144** 673
[1026] Andrieu S, Piecuch M and Bobo J F 1992 *Phys. Rev.* B **46** 4909
[1027] Andrieu S, Ravet M F, Lenoble O, Dupuis V, Piecuch M, Pizzini S, Baudelet F and Fontaine A 1992 *Europhys. Lett.* **18** 529
[1028] Andrieu S, Piecuch M, Bobo J F, Lenoble O and Bauer P 1992 *J. Physique* IV **C3** 147
[1029] Sanchez J P, Ravet M F, Piecuch M and Maurer M 1990 *Hyperfine Interact.* **57** 2077
[1030] Baudelet F, Fontaine A, Tourillon G, Guay D, Maurer M, Piecuch M, Ravet M F and Dupuis V 1993 *Phys. Rev.* B **47** 2344
[1031] Saint-Lager M C, Raoux D, Brunel M, Piecuch M, Elkaïm E and Lauriat J P 1995 *Phys. Rev.* B **51** 2446
[1032] Spišák D, Lorenz R and Hafner J 2001 *Phys. Rev.* B **63** 094424
[1033] Spišák D, Lorenz R and Hafner J 2001 *J. Appl. Phys.* **89** 7080
[1034] Totland K, Fuchs P, Gröbli J C and Landolt M 1993 *Phys. Rev. Lett.* **70** 2487
[1035] Wu R and Freeman A J 1991 *Phys. Rev.* B **44** 4449
[1036] Knab D and Koenig C 1991 *J. Magn. Magn. Mater.* **98** 10
[1037] Knab D and Koenig C 1991 *J. Magn. Magn. Mater.* **93** 398
[1038] Zenia H, Bouarab S and Demangeat C 2002 *Surf. Sci.* **515** 245
[1039] Zenia H, Bouarab S and Demangeat C 2002 *Surf. Sci.* **521** 49

[1040] Kohlhepp J and Gradmann U 1995 *J. Magn. Magn. Mater.* **139** 347
[1041] Fritzsche H, Kohlhepp J and Gradmann U 1995 *Phys. Rev.* B **51** 15933
[1042] Pasyuk V, Lauter H J, Johnson M T, den Broader F J A, Janssen E, Bland J A C and Petrenko A V 1993 *Appl. Surf. Sci.* **65–66** 118
[1043] Pasyuk V, Lauter H J, Johnson M T, den Broader F J A, Janssen E, Bland J A C, Petrenko A V and Gay J M 1993 *J. Magn. Magn. Mater.* **121** 180
[1044] Beauvillain P, Chappert C, Grolier V, Mégy R, Ould-Mahfoud S, Renard J P and Veillet P 1993 *J. Magn. Magn. Mater.* **121** 503
[1045] Blügel S, Weinert M and Dederichs P H 1988 *Phys. Rev. Lett.* **60** 1077
[1046] Pescia D, Zampieri G, Stampanoni M, Bona G L, Willis R F and Meier F 1987 *Phys. Rev. Lett.* **58** 933
[1047] de Miguel J J, Cebollada A, Gallego J M, Ferrer S, Miranda R, Schneider C M, Bressler P, Garbe J, Bethke K and Kirschner J 1989 *Surf. Sci.* **211–212** 732
[1048] de Miguel J J, Cebollada A, Gallego J M, Miranda R, Schneider C M, Schuster P and Kirschner J 1991 *J. Magn. Magn. Mater.* **93** 1
[1049] Johnson M T, de Vries J J, McGee N W E, aan de Stegge J and den Broeder F J 1992 *Phys. Rev. Lett.* **69** 3575
[1050] Lee J, Lauhoff G and Bland J A C 1997 *Phys. Rev.* B **56** R5728
[1051] Vaz C A F and Bland J A C 2000 *Phys. Rev.* B **61** 3098
[1052] Bland J A C, Pescia D and Willis R F 1987 *Phys. Rev. Lett.* **58** 1244
[1053] Willis R F, Bland J A C and Schwarzacher W 1988 *J. Appl. Phys.* **63** 4051
[1054] Pescia D, Willis R F and Bland J A C 1987 *Surf. Sci.* **189–190** 724
[1055] Lauhoff G, Lee J, Bland J A C, Schillé J P and van der Laan G 1998 *J. Magn. Magn. Mater.* **177–181** 1253
[1056] Lauhoff G, Bland J A C, Lee J, Langridge S and Penfold J 1999 *Phys. Rev.* B **60** 4087
[1057] Lauhoff G, Lee J, Bland J A C, Langridge S and Penfold J 1999 *J. Magn. Magn. Mater.* **198–199** 331
[1058] Lauhoff G, Hirohata A, Lee J, Bland J A C, Langridge S and Penfold J 1999 *J. Phys.: Condens. Matter* 6707
[1059] Vaz C A F, Lauhoff G, Bland J A C, Langridge S, Bucknall D, Penfold J, Clarke J, Halder S K and Tanner B K 2007 *J. Magn. Magn. Mater.* **313** 89
[1060] Tischer M, Hjortstam O, Arvanitis D, Dunn J H, May F, Baberschke K, Trygg J, Willis J M, Johansson B and Eriksson O 1995 *Phys. Rev. Lett.* **75** 1602
[1061] Daalderop G H O, Kelly P J and den Broeder F J A 1992 *Phys. Rev. Lett.* **68** 682
[1062] Johnson M T, der Broeder F J A, de Vries J J, McGee N W E, Jungblut R and aan de Stegge J 1993 *J. Magn. Magn. Mater.* **121** 494
[1063] Vaz C A F, Lauhoff G, Lee J and Bland J A C 1999 *IEEE Trans. Magn.* **35** 3850
[1064] Bland J A C, Johnson A D, Bateson R D and Lauter H T 1992 *J. Magn. Magn. Mater.* **104–107** 1798
[1065] Bland J A C, Daboo C, Gehring G A, Kaplan B, Ives A J R, Hicken R J and Johnson A D 1995 *J. Phys.: Condens. Matter* **7** 6467
[1066] Fredrikze H, de Haan P, Lodder J C and Rekveldt M T 1993 *J. Magn. Magn. Mater.* **120** 369
[1067] Prinz G A, Vittoria C, Krebs J J and Hathaway K B 1985 *J. Appl. Phys.* **57** 3672
[1068] Bland J A C, Bateson R D, Riedi P C, Graham R G, Lauter H J, Penfold J and Shackleton C 1991 *J. Appl. Phys.* **69** 4989
[1069] Houdy P, Boher P, Giron F, Pierre F, Chappert C, Beauvillain P, Dang K L, Veillet P and Velu E 1991 *J. Appl. Phys.* **69** 5667
[1070] Blundell S J, Gester M, Bland J A C, Daboo C, Gu E, Baird M J and Ives A J R 1993 *J. Appl. Phys.* **73** 5948
[1071] Dekoster J, Jedryka E, Wójcik M and Langouche G 1993 *J. Magn. Magn. Mater.* **126** 12
[1072] Respaud M *et al* 1998 *Phys. Rev.* B **57** 2925
[1073] Ryan P, Winarski R P, Keavney D J, Freeland J W, Rosenberg R A, Park S and Falco C M 2004 *Phys. Rev.* B **69** 054416
[1074] Lee C H, Yu K L, Lee M H, Huang J A C and Felcher G P 2000 *J. Magn. Magn. Mater.* **209** 110
[1075] Stearns M B, Lee C H and Groy T L 1989 *Phys. Rev.* B **40** 8256
[1076] Metoki N, Donner E and Zabel H 1994 *Phys. Rev.* B **49**17351
[1077] Bagayoko D, Ziegler A and Callaway J 1983 *Phys. Rev.* B **27** 7046
[1078] Victora R H and Falicov L M 1984 *Phys. Rev.* B **30** 259
[1079] Herman F, Lambin P and Jepsen O 1985 *Phys. Rev.* B **31** 4394
[1080] Herman F, Lambin P and Jepsen O 1985 *J. Appl. Phys.* **57** 3654
[1081] Moruzzi V L, Marcus P M, Schwarz K and Mohn P 1986 *J. Magn. Magn. Mater.* **54–57** 955
[1082] Singh D J 1992 *Phys. Rev.* B **45** 2258
[1083] Sandratskii L M and Kübler J 1993 *Phys. Rev.* B **47** 5854
[1084] Liu A Y and Singh D J 1993 *Phys. Rev.* B **47** 8515
[1085] Alippi P, Marcus P M and Scheffler M 1997 *Phys. Rev. Lett.* **78** 3892
[1086] Liu A Y and Singh D J 1993 *J. Appl. Phys.* **73** 6189
[1087] Valvidares S M, Schroeder T, Robach O, Lee C Q T L and Ferrer S 2004 *Phys. Rev.* B **70** 224413
[1088] Giordano H, Atrei A, Torrini M, Bardi U, Gleeson M and Barnes C 1996 *Phys. Rev.* B **54** 11762
[1089] Li H and Tonner B P 1989 *Phys. Rev.* B **40** 10241
[1090] Kim S K, Petersen C, Jona F and Marcus P M 1996 *Phys. Rev.* B **54** 2184
[1091] Gazzadi G C and Valeri S 1999 *Europhys. Lett.* **45** 501
[1092] Duò L, Bertacco R, Isella G, Ciccacci F and Richter M 2000 *Phys. Rev.* B **61** 15294
[1093] Wieldraaijer H, Kohlhepp J T, LeClair P, Ha K and de Jonge W J M 2003 *Phys. Rev.* B **67** 224430
[1094] Scheurer F, Carrière B, Deville J P and Beaurepaire E 1991 *Surf. Sci. Lett.* **245** L175
[1095] Fölsch S, Helms A, Steidinger A and Rieder K H 1998 *Phys. Rev.* B **57** R4293
[1096] Fölsch S, Helms A, Steidinger A and Rieder K H 1999 *J. Magn. Magn. Mater.* **191** 38
[1097] Fölsch S, Helms A, Steidinger A and Rieder K H 1999 *J. Magn. Magn. Mater.* **198–199** 746
[1098] Wang C P, Wu S C, Jona F and Marcus P M 1994 *Phys. Rev.* B **49** 17385
[1099] Kim S K, Jona F and Marcus P M 1995 *Phys. Rev.* B **51** 5412
[1100] Wormeester H, Hüger E and Bauer E 1996 *Phys. Rev.* B **54** 17108
[1101] Wulfhekel W, Gutjahr-Löser T, Zavaliche F, Sander D and Kirschner J 2001 *Phys. Rev.* B **64** 144422
[1102] Man K L, Zdyb R, Huang S F, Leung T C, Chan C T, Bauer E and Altman M S 2003 *Phys. Rev.* B **67** 184402
[1103] Spiridis N, Ślęzak T, Zajak M and Korecki J 2004 *Surf. Sci.* **566–568** 272
[1104] Xu F, Joyce J J, Ruckman M W, Chen H W, Boscherini F, Hill D M, Chambers S A and Weaver J H 1987 *Phys. Rev.* B **35** 2375
[1105] Teodorescu C M, Martin M G, Franco N, Ascolani H, Chrost J, Avila J and Asencio M C 1999 *J. Electron Spectrosc. Relat. Phenom.* **101–103** 493

[1106] Wu Y Z, Ding H F, Jing C, Wu D, Liu G L, Gordon V, Dong G S, Jin X N, Zhu S and Sun K 1998 *Phys. Rev.* B **57** 11935

[1107] Nath K G, Maeda F, Suzuki S and Watanabe Y 2001 *J. Appl. Phys.* **90** 1222

[1108] Lauhoff G, Bruynseraede C, Boeck J D, Roy W V, Bland J A C and Borghs G 1997 *Phys. Rev. Lett.* **79** 5290

[1109] Bland J A C, Blundell S J, Gester M, Bateson R D, Singleton J, Cox U J, Lucas C A, Poon W C K and Penfold J 1992 *J. Magn. Magn. Mater.* **115** 359

[1110] Lüdge K, Schultz B D, Vogt P, Evans M M R, Braun W, Palmstrøm C J, Richter W and Esser N 2002 *J. Vac. Sci. Technol.* B **20** 1591

[1111] Palmstrøm C J, Chang C C, Yu A, Galvin G J and Mayer J W 1987 *J. Appl. Phys.* **62** 3755

[1112] Mangan M A, Spanos G, Ambrose T and Prinz G A 1999 *Appl. Phys. Lett.* **75** 346

[1113] Wu Y Z, Ding H F, Jing C, Dong G S, Jin X N, Sun K and Zhu S 1999 *J. Electron Spectrosc. Relat. Phenom.* **198–199** 297

[1114] Subramanian S, Sooryakumar R, Prinz G A, Jonker B T and Idzerda Y U 1994 *Phys. Rev.* B **49** 17319

[1115] Subramanian S, Liu X, Stamps R L, Sooryakumar R and Prinz G A 1995 *Phys. Rev.* B **52** 10194

[1116] Dekoster J, Jedryka E, Mény C and Langouche G 1993 *Europhys. Lett.* **22** 433

[1117] Bruynseraede C, Lauhoff G, Bland J A C, Strijkers G, Boeck J D and Borghs G 1998 *IEEE Trans. Magn.* **34** 861

[1118] Jay J P, Jêdryka E, Dekoster J, Langouche G and Panissod P 1996 *Z. Phys.* B **101** 329

[1119] Swinnen B, Dekoster J, Meersschaut J, Cottenier S, Demuynck S, Langouche G and Rots M 1997 *Appl. Phys. Lett.* **70** 3302

[1120] Swinnen B, Meersschaut J, Dekoster J, Langouche G, Cottenier S, Demuynck S and Rots M 1997 *Phys. Rev. Lett.* **78** 362

[1121] Swinnen B, Meersschaut J, Dekoster J, Langouche G, Cottenier S, Demuynck S and Rots M 1998 *Phys. Rev. Lett.* **80** 1569

[1122] Swinnen B, Dekoster J, Meersschaut J, Demuynck S, Cottenier S, Langouche G and Rots M 1997 *J. Magn. Magn. Mater.* **175** 23

[1123] Pizzini S, Fontaine A, Dartyge E, Giorgetti C, Baudelet F, Kappler J P, Boher P and Giron F 1994 *Phys. Rev.* B **50** 3779

[1124] Šljivančanin Ž V and Vukajlović F R 1998 *Phys. Rev. Lett.* **80** 1568

[1125] Šljivančanin Ž V and Vukajlović F R 2002 *Int. J. Mod. Phys.* B **16** 3655

[1126] Makhlouf S A, Ivanov E, Sumiyama K and Suzuki K 1992 *J. Alloys Compounds* **189** 117

[1127] van der Laan G, Hoyland M A, Surman M, Flipse C F J and Thole B T 1992 *Phys. Rev.* B **69** 3827

[1128] van der Laan G 1998 *J. Magn. Magn. Mater.* **190** 318

[1129] Hope S *et al* 1997 *Phys. Rev.* B **55** 11422

[1130] Lee J, Lauhoff G, Tselepi M, Hope S, Rosenbusch P, Bland J A C, Dürr H A, van der Laan G, Schillé J P and Matthew J A D 1997 *Phys. Rev.* B **55** 15103

[1131] Lee J, Lauhoff G, Hope S, Daboo C, Bland J A C, Schillé J P, van der Laan G and Penfold J 1997 *J. Appl. Phys.* **81** 3893

[1132] Gubbiotti G, Carlotti G, Ciria M and O'Handley R C 2002 *IEEE Trans. Magn.* **38** 2649

[1133] Yang Z, Gavrilenko V I and Wu R 2000 *Surf. Sci.* **447** 212

[1134] Lee J and Bland J A C 1997 *Surf. Sci.* **382** L672

[1135] Lindner J, Poulopoulos P, Wilhelm F, Farle M and Baberschke K 2000 *Phys. Rev.* B **62** 10431

[1136] Rosenbusch P, Lee J, Lauhoff G and Bland J A C 1997 *J. Magn. Magn. Mater.* **172** 19

[1137] Vaz C A F, Lauhoff G, Bland J A C, Hase B D F T P A, Tanner B K, Langridge S and Penfold J 2001 *J. Magn. Magn. Mater.* **226–230** 1618

[1138] Wu R, Chen L and Freeman A J 1997 *J. Appl. Phys.* **81** 4417

[1139] Vaz C A F, Steinmuller S J, Moutafis C, Bland J A C and Babkevich A Y 2007 *Surf. Sci.* **601** 1377

[1140] Sorg C, Ponpandian N, Scherz A, Wende H, Nünthel R, Gleitsmann T and Baberschke K 2004 *Surf. Sci.* **565** 197

[1141] Chakraborty M, Mookerjee A and Bhattacharya A K 2005 *J. Magn. Magn. Mater.* **285** 210

[1142] Lee J, Lauhoff G, Fermon C, Hope S, Bland J A C, Schillé J P, van der Laan G, Chappert C and Beauvillain P 1997 *J. Phys.: Condens. Matter* **9** L137

[1143] Lin T, Schwickert M M, Tomaz M A, Chen H and Harp G 1999 *Phys. Rev.* B **59** 13911

[1144] Heinrich B, Arrott A S, Cochran J F, Purcell S T, Urquhart K B and Myrtle K 1987 *J. Cryst. Growth* **81** 562

[1145] Wieczorek M D, Keavney D J, Storm D F and Walker J C 1993 *J. Magn. Magn. Mater.* **121** 34

[1146] Vogel J, Panaccione G and Sacchi M 1994 *Phys. Rev.* B **50** 7157

[1147] Vogel J and Sacchi M 1996 *Phys. Rev.* B **53** 3409

[1148] Kamada Y, Matsui M and Asada T 1997 *J. Phys. Soc. Japan* **66** 466

[1149] Tian C S *et al* 2005 *Phys. Rev. Lett.* **94** 137210

[1150] Marcus P M, Moruzzi V L, Wang Z Q, Li Y S and Jona F 1987 *Mater. Res. Soc. Symp. Proc.* **83** 21

[1151] Heinrich B, Arrott A S, Cochran J F, Liu C and Myrtle K 1986 *J. Vac. Sci. Technol.* A **4** 1376

[1152] Heinrich B, Arrott A S, Cochran J F, Purcell S T, Urquhart K B, Alberding N and Liu C 1987 *Thin Film Growth Techniques for Low-Dimensional Structures* (*NATO ASI Series B, Physics* 163) ed R F C Farrow *et al* (New York: Plenum) p 521

[1153] Heinrich B, Cochran J F, Arrott A S, Purcell S T, Urquhart K B, Dutcher J R and Egelhoff W F Jr 1989 *Appl. Phys.* A **49** 473

[1154] Wang Z Q, Li Y S, Jona F and Marcus P M 1987 *Solid State Commun.* **61** 623

[1155] Kern R and Müller P 1997 *Surf. Sci.* **392** 103

[1156] Mijiritskii A V, Smulders P J M, Chumanov V Y, Rogojanu O C, James M A and Boerma D O 1998 *Phys. Rev.* B **58** 8960

[1157] Purcell S T, Arrott A S and Heinrich B 1988 *J. Vac. Sci. Technol.* B **6** 794

[1158] Gutierrez C J, Wieczorek M D, Qiu Z Q, Tang H and Walker J C 1991 *J. Magn. Magn. Mater.* **93** 369

[1159] Lee J I, Hong S C and Freeman A J 1992 *J. Magn. Magn. Mater.* **104–107** 1684

[1160] Lee J I, Hong S C, Freeman A J and Fu C L 1993 *Phys. Rev.* B **47** 810

[1161] Tang W X, Qian D, Wu D, Dong G S, Jin X N, Shen S M, Jiang X M, Zhang X X and Zhang Z 2002 *J. Magn. Magn. Mater.* **240** 404

[1162] Vaz C A F, Godinho M, Dormann J L, Noguès M, Ezzir A, Tronc E and Jolivet J P 1997 *Mater. Sci. Forum* **235** 813

[1163] Dormann J L, Fiorani D and Tronc E 1997 *Adv. Chem. Phys.* **98** 283

[1164] Bauer E 1994 *Rep. Prog. Phys.* **57** 895

[1165] Donath M 1999 *J. Phys.: Condens. Matter* **11** 9421

[1166] Poulopoulos P, Lindner J, Farle M and Baberschke K 1999 *Surf. Sci.* **437** 277

[1167] Bayreuther G, Dumm M, Uhl B, Meier R and Kipferl W 2003 *J. Appl. Phys.* **93** 8230

[1168] Victora R H and MacLaren J M 1993 *Phys. Rev.* B **47** 11583

[1169] Wang D S, Wu R and Freeman A J 1994 *J. Magn. Magn. Mater.* **129** 237

[1170] Bruno P 1989 *Phys. Rev.* B **39** 865

[1171] Daalderop G H O, Kelly P J and Schuurmans M F H 1994 *Ultrathin Magnetic Structures I* ed J A C Bland and B Heinrich (Berlin: Springer) p 40
[1172] Yafet Y and Gyorgy E M 1988 *Phys. Rev.* B **38** 9145
[1173] Williams C D H, Evans D and Thorp J S 1988 *J. Magn. Magn. Mater.* **73** 123
[1174] Farle M, Berghaus A and Baberschke K 1989 *Phys. Rev.* B **39** 4838
[1175] Lee E W 1955 *Rep. Prog. Phys.* **18** 184
[1176] Chappert C and Bruno P 1988 *J. Appl. Phys.* **64** 5736
[1177] Shick A B, Novikov D L and Freeman A J 1997 *Phys. Rev.* B **56** R14259
[1178] Sander D, Enders A and Kirschner J 1999 *J. Magn. Magn. Mater.* **200** 439
[1179] Ha K and O'Handley R C 1999 *J. Appl. Phys.* **85** 5282
[1180] Chambers S A, Chen H W, Vitomirov I M, Anderson S B and Weaver J H 1986 *Phys. Rev.* B **33** 8810
[1181] Tsao J Y 1993 *Materials Fundamentals of Molecular Beam Epitaxy* (New York: Academic)
[1182] Bochi G, Ballentine C A, Inglefield H E, Thompson C V and O'Handley R C 1996 *Phys. Rev.* B **53** R1729
[1183] Bochi G, Ballentine C A, Inglefield H E, Thompson C V and O'Handley R C 1996 *J. Appl. Phys.* **79** 5845
[1184] O'Handley R C and Sun S W 1991 *Science and Technology of Nanostructured Magnetic Materials* (*NATO ASI series* vol 259) ed G C Hadjipanayis and G A Prinz (New York: Plenum) p 109
[1185] O'Handley R C, Song O S and Ballentine C A 1993 *J. Appl. Phys.* **74** 6302
[1186] Bochi G, Song O and O'Handley R C 1994 *Phys. Rev.* B **50** 2043
[1187] Song O, Ballentine C A and O'Handley R C 1994 *Appl. Phys. Lett.* **64** 2593
[1188] Szymczak H 1997 *J. Appl. Phys.* **81** 5411
[1189] Gutjahr-Löser T, Sander D and Kirschner J 2000 *J. Appl. Phys.* **87** 5920
[1190] Farle M, Mirwald-Schulz B, Anisimov A N, Platow W and Baberschke K 1997 *Phys. Rev.* B **55** 3708
[1191] Farle M, Platow W, Anisimov A N, Poulopoulos P and Baberschke K 1997 *Phys. Rev.* B **56** 5100
[1192] Dhesi S S, Dürr H A and van ver Laan G 1999 *Phys. Rev.* B **59** 8408
[1193] Klein C, Ramchal R, Schmid A K and Farle M 2007 *Phys. Rev.* B **75** 193405
[1194] Callen H B and Callen E 1966 *J. Phys. Chem. Solids* **27** 1271
[1195] Farle M, Platow W, Kosubek E and Baberschke K 1999 *Surf. Sci.* **439** 146
[1196] Zakeri K, Kebe T, Lindner J and Farle M 2006 *Phys. Rev.* B **73** 052405
[1197] Zakeri K, Kebe T, Lindner J and Farle M 2006 *J. Magn. Magn. Mater.* **299** L1
[1198] Zakeri K, Kebe T, Lindner J and Farle M 2007 *J. Magn. Magn. Mater.* **316** e334
[1199] Mryasov O N, Nowak U, Guslienko K Y and Chantrell R W 2005 *Europhys. Lett.* **69** 805
[1200] Staunton J B, Szunyogh L, Buruzs A, Gyorffy B L, Ostanin S and Udvardi L 2006 *Phys. Rev.* B **74** 144411
[1201] Skomski R, Mryasov O N, Zhou J and Sellmyer D J 2006 *J. Appl. Phys.* **99** 08E916
[1202] Buruzs Á, Weinberger P, Szunyogh L, Udvardi L, Chleboun P I, Fischer A M and Staunton J B 2007 *Phys. Rev.* B **76** 064417
[1203] Stanley H E 1971 *Introduction to Phase Transitions and Critical Phenomena* (New York: Oxford University Press)
[1204] Weber W, Bischof A, Allenspach R, Back C H, Fassbender J, May U, Schirmer B, Jungblut R J, Güntherodt G and Hillebrands B 1996 *Phys. Rev.* B **54** 4075
[1205] Bozorth R M 1993 *Ferromagnetism* (New York: IEEE)
[1206] Nishizawa T and Ishida K 1990 *Binary Alloy Phase Diagrams* vol 2, ed T B Massalski (Materials Park, OH: ASM International) p 1181
[1207] Steigerwald D A and Egelhoff W F Jr 1987 *Surf. Sci.* **192** L887
[1208] Mankey G J, Kief M T and Willis R F 1991 *J. Vac. Sci. Technol.* A **9** 1595
[1209] Kief M T, Mankey G J and Willis R F 1991 *J. Appl. Phys.* **69** 5000
[1210] Schmid A K, Atlan D, Itoh H, Heinrich B, Ichinokawa T and Kirschner J 1993 *Phys. Rev.* B **48** 2855
[1211] Gonzalez L, Miranda R, Salmerón M, Vergés J A and Ynduráin F 1981 *Phys. Rev.* B **24** 3245
[1212] Chen Q, Onellion M, Walt A and Dowben P A 1992 *J. Phys.: Condens. Matter* **4** 7985
[1213] Bernhard T, Pfandzelter R, Gruyters M and Winter H 2005 *Surf. Sci.* **575** 154
[1214] Fassbender J, Allenspach R and Dürig U 1997 *Surf. Sci.* **383** L742
[1215] Kim S K, Kim J S, Han J Y, Seo J M, Lee C K and Hong S C 2000 *Surf. Sci.* **453** 47
[1216] Lee H, Lee D, Kim W, le Hung N, Kim H and Hwang C 2007 *Phys. Status Solidi* b **244** 4411
[1217] Sandratskii L M and Kübler J 1992 *J. Phys.: Condens. Matter* **4** 6927
[1218] Ramsperger U, Vaterlaus A, Pfäffli P, Maier U and Pescia D 1996 *Phys. Rev.* B **53** 8001
[1219] May U, Fassbender J and Güntherodt G 1997 *Surf. Sci.* **377–379** 992
[1220] Miron R A and Fichthorn K A 2005 *Phys. Rev.* B **72** 035415
[1221] Clarke A, Jennings G, Willis R F, Rous P J and Pendry J B 1987 *Surf. Sci.* **187** 327
[1222] Beier T, Jahrreiss H, Pescia D, Woike T and Gudat W 1988 *Phys. Rev. Lett.* **61** 1875
[1223] Baberschke K 1999 *Surf. Rev. Lett.* **6** 735
[1224] Hillebrands B, Krams P, Fassbender J, Mathieu C, Günderodt G, Jungblut R and Johnson M T 1994 *Acta Phys. Pol.* A **85** 179
[1225] Weber W, Bischof A, Allenspach R, Würsch C, Back C H and Pescia D 1996 *Phys. Rev. Lett.* **76** 3424
[1226] Kowalewski M, Schneider C M and Heinrich B 1993 *Phys. Rev.* B **47** 8748
[1227] Every A G and McCurdy A K 1992 *Landolt–Börnstein—Group III: Crystal and Solid State Physics* vol 29a ed D F Nelson (Berlin: Springer) p 1
[1228] Gump J, Xia H, Chirita M, Sooryakumar R, Tomaz M A and Harp G R 1999 *J. Appl. Phys.* **86** 6005
[1229] Hillebrands B, Fassbender J, Jungblut R, Güntherodt G, Roberts D J and Gehring G A 1996 *Phys. Rev.* B **53** R10548
[1230] Hartmann D, Weber W, Wesner D, Popovic S and Güntherodt G 1993 *J. Magn. Magn, Mater.* **121** 160
[1231] Engel B N, Wiedmann M H, Leeuwen R A V and Falco C M 1993 *Phys. Rev.* B **48** 9894
[1232] Beauvillain P, Bounouh A, Chappert C, Mégy R, Ould-Mahfoud S, Renard J P, Veillet P, Weller D and Corno J 1994 *J. Appl. Phys.* **76** 6078
[1233] Weber W, Back C H, Bischof A, Pescia D and Allenspach R 1995 *Nature* **374** 788
[1234] Schumann F O, Buckley M E and Bland J A C 1994 *J. Appl. Phys.* **76** 6093
[1235] Buckley M E, Schumann F O and Bland J A C 1995 *Phys. Rev.* B **52** 6596
[1236] Buckley M E, Schumann F O and Bland J A C 1996 *J. Phys.: Condens. Matter* **58** L147
[1237] Engel B N, Wiedmann M H, Leeuwen R A V and Falco C M 1993 *J. Appl. Phys.* **73** 6192

[1238] Engel B N, Wiedmann M H and Falco C M 1994 *J. Appl. Phys.* **75** 6401
[1239] Bennett W R, Schwarzacher W and Egelhoff W F Jr 1990 *Phys. Rev. Lett.* **65** 3169
[1240] Johnson M T, Purcell S T, McGee N W E, Coehoorn R, aan de Stegge J and Hoving W 1992 *Phys. Rev. Lett.* **68** 2688
[1241] Qiu Z Q, Pearson J and Bader S D 1992 *Phys. Rev.* B **46** 8659
[1242] Weber W, Allenspach R and Bischof A 1995 *Europhys. Lett.* **31** 491
[1243] Weber W, Allenspach R and Bischof A 1995 *Europhys. Lett.* **32** 379
[1244] Kawakami R K, Rotenberg E, Escorcia-Aparicio E J, Choi H J, Wolfe J H, Smith N V and Qiu Z Q 1999 *Phys. Rev. Lett.* **82** 4098
[1245] van Belle F, Vaz C A F and Bland J A C 2007 *Phys. Rev.* B **76** 184411
[1246] Allenspach R, Bischof A and Dürig U 1997 *Surf. Sci.* **381** L573
[1247] Smirnov A V and Bratkovsky A M 1996 *Phys. Rev.* B **54** R17371
[1248] Fassbender J, May U, Schirmer B, Jungblut R M, Hillebrands B and Güntherodt G 1995 *Phys. Rev. Lett.* **75** 4476
[1249] Weber W, Back C H, Bischof A and Allenspach C W R 1996 *Phys. Rev. Lett.* **76** 1940
[1250] Hope S, Gu E, Tselepi M, Buckley M E and Bland J A C 1998 *Phys. Rev.* B **57** 7454
[1251] Fassbender J, Güntherodt G, Mathieu C, Hillebrands B, Jungblut R, Kohlhepp J, Johnson M T, Roberts D J and Gehring G A 1998 *Phys. Rev.* B **57** 5870
[1252] Fassbender J, Mathieu C, Hillebrands B, Güntherodt G, Jungblut R and Johnson M T 1994 *J. Appl. Phys.* **76** 6100
[1253] Fassbender J, Mathieu C, Hillebrands B, Güntherodt G, Jungblut R and Johnson M T 1995 *J. Magn. Magn. Mater.* **148** 156
[1254] Kopper K P, Küpper D, Reeve R, Mitrelas T and Bland J A C 2007 *J. Appl. Phys.* **103** 07C904
[1255] Albrecht M, Furubayashi T, Gradmann U and Harrison W A 1992 *J. Magn. Magn. Mater.* **104–107** 1699
[1256] Oepen H P, Berger A, Schneider C M, Reul T and Kirschner J 1993 *J. Magn. Magn. Mater.* **121** 490
[1257] Néel L 1962 *Comptes Rendus* **255** 1545
[1258] Schlömann E 1970 *J. Appl. Phys.* **41** 1617
[1259] Bruno P 1988 *J. Phys. F: Met. Phys.* **18** 1291
[1260] Bruno P 1988 *J. Appl. Phys.* **64** 3153
[1261] Zhao Y P, Palasantzas G, Wang G C and Hosson J T M D 1999 *Phys. Rev.* B **60** 1216
[1262] Choe S B and Shin S C 2000 *J. Magn. Magn. Mater.* **221** 255
[1263] Schlömann E and Joseph R I 1970 *J. Appl. Phys.* **41** 1336
[1264] Park Y, Fullerton E E and Bader S D 1995 *Appl. Phys. Lett.* **66** 2140
[1265] Arias R and Mills D L 1999 *Phys. Rev.* B **59** 11871
[1266] Wolfe J H, Kawakami R K, Ling W L, Qiu Z Q, Arias R and Mills D L 2001 *J. Magn. Magn. Mater.* **232** 36
[1267] Néel L 1962 *Comptes Rendus* **255** 1676
[1268] Hill E W, Thomlinson S L and Li J P 1993 *J. Appl. Phys.* **73** 5978
[1269] Altbir D, Kiwi M, Ramírez R and Schuller I K 1995 *J. Magn. Magn. Mater.* **149** L246
[1270] Wei D and Bertram H N 1996 *IEEE Trans. Magn.* **32** 3434
[1271] Leal J L and Kryder M H 1996 *IEEE Trans. Magn.* **32** 4642
[1272] Han D H, Zhu J G and Judy J H 1997 *J. Appl. Phys.* **81** 4996
[1273] Schrag B D *et al* 2000 *Appl. Phys. Lett.* **77** 2373
[1274] Chopra H D, Yang D X, Chen P J, Parks D C and Egelhoff W F Jr 2000 *Phys. Rev.* B **61** 9642
[1275] Tiusan C, Hehn M and Ounadjela K 2002 *Eur. Phys. J.* B **26** 431
[1276] Egelhoff W F Jr, McMichael R D, Dennis C L, Stiles M D, Shapiro A J, Maranville B B and Powell C J 2006 *Appl. Phys. Lett.* **88** 162508
[1277] Vaz C A F, Steinmuller S J and Bland J A C 2007 *Phys. Rev.* B **75** 132402
[1278] Steinmuller S J, Vaz C A F, Ström V, Moutafis C, Gürtler C M, Kläui M, Bland J A C and Cui Z 2007 *Phys. Rev.* B **76** 054429
[1279] Steinmuller S J, Vaz C A F, Ström V, Moutafis C, Gürtler C M, Kläui M, Bland J A C and Cui Z 2007 *J. Appl. Phys.* **101** 09D113
[1280] Chang C A 1990 *J. Appl. Phys.* **68** 4873
[1281] Jungblut R, Johnson M T, aan de Stegge J, Reinders A and den Broeder F J A 1994 *J. Appl. Phys.* **75** 6424
[1282] O'Brien W L, Droubay T and Tonner B P 1996 *Phys. Rev.* B **54** 9297
[1283] Marioni M A, Pilet N, Ashworth T, O'Handley R C and Hug H J 2006 *Phys. Rev. Lett.* **97** 027201
[1284] Matthews J W and Crawford J L 1970 *Thin Solid Films* **5** 187
[1285] Tjeng L H, Idzerda Y U, Rudolf P, Sette F and Chen C T 1992 *J. Magn. Magn. Mater.* **109** 288
[1286] Idzerda Y and Prinz G A 1993 *Surf. Sci.* **284** L394
[1287] Stuhlmann C and Ibach H 1989 *Surf. Sci.* **219** 117
[1288] Schulz B and Baberschke K 1994 *Phys. Rev.* B **50** 13467
[1289] Shen J, Giergiel J and Kirschner J 1995 *Phys. Rev.* B **52** 8454
[1290] Lindner J, Poulopoulos P, Nünthel R, Kosubek E, Wende H and Baberschke K 2003 *Surf. Sci.* **523** L65
[1291] Nünthel R *et al* 2003 *Surf. Sci.* **531** 53
[1292] Naik R, Kota C, Payson J S and Dunifer G L 1993 *Phys. Rev.* B **48** 1008
[1293] Chang C A 1989 *Appl. Phys. Lett.* **55** 2754
[1294] Chang C A 1990 *J. Appl. Phys.* **67** 566
[1295] Chang C A, Liu J C and Angilello J 1990 *Appl. Phys. Lett.* **57** 2239
[1296] Parkin S S P, Li Z G and Smith D J 1991 *Appl. Phys. Lett.* **58** 2710
[1297] Demczyk B G, Naik V M, Auner G, Kota C and Rao U 1994 *J. Appl. Phys.* **75** 1956
[1298] Hashim I, Park B and Atwater H A 1993 *Appl. Phys. Lett.* **63** 2833
[1299] Echigoya J, Enoki H, Satoh T, Waki T, Ohmi T, Otsuki M and Shibata T 1992 *Appl. Surf. Sci.* **56–58** 463
[1300] Liu C S and Chen L J 1996 *Appl. Surf. Sci.* **92** 84
[1301] Krastev E T, Voice L D and Tobin R G 1996 *J. Appl. Phys.* **79** 6865
[1302] Masten A and Wissmann P 2001 *Appl. Surf. Sci.* **179** 68
[1303] O'Brien W L and Tonner B P 1996 *J. Appl. Phys.* **79** 5623
[1304] Farle M, Platow W, Anisimov A N, Schulz B and Baberschke K 1997 *J. Magn. Magn. Mater.* **165** 74
[1305] Uiberacker C, Zabloudil J, Weinberger P, Szunyogh L and Sommers C 1999 *Phys. Rev. Lett.* **82** 1289
[1306] Lauhoff G, Vaz C A F, Bland J A C, Lee J and Suzuki T 1999 *IEEE Trans. Magn.* **35** 3883
[1307] Lauhoff G, Vaz C A F, Bland J A C, Lee J and Suzuki T 2000 *Phys. Rev.* B **61** 6805
[1308] O'Brien W L and Tonner B P 1994 *Phys. Rev.* B **49** 15370
[1309] Zhang W, Vaz C A F, Hirohata A and Bland J A C 1999 *J. Appl. Phys.* **85** 4806